

Dissertation zur Erlangung des Doktorgrades  
der Fakultät für Chemie und Pharmazie  
der Ludwig-Maximilians-Universität München

# Design and Synthesis of Selective Ligands for the FK506-binding Protein 51

---

**Steffen Paul-Günter Gaali**

aus

München, Deutschland

2012

Erklärung

---

**Erklärung**

Diese Dissertation wurde im Sinne von § 7 der Promotionsordnung vom 28. November 2011 von Herrn Prof. Christoph Turck betreut.

Eidesstattliche Versicherung

Diese Dissertation wurde eigenständig und ohne unerlaubte Hilfe erarbeitet.

München, 03.05.2012

.....  
(Unterschrift des Autors / der Autorin)

Dissertation eingereicht am 03.05.2012

1. Gutachter: Prof. Christoph Turck

2. Gutachter: Prof. Roland Beckmann

Mündliche Prüfung am 17.07.2012

## **Danksagung**

An dieser Stelle möchte ich mich bei Prof. Dr. Dr. Florian Holsboer für die Möglichkeit bedanken, diese Arbeit am Max-Planck-Institut für Psychiatrie durchzuführen.

Besonders bedanken möchte ich mich bei Dr. Felix Hausch, der mir ermöglicht hat diese interessante und fordernde Doktorarbeit in seiner Forschungsgruppe durchzuführen. Seine hohe fachliche Kompetenz und die stete Diskussionsbereitschaft haben mir oftmals sehr weiter geholfen und ich habe viel für meine wissenschaftliche Zukunft gelernt.

Sehr herzlich möchte ich mich bei Prof. Turck und Prof. Beckmann bedanken für die Bereitschaft als Gutachter für meine Doktorarbeit zu fungieren. Des Weiteren bedanke ich mich bei Prof. Wanner, Prof. Heuschmann, Prof. Bracher und Prof. Hoffmann-Röder dafür als Prüfer zur Verfügung zu stehen.

Ich danke allen meinen Kollegen für das tolle Arbeitsklima und die Zeit die wir in und außerhalb des Labors miteinander verbracht haben. Besonderer Dank geht an die Chemie Crew von Labor 208 Christian Devigny und Yansong Wang für die tolle Zusammenarbeit und den Spaß im Labor, der das Arbeiten leicht gemacht hat und an meine persönliche Assay Abteilung Alexander Kirschner für das unermüdliche säen, ernten und mikroskopieren von verschiedensten Zellen, um meine Inhibitoren zu testen.

Ich bedanke mich bei Frau Dubler und Herr Dr. Stephenson von der NMR-Abteilung des Departments Chemie der LMU München.

Mein größter Dank gilt meiner Frau Maria sowie meinen Eltern, meinem Bruder und meinen Freunden ohne deren Rückhalt und Unterstützung in allen Lebenslagen ich nie so weit gekommen wäre.

## **Abstract**

The large FK506-binding proteins FKBP51 and FKBP52 are Hsp90 associated cochaperones that modulate steroid hormone receptor signaling. It has been shown that FKBP51 is a negative regulator whereas FKBP52 is a positive regulator of the glucocorticoid receptor. A majority of patients suffering from depression show an altered response to glucocorticoids. Furthermore, polymorphisms in the FKBP51 encoding gene were associated with human stress response and several psychiatric disorders. Recently, FKBP51 knockout or knockdown was shown to have a protective effect on stress-coping behavior in animal models of anxiety and depression.

In a neuroblastoma cell line FKBP51 suppresses the elongation of neurites whereas FKBP52 enhanced it. All FKBP ligands reported so far, including rapamycin and FK506, show only negligible selectivity between FKBP51 and FKBP52, since the residues within the active site are completely conserved both on the sequence and the structural level. Due to the antagonistic effect of FKBP51 and FKBP52, the opposing activity of these proteins cannot be examined with the present FKBP inhibitors. Therefore, we envisioned a chemical genomics tool to address these selectivity problems. Using structure-based design and protein mutagenesis we engineered an enlarged cavity into the active sites of FKBP51 and FKBP52. In turn, we synthesized a series of complementary ligands with protruding side chains that were designed to fit into this new cavity and to prevent binding to the wild-type proteins. The best ligands of this series showed low nanomolar affinities while maintaining 500 to 1000-fold selectivity for mutated FKBP51/52 over wildtype proteins.

Using these artificially selective ligands in a cell model of neuronal differentiation (N2a cells), we showed that specific inhibition of overexpressed FKBP51 restores neurite outgrowth whereas specific inhibition of overexpressed FKBP52 has the opposite effect. This is the first proof of pharmacological activity of FKBP51 ligands in a relevant cellular model. Furthermore we unambiguously show that selectivity is crucial for the effect. This could at least in part explain the inconsistencies and conflicting results that have plagued the field of neuroimmunophilin FKBP ligands in the past.

During our synthesis campaign we made the discovery that certain ligands can induce a conformational change in the binding pocket of FKBP51 and that these substances consistently show substantial selectivity versus FKBP52. Based on several co-crystal structures we rationally designed a series of these induced fit ligands which finally led to inhibitors (**iFit-1**, **iFit-2**) with low nanomolar affinities (4-6 nM) for wildtype FKBP51 and up to 10000 fold selectivity versus FKBP52. These ligands are the most potent and selective ligands reported for FKBP51 so far. In a neurite outgrowth assay they enhanced neurite outgrowth whereas FK506 was less active. These ligands provide the basis for the development of drug-like FKBP51 inhibitors to pharmacologically probe the role of FKBP51 in a whole animal context.

A. Introduction .....	1
<b>1. The biology of Immunophilins</b> .....	<b>1</b>
1.1 FK506-binding proteins and Cyclophilins.....	1
1.2 The biology of FKBP51 and FKBP52 .....	4
1.2.1 Structure and function of FKBP51 and FKBP52 .....	4
1.2.2 The role of FKBP51 and FKBP52 in steroid receptor signaling .....	5
1.2.3 Effects of FKBP51 and FKBP52 on the endocrine system.....	7
1.2.3.1 FKBP52 knockout mouse .....	7
1.2.3.2 FKBP51 knockout mouse .....	7
1.2.4 FKBP51 in stress related diseases.....	8
1.2.5 Cancer and cell proliferation .....	9
1.2.6 Immune function .....	10
1.2.7 Effect on neurodegenerative diseases .....	10
1.3 Chemical biology of FKBP ligands .....	11
1.3.1 Immunosuppressive FKBP ligands .....	11
1.3.2 Non-immunosuppressive FKBP ligands .....	12
1.4 Targeting the PPIase binding pocket of FKBP51 and FKBP52 .....	15
1.5 Artificially selective ligands .....	19
<b>2. Aim of the study</b> .....	<b>22</b>
B. Results and Discussion .....	23
<b>1. Chemical genomics to selectively address FKBP-sub-types</b> .....	<b>23</b>
1.1 Design of FKBP mutant specific engineered (FMSE) ligands .....	23
1.2 Synthesis of the FMSE ligands.....	24
1.3 Biochemical characterization of the FMSE-ligand-mutant pairs .....	27
1.4 Effect of selective inhibition of mutated FKBP51 and 52 on neurite outgrowth in N2a neuroblastoma cells.....	31
<b>2. Solving the selectivity issue by an induced fit mechanism</b> .....	<b>35</b>
2.1 Induced fit as a basis for selectivity .....	35
2.2 Synthesis of iFit FKBP51 ligands .....	38
2.2.1 Cyclopropylmethyl and benzyl series .....	39
2.2.1.1 Design and synthesis of C <sub>α</sub> cyclopropylmethyl and benzyl ligands .....	39
2.2.1.2 Biochemical activity of cyclopropylmethyl and benzyl ligands .....	41
2.2.2 Cyclohexenyl/Cyclohexyl series.....	45

2.2.2.1 Design and synthesis of cyclohexenyl/cyclohexyl ligands .....	45
2.2.2.2 Biochemical activity of cyclohexenyl/cyclohexyl ligands .....	47
2.2.2.3 Effect of iFit ligands on neurite outgrowth .....	52
2.2.3 C <sub>α</sub> -hydroxy series .....	53
2.2.4 C <sub>α</sub> symmetric ligand series .....	55
2.2.5 Synthesis of C <sub>α</sub> substituted rapamycin .....	56
2.3 Structural basis for the selectivity .....	58
2.3.1 Structure-activity relationship of the iFit ligands .....	58
2.3.2 Quantification of the induced conformational change .....	60
2.3.3 Evaluation of the co-crystal structures .....	61
2.3.3.1 The C <sub>α</sub> -Substituent .....	61
2.3.3.2 The Trimethoxyphenyl Moiety .....	62
2.3.3.3 The Top Group .....	63
<b>3. Summary and Outlook on Selective FKBP Ligands .....</b>	<b>65</b>
<b>4. Fluorescent Immunophilin Tracers .....</b>	<b>67</b>
4.1 Synthesis of fluorescent rapamycin derivatives .....	67
4.2 Synthesis of a fluorescent iFit ligand .....	69
4.3 Facile synthesis of a fluorescent CsA analogue to study Cyclophilin 40 and Cyclophilin 18 ligands .....	70
4.3.1 Synthesis of the tracer .....	71
4.3.2 Development of a fluorescence polarization assay for cyclophilin 40 and Cyp18 .....	72
<b>C. Experimental Section .....</b>	<b>74</b>
<b>1. Analytical Methods .....</b>	<b>74</b>
1.1 Nuclear magnetic resonance .....	74
1.2 Mass spectroscopy .....	74
1.3 HPLC .....	74
1.4 Silica chromatography .....	76
1.5 Data analysis of neurite outgrowth .....	77
<b>2. Reagents and solvents .....</b>	<b>77</b>
2.1 Reagents .....	77
2.2 Non-commercial reagents .....	80
2.3 Solvents .....	80
<b>3. General procedures .....</b>	<b>81</b>

<b>4. Synthesis of used compounds .....</b>	<b>81</b>
4.1 General synthesis procedure A for the coupling of morpholine containing top-groups .....	81
4.2 General synthesis procedure B for the coupling of free acid top-groups .....	82
4.3 Synthetic procedures .....	82
4.4 Biochemical Methods .....	147
<b>D. Abbreviations.....</b>	<b>149</b>
<b>E. Annex .....</b>	<b>151</b>
<b>F. References.....</b>	<b>155</b>
<b>G. Curriculum Vitae .....</b>	<b>164</b>

## A. Introduction

### 1. The biology of Immunophilins

#### 1.1 FK506-binding proteins and Cyclophilins

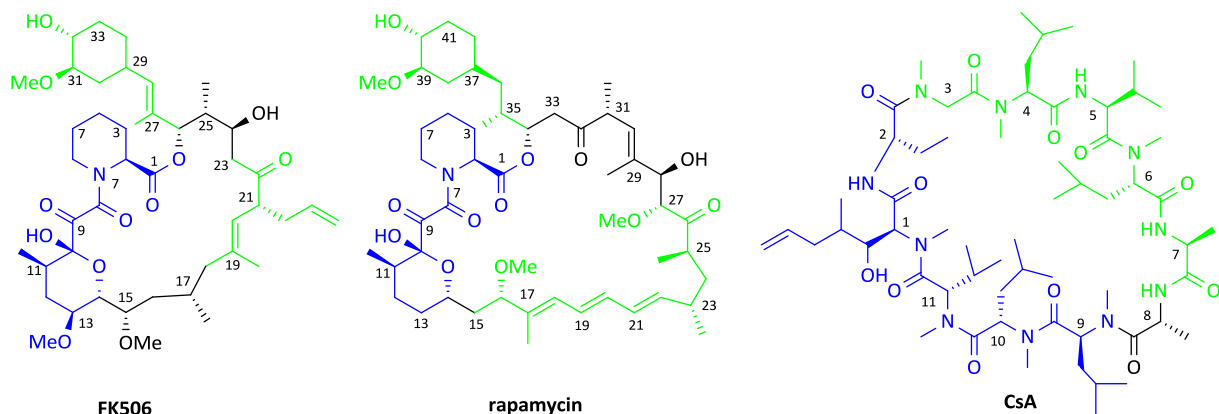


**Fig. 1:** The prototypic FKBP ligands FK506 and rapamycin and the cyclophilin ligand CsA. **Blue** (FK506, rapamycin): FKBP binding domain, **blue** (CsA) cyclophilin binding domain. **Green** (CsA, FK506) calcineurin binding domain, **green** (rapamycin) mTOR binding domain.

FK506-binding proteins (FKBP) and cyclophilins (Cyp) belong to the class of immunophilins which are defined by their ability to bind immunosuppressive ligands like FK506, rapamycin (Rap), and Cyclosporin A (CsA, **Fig. 1**). FKBP and Cyps minimally contain a peptidyl-prolyl-isomerase (PPIase) domain that catalyzes the interconversion of cis-trans isomers of X-Pro peptides and that binds to immunosuppressive drugs. For all aminoacids except proline the equilibrium of cis/trans isomerization lies on the trans side. In proteins these 19 aminoacids adopt almost exclusively the trans configuration. X-Proline dipeptides can occur either in the cis or the trans configuration in folded proteins, whereas in the unfolded state there is an ratio of cis/trans 2:8. Therefore in many protein folding processes the cis/trans isomerization of X-Pro displays the rate determining step. PPIases help proteins to fold in a correct way by catalyzing the isomerization of proline residues.<sup>1</sup>

The immunosuppression is not mediated by inhibition of the PPIase activity but by enabling FKBP to form a ternary complex with calcineurin (for FK506) or mTOR (for Rap). In complex with FKBP-FK506 calcineurin is not able to dephosphorylate nuclear factor of activated T-cells (NF-AT) which is needed for IL-2 expression and T-cell activation. The main mediators are FKBP12, and partially FKBP12.6 and

## A. Introduction

FKBP51.<sup>2</sup> mTOR assembles two complexes mTORC1 and mTORC2. The kinase activity of mTORC1 can be specifically inhibited by FKBP-Rap complexes which in turn leads to less phosphorylation of p70S6Kinase and 4E-BP1, both key regulators in protein translation and thereby causing the immunosuppressive effect.<sup>2, 3,4</sup>

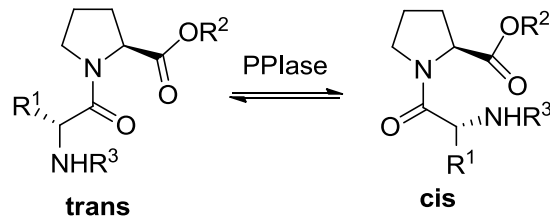


Fig 2: Proline cis/trans isomerization

The human genome encodes 17 different FKBP, which are named according to their size in kilodaltons (e.g., FKBP12, FKBP38, FKBP51 and FKBP52). **Table 1** shows the different known FKBP and their biochemical roles in mammalian cells known so far<sup>5</sup>.

Name	Associated Binding Partners	Functions	Cellular Compartment
hFKBP12a <sup>6,7</sup> hFKBP12.6 <sup>8,9</sup> hFKBP12c <sup>5</sup>	FK506/Calcineurin Rap/mTOR Type I TGFβ receptor Muscle ryanodine receptor Inositol receptor cardiac ryanodine receptor	regulator of cell cycle	Cytosol
hFKBP15p <sup>5</sup> hFKBP22p <sup>5</sup> hFKBP25p <sup>5</sup> hFKBP24p <sup>5</sup> hFKBP63p <sup>5</sup> hFKBP65p <sup>10</sup>		Protein coding cofactor     elastin chaperone	ER
hFKBP36 <sup>11,12</sup>	clathrin and Hsp72	glyceraldehyde-3-phosphate dehydrogenase inhibitor	Nuclear
hFKBP37 <sup>13</sup>	Aryl receptor	Transcription of genes	Cytosol
hFKBP37i <sup>14</sup>		Amarosis syndrome	Cytosol
hFKBP38 <sup>15</sup>	Bcl, FK506	Development of cancer cells	Cytosol

## A. Introduction

---

		Hedgehog signalling	
hFKBP51 <sup>16</sup>	SHR, HSP90, Akt	Negative Modulator of SHR	Cytosol
hFKBP52 <sup>17</sup>	SHR, HSP90	Positive Modulator of SHR	Cytosol
hFKBP25n <sup>18</sup>	YY1, HMG-II	Transcription of genes	Nuclear/Cytosolic
hFKBP135 <sup>5</sup>	F-Actin	Colocalized with F-Actin in growth cones of dorsal root ganglion neurons	Cytosol

**Table 1:** Biochemical roles and distribution of human FKBP5

The second class of immunophilins are the cyclophilins. The human genome encodes at least 16 unique cyclophilins, all containing a highly conserved Cyp18-homology domain, which shows PPIase activity. Many of them bind tightly to the unselective cyclophilin ligands CsA and sanglifehrin A.<sup>19, 20</sup> The Cyp-CsA complex forms a ternary complex with the phosphatase calcineurin (CN) similar to FKBP12-FK506. In this heterocomplex calcineurin is also unable to dephosphorylate its substrate NF-AT which is required for T-cell activation which again leads to the immunosuppressive effect<sup>3</sup>.

## 1.2 The biology of FKBP51 and FKBP52

### 1.2.1 Structure and function of FKBP51 and FKBP52

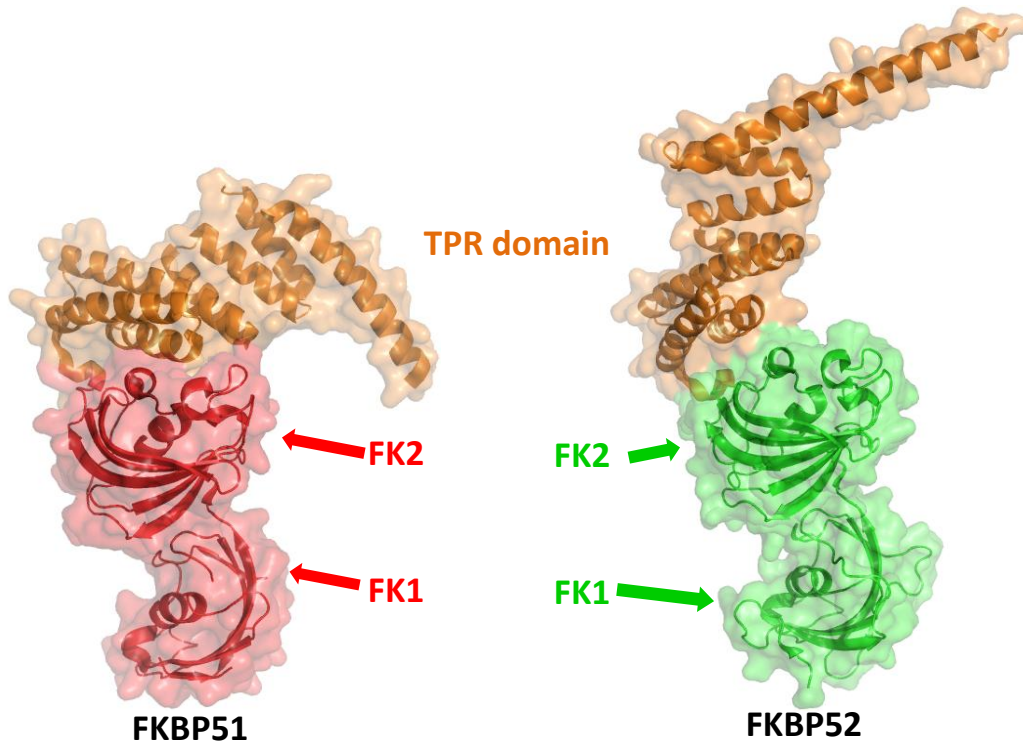


**Fig 3:** Crystal structures of FKBP51 and FKBP52

The large FKBP homologs FKBP51 and FKBP52 have first been identified in complex with steroid hormone receptors (SHR).<sup>21, 22</sup> The binding to SHRs is mediated by the heatshock protein 90 (Hsp90), where they act as co-chaperones.<sup>23</sup> Since then these proteins received great attention because of their steroid hormone signaling-regulating roles. Many endocrine related diseases are known for which FKBP51 and FKBP52 are potential therapeutic targets, such as for example stress related diseases, prostate cancer, breast cancer, male and female contraception and metabolic diseases. To better understand the role of these FKBP51 and FKBP52 in these diseases new non-immunosuppressive ligands are needed.

FKBP51 and FKBP52 are close homologs and share 70% sequence similarity.<sup>23</sup> They possess a similar domain architecture (**Fig. 3**), consisting of the FKBP12 like N-terminal PPIase domain (FK1), followed by another FKBP12 like domain (FK2) which although structurally similar to FK1 possesses no PPIase activity. At the C-terminus a tetratricopeptide (TPR) domain facilitates the binding to the EEVD motif at the C-terminus of Hsp90.<sup>24, 25</sup> The overall architecture of the domains of FKBP51 and FKBP52 is very similar. The orientation of FK1 and FK2 differ only slightly but the TPR domain orientation of FKBP52 is tilted compared to that of FKBP51. It has to be considered that FKBP52 was not crystalized

as a whole, but in two parts due to its instability in solution. The crystal structure in **Fig. 3** shows the reconstruction based on the two parts. The loop linking the FK2 and the TPR domain could be flexible and the orientations of the TPR domains could be due to different crystal packing.

The FK1 and FK2 domain are connected by a linker of seven to nine amino acids. FKBP52 has a casein kinase 2 phosphorylation (CK2) sequence (TEEED) in this linker which is not present in FKBP51 (the correspondent sequence is FED). It is thought that the phosphorylation of FKBP52 by CK2 at T143 decreases binding to Hsp90 and thereby abrogates the activating effect. This effect could be due to a reorientation of the FK1 domain upon phosphorylation.<sup>26</sup>

### 1.2.2 The role of FKBP51 and FKBP52 in steroid receptor signaling

FKBP51 and FKBP52 are regulators of steroid hormone receptor (SHR) binding activity. In most reports FKBP51 acts as a negative modulator on SHRs<sup>27</sup>, whereas FKBP52 is a positive regulator of androgen receptor (AR)<sup>28</sup>, glucocorticoid receptor (GR)<sup>29</sup> and progesterone receptor (PR)<sup>30</sup>. **Fig. 4** shows a model of the maturation and regulation of SHRs. Either FKBP51 or FKBP52 enters the mature Hsp90-dimer-SHR complex, which is stabilized by p23. The FKBP binds to the C-terminus of Hsp90 via the TPR domain. The present model proposes the FK1 domain and especially the proline rich loop of FKBP51 and FKBP52 interacts directly with the ligand binding domain of the SHR. If FKBP51 is present the binding affinity for the respective hormone decreases, whereas if FKBP52 is in the complex the binding affinity is increased.<sup>31</sup>

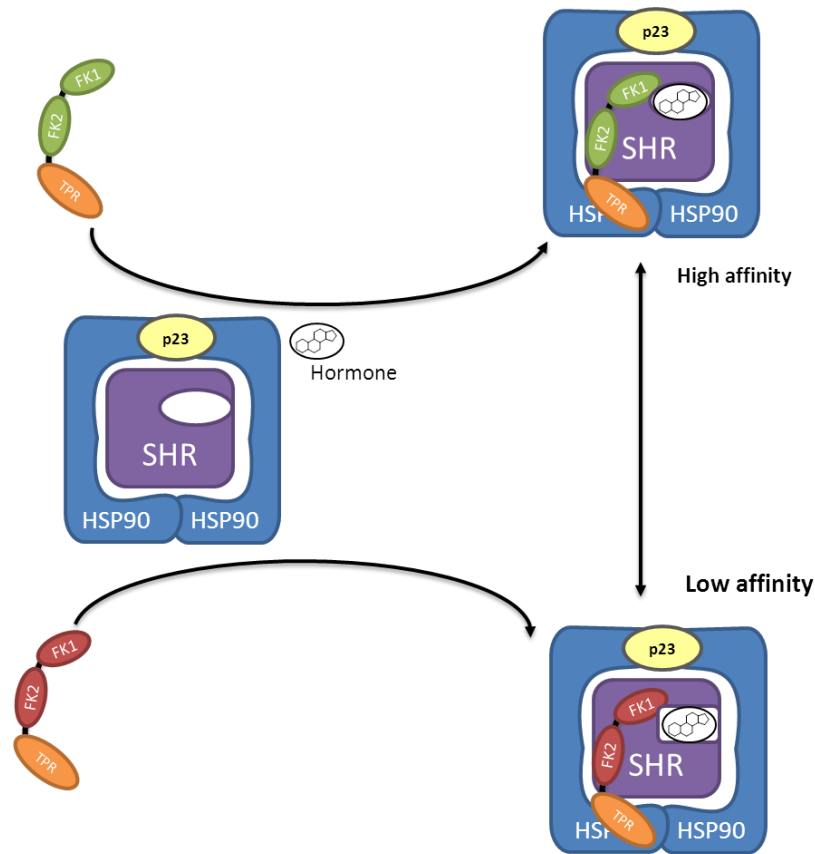


**Fig. 4:** Model of FKBP51 and 52 on steroid hormone maturation and ligand binding.

The PPIase enzymatic activity is not required for the modulation of the SHRs, but the FK1 domain and especially the proline rich loop which sits on top of the binding pocket, is crucial.<sup>32</sup> Differences in this loop seem to be the cause for the different functions of the FKBP5s, shown by the mutations, A116V and L119P in FKBP51 that switched the activity to full FKBP52-like characteristics towards AR activation.<sup>32</sup>

FKBP51 and FKBP52 also play a role in steroid hormone receptor localization. In the ligand free state the SHRs primarily stay in the cytoplasm, whereas ligand bound SHRs are mainly nuclear or translocate to the nucleus.<sup>33, 34</sup> It has been suggested that the accumulation of ligand bound SHR in the nucleus is enhanced by active retrograde transport driven by the dynein-dynactin complex which co-immunoprecipitate with the Hsp90-FKBP52 and with the GR and MR.<sup>35, 36</sup>

## **1.2.3 Effects of FKBP51 and FKBP52 on the endocrine system**

### **1.2.3.1 FKBP52 knockout mouse**

FKBP52 knockout mice (52KO) are viable but females are completely infertile. Male 52KO mice display a phenotype consistent with androgen insensitivity syndrome, hypospadias, penis length and weight of the penis was reduced, smaller seminal vesicles, smaller prostate glands, slightly lower sperm motility, collectively showing that mainly secondary sex organs are affected whereas primary sex organs like testes seemed to be unaffected.<sup>28, 37</sup> Female 52KO mice show no big change in phenotype but are sterile. This is due to progesterone insensitivity causing failures in decidualization and embryonic implantation.<sup>38</sup> Thus, FKBP52 is crucial for correct development of reproductive organs in male and female mice which is mainly caused by AR and PR insensitivity.

### **1.2.3.2 FKBP51 knockout mouse**

Under basal conditions FKBP51 knockout mice (51KO) show no robust phenotype. 51KO male and female mice are fertile and males show normal reproductive organs. Thus AR signaling is unaffected and also no changes in GR activity could be observed.<sup>37</sup> A possible explanation for the unanticipated absence of an effect on GR is the nature of the cortisol secretion under stress, and indeed recently Touma and coworkers could show, that 51KO in mice leads to a more active coping behavior after exposure to different types of stress. Additionally the hypothalamus-pituitary-adrenal (HPA) axis response on stress was altered. 51KO mice showed a stronger suppression of corticosterone secretion after treatment with a low dose of dexamethasone.<sup>39</sup> These findings were supported by the results of Hartmann et al. who showed in a chronic model of social defeat stress, that 51KO mice responded less to a novel acute stimulus and showed an enhanced recovery, as well as more active stress-coping behavior.<sup>40</sup> Additionally O'Leary and coworkers demonstrated that FKBP51 deficiency in aged mice led to more active stress-coping in the forced swim test and the tail suspension test. Both are well established paradigms to assess antidepressive effects.<sup>41</sup> All these findings strongly support the hypothesis that FKBP51 plays an important role in endocrine regulation of the HPA axis by reducing GR responsiveness. This makes FKBP51 a promising target in stress related diseases.

### 1.2.4 FKBP51 in stress related diseases

In stress related diseases such as major depression, bipolar disorder, post-traumatic stress disorder (PTSD) and anxiety disorder patients often display an imbalance in the stress hormone system called the hypothalamus-pituitary-adrenal (HPA) axis (**Fig. 5**). In healthy individuals this hormone system triggers the physiological and behavioral response to stressors. This can be measured by an increase in blood cortisol levels that peaks after 15-30 min and then slowly declines after termination of the stressor. Cortisol is a catabolic steroid hormone that activates energy metabolism in various tissues and acts as a negative regulator on the HPA axis.<sup>42</sup>

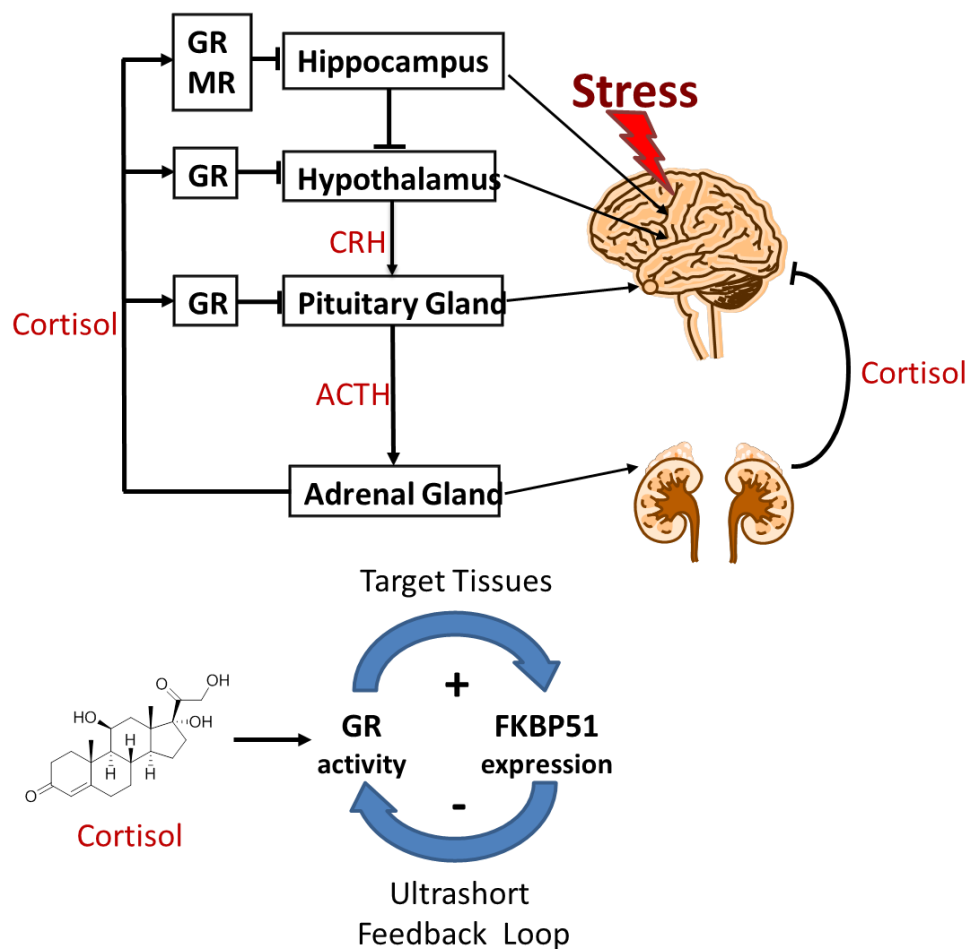


**Fig. 5:** Hypothalamus-pituitary-adrenal axis with hormone regulation cascades

Upon stress the hypothalamus secretes corticotropin releasing hormone (CRH) which induces the production of adrenocorticotropic hormone (ACTH) in the pituitary gland. ACTH in turn increases the release of cortisol in the adrenal gland into the blood. Cortisol is binding to the GR and MR which in turn inhibit the further release of CRH and ACTH thereby maintaining homeostasis of the HPA axis. Additionally, an ultrashort feedback loop is thought to be present at the cellular level. Activated GR

increases the FKBP51 expression which in turn decreases the affinity of the GR for cortisol. Malfunctions in these negative feedback loops are thought to be a cause for an inappropriate reaction of the HPA axis to stress which is often observed in depressive patients.

FKBP51 is a known negative modulator of GR activity. Its physiological relevance was supported by findings in squirrel monkeys which show an increased blood cortisol level associated to decreased GR activity and an overexpression of the more potent squirrel monkey FKBP51.<sup>43, 44</sup> These findings initiated human genetic studies on FKBP51 in major depression. In these studies identified single nucleotide polymorphisms in the FKBP51 encoding gene were associated with the response to antidepressants and with more lifetime depressive episodes.<sup>45</sup> Similar studies followed that confirmed these findings<sup>46, 47</sup> and found gender-specific effects.<sup>47, 48</sup> FKBP51 genetic variants could also be linked to bipolar disorders<sup>48</sup> and significant associations were also found to suicidal events.<sup>49-52</sup> Polymorphisms in the FKBP51 encoding gene also influence the recovery from psychosocial stress in healthy individuals<sup>53</sup>. Another link could be observed from FKBP51 gene variants to peritraumatic dissociation<sup>54</sup> which is an important risk factor for development of a PTSD.<sup>55</sup> The connection to PTSD was also found in other studies.<sup>56</sup> All these findings clearly show that FKBP51 contributes to the etiology of stress-related psychiatric disorders.

### 1.2.5 Cancer and cell proliferation

FKBP51 is up-regulated by androgens (natural: dehydrotestosterone, synthetic: R1881) which made it an interesting target for androgen dependent cancer types. Indeed, FKBP51 has consistently been reported to be up-regulated in human prostate cancer cells.<sup>57</sup> FKBP51 was also found to be up-regulated in prostatic hyperplasia.<sup>58</sup> Further FKBP51 was shown to promote the assembly of the Hsp90 chaperone complex and thereby regulates androgen receptor signaling in prostate cancer cells.<sup>59, 60</sup> However, the unanticipated potentiation of AR by FKBP51 is a very special case because in all other reported studies FKBP51 is a negative regulator of SHR. Although, this effect was not seen in all reported studies and seems to be cell-type dependent.<sup>61</sup> The FKBP unselective ligand FK506 was shown to inhibit cell growth after androgen stimulation in a new prostate cancer type where FKBP51 and FKBP52 are overexpressed.

It was demonstrated that FKBP51 suppresses the proliferation of colorectal adenocarcinoma, possibly due to its deactivating effect on glucocorticoid receptors<sup>62</sup>. Following dexamethasone treatment myeloma cells show prior cell death up-regulation of FKBP51. This could be exploited to enhance the myeloma killing effect of dexamethasone in future<sup>63</sup>. By an siRNA approach a link of FKBP51 to drug-induced NF- $\kappa$ B activation in human acute lymphoblastic leukemia could be shown.

This was supported by inhibition using rapamycin<sup>64</sup>. In a recent study the role of FKBP51 in melanocyte malignancy was outlined<sup>65</sup>. In a different cell line Pei and coworkers were able to identify FKBP51 as a negative regulator of the Akt pathway by serving as a scaffolding protein for PHLPP. A reduced expression of FKBP51 in certain cancer types could be correlated with increased AKT phosphorylation which resulted in a reduced cell sensitivity to chemotherapeutics<sup>66</sup>.

Much less is known about the implications of FKBP52 in cancer but recently it could be shown that prevention of hormone-induced dissociation of the Hsp90-FKBP52-AR complex results in inhibition of androgen-stimulated prostate cancer cell proliferation<sup>67</sup>.

Due to their modulating actions on steroid hormone receptors and their implications in the according diseases, FKBP51 and FKBP52 represent promising drug targets for anti-cancer therapy.

### 1.2.6 Immune function

FKBPs also play a role in immune function and inflammation. The best known effect of FKBP51 is their ability to form ternary complexes with the immunosuppressive drugs FK506 and rapamycin (see **Chapter 1.1**). Besides these prominent immunosuppressive effects various other implications were published during the last years. Recent studies showed FKBP51 to be up-regulated in CD34+ bone marrow cells in patients with rheumatoid arthritis.<sup>68, 69</sup> Park and co-workers demonstrated that FKBP51 can modulate NF- $\kappa$ B-dependent gene expression in Newcastle disease virus-infected chickens.<sup>70</sup> Further it was shown that FKBP51 modulates the stability of I $\kappa$ B and the phosphorylation of NF- $\kappa$ B and enhances its DNA binding.<sup>71</sup> A very recent study connects FKBP51 expression with asthma after administration on inhaled corticosteroids.<sup>72</sup> Additionally, in patients suffering from chronic obstructive pulmonary disease an up-regulation of FKBP51 could be observed.<sup>73</sup> FKBP51 plays also a role in endogenous MHC class II-restricted antigen presentation. FK506 was able to inhibit the presentation of endogenous MHC class II-restricted minor histocompatibility antigens in primary dendritic cells (DC) in vitro. This effect could be rescued by RNAi mediated reduction of FKBP51.<sup>74</sup>

### 1.2.7 Effect on neurodegenerative diseases

Besides their role in immunosuppression, FKBP51 have repeatedly been linked to neurodegeneration in several animal models like transient focal cerebral ischemia in rats or in MPTP mouse models of Parkinson's disease.<sup>75, 76</sup> Gold et al. showed in a rat sciatic nerve crush model that the immunosuppressive drug FK506 accelerated nerve (re-)generation.<sup>77</sup> This effect could also be

transferred to human patients receiving hand transplants.<sup>78</sup> FK506 binds unselectively to FKBP proteins and the mediator of the neuroprotective effect could not be elucidated so far. Early research was focused on the most abundant FKBP12 as the main mediator of the neuroprotective effect of FK506. It could be shown that adding FK506 to primary neurons during or after glucose deprivation limited the induced damage. This effect could be reverted by a FKBP12 antibody or the competitive inhibitor rapamycin.<sup>79</sup> Importantly, the use of non-immunosuppressive derivatives of FK506 which are not able to form a ternary complex ruled out a calcineurin-dependent mechanism for the observed neuroprotective activity.<sup>80, 81</sup> In primary hippocampal cell cultures from FKBP12 knockout mice FK506 retained neurotrophic activity, thus devalidating the prototypic FKBP12 as the relevant target in this model. The mitochondrial FKBP38 and the Hsp90 co-chaperone FKBP52 have been suggested as alternative targets<sup>82, 83</sup> (for detailed reviews see<sup>84,85</sup>). Present FKBP ligands that show neuroprotective effects bind unselectively the whole group of FKBP, with most research focused on FKBP12, FKBP38 and FKBP52. Quinta and co-workers could show that neurite outgrowth in mouse N2a cells is favored by FKBP52 over-expression or FKBP51 knock-down, and is impaired by FKBP52 knock-down or FKBP51 over-expression, nicely showing the antagonistic activities of FKBP51 and 52 on neuronal differentiation.<sup>86</sup> FKBP51 and FKBP52 were also found to play a role in tau turnover which is a key phenomenon in Alzheimer's disease.<sup>87, 88</sup>

All these findings suggest that immunophilins and especially the larger homologs FKBP51 and FKBP52 are important for neuronal processes involved in neuroprotection, neuroregeneration and neuronal differentiation. Additionally, because of the antagonistic effects of FKBP51 and FKBP52 in different systems it is particularly important to develop FKBP subtype selective Ligands to dissect the opposing roles of these proteins.

### 1.3 Chemical biology of FKBP ligands

#### 1.3.1 Immunosuppressive FKBP ligands

Since the discovery of FK506 and rapamycin (**Fig. 1**) in the 1990s and the characterization of their immunosuppressive effect a lot of research has been devoted to the improvement of these ligands in terms of side effects, solubility and efficacy. **Fig. 6** shows FK506 and rapamycin analogs that are used in the clinic. The efforts in this field increased even more after the discoveries that rapamycin has beneficial effect on longevity in mice<sup>89</sup>, improves behavioral and cognitive deficits in models of

neurodegeneration like Alzheimer's<sup>90</sup>, Parkinson's<sup>91</sup> and Huntington's disease<sup>92</sup> and in cancers due to misregulated mTOR pathway.<sup>93</sup>

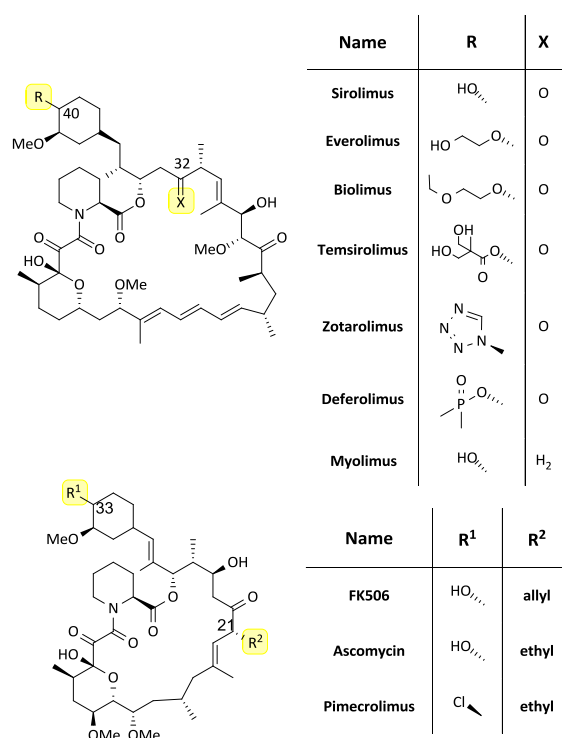
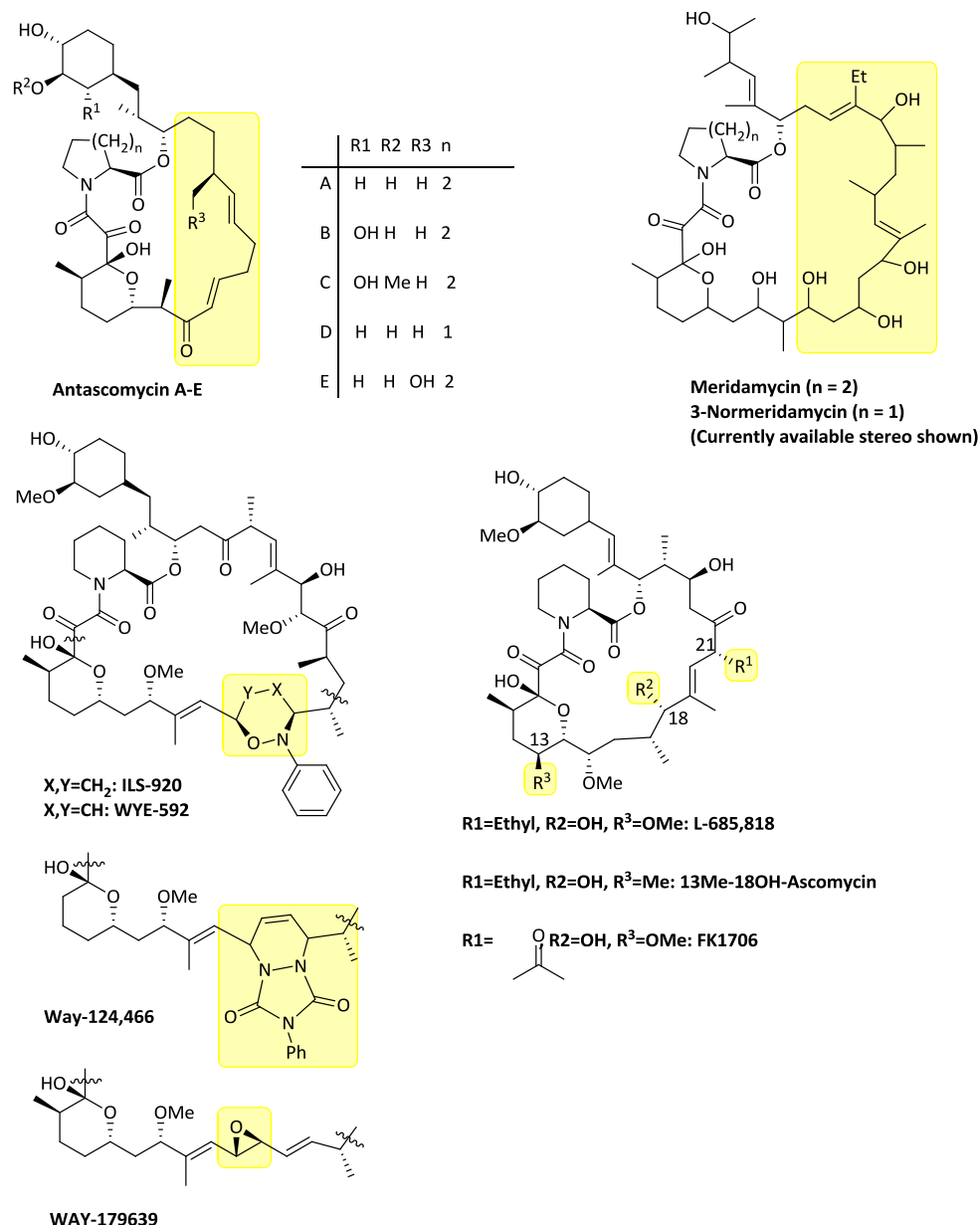


Fig. 6: Clinically used FK506 and rapamycin analogs<sup>84</sup>

### 1.3.2 Non-immunosuppressive FKBP ligands

Up to now almost no drugs are available to treat chronic neurodegenerative diseases. Gold and co-workers found in the early 1990s that besides its immunosuppressive effects FK506 has also neurotrophic activity. These effects were shown in a rat sciatic nerve model.<sup>77, 94</sup> These findings stimulated a whole field to search for non-immunosuppressive immunophilin ligands that still display this neuroprotective effect. These ligands were termed neuroimmunophilin ligands.

Almost 20 years of medicinal chemistry and biochemistry efforts produced a variety of non-immunosuppressive ligands based on the known natural products (**Fig. 7**) where the effector domain is changed. This abolished the binding to calcineurin/ mTOR (e.g., FK1706, meridamycin, normeridamycin, ILS920, Way-124466, Wye-592, L685-818). These ligands demonstrated their effect in animal models of cerebral ischemia<sup>83, 95</sup>, traumatic brain injury<sup>96</sup>, diabetic neuropathy<sup>97</sup>, Parkinson's disease<sup>75, 98, 99</sup>, and various types of physical neuronal injury.<sup>81, 100-102</sup>



**Fig. 7:** Neuroimmunophilin ligands based on biosynthetic or semi-synthetic analogs of FK506 or rapamycin<sup>84</sup>

In addition a vast number of synthetic FKBP ligands have been reported which are based on the pipercolyl/prolyl diketoamide core derived from FK506 and rapamycin. All these compounds lack the effector domain of FK506 and are thus not immunosuppressive. **Fig. 8** shows a collection of reported synthetic neuroimmunophilin ligands that showed neurotrophic activity. VX-10,367 and VX-7109 were patented for stimulating neurite growth in nerve cells and are the most potent FKBP12 ligands known to date.<sup>103</sup> GPI1046 received a lot of attention due to its effect on neurite outgrowth from sensory neuronal cultures with reports of picomolar potency *In vivo*. Additionally GPI-1046 stimulated the regeneration of lesioned sciatic nerve axons.<sup>80, 104</sup> Analogs of GPI1046 were also published to be neurotrophic (GPI1485, JNJ460).<sup>105</sup> However these results were challenged by other

## A. Introduction

groups.<sup>104, 106</sup> Moreover, GPI1046 was also reported to be inactive in PPIase assay by us and others.<sup>85</sup> Our own unpublished data shows that GP1046 is also inactive for the higher homologs FKBP51 and FKBP52.

Most of the studies in the literature are focused on FKBP12 but Gold and coworkers showed that also other proteins can mediate the effect.<sup>82</sup> This was corroborated by using various FK506 analogs that are claimed not to bind FKBP12 (VX-853, V-13,661 and V-13,670, **Fig. 8**).<sup>75, 102</sup> Furthermore the selective FKBP38 inhibitor DM-CHX was shown to be active in an animal model of focal cerebral ischemia.<sup>83</sup>

All these results show that FKBP ligands can have neuroprotective or neurotrophic activities and may be potentially useful in certain neurodegenerative diseases or after neuronal loss. Although a lot of inconsistencies still exist possibly by differences in cellular and animal models or ligands used. Also the relevant targets are still controversially discussed.<sup>85</sup>

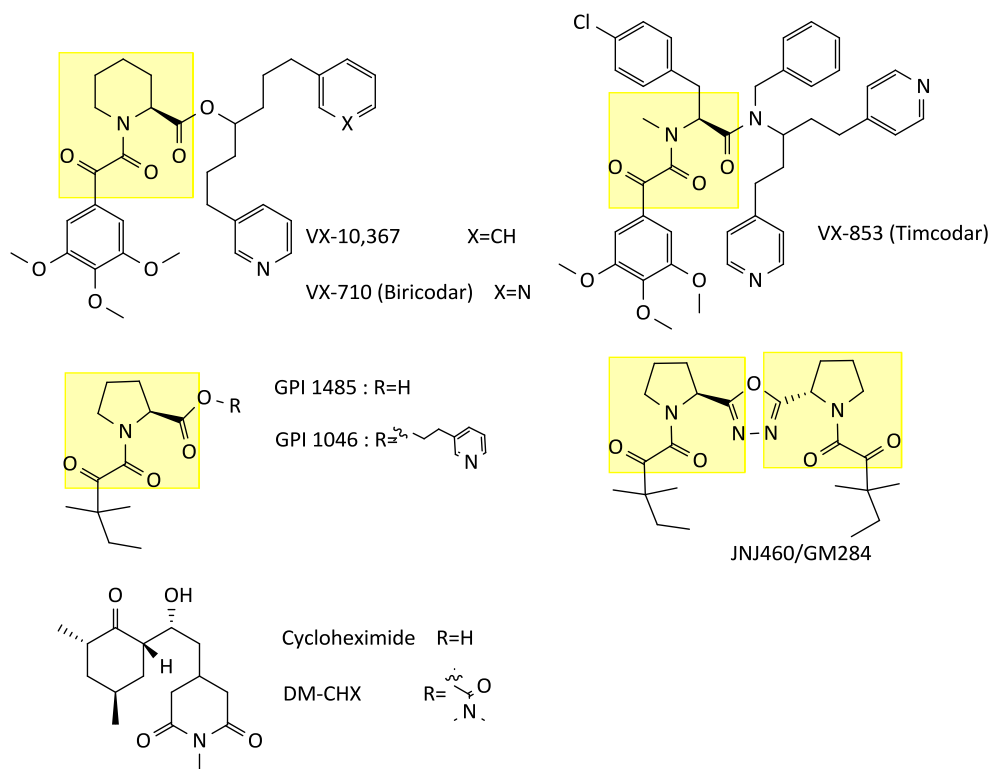


**Fig.8:** Synthetic neuroimmunophilin ligands. The core of FK506 or rapamycin or equivalent groups are shown in yellow<sup>84</sup>

## 1.4 Targeting the PPIase binding pocket of FKBP51 and FKBP52

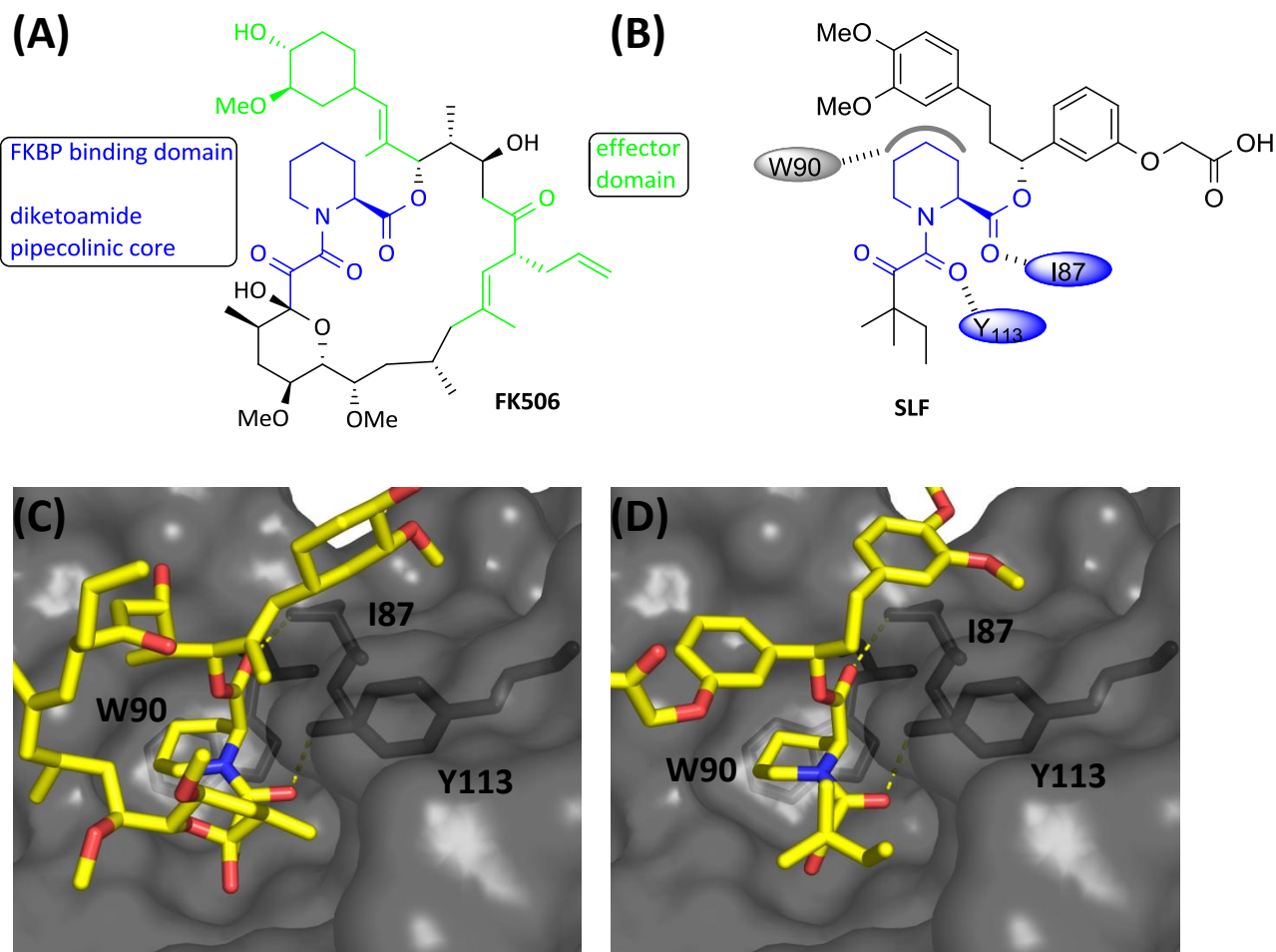


**Fig. 9:** (A) Natural product FKBP ligand FK506, FKBP binding domain (blue), effector domain (green). (B) Synthetic FKBP ligand SLF FKBP binding domain (blue). (C) Co-crystal structure of FK506 and FKBP51. (D) Co-crystal structure of SLF and FKBP51.

As outlined in the previous chapter most of the synthetic immunophilin ligands were designed to bind FKBP12. These ligands were derived from the diketoamide pipercolinic core of FK506 and rapamycin lacking the effector domain and are exemplified by **SLF**<sup>107</sup> (Fig. 9). The pyranose ring was exchanged by a tert-pentyl group which proved to be a good isoster. **SLF** showed binding affinity for FKBP12 in the range of FK506 (low nanomolar) but for the larger homologs FKBP51 and FKBP52 it was substantially less affine (low micromolar).<sup>108</sup> Therefore, the Hausch group solved the co-crystal structure of **SLF** and FKBP51<sup>109</sup> and compared it to the co-crystal structure of FK506 and FKBP51<sup>110</sup> as a starting point for rational ligand design. The amino acids of the binding pocket are almost superimposeable and **SLF** also shows the important hydrogen bonds from I87 to the pipercolate carbonyl group and from Y113 to the amide carbonyl group. W90 forms the bottom of the binding pocket and the pipercolyl ring sits on top of the indole ring. **SLF** was the only ligand in the literature

## A. Introduction

that was described for FKBP51<sup>108</sup> at the start of this thesis while for FKBP52 three ligands were known.<sup>95, 105</sup>

Gopalakrishnan and co-workers performed the first structure activity relationship (SAR) analysis to determine the contributions of individual substructures of **SLF** (**Fig. 10**).<sup>109</sup> The affinities were measured using the fluorescence polarization assay described by Kozany et al.<sup>108</sup> **SLF** bound to FKBP51 with  $\sim 8\mu\text{M}$  and to FKBP52 with  $\sim 10\mu\text{M}$ .

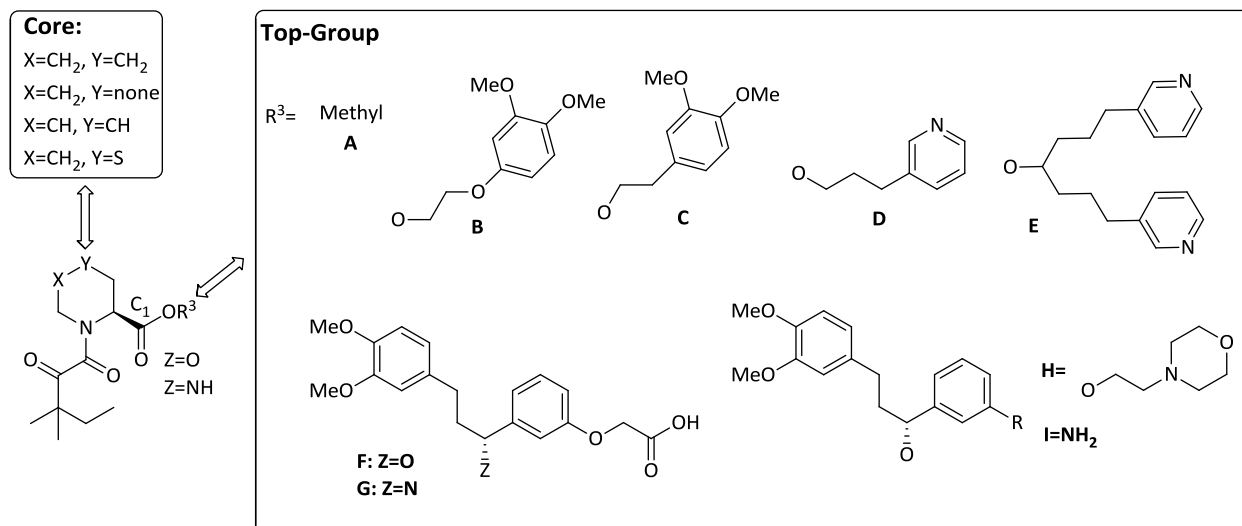


**Fig. 10:** Synthetic analogs of **SLF** for SAR analysis

Replacement of the pipercolyl core by proline or 4,5-dehydropipercolinic acid resulted in a 4-6 fold reduction in potency. The change to thiomorpholine-3-carboxylic acid abolished binding to FKBP51 and FKBP52.

Furthermore they employed different top-groups. The smaller groups (**Fig. 10, A-D**) showed no binding to FKBP51 and FKBP52. To eliminate the free charge at the free acid moiety of **F** and **G** they changed it to morpholine **H** which increased the binding affinity by 2-4 fold compared to **SLF** and a slight preference for FKBP52 could be observed. This trend could also be seen in a sulfonamide series of compounds also published by the Hausch group<sup>111</sup>. They replaced the ester at C1 **G** by an amide which abolished binding to FKBP51 and FKBP52. Finally, they replaced the oxyacetyl group of the **SLF** top-group by an amine **I** which resulted in the best binding compound **1** (**Fig. 11**) of this series. It showed binding to FKBP51 of  $\sim 4\mu\text{M}$  and to FKBP52 of  $\sim 1\mu\text{M}$ .

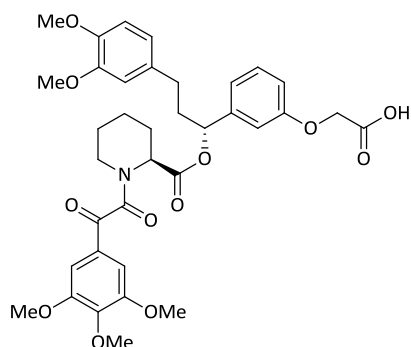
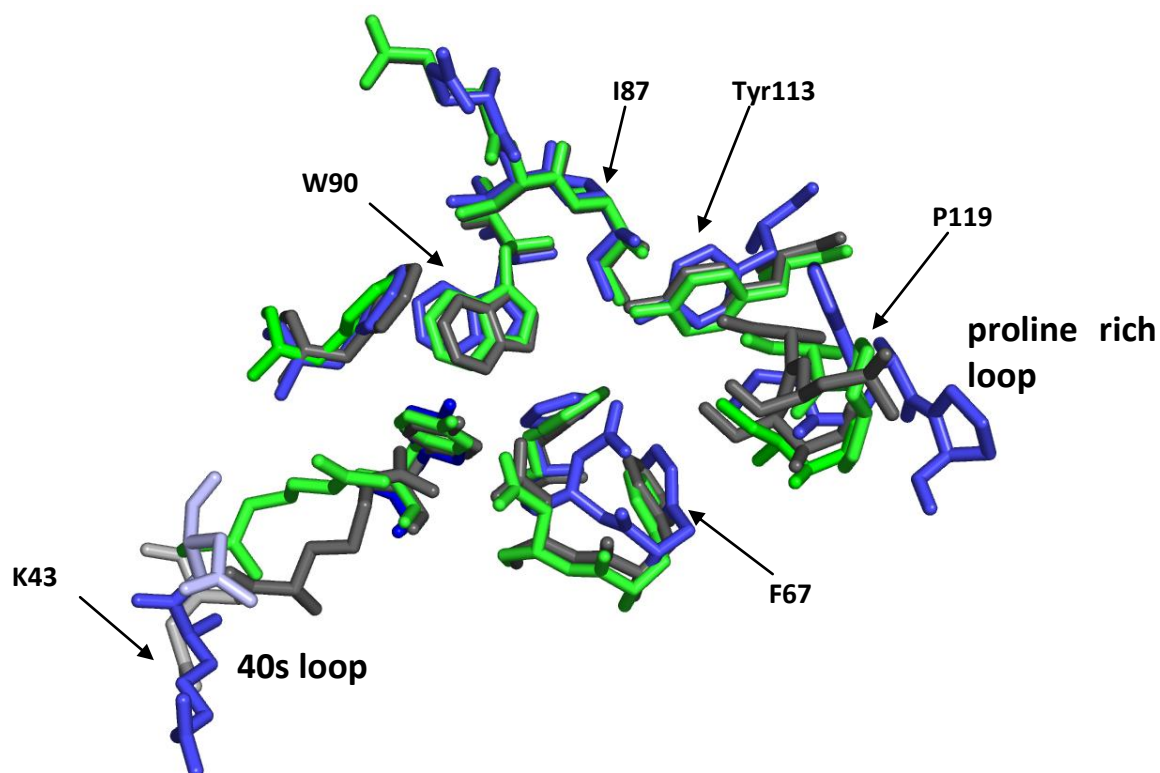


**Fig. 11:** Exchange of tert-pentyl by 3,4,5-trimethoxyphenyl

They continued by replacing the tert-pentyl group with 3,4,5-trimethoxyphenyl (**Fig. 11**) which resulted in a 2 fold decrease in binding for the larger FKBP5s. Additionally two clinically used non-immunosuppressive FK506 analogs were tested on their binding to FKBP51 and FKBP52 (**Fig. 8**). Biricodar showed affinity in the range of SLF  $\sim 8 \mu\text{M}$  whereas Timcodar showed no affinity for any FKBP tested.



<b>FKBP12</b>	26	36	37	42	<b>N<sup>43</sup></b>	46	<b>E<sup>54</sup></b>	55	56	59	82	<b>H<sup>87</sup></b>	<b>P<sup>88</sup></b>	91	99
<b>FKBP51</b>	57	67	68	73	<b>N<sup>74</sup></b>	77	<b>Q<sup>85</sup></b>	86	87	90	113	<b>S<sup>118</sup></b>	<b>L<sup>119</sup></b>	122	130
<b>FKBP52</b>	57	67	68	73	<b>K<sup>74</sup></b>	77	<b>E<sup>85</sup></b>	86	87	90	113	<b>S<sup>118</sup></b>	<b>P<sup>119</sup></b>	122	130

**Fig. 12:** Overlay of the important amino acids of the binding pocket of FKBP12, FKBP51 and FKBP52. The not conserved amino acids are marked in red.

## A. Introduction

The binding pocket of all FKBP is highly conserved. The most prominent changes are found in the 70s loop (amino acids 71-76 of FKBP51/52) and the proline rich loop (amino acids 118-122 of FKBP51/52) (**Fig. 12**). The most important change in the amino acid sequence between FKBP51 and FKBP52 can be found in position 119 in the proline rich loop. A L119P mutation in FKBP51, which introduces the proline found in FKBP52, conferred significant potentiation activity towards steroid hormone receptors, whereas the converse P119L mutation in FKBP52 decreased potentiation.<sup>32</sup>

Thus, they planned to target the proline rich loop with a new series of compounds comprising a substituted cyclohexyl ring (**Fig. 13**) instead of the tert-pentyl. This would be more close to the pyranose ring of FK506.

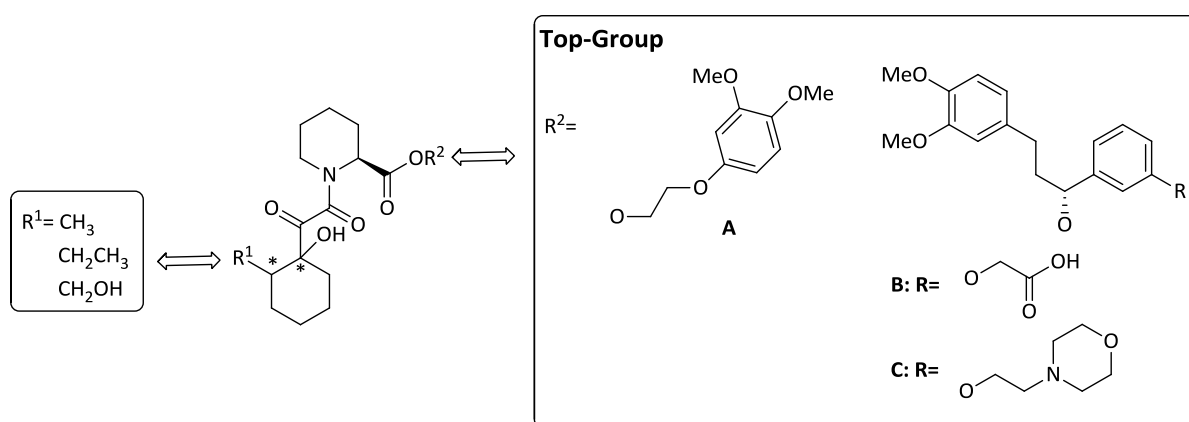


**Fig. 13:** Cyclohexyl substituted ligand series targeting the proline rich loop

The SAR of these compounds and the crystal structures that they published showed that FKBP51 and FKBP52 are tolerant to different stereochemistries at the cyclohexyl substituent. The best binding compounds of this series **C1** and **C2** (**Fig. 14**) show binding affinities of  $1 \mu\text{M}$  to  $4 \mu\text{M}$ .

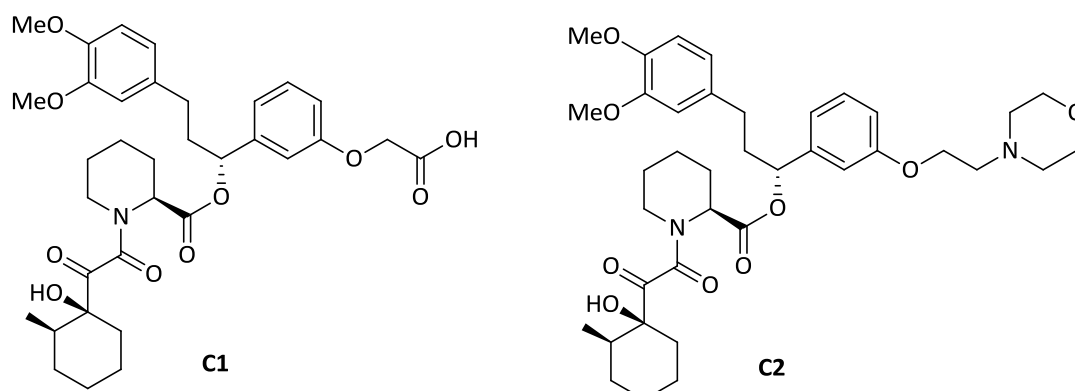


**Fig. 14:** Best binding examples of the substituted cyclohexyl ligand series.

For FKBP12 it was shown that the diketo amide moiety can be bioisosterically exchanged to sulfonamide<sup>112, 113</sup>. To determine the binding of sulfonamide ligands to FKBP51 and FKBP52 Gopalakrishnan et al. developed a solid phase strategy for the synthesis of a focused sulfonamide library<sup>111</sup>.

Out of 36 compounds with aromatic sulfonamides they identified 5 hits for the binding to FKBP51 and FKBP52 which displayed a slight preference for FKBP52. The hits showed moderate binding affinities with  $\sim 10 \mu\text{M}$ .

For the best hits the morpholine top-group (**Fig. 15**) was employed and increased the binding affinity to nanomolar levels for **S1** and to low micromolar for **S2**. Therefore ligand **S1** displays the best known ligand for the large FKBP5s to date. With this strategy they could show that a bioisosteric replacement of the diketo amide to sulfonamide with conservation of the hydrogen bonds leads to potent FKBP51 and FKBP52 inhibitors.

All of the described ligands in this chapter unfortunately show no selectivity between FKBP51 and FKBP52 and at least 10 to 100-fold higher affinity for FKBP12.

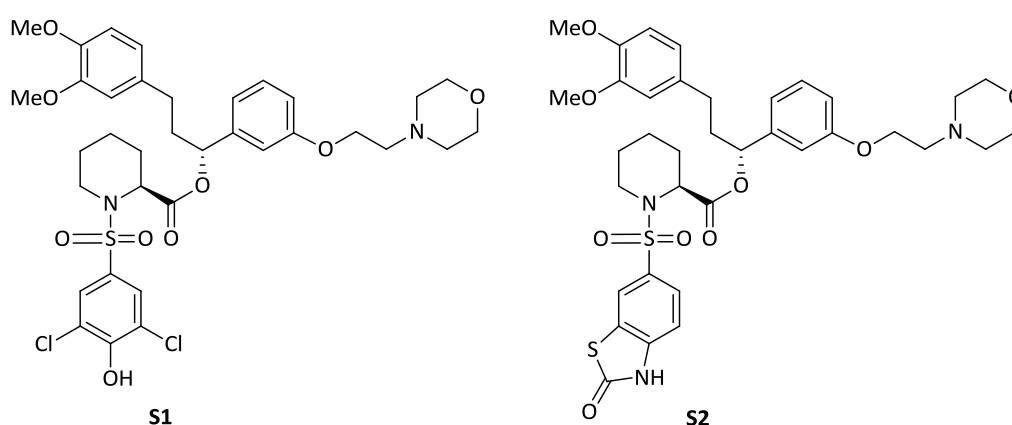


Fig. 15: Top-group substitutions of the best hits

## 1.5 Artificially selective ligands

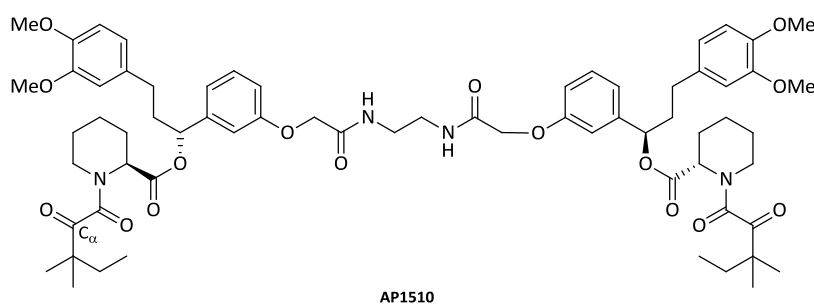
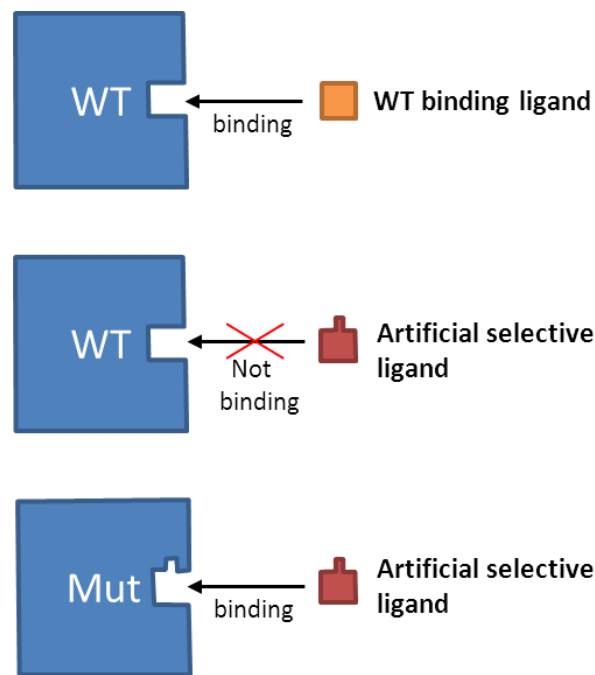


Fig. 16: Chemical inducer of dimerization **AP1510** based on an **SLF** dimer

In the early 1990s Spencer et al.<sup>114</sup> developed chemical inducers of dimerization (CID) to control intracellular signal pathways that are normally controlled by protein-protein interactions. Therefore, they conjugated two FK506 molecules together via a linker and termed it FK1012. This was improved by the development of the bivalent synthetic analog **AP1510**<sup>115</sup> (**Fig. 16**). These CIDs can bind and dimerize proteins of interest which are fused to a FKBP12 “tag” and thereby specifically activate signaling. The major disadvantage is the high affinity to endogenous FKBP12 which are highly expressed. This leads to unwanted heterodimers that interfere with the signaling pathways which are to be observed.



**Fig. 17:** Principle of artificial selective ligands. Bulky modification at the ligand abolishes binding to the wildtype but allows binding to the mutant

To address this selectivity problem the group of Holt<sup>116</sup> used a chemical genomics approach to redesign the FKBP12-ligand interface by engineering a new pocket into the active site. At the same time they synthesized ligands that exploit the newly formed cavity in the binding pocket (**Fig. 17 and Fig. 18**). These ligands showed a substantial decrease in binding affinity to the wildtype but high affinity to the mutant protein. This technique is also called the bump and hole concept.

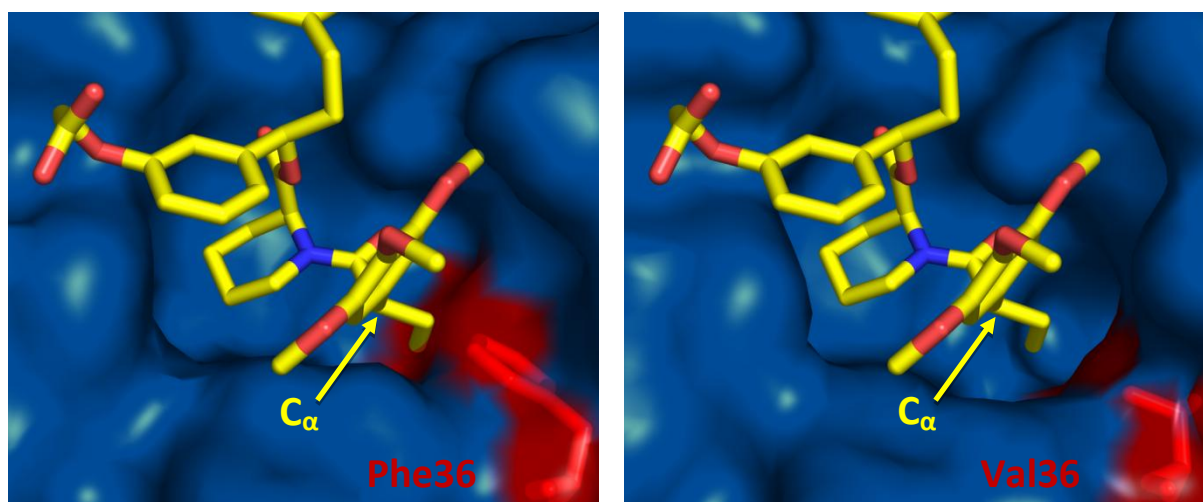


**Fig. 18:** (A) Model of ligand **10** in the crystal structure of FKBP12<sup>WT</sup>. Steric clash of the C<sub>α</sub> substituent with Phe36 (red). (B) Co-crystal structure of **10** with the mutated FKBP12<sup>F36V</sup>. C<sub>α</sub> substituent fits into the new formed cavity.

To achieve that goal they investigated the co-crystal structure of FK506 and FKBP12 and concluded that an exchange of the C<sub>α</sub> carbonyl to larger substituents would sterically clash with either Tyr26 or Phe36 and should abolish or decrease binding. In turn a compensating mutation at one of these amino acids would restore binding (**Fig. 17** and **Fig. 18**). The best ligand (**1**, **Fig. 20**) showed an affinity of 1.8 nM to the F36V mutant of FKBP12 and to the wildtype FKBP12 of 2930 nM. This ligand can differentiate 1,000-fold between WT and was further dimerized via a short linker to form **AP20187** (**Fig. 19**) which was then used to activate Fas signaling in a mouse model of conditional cell ablation<sup>116</sup>.

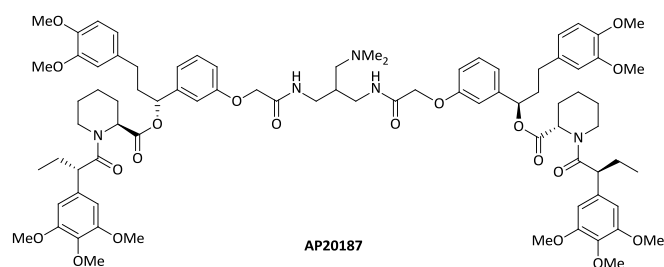


**Fig. 19** Mutant selective FKBP12 CID **AP20187**.

CIDs have been used in a broad range of applications for dimerization of for example membrane receptors: Erythropoietin receptor<sup>117</sup>, PDGF-β-R / Insulin receptor<sup>118</sup>, epithelial growth factor receptors / hepatocyte growth factor / thrombopoietin receptor<sup>119</sup> or for the induced activation of apoptosis by dimerization of the FAS receptor or the dimerization of caspases<sup>115, 120-122</sup>.

Banaszynski et al. from the Wandless group further expanded that field by designing a method to reversibly regulate protein stability in living cells using a synthetic analog termed **Shield-1**<sup>123</sup>

Another very prominent example of the bump and hole strategy is the selective inhibition of mutant kinases shown by Bishop from the lab of Kevan Shokat.<sup>124</sup> With this technique they designed a selective cdc28 inhibitor and showed for the first time the effect of the inhibition of this specific kinase. This technique was also applied to other kinases.<sup>125</sup>

## 2. Aim of the study

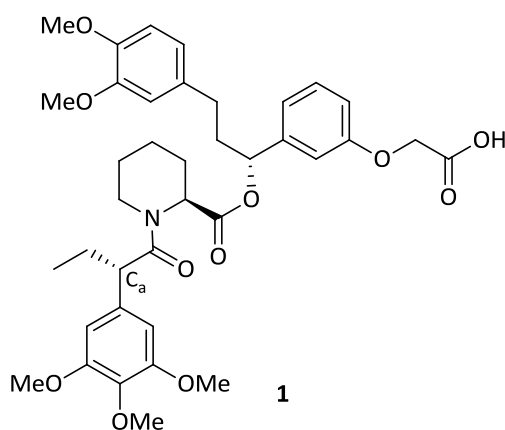


**Fig. 20:** Starting point of the synthetic campaign

FKBP51 is a known negative modulator of glucocorticoid receptor (GR) activity whereas its closest homolog FKBP52 activates the GR.

The natural product FK506, rapamycin and all other reported FKBP ligands show if at all a selectivity for FKBP12 because of their high structural and sequence similarity<sup>84</sup>. Due to the opposing effects of FKBP51 and FKBP52 these ligands are not suited to study the role of these proteins in GR signalling.

The goal of the study was to design and synthesize ligands that solve that selectivity issue of the known FKBP ligands.

We envisioned a chemical genomics tool to artificially design selective ligand mutant pairs for FKBP51 and FKBP52. Therefore structure-based design should be used to synthesize ligands with protruding C<sub>α</sub> substituents and site directed mutagenesis to introduce an enlarged cavity into the active sites of FKBP51 and FKBP52 to compensate for the C<sub>α</sub> substituent. Starting point for the synthesis was the FKBP12<sup>F36V</sup> mutant selective ligand **1**<sup>116</sup> (**Fig. 20**). This chemical genomics tool was intended to be applied to more complex in vitro GR binding assays and cellular assays like GR reporter gene assays to probe the pharmacological tractability of FKBP51 and its potential as a druggable target.

## B. Results and Discussion

### 1. Chemical genomics to selectively address FKBP-sub-types

#### 1.1 Design of FKBP mutant specific engineered (FMSE) ligands

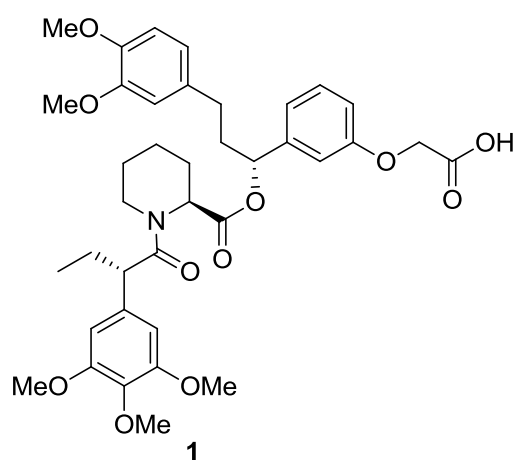
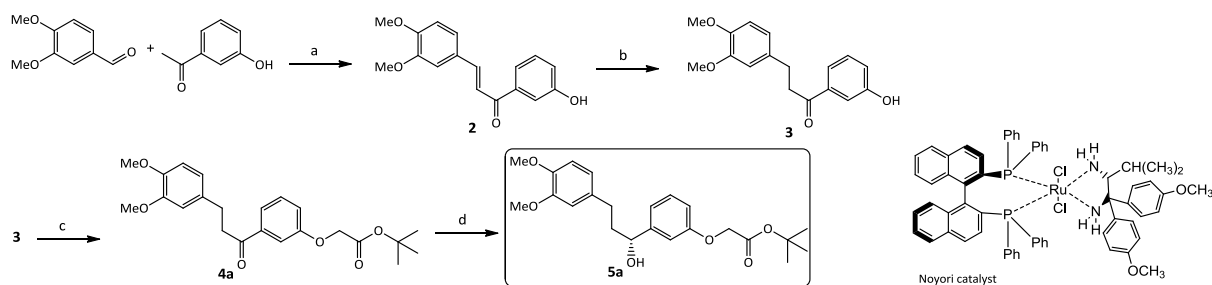


Fig. 21: FKBP mutant-specific engineered ligand 1

All FKBP ligands reported so far, including rapamycin and FK506, show only negligible selectivity for individual FKBP homologs since the residues within the active site are completely conserved both on the sequence and the structural level except for FKBP38.<sup>110</sup> FKBP51 and 52 have been shown to have opposing effects on steroid hormone receptors as well as on neurite outgrowth. FKBP51 in most cases reduces receptor sensitivity, whereas FKBP52 is a positive regulator of SHRs.<sup>31</sup> Likewise in a neuroblastoma cell line FKBP51 suppressed the elongation of neurites whereas FKBP52 enhanced it.<sup>86</sup> Due to these antagonistic effects, these proteins cannot be examined with present FKBP inhibitors. Chemical genomics provides for this case the perfect tool to artificially overcome this selectivity issue by engineered mutant-ligand pairs. A large hydrophobic amino acid in the active site is mutated to a smaller amino acid, which generates a new hole in the binding pocket. In turn, a complementary ligand is engineered with a protruding sidechain that fits into this new cavity. This sidechain performs two tasks; first it should increase the affinity to the mutated protein and second decrease the affinity to the wildtype. In previous work in the Hausch lab phenylalanine 67 was mutated to valine to open a new cavity in the binding pocket. Complementarily, compound **1**



## B. Results and Discussion



**Fig 23:** (a) KOH, EtOH/H<sub>2</sub>O, 80-99%, RT. (b) Pd/C/BaSO<sub>4</sub>, H<sub>2</sub> 30-40 bar, MeOH, 88-95%. (c) K<sub>2</sub>CO<sub>3</sub>, BrCH<sub>2</sub>COOtBu, acetone, 60-75%. (d) Noyori cat, H<sub>2</sub>, i-propanol, 80%, >95% ee.

The pipercolinic acid analogs **7a** and **b** were synthesized from commercially available (*S*)-Pipercolinic respective (*S*)-thiopipercolinic acid using standard Fmoc protection (**Fig. 24**). **7a** and **7b** and the Fmoc- (*S*)-Proline analog **7c** were further esterified with the alcohols **5a** and **b**.

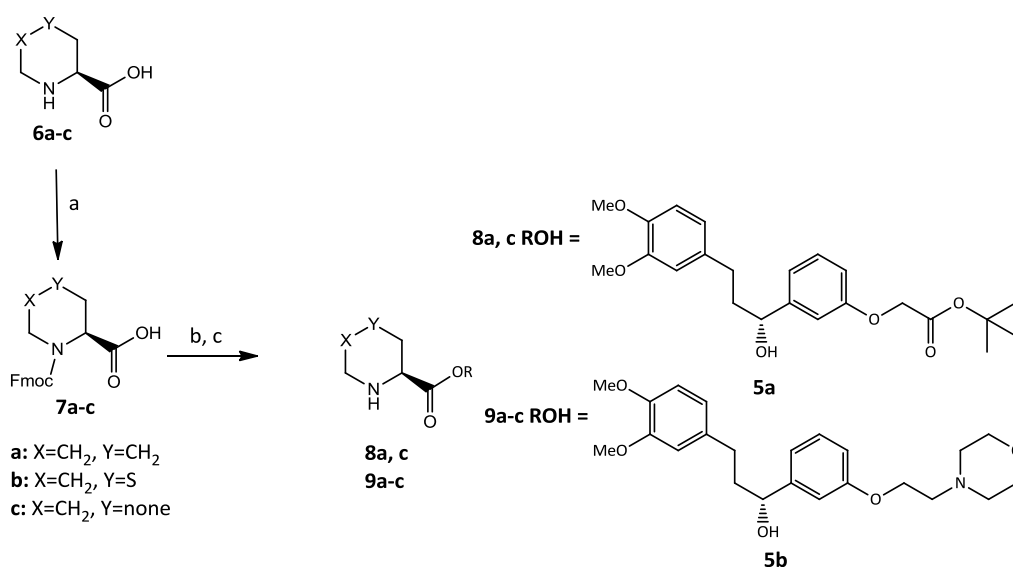


**Fig. 24:** (a) TEA, Fmoc-Cl, DCM, RT, 90-95%. (b) **5a** or **5b** EDC, DCM, RT, 50-70%. (c) 4-Methyl-piperidine, DCM, RT, 70-90%

Based on the FKBP12<sup>F36V</sup> co-crystal structure with compound **1** it is clear that the C<sub>α</sub> substituent has to be in the (*S*)-configuration to fit best into the new hole (**Fig 21**)<sup>107</sup>. First attempts to synthesize different C<sub>α</sub> substituted ligands were performed by non-stereoselective alkylation of commercially available 2-(3,4,5 trimethoxyphenyl)acetic acid using various alkylbromides, and eventually separation of the diastereomers of the final product. Unfortunately, the coupling of **17-19** (**Fig. 25**) to **8** resulted in almost exclusive formation of the unwanted C<sub>α</sub> (*R*)-configuration which was determined by comparison with the HPLC shift of the active isomer of compound **1** and is in line with the low binding affinity of the products 24dia (data not shown). This was subsequently corroborated with the

HPLC shifts of the active compound which were later synthesized in a stereoselective manner (compounds **24-28**).

We envisioned a stereoselective synthesis using the Evans auxiliary (**Fig. 26**) to obtain  $C_\alpha$  substitutions in (*S*)-configuration.<sup>126</sup> We chose allyl because of its larger size compared to ethyl and because the literature shows broad application of allyl halides in stereoselective Evans alkylation.<sup>127, 128</sup> Therefore 2-(3,4,5-trimethoxyphenyl)acetic acid **11** was converted to the stable active pentafluorophenol ester to give **20** which was then coupled with (*S*)-isopropylloxazolidinone to give the imide **21**.

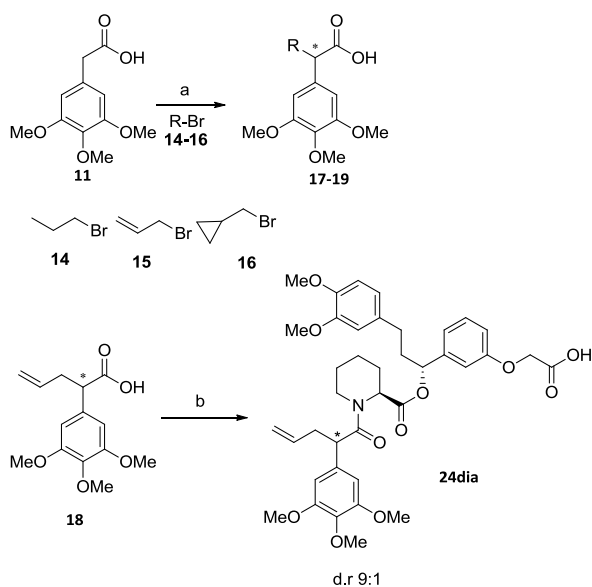


**Fig. 25:** (a) LiHMDS 2.2 eq, R-Br, THF, RT, 60-80% (b) HATU, DIEPA, DCM, 50-60%.

The key step in this synthesis, the stereoselective alkylation was performed after formation of the sodium enolate, which reacted with allyl bromide to give **22** with 60% yield and *dr* >95:5 (determined by HPLC and NMR). The imide was cleaved to give the free acid **23**.

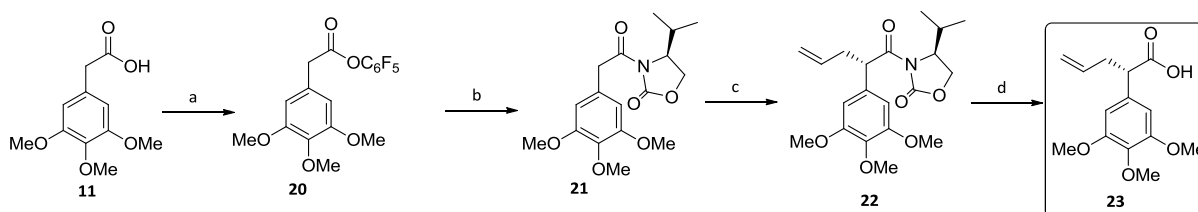


**Fig. 26:** (a) EDC,  $C_6H_5OH$ , DCM, RT 90-95%. (b) BuLi, (*S*)-isopropylloxazolidinone, THF,  $-78^\circ C-0^\circ C$ , 60-80%. (c) NaHMDS, THF, allyl bromide,  $-78^\circ C$ , 50-60%. (d) LiOH,  $H_2O_2$ , THF/ $H_2O$  8:5,  $0^\circ C-RT$ , 60-90%

The allyl substituted ligand series was synthesized by amide bond formation of **8a-c/9a-c** with **23** to give the final compounds **24-28** with a dr of >90:10 (determined by HPLC and NMR). Compounds **18** and **19** were obtained after tert-butyl deprotection with 10% TFA in DCM with 50% yield. The 3,4-dehydropipecolinic ester core **33** was synthesized from (*S*)-allylglycine **29** according to the published procedure of Varray et al.<sup>129</sup> **33** was coupled to **23** and the ester was cleaved to give **34**, which was esterified with the morpholine top group **5b** providing the ligand **35** with dr of >95:5.

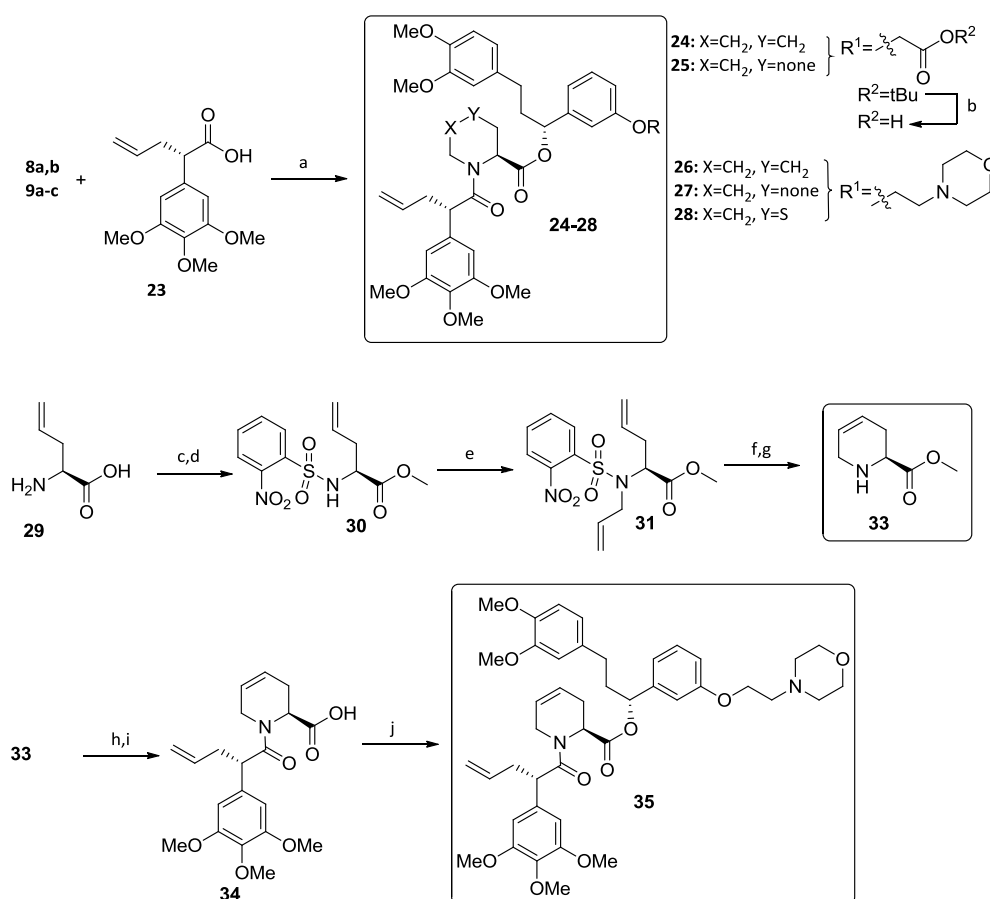
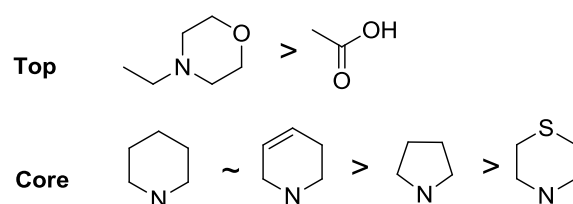


**Fig. 27:** (a) HATU, DIPEA, DCM, RT, 40-50%. (b) TFA, DCM, 0°-RT, 50-60%. (c) *o*-nitrobenzenesulfonyl chloride, TEA, DCM, RT, 60%. (d) TMSCl, MeOH, 0°C-RT, 99%. (e) Allylbromide, K<sub>2</sub>CO<sub>3</sub>, DMF, RT, 83%. (f) RT, Grubbs Cat. II, DCM, reflux, 90%. (g) Thiophenol, Cs<sub>2</sub>CO<sub>2</sub>, CH<sub>3</sub>CN, RT, 81%. (h) HATU, DIPEA, **23**, DCM, RT, 68%. (i) LiOH, THF/H<sub>2</sub>O, RT, 80%. (j) EDC-HCl, DMAP, **5b**, DCM, 0°C-RT, 62%.

### 1.3 Biochemical characterization of the FMSE-ligand-mutant pairs

To determine the IC<sub>50</sub> values of the engineered ligands to the proteins, we performed *in vitro* fluorescence polarization binding assays with the FK1-domains of FKBP51, FKBP52 and the corresponding mutated FK1-domains according to Kozany et al.<sup>108</sup> **Table 1** shows the binding

affinities of the synthesized ligands. We generated a series of C<sub>α</sub> allyl compounds bearing different core and top groups. The final compounds were synthesized either with a hydrophilic top group, containing a free acid moiety for better solubility, or a morpholine group for better cell permeability. Compound **24** was the first synthesized and showed already an improvement compared to the ethyl compound **1**. The affinity for FKBP51<sup>F67V</sup> increased upon exchange of ethyl to allyl to 0.7 μM showing that the artificial cavity in the mutated proteins can accommodate bigger substituents than ethyl. We next exchanged the pipercolinic core to proline to probe the effect of a smaller ring on binding. The IC<sub>50</sub> of the proline derivative **25** increased by 2-fold for the mutated proteins but also 4-fold for the wildtypes. Thus, the selectivity vs the wild type proteins decreased slightly. By exchanging the hydrophilic acid moiety by morpholine a strong increase in binding affinity occurred. Substitution of the free acid of **24** by morpholine yielded **26** and increased the affinity by 12-fold for the wildtype proteins and by almost 100-fold for the mutated proteins. The selectivity of mutated vs wildtype proteins increased to 1000-fold. Encouraged by this effect we synthesized the proline derivative **27**, unfortunately the binding affinity decreased by 3-fold for the wildtype, and 10-fold for the mutant. This is in contrast to proline compound **25** with the free acid top group where this proline modification resulted in an increase of affinity compared to pipercolate. The selectivity of **27** also decreased slightly. We further substituted the core by thiomorpholine **28**, which caused a drop of 10-fold in affinity whereas exchange to the 3,4-dehydropipercolinic core **35** showed affinity in the range of **26**. **Tab. 1** shows the SAR of the allyl series.



**Tab. 1:** SAR of the allyl series for FKBP51F67V

**Fig. 28** shows the binding curves of the two best compounds **26** and **35**. Compound **26** was kindly synthesized by the LDC based on our results as a control for further experiments.

In summary, we improved the binding affinity to the mutated proteins by 1000-fold compared to compound **1** while maintaining 500 to 1000-fold selectivity for mutated FKBP51/52 over wildtype proteins. These selective ligand-mutant pairs can be used in a model system created by chemical genomics to examine the selective inhibition of FKBP51 and 52. This system can be used in different cellular assays (e.g. reporter gene, neurite outgrowth assay) where FKBP mutant proteins can be

overexpressed. The best ligands bind with  $IC_{50}$  in the low nanomolar range, which enables for specific inhibition of mutated protein over endogenous proteins.

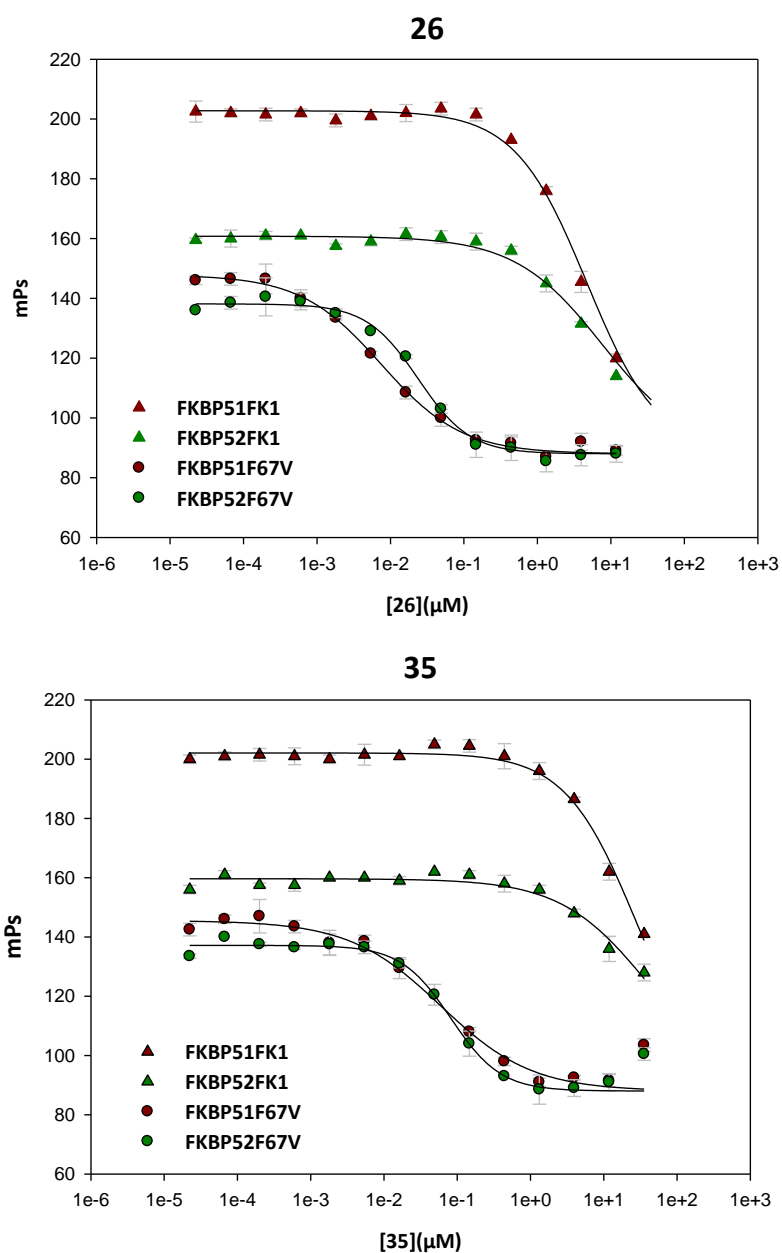
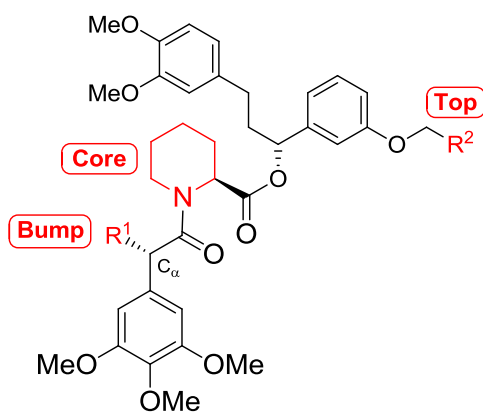


**Fig.28:** Biochemical characterization of artificially selective FKBP mutant-ligand pairs with **26** and **35**. Purified FK1-domains of 51wt (2 nM), 52wt (2 nM), 51mut (2 nM) and 52mut (10 nM) were measured in a fluorescence polarization binding assay by titrating **26** or **35** using 3nM of compound **F2** (Chapter 4.1) as a tracer<sup>108</sup>.



Name	Core	R <sup>2</sup>	R <sup>1</sup>	51 <sup>WT</sup>	51 <sup>F67V</sup>	52 <sup>WT</sup>	52 <sup>F67V</sup>
1				>70	1.8 ± 3.1	>100 <sup>(a)</sup>	22.6 ± 1.5
24				60.9 ± 16.1	0.7 ± 0.1	>100 <sup>(a)</sup>	2.2 ± 0.2
25 <sup>(b)</sup>				16.1 ± 3.8	0.3 ± 0.1	47.3 ± 16.5	0.7 ± 0.2
26 <sup>(b)</sup>				4.7 ± 1.4	<b>0.01 ± 0.001</b>	7.7 ± 5.8	0.024 ± 0.003
27				>15	<b>0.09 ± 0.05</b>	2.87 ± 1.10	0.16 ± 0.08
28				>60 <sup>(a)</sup>	0.47 ± 0.14	>60 <sup>(a)</sup>	0.6 ± 0.1
35				>30 <sup>(a)</sup>	<b>0.06 ± 0.03</b>	>40 <sup>(a)</sup>	0.08 ± 0.02

**Tab.2:** General structure of the ligands, and binding affinities (IC<sub>50</sub>) in μM. Purified FK1-domains of 51wt (2 nM), 52wt (2 nM), 51mut (2 nM) and 52mut (10 nM) were measured in a fluorescence polarization binding assay by titrating the compounds using 3nM of compound **F2** (Chapter 4.1) as a tracer<sup>108</sup>. (a) Solubility limit. (b) Compounds were provided by a collaboration with the Lead Discovery Center GmbH (LDC)

## 1.4 Effect of selective inhibition of mutated FKBP51 and 52 on neurite outgrowth in N2a neuroblastoma cells

FK506 analogs have repeatedly shown neurotrophic or neuroregenerative effects in cellular and animal models. However, due to overlapping functions of FK506-binding proteins and the lack of selectivity of the ligands it proved difficult so far to exactly pinpoint the relevant FKBP. Some FKBP5s show negative and others positive effects on neuronal function.

To pharmacologically probe the role of FKBP51 and FKBP52 on neuronal function we used N2a cells as a cellular model for the differentiation of neuronal progenitor cells. Quinta et al. had previously shown that FKBP51 and FKBP52 have opposing effects in this model.<sup>86</sup> Similar effects were observed in our system. Overexpressing FKBP51 inhibited neurite outgrowth (**Fig. 29B**, lanes 3 in **Figs. 29C/D**) compared to control transfection. In contrast, overexpression of FKBP52 enhanced the outgrowth of neurites compared to control (**Fig. 30**, lane 3). Fortunately, the neurite outgrowth-suppressing or stimulating effects of FKBP51 or FKBP52 were not affected by the point mutation F67V in the active site.

As we were especially interested in whether FKBP51 can be pharmacologically targeted, we tested the effect of the selective inhibitors on FKBP-modulated neurite outgrowth. Transfection with empty vector pRk5 displays the basal neurite length after starvation (**Fig. 29A**, **Fig. 29D/E**, lane 1). The addition of **26** and **35** only marginally affected neurite outgrowth under these conditions. Likewise they did not revert the neurite outgrowth suppression by overexpressed wildtype FKBP51 (**Fig 29D/E**, lane 4), to which they bind with 1000-fold less affinity than to the mutant FKBP. However, the neurite outgrowth suppressed by the mutated FKBP51 was almost completely rescued by the mutant-selective inhibitors **35** (**Fig. 29C**, **Fig. 29D**, lane 6). Almost identical results were obtained with the ligand **26** (**Fig. 29E**, lane 6).

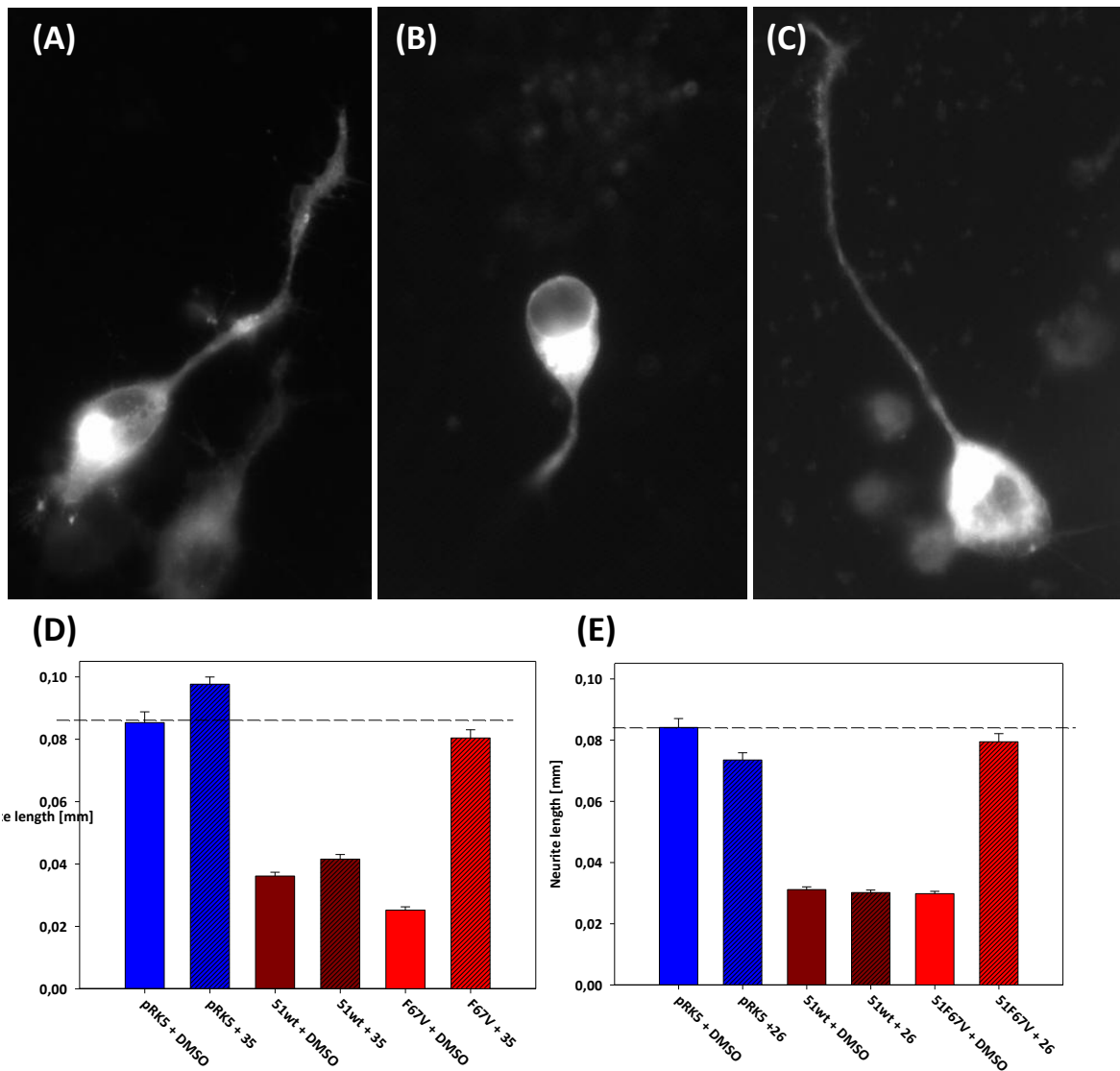


**Fig. 29:** Rescue of neurite outgrowth assay in N2a-cells overexpressing FKBP51 by artificially selective ligand **26** and **35**. (A) Transfection control vector prk5 and application of DMSO (B) Overexpression of FKBP51F67V and application of DMSO (C) Overexpression of FKBP51F67V and application of 20  $\mu$ M Compound **35**. (D) and (E) Each bar represents the mean of the neurite length (in mm) of 20-30 cells after the indicated treatment.

Next we tested the consequence of selective inhibition of FKBP52 on neurite outgrowth. Again, **35** did not inhibit the basal neurite outgrowth or the enhancement induced by the wildtype FKBP52 (**Fig. 30**, lane 2 and 4). In contrast, inhibition of the mutated FKBP52 abolished the neurite stimulation completely even below basal level (**Fig. 30**, lane 6).

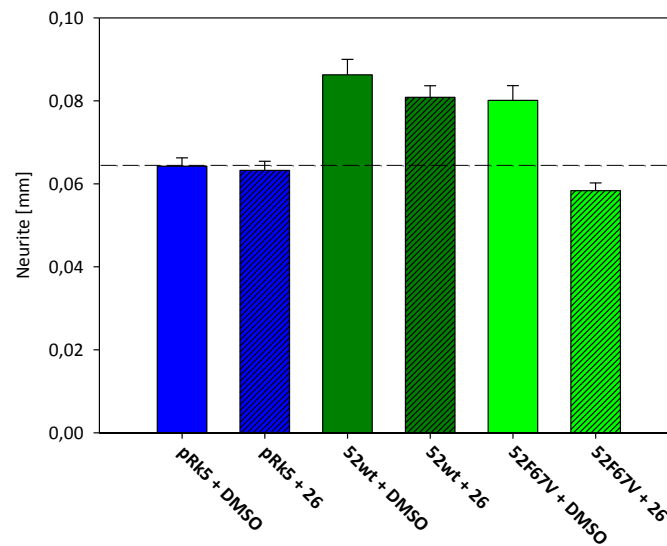


**Fig. 30:** Suppression of FKBP52 enhanced neurite outgrowth in N2a-cells overexpressing FKBP52 by artificially selective ligand **35**.

The previous results strongly suggested inhibition of FKBP51 and FKBP52 to have opposite effects. To unambiguously prove this we co-overexpressed FKBP51 (wildtype and mutant) and FKBP52 (wildtype and mutant) in all four possible combinations and monitored the effects of the mutant-selective ligand **35** on neurite outgrowth behavior (**Fig. 31**). Simultaneous overexpression of FKBP51 and 52 wildtype and mutants in all combinations (**Fig. 31**, lane 3, 5, 7 and 9) resulted in neurite length comparable with basal conditions (overexpression of control vector) which can be attributed to the opposing effects of FKBP51 and FKBP52. As expected, **35** had no effect on basal conditions, and only a small effect on cells overexpressing wildtype FKBP51 and wildtype FKBP52 (**Fig. 31**, lane 2, 4). Likewise, inhibition of mutated FKBP52 coexpressed with wildtype FKBP51 by **35** caused a shortening of the neurites due to selective, blocking the positive effect of FKBP52 while sparing the suppressing effect of FKBP51 (**Fig. 31**, lane 7 and 8). Selective inhibition of mutated FKBP51 co-expressed with wildtype FKBP52 by **35** lead to neurite outgrowth in line with leaving the positive effect of FKBP52 (**Fig. 31**, lane 5 and 6). Importantly inhibiting the two mutated proteins at the same time resulted in neurites with the same length as the corresponding DMSO control (**Fig 31** lane 10) consistent with a mutually canceling effect of simultaneously inhibiting both FKBP5s. Taken together, in these model experiments with artificially selective ligand mutant pairs, we unambiguously showed that FKBP inhibiting ligands can have neurite outgrowth-stimulating or suppressing effects, depending whether FKBP51 or FKBP52 is more relevant in the system.

In summary, we for the first time demonstrated activity of FKBP51 ligands in a relevant cellular model thereby providing the first experimental proof of concept for the feasibility to

pharmacologically target FKBP51. We showed in a cell model of neuronal differentiation, that specific inhibition of overexpressed FKBP51 restores neurite outgrowth whereas specific inhibition of overexpressed FKBP52 has the opposite effect. We therefore propose FKBP51-selective ligands as neuroprotective agents and that selectivity vs. FKBP52 will be crucial for a therapeutic benefit. This could be helpful for neurodegenerative diseases like Alzheimer's and Parkinson's disease but also during stress or in depression, which are characterized by neural loss or atrophy.

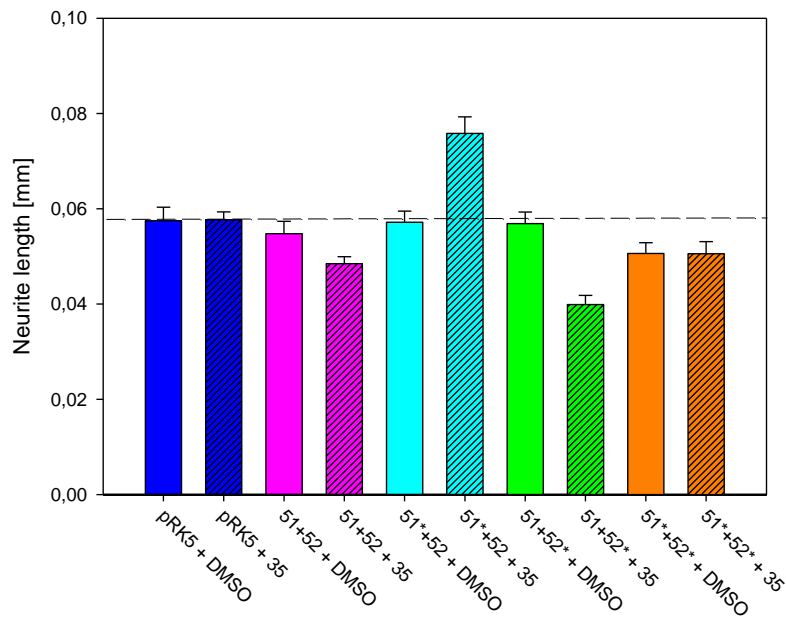


**Fig. 31:** Co-expression of FKBP51 and 52 and engineered sensitive mutants thereof. Either addition of DMSO or inhibition by **35**.

\* indicates mutated proteins

## 2. Solving the selectivity issue by an induced fit mechanism

### 2.1 Induced fit as a basis for selectivity

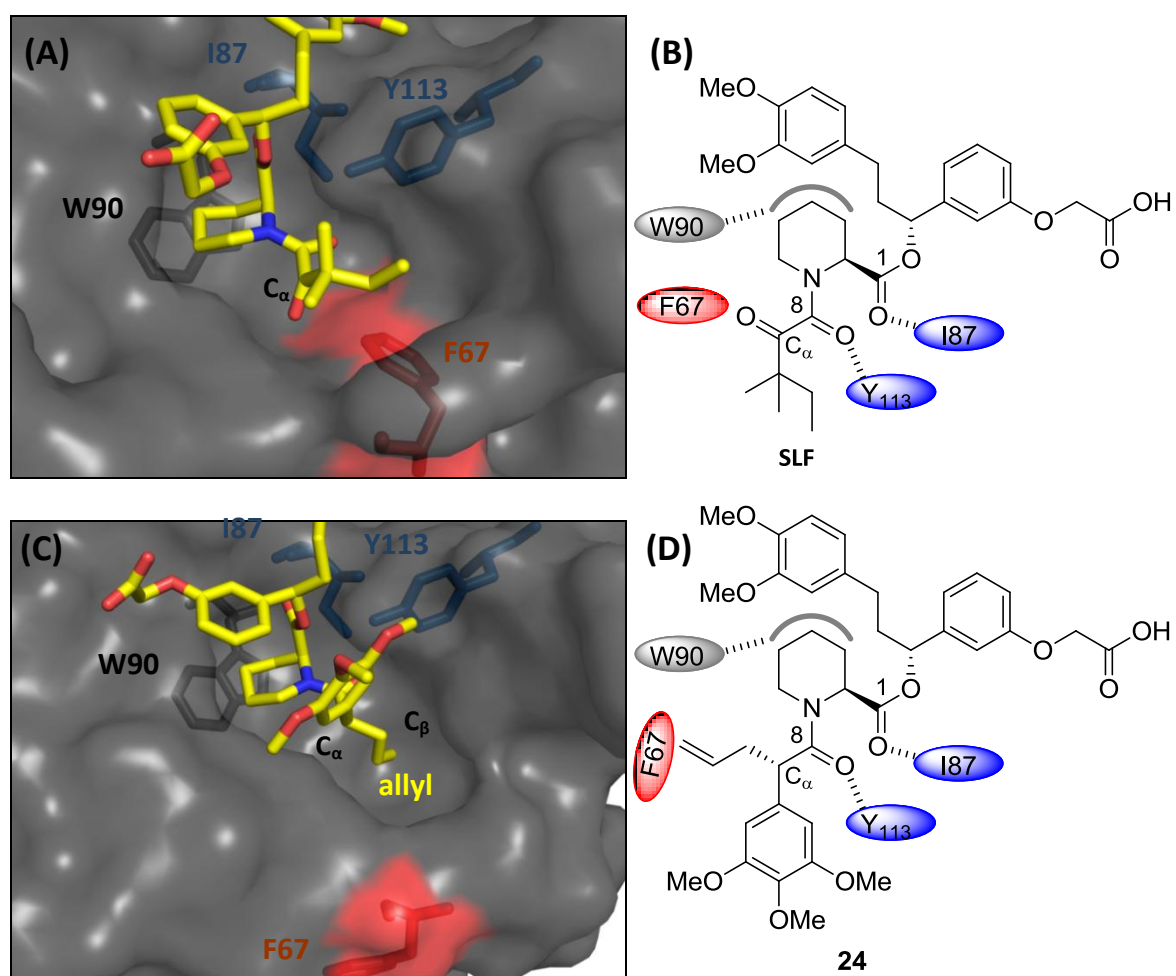


**Fig 32:** (A) Co-crystalstructure of **SLF** and FKBP51FK1. (B) Structure of IF63. (C) Co-crystalstructure of **24** and FKBP51FK1. For better visibility of the binding pocket K121 was removed from the crystal structures) highlighted are in blue the important hydrogen bonds from I87 to the C1 carbonyl group and from Y113 to the pipercolinic amide carbonyl C8. Further W90 is shown which displays the bottom of the binding pocket. F67 that is displaced to accommodate **24** is indicated in red.

Our model system (**chapter 1.3**) showed that selectivity between FKBP51 and FKBP52 is necessary. However, the design of wildtype selective ligands for the wildtype proteins is extremely challenging due to the structural similarity of the binding pocket of the different FKBP subtypes. All ligands tested before showed almost the same binding affinity for FKBP51 and 52.

In the assay results of our model system we noticed a slight preference of some of the C $\alpha$ -substituted compounds for FKBP51 (**1**, **24**, **25**, **26**, **Tab. 2**). This was unexpected as the C $\alpha$ -allyl group would clash

with F67 in a binding mode typical for FKBP ligands (Fig. 32A, 34A). Intrigued by this finding we solved the co-crystal structures of **24** at a resolution of 1.4 Å and compared it with the co-crystal structure of the unselective FKBP ligand **SLF** with FKBP51 (Fig. 32A). This revealed that compound **24** induces a conformational change in the binding pocket of FKBP51 that allows the protruding C<sub>α</sub> allyl group to fit into a newly formed hole. More precisely, the C<sub>α</sub> allyl substituent of **24** displaces F67 (Fig. 32C) which flips out of the binding pocket to form a new hole in the binding pocket. Fig. 33 shows the superposition of the co-crystal structures of FKBP51FK1/**24** and FKBP51FK1/**SLF**. The major changes are found in the 60s and 70s loop which together with the proline rich loop contains the most important structural differences between the FK1 domains of FKBP51 and FKBP52. The 40s and the proline rich loop are known to be the most flexible part of the protein.<sup>109, 110</sup>

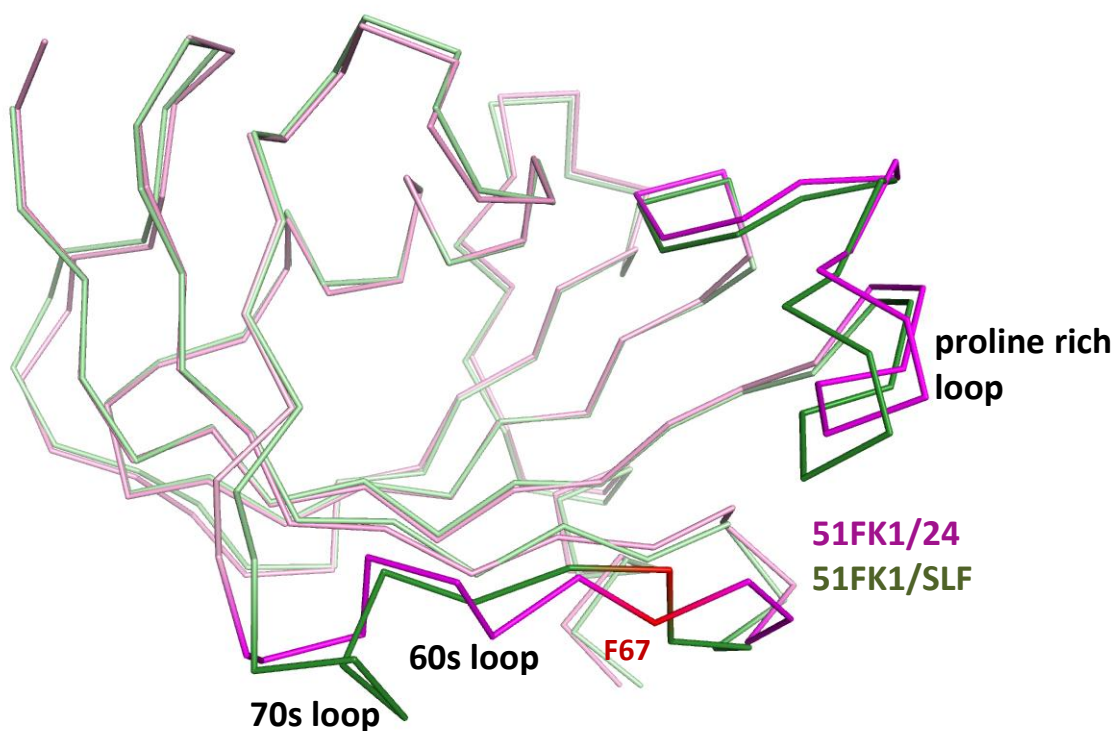


**Fig. 33:** Superposition of the backbone traces of the co-crystal structure of FKBP51FK1/**24** (pink) and the co-crystal structure of FKBP51FK1/**SLF** (green).

The most interesting and prominent structural changes are observed in the amino acid sequence from G64 to N74 (GKKFDSSHERN, 60s to 70s loop Fig. 33, Fig. 34). The flip of F67 causes most of the surrounding amino acids to change their conformation. The side chains of K65 and K66 are not defined in the crystal structure, probably due to their flexibility, as they are solvent accessible. No ordered electron density for these amino acids could be observed. Interestingly, D68 almost retains the conformation compared to the co-crystal structure of FKBP51FK1/**SLF** although it is directly

neighboring F67 and it lost its saltbridge to R73, which possibly is replaced by S70. The conformation of S69 stays the same whereas S70 is flipped upwards together with a large conformational change of H71. The orientation of D72 only slightly changes whereas the orientation of R73 and N74 are completely changed.

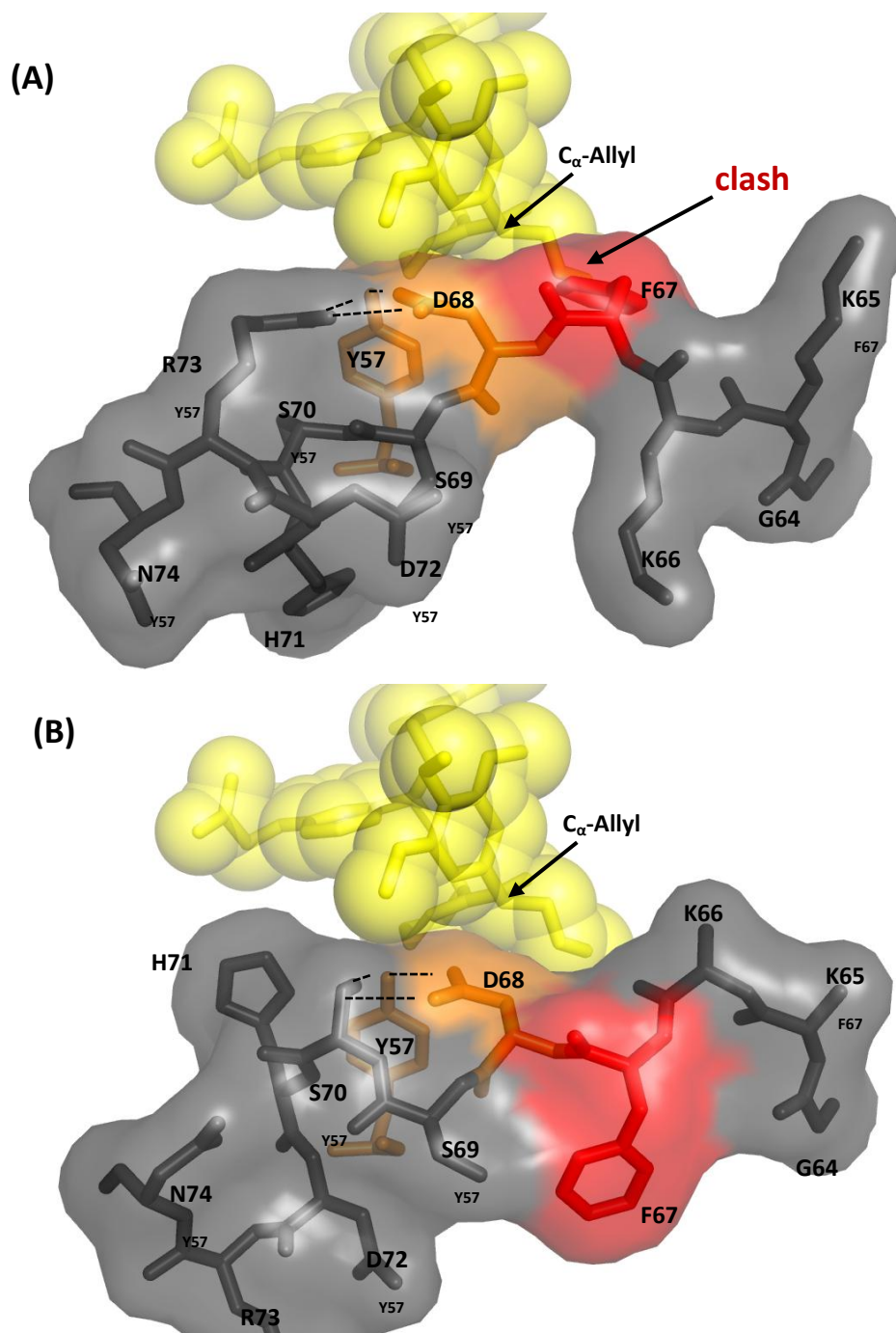


**Fig. 34:** Structural changes of G64 to F67 (60s and 70s) induced by 24. **(A)** 24 modeled into the co-crystal structure of FKBP51FK1/SLF. **(B)** co-crystal structure of FKBP51FK1/24

These extraordinary results provided a structural explanation for the unexpected binding of **24** to FKBP51. We therefore started the synthesis of a series of variously  $C_\alpha$  substituted ligands to further elaborate the scope of this induced fit mechanism.

## 2.2 Synthesis of iFit FKBP51 ligands

The iFit (inducing fit) ligands were synthesized by a similar synthetic route as the FKBP subtype specific engineered ligands.

We synthesized ligands consisting of three main parts the “Core”, the “ $C_\alpha$ -Sub” and the “Top group” (**Fig. 35**). Core structures are either (*S*)-proline or (*S*)-pipercolinic acid. The “Top group” is a complex alcohol or amine, containing one or two substituted phenyl/pyridine rings with an ionizable moiety (acid, morpholine or pyridine) to increase solubility or cell permeability. The “ $C_\alpha$ -Sub” is an alkyl substituent in  $C_\alpha$ -position of the Core with (*S*)-conformation that protrudes into the hydrophobic binding pocket of FKBP proteins and induces the conformational rearrangement. We synthesized  $C_\alpha$  substituents of different sizes ranging from allyl to benzyl to identify the best group for the induced sub-pocket.

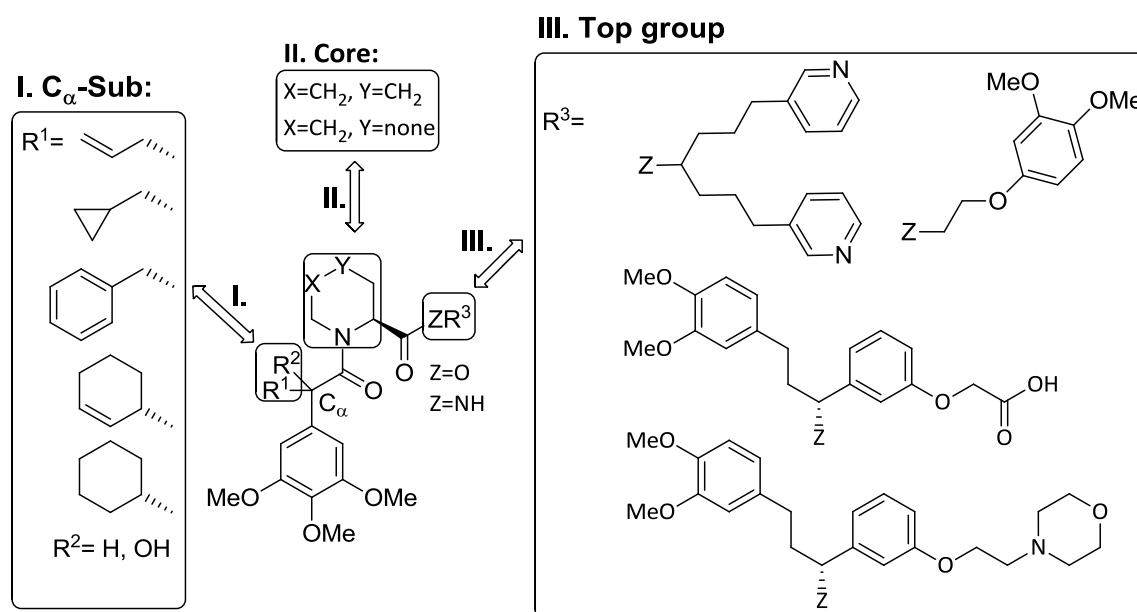


**Fig. 35:** General structure of synthesized iFit ligands

## 2.2.1 Cyclopropylmethyl and benzyl series

### 2.2.1.1 Design and synthesis of C<sub>α</sub> cyclopropylmethyl and benzyl ligands

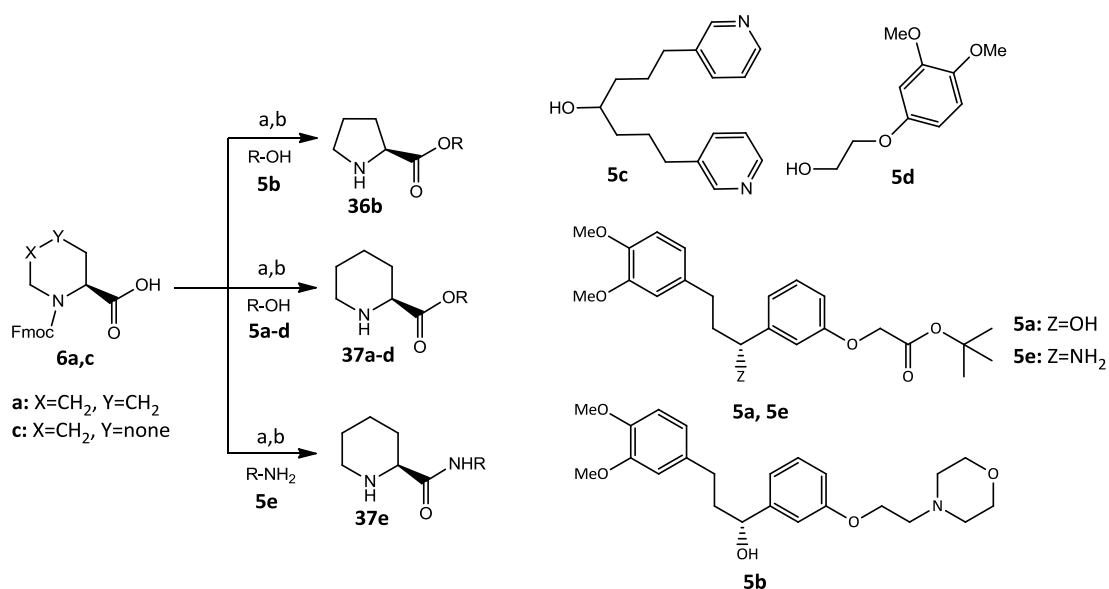


**Fig. 36:** (a) EDC, DCM, RT, 50-70%. (b) 4-Methyl-piperidine, DCM, RT, 70-90%

Fmoc-(S)-pipecolate **6a** and Fmoc-(S)-Proline **6c** were esterified with alcohols **5a-d** and after Fmoc cleavage the Products **36b** and **37a-e** could be obtained with good yields.

We aimed to enlarge the C<sub>α</sub> bump from allyl to cyclopropylmethyl because the co-crystal structure of **24** clearly indicated that a cyclopropyl ring would fit better into the induced sub-pocket than the smaller allyl group. The synthesis of the cyclopropylmethyl substituent under the conditions used for allyl proved to be challenging. The stereoselective alkylation of the Evans imide with cyclopropylmethyl bromide only gave trace amount of the desired product (**Fig. 37**).

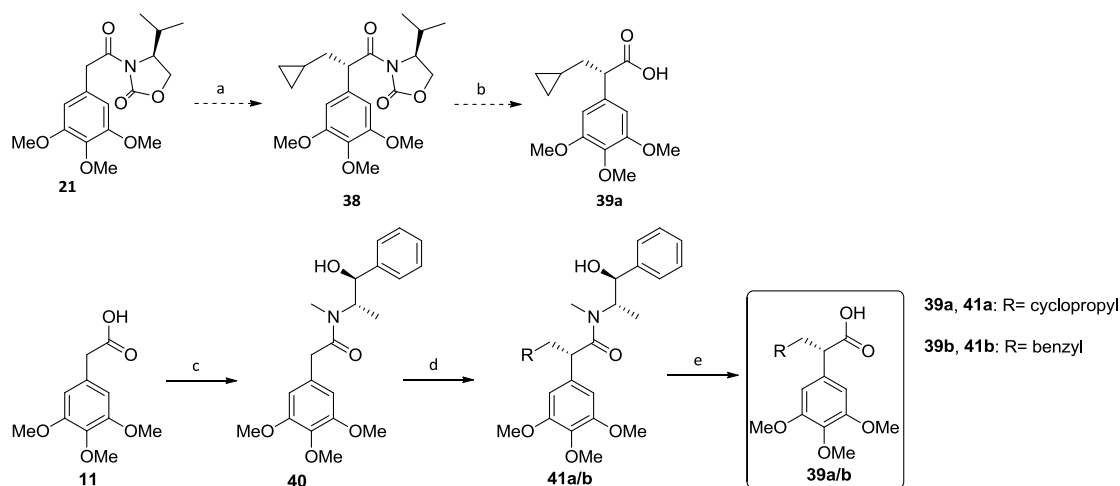


**Fig. 37:** (a) NaHMDS, THF, R-Br,  $-78^{\circ}\text{C}$ , <5%. (b) LiOH,  $\text{H}_2\text{O}_2$ , THF/ $\text{H}_2\text{O}$  8:5,  $0^{\circ}\text{C}$ -RT, (c) EDC, (S),(S)-pseudoephedrine, DCM, RT, 80-90%. (d) LiHMDS, LiCl, cyclopropylmethyl iodide or benzyl bromide, THF,  $-78^{\circ}\text{C}$ - $0^{\circ}\text{C}$ , 40-50%. (e) 4 M  $\text{H}_2\text{SO}_4$ , dioxane,  $0^{\circ}\text{C}$ -reflux, 50-60%.

We concluded that the Evans imide was too deactivated to be properly reacted with non-allylic primary or secondary alkylbromides. We therefore decided to use a more active amide auxiliary for this type of substrate, the Myers pseudoephedrine (**Fig. 37**). This auxiliary shows a higher scope of possible alkylations in the literature.<sup>130</sup> Using the Myers auxiliary the primary cyclopropylmethyl halide could be successfully reacted with moderate yield. Towards this end 2-(3,4,5-trimethoxyphenyl) acetic acid **11** was first coupled with (S),(S)-pseudoephedrine to give **40**. The amide enolate was formed using LiHMDS and was further alkylated with either cyclopropylmethyl bromide or benzyl bromide, to give **41a** and **b**. For the reactions to occur, it proved to be crucial to dry the LiCl at  $150^{\circ}\text{C}$  over night in high vacuum and additionally flame dry it under high vacuum prior use. The acids **39a** and **b** were liberated, using 4 M  $\text{H}_2\text{SO}_4$  in dioxane under reflux.

**39a** and **b** were coupled to **36b**, **37a** and to **37b** by the same conditions using HATU to provide the ligands **42-45** (**Fig. 38**).

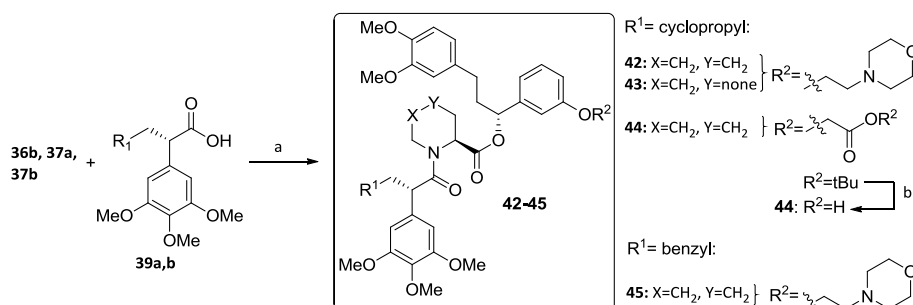


**Fig. 38:** (a) HATU, DIPEA, DCM, RT, 40-50%. (b) TFA, DCM,  $0^{\circ}$ -RT, 50-60%.

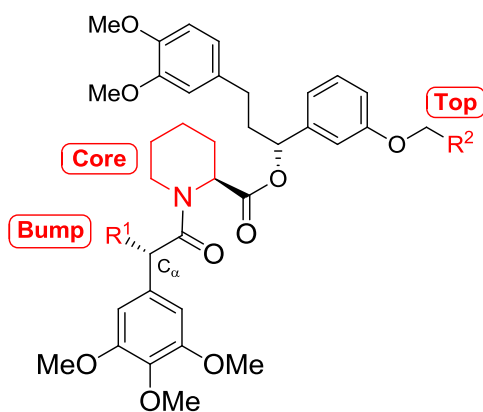
### 2.2.1.2 Biochemical activity of cyclopropylmethyl and benzyl ligands

We tested this series of compounds in our in vitro FP competition assay (**Tab. 3**). From our FKBP subtype-specific engineered ligand screen we knew that changing from a pipercolinic core to proline core and exchange of the free acid moiety to morpholine can increase the binding affinity to the wildtype FKBP in the allyl series (see **Tab. 2**) but at a cost of reduced selectivity. Fortunately, the larger C $\alpha$  substituent cyclopropyl-methyl, restored selectivity and further increased the affinity (**Tab. 3**). Compound **42** binds to FKBP51 with 9.9  $\mu$ M and shows no binding to FKBP52 up to the solubility limits of compound **42**. To explore the limits of the induced cavity, we enlarged the C $\alpha$  substituent from cyclopropylmethyl to benzyl. Compound **45** lost completely its ability to bind to either wildtype FKBP51 or FKBP52, indicating that the protruding phenyl ring is too big to be accommodated by the protein. Another interesting effect is that **42** shows affinity for FKBP12 in the range of FKBP52 which is not the case for all other compound series tested so far. Up to now all ligands show much higher affinity for FKBP12, typically 10-1000 fold.

With increasing from allyl to cyclopropylmethyl we were able to increase the affinity to FKBP51 around 2-fold, increase the selectivity vs FKBP52 at least >10-fold and further discovered the first iFit ligands that show binding to FKBP12 in the same range as to FKBP51 (e.g. compound **42**).

To explore whether the induced fit binding mode observed with **24** also extended to this new series we solved the co-crystal structures of FKBP51FK1 and **27** at a resolution of 1.2 Å and that of **42** with a 2.1 Å resolution (**Fig. 39A, 39C**). The ligands adopt a very similar conformation as **24**, and retain the two important hydrogen bonds to I87 and Y113. The overall architecture of the proteins is mostly superimposable (**Fig. 40A**). The main differences are in the 40s and the proline rich loop. The 40s loop of the **27** and **42** co-crystal structure is superimposable and adopts from S69 to N74 almost the same conformation as the co-crystal structure with **SLF**, interestingly, a flip of these amino acids as observed in the co-crystal structure of **24** does not occur (**Fig. 34A,B**). G64 to D68 is superimposable in the three induced fit crystal structures. The proline rich loop of all co-crystal structures diverge likely due to the flexibility of this region that has been observed earlier.<sup>109, 110</sup>

The proline cores of **24** and **42** adopt two different envelope conformations (**Fig. 40C**) which has an impact on the orientation of the C $_1$  carbonyl to C $\alpha$  segment. Especially the orientation at the C $_1$  and the C $_8$  carbonyl which form the important hydrogen bonds to I87 and Y113 is important. Although the proline core cannot be perfectly overlapped to the pipercolate core, the C $_1$  carbonyl to C $\alpha$  segment of **27** resembles much better the conformation of **24** than the conformations of the closer homolog **42** (**Fig. 40C**).



Name	Core	Top (R)	Bump	51WT	52WT	12WT
24				60.9 ± 16.1	>100	24.0 ± 3.5
25				16.1 ± 3,8	47.3 ± 16,5	0.7 ± 0,2
26				4.7 ± 1.4	7.7 ± 5.8	0.024 ± 0.003
27				>15	2.9 ± 1.1	0.88 ± 0.08
42				9.9 ± 1.8	>100	6.4 ± 1.2
43				22.6 ± 3.8	>100	1.9 ± 0.2
44				7.1 ± 4.0	>30	0.9 ± 0.3
45				>100	>100	>100

**Tab. 3:** General structure of the ligands, and binding affinities ( $IC_{50}$ ) in  $\mu M$ . Purified FK1-domains of FKBP51<sup>WT</sup> (2 nM), FKBP52<sup>WT</sup> (2 nM), FKBP51<sup>F67V</sup> (2 nM) and FKBP52<sup>F67V</sup> (10 nM) were measured in a fluorescence polarization binding assay by titrating the compounds using 3nM of compound **F2** (Chapter 4.2) as a tracer.<sup>108</sup>

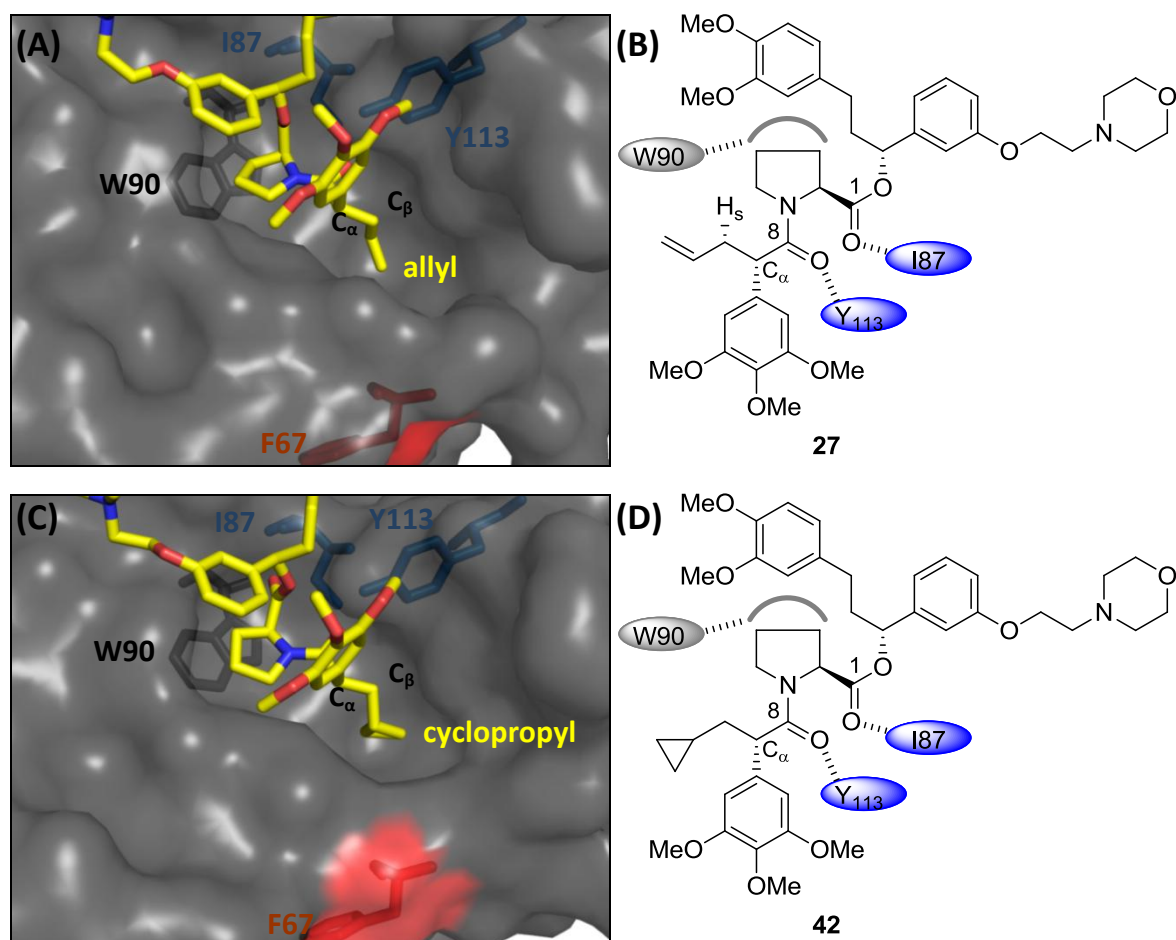


**Fig 39:** (A) Co-crystal structure of **27** and FKBP51FK1. (B) Structure of **27**. (C) Co-crystal structure of **42** and FKBP51FK1. (D) Structure of **42**. For better visibility of the binding site K121 was removed from the crystal structures

From these crystal structures it is not obvious why **26** or **27** lost selectivity compared to **24** and **42**. It seemed that increasing the size of the  $C_{\alpha}$  substituent accounts for increasing selectivity, which is displayed by the binding affinities (**Table 3**). The co-crystal structures of the iFit ligands revealed that the pro-(S)-proton at  $C_{\beta}$  of the iFit ligands pointed into the open space of the binding pocket. We therefore decided to introduce a substituent at the  $C_{\beta}$  (**Fig. 39C**) position, that additionally could be cyclized with the allyl substituent. We thus continued with the synthesis of the cyclohexenyl/cyclohexyl series of compounds.

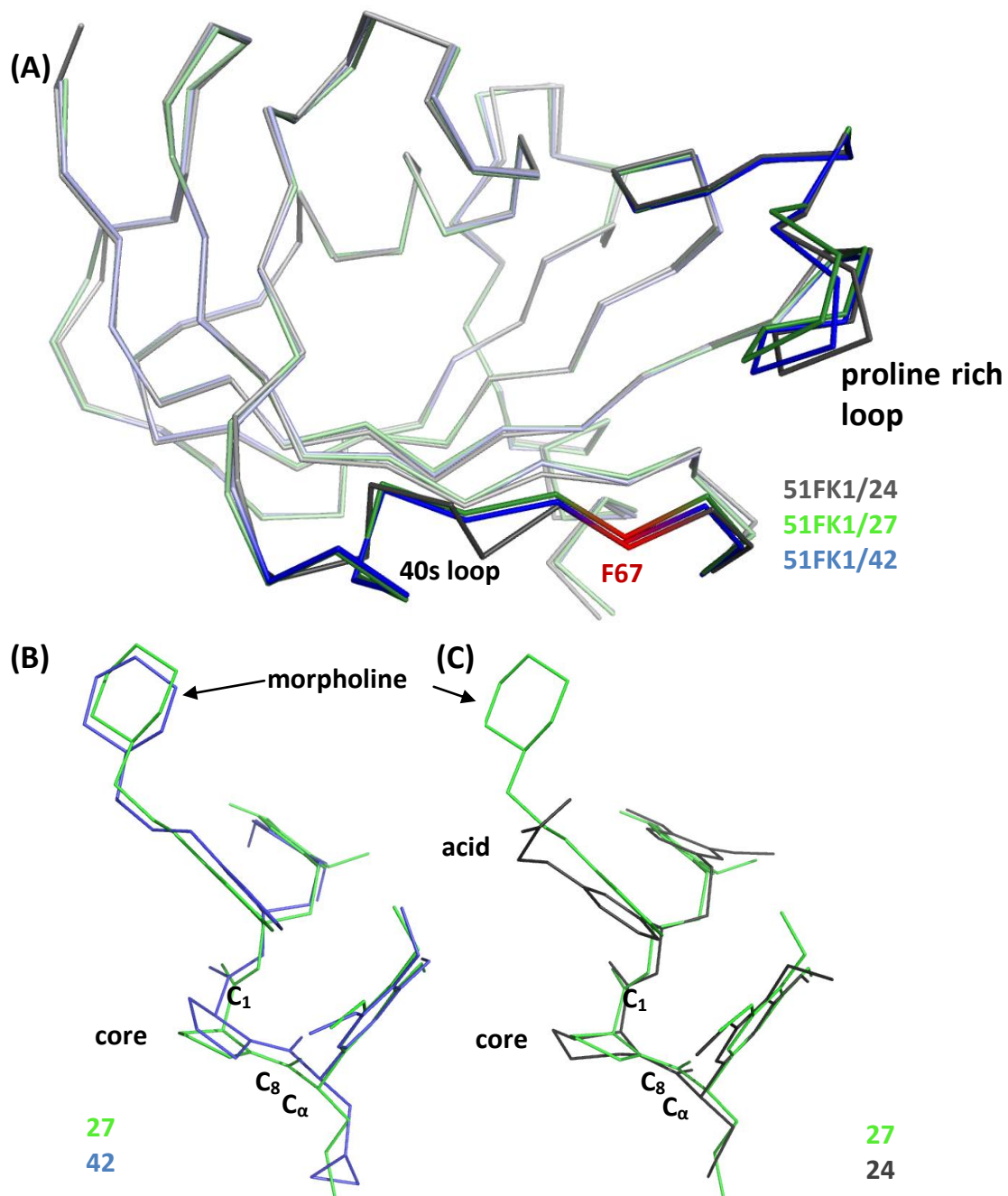


**Fig. 40.** (A) Superposition of the backbone traces of the co-crystal structure of FKBP51FK1/24 (grey) and the co-crystal structure of FKBP51FK1/27 (green). (B) Overlay of 27 (green) and 42 (blue). (C) Overlay of 27 (green) and 24 (grey).

## 2.2.2 Cyclohexenyl/Cyclohexyl series

### 2.2.2.1 Design and synthesis of cyclohexenyl/cyclohexyl ligands

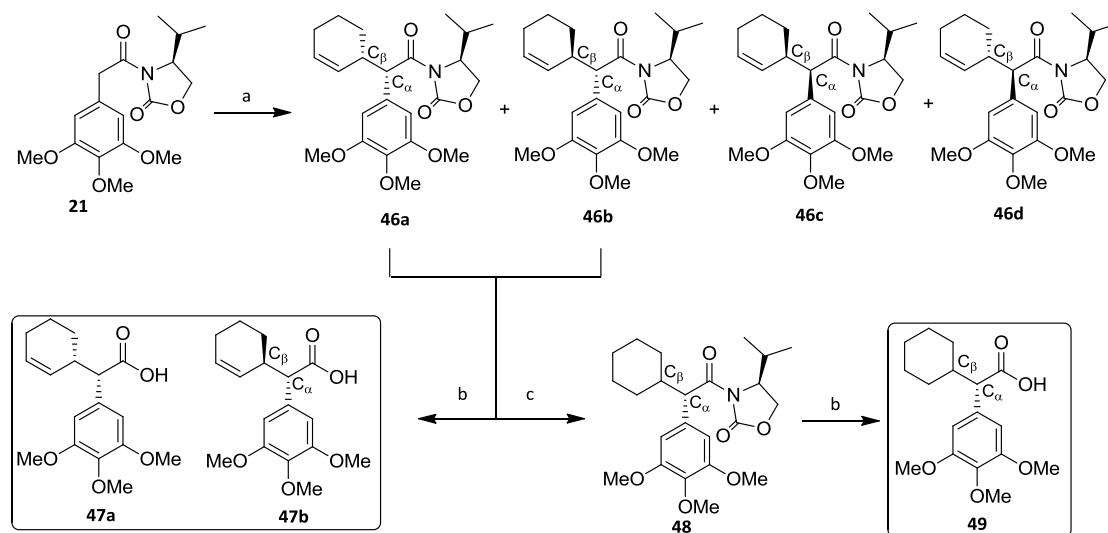


**Fig. 41** (a) NaHMDS, THF, cyclohexenyl-bromide, -78°C, 50-60%. (b) LiOH, H<sub>2</sub>O<sub>2</sub>, THF/H<sub>2</sub>O 8:5, 0°C-RT, 60-90%. (c) Pd/C, 30 bar H<sub>2</sub>, MeOH, RT, 90-99%.

The Evans auxiliary modified trimethoxyphenylacetic acid building block **21** could be successfully reacted with cyclohexenyl bromide under the same conditions as established for allyl bromide to give **46** as a mixture of four diastereomers with an overall yield of 63% (**Fig. 41, Annex Fig. A**). After flash chromatography, the mixture could be separated to obtain fractions of **46a/b** with 55% and fractions of **46c/d** with 8% yield (**Annex Fig. B and C**). **46a/b** and **46c/d** were each obtained with a diastereomeric rate at C<sub>α</sub> of 99%. The reaction also showed a preference for one diastereomer at the C<sub>β</sub> position. **46a/b** was obtained as a 85:15 mixture of diastereomers. This annotation is supported by analytical HPLC and finally analyzed by <sup>13</sup>C NMR analysis (analytical HPLC, **Annex Fig. C**, NMR, **Annex Fig. D**). **46a/b** could not be separated and was subsequently used as mixture of diastereomers. The absolute configuration of the preferred diastereomer was finally determined in the co-crystal structure of the cyclohexenyl-containing ligand **51** and will be discussed later. The imide **46a/b** was cleaved to give the free acid **47a/b** as a 85:15 mixture of diastereomers which could be partially resolved by analytical HPLC (**Annex Fig. E**). In parallel, the double bond of **46a/b** was reduced to give **48** with a diastereomeric excess of 99% at C<sub>α</sub>. No tailing in the analytical HPLC (**Annex Fig. F**) and no additional peaks in the NMR (**Annex Fig. G**) can be observed for **48**. The acid **49** was liberated as described for **47**.

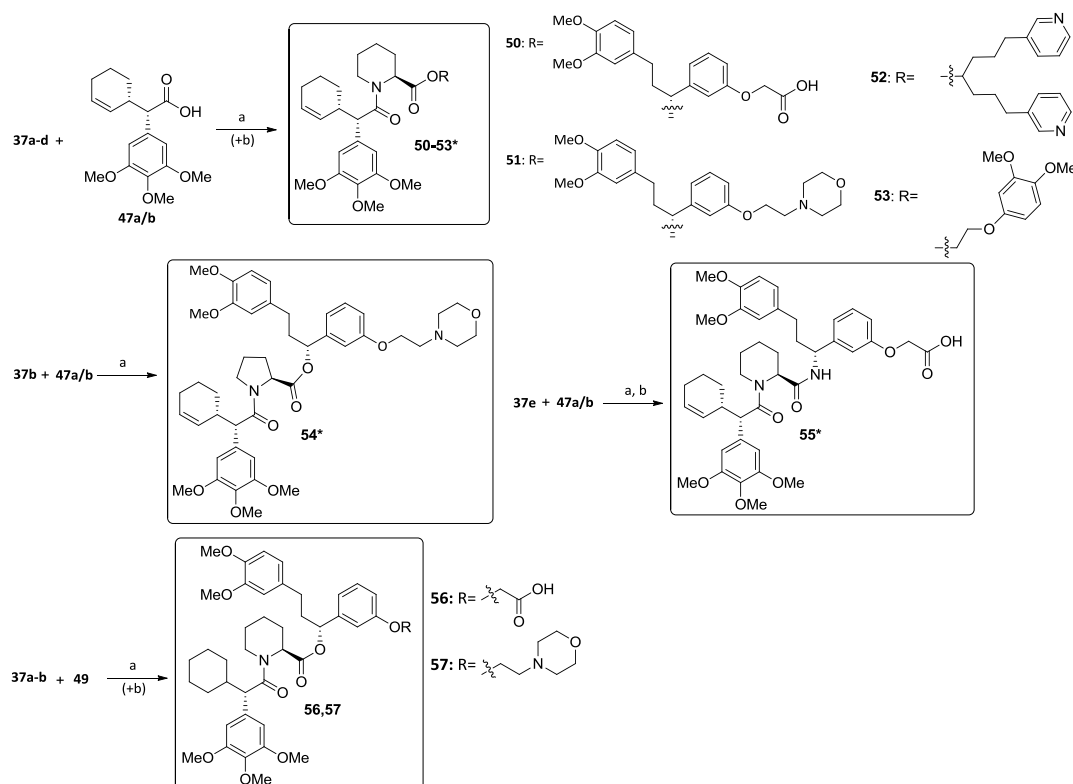


**Fig. 42:** (a) HATU, DIPEA, DCM, RT, 40-70%. (b) 10% TFA, DCM, RT, 50-70% (for 50, 55 and 56). \* 85:15 mixture of diastereomers

Coupling of **47a/b** to **37a-d** readily provided the cyclohexenyl derivatives **50-53** (Fig. 42) as mixtures of diastereomers at  $C_{\beta}$  of 85:15 which could not be further separated. The di-amide ligand **55** was synthesized like its ester homologs **50-53** and was also obtained as a 85:15 mixture of diastereomers. To further explore different  $C_{\alpha}$  substituents and to remove the  $C_{\beta}$  stereocenter we synthesized cyclohexyl analogs **56** and **57** from **37a** and **37b** coupled with **49**. Table 4 shows the inhibition constants ( $K_i$ ) of the cyclohexenyl/cyclohexyl series calculated from the binding data obtained with the fluorophores **F2** and **F4**. Due to the high binding affinity of the cyclohexyl/cyclohexenyl-containing ligands tracer **F2** was not sufficient anymore. We therefore had to design a new tracer **F4** for our fluorescence polarization assay (for a detailed description see Chapter 4.3).

We were pleased to see our rationale confirmed. The cyclization at the  $C_{\beta}$  position increased the affinity substantially to low nanomolar levels. The best iFit ligands to date, compounds **56** and **57**, show a  $K_i$  of  $4 \pm 0.3$  nM and  $6 \pm 2$  nM for FKBP51FK1. This is comparable to the natural product rapamycin ( $K_i$   $6 \pm 1$  nM) and almost one order of magnitude better than the natural product FK506 ( $K_i$   $93 \pm 19$  nM). Most important, the compounds showed no binding or very weak binding to FKBP52. Another interesting fact of the compounds is the preference over FKBP12. All cyclohexenyl/cyclohexyl compounds show at least 4-5 fold selectivity for FKBP51 over FKBP12 which makes them the first of this kind. For the cyclohexyl iFit ligands the selectivity of FKBP51 vs FKBP12

increased to >15-20 fold. All known FKBP ligands show a strong preference for FKBP12 over FKBP51 and FKBP52 of 100 to 1000 fold. Further optimization of this feature could lead to even more FKBP51 selective ligands.

### 2.2.2.2 Biochemical activity of cyclohexenyl/cyclohexyl ligands

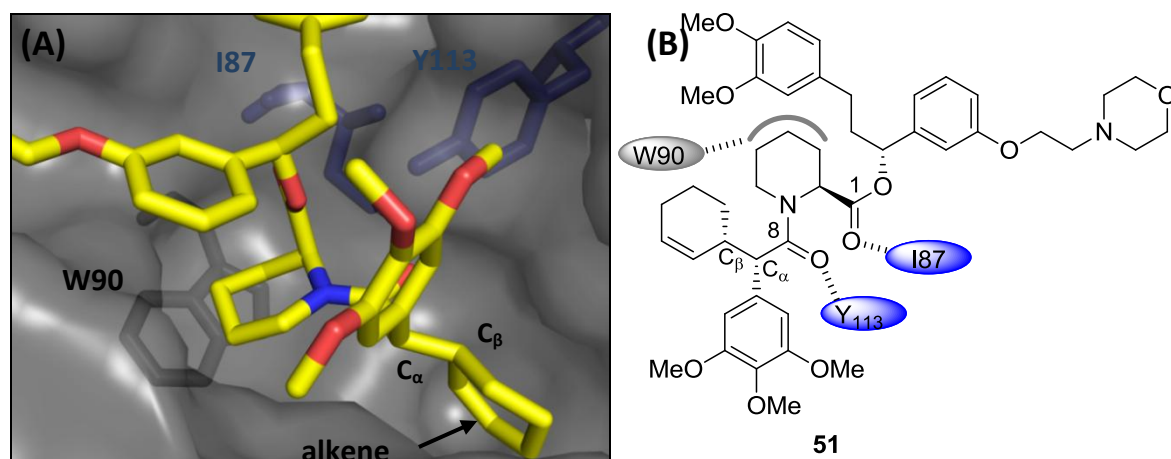


**Fig. 43:** (A) Co-crystal structure of **43** and FKBP51. (B) Structure of **51**. For better visibility of the binding pocket K121 was removed from the crystal structures

We solved a co-crystal structure of **51** and FKBP51 of a resolution of 1.25 Å (**Fig. 43A**). The pipercolinic core of **51** adopts a chair conformation. The whole ligand is except the core and the C<sub>α</sub> substituent almost superimposable to **27** (**Fig. 44A**). With the help of the co-crystal structure we were able to define the preferred configuration at the C<sub>β</sub> carbon. As indicated in **Fig. 43B** the best binding configuration at C<sub>β</sub> is (*S*). Probably **47a** is also the major diastereomer of the alkylation (**Fig. 41**). However, we cannot exclude the possibility, that **47a** is the minor diastereomer formed in the alkylation but has a much higher binding affinity.

The cyclohexenyl ring sits tightly in the induced subpocket with the alkene moiety pointing into the binding pocket (**Fig. 43A**).



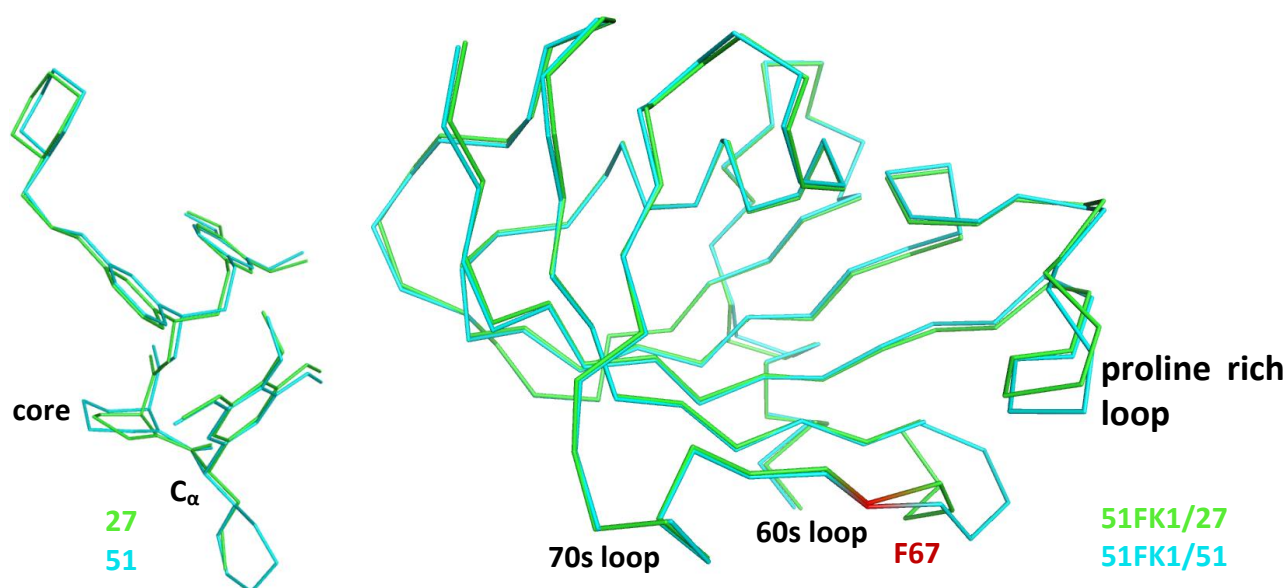


**Fig. 44:** (A) Overlay of ligand **27** and **51** in complex with FKBP51FK1. (B) Ribbon. (B) Superposition of the backbone traces of the co-crystal structure of FKBP51FK1/**27** (green) and the co-crystal structure of FKBP51FK1/**51** (cyan)

The overall architecture of the co-crystal structures **27**, **42** and **51** are superimposable except the 60s and the proline rich loop. **Fig. 44B** shows the ribbon overlay of the 51FK1/**27** and 51FK1/**51** co-crystal structure. The major differences can be found in the amino acids L61 to F66 (60s loop). The amino acids have to further reorientate to accommodate to the larger cyclohexenyl substituent (**Fig. 45**). The proline rich loop shows its slight flexibility which was also visible in the other co-crystal structures (**Fig. 44B**).

To further elaborate the binding properties of cyclohexenyl substituted ligands we synthesized four more compounds with different top groups **50-53** and one with a proline core **54**. For ligand **52** ( $K_i = 50 \pm 62$  nM) we chose the symmetric dipyridine top group known from the structurally related drug candidate Biricodar (Vertex Pharmaceuticals). The pyridine rings replace the substituted phenyl rings; pyridine constitutes a good compromise between hydrophobicity and solubility due to the protonizable amine. The advantage is lower molecular weight and a decrease in complexity by losing one stereocenter. The exchange resulted in a slight loss in affinity compared to **51** ( $K_i = 26 \pm 4$  nM), but retained selectivity for FKBP51. Replacement of the morpholine by a free acid **50** ( $K_i = 23 \pm 4$  nM) showed no substantial difference in binding affinities but strongly increases the water solubility. The top group of **53** was identified in a different ligand series in our group, as a smaller replacement for the bisubstituted top groups of the described ligands. Even more than the bipyridine top group it decreases molecular weight and removes one stereocenter. The binding affinity of the resulting compound **53** dropped substantially but selective binding for FKBP51 was still clearly

detectable at low micromolar levels. The exchange of the pipecolate core to proline **54** ( $K_i = 40 \pm 6$  nM) resulted in a slight decrease of binding affinity compared to **51**. The exchange of the top-group ester by an amide **55** ( $K_i = 328 \pm 40$  nM) decreased the affinity by more than 10 fold compared to **52** ( $K_i = 23 \pm 4$  nM). This could be due to the additional H-donor of the amide which is predicted to intramolecularly point to the trimethoxyphenyl group in a typical FKBP bound conformation. This interaction is likely less favorable than the van-der-Waals contacts of the corresponding pipecolate ester. It is noteworthy that **55** is the first pipecolate amide ligand with clearly detectable affinity for FKBP51. This is important as the pipecolate ester represents an undesired metabolic liability. The best compounds of this series and the best binding iFit ligands to date are **56** ( $K_i = 4 \pm 0.3$  nM) and **57** ( $K_i = 6 \pm 2$  nM). The reduction of the double bond of the cyclohexenyl ring resulted in a 4-fold increase in binding affinity.

These compounds are the first reported FKBP51 ligands which bind with low nanomolar affinity and additionally show selectivity of more than 10000-fold over FKBP52. Another important point is the selectivity vs FKBP12. **56** and **57** are the first FKBP ligands that have selectivity  $> 10$  for FKBP51 vs FKBP12.

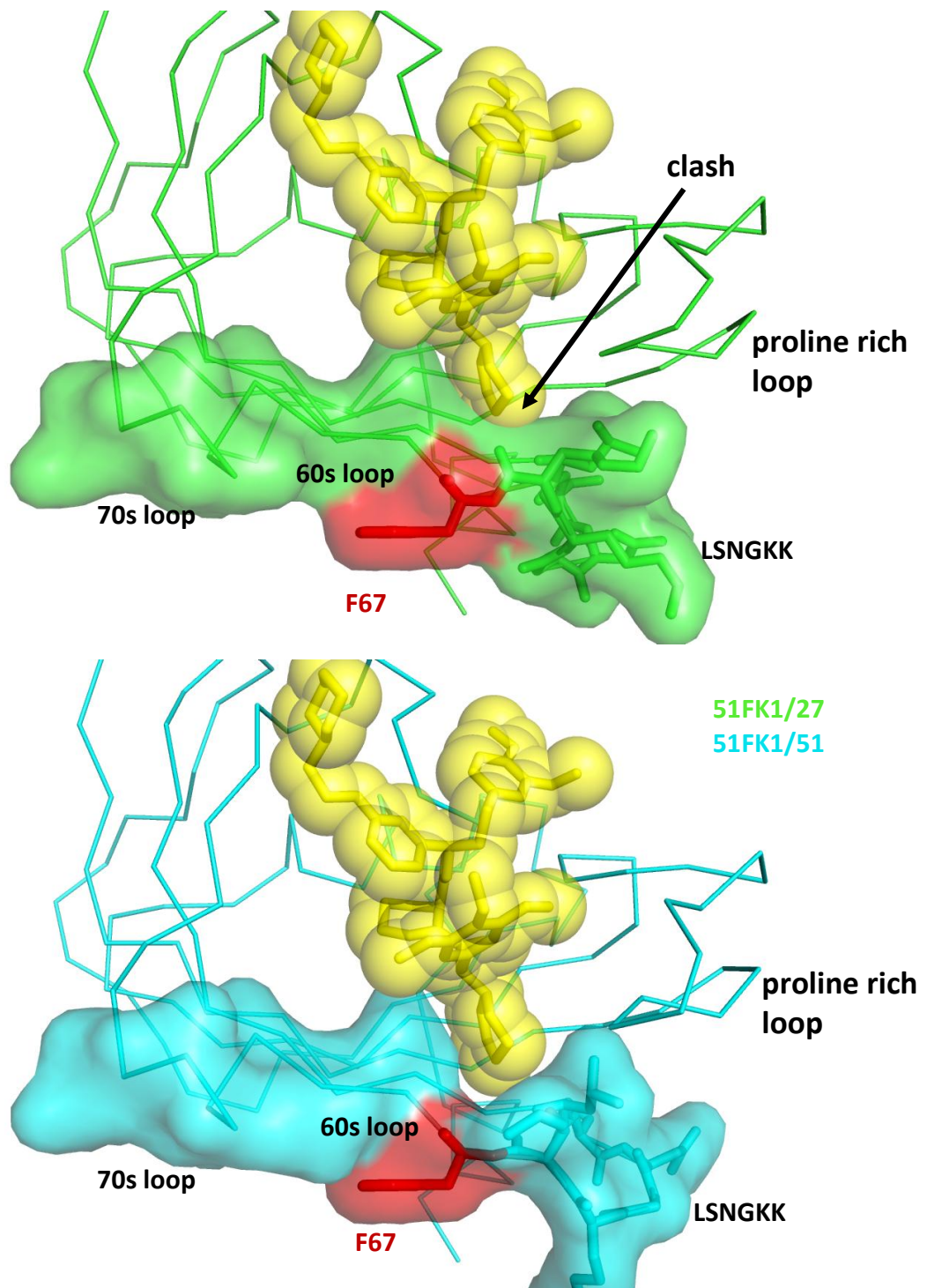


**Fig. 45:** (A) Structural change of the 60s loop induced by 51. (A) 51 modeled into the co-crystal structure of FKBP51FK1/27(**green**). (B) co-crystal structure of FKBP51FK1/51 (**cyan**).

### 2.2.2.3 Effect of iFit ligands on neurite outgrowth

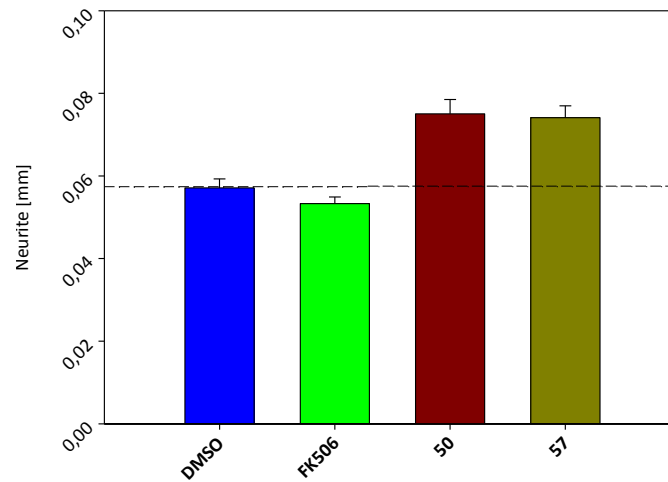


**Fig. 46:** Selective inhibition of FKBP51 wildtype by FK506, **50** and **57** at 1  $\mu$ M

**Fig. 46** shows our first results using iFit ligands in a neurite outgrowth assay performed under basal conditions without overexpression of FKBP51 or FKBP52 proteins. The first lane (blue) displays the DMSO control, which reflects the basal length of neurite outgrowth in this assay. By adding the unselective FK506 we observe no increase in neurite length but rather a slight decrease. This result is different to the results reported by Quinta et al<sup>86</sup> but it is consistent with our previous results which showed that inhibition of both FKBP51 and FKBP52 at the same time show no effect (**Fig. 46**). In contrast selective ligands **50** and **57** significantly increased the neurite lengths. These results support our previous hypothesis that selectivity for FKBP51 could be beneficial for the development of ligands with neuroregenerative properties.

### 2.2.3 C<sub>α</sub>-hydroxy series

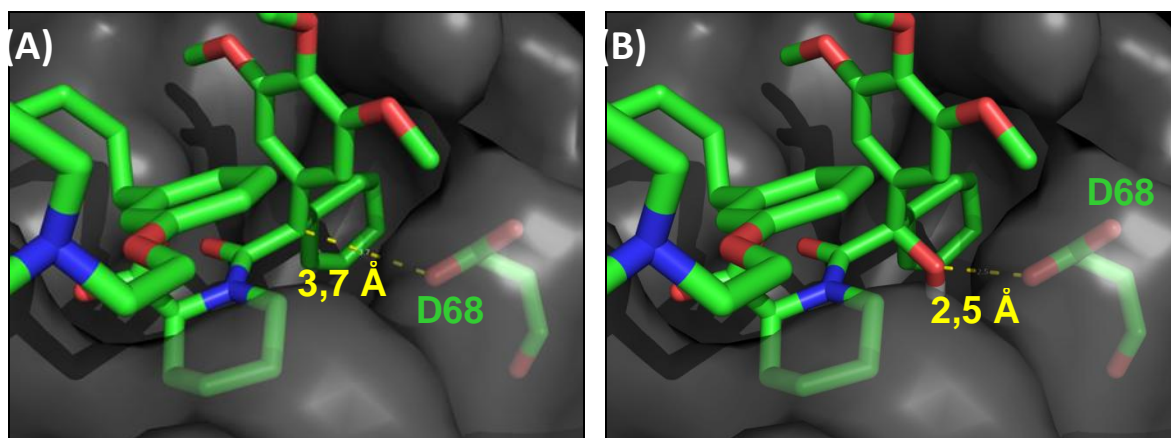


**Fig 47:** (A) Co-crystal structure of **51** and FKBP51. (B) Modeling of the **64a** into the co-crystal structure of **51**

Molecular modeling revealed that a potential hydrogen bond could be formed between D68 and an hydrogen donor group at C<sub>α</sub> (**Fig. 47**). To test if an additional hydroxy group at C<sub>α</sub> is tolerated, we first synthesized compound **60** (**Fig. 48**). We started from commercially available 2-(3,4,5 trimethoxyphenyl)acetic acid and oxidized it with seleniumdioxide<sup>131</sup> to obtain **58** the α-keto acid was alkylated with allylmagnesium bromide to give racemic **59**. The racemate was coupled to **37a** to give **60** as a 1:1 mixture of diastereomers with modest 25% yield. Upon treatment of **60** with 10% TFA to deprotect the t-Bu-group, however the C<sub>α</sub> hydroxy group readily eliminated to give the undesired **62** as the major product and only trace amounts of **61**. As expected **62** showed no affinity for FKBP51 or **52** (data not shown).

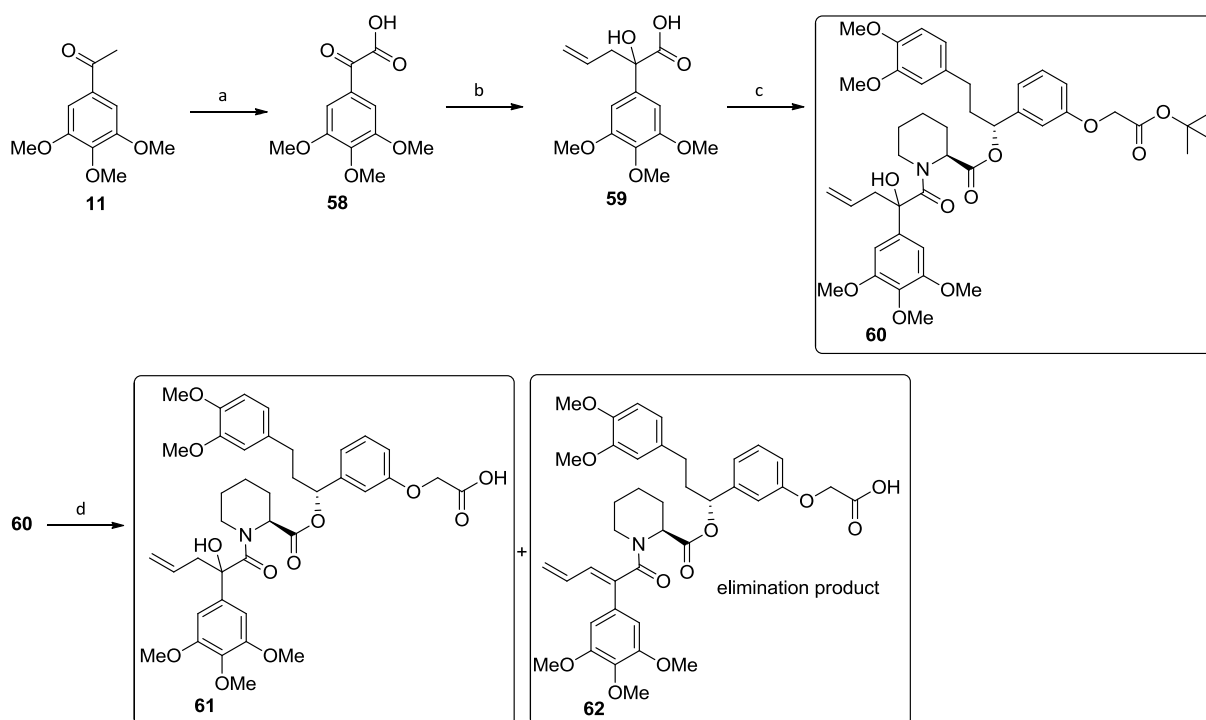


**Fig. 48:** (a)  $\text{SeO}_2$ , pyridine, reflux, 92%. (b) Allylmagnesium bromide, THF,  $-78^\circ\text{C}$ -RT, 60%. (c) 37a, HATU, DIPEA, DCM, RT, 25%. (d) 10% TFA/DCM,  $0^\circ\text{C}$ -RT

To solve this problem we designed a different synthetic route where the alkylation was performed in the last step (**Fig. 49**). First, we synthesized Biricodar/**63**.<sup>132</sup> Then the  $\text{C}_\alpha$ -carbonyl was alkylated using cyclohexylmagnesium bromide which readily yielded a racemic mixture of **64a/b**. The diastereomers **64a** and **64b** could be separated using reversed phase HPLC. Under these conditions no elimination of the  $\text{C}_\alpha$  hydroxy group was observed.

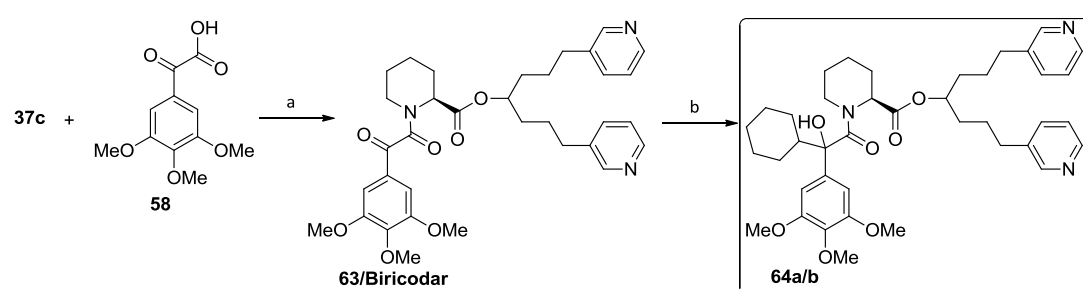


**Fig. 49:** (a) HATU, DIPEA, DCM, RT, 40-70%. (b) Cyclohexylmagnesium bromide, THF,  $-78^\circ\text{C}$

Of these only one diastereomer **64a** ( $K_i = 77 \pm 11$  nM, **Tab. 4**) bound with good binding affinity in the nanomolar range, whereas the other diastereomer did not show any binding within the limits of the assay. Thus, addition of a hydroxy group at  $\text{C}_\alpha$  seems to be tolerated (in the correct stereochemical configuration) but overall it does not seem to add additional binding energy. However, it highly simplifies the synthesis of the ligands and allows simple access to a broad range of potential  $\text{C}_\alpha$  substituents (described in the outlook).

We plan to expand these series of compounds to the morpholine top group to improve the binding affinity. Main advantage of this methodology is that a broad scope of Grignard reagents can be used. Furthermore, it is not dependent on tedious stereoselective alkylations using auxiliaries although it requires separation of the diastereomers by preparative HPLC.

### 2.2.4 C<sub>α</sub> symmetric ligand series

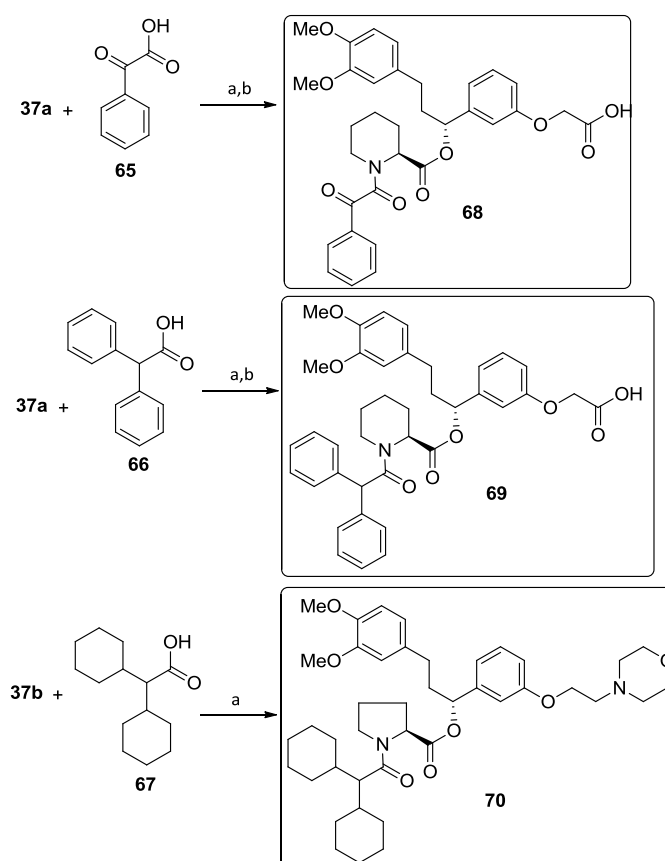


Fig. 50: (a) HATU, DIPEA, DCM, RT, 74-78%. (b) 10% TFA/DCM, RT, 64-82%

To estimate the contribution on binding of the three methoxy groups of the lower part of the ligands, we synthesized compound **68** from commercially available α-keto-2-phenylacetic acid. In addition we synthesized the symmetric C<sub>α</sub> ligand **69** from 2,2-diphenylacetic acid. Due to the high binding affinity of the cyclohexyl ligand series we also synthesized the symmetric dicyclohexyl ligand **70**. Both symmetric ligands lost their affinity to the larger FKBP12 completely and only C<sub>α</sub> keto analogue showed moderate affinity for FKBP12 (Table 6).

Name	Core	R <sup>2</sup>	R <sup>1</sup>	51WT	52WT	12WT
68				>150	>200	10.03 ± 1.64
69				>150	>200	>150
70				>150	>150	>150

**Tab. 7:** General structure of the ligands, and binding affinities (IC<sub>50</sub>) in μM. Purified FK1-domains of FKBP51<sup>WT</sup> (280 nM), FKBP52<sup>WT</sup> (400 nM), FKBP12<sup>WT</sup> (10 nM) were measured in a fluorescence polarization binding assay by titrating the compounds using 20 nM **F2** as a tracer for FKBP51<sup>WT</sup>/52<sup>WT</sup> and 3 nM for FKBP12<sup>WT</sup>.

### 2.2.5 Synthesis of C<sub>α</sub> substituted rapamycin

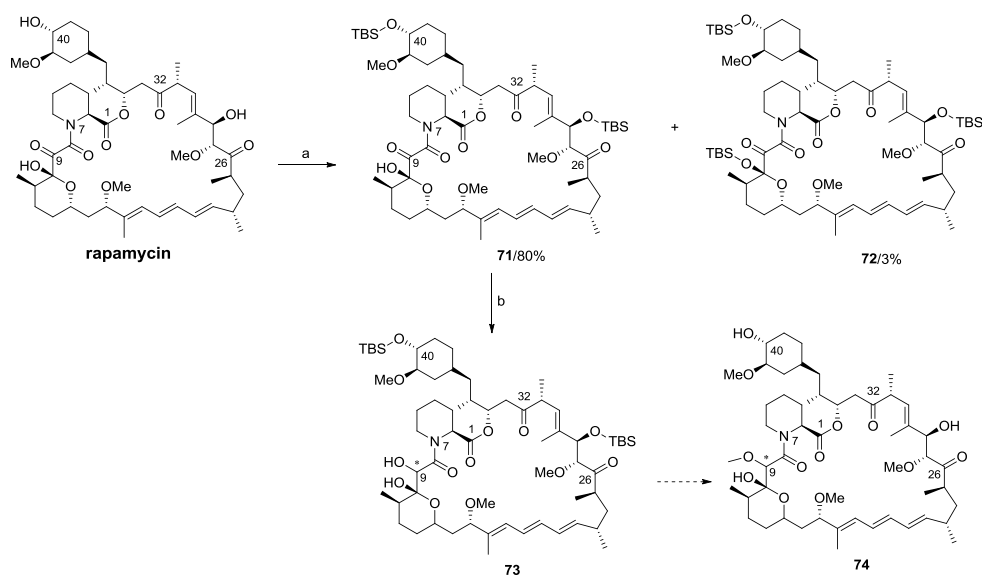


**Fig. 51:** (a) TBSOTf, 2,6-Lutidine, RT, 80%. (b) NaCNBH<sub>3</sub>, MeOH, 0°C-50°C, 20%.

The immunosuppressive effect of rapamycin results from inducing ternary protein complexes with the FKBP and the kinase mTOR, an important regulator of cell growth and proliferation. The most prominent partner of rapamycin is believed to be FKBP12. Research in Hausch lab showed that rapamycin complexes of larger FKBP protein family members can tightly bind to mTOR and potently inhibit its kinase activity (März et al. Manuscript in preparation).

To investigate the role of the different FKBP involved in the ternary FKBP-rapamycin-mTOR complexes a FKBP subtype-selective rapamycin analog is needed. We intended to synthesize a C $\alpha$  modified rapamycin derivative as depicted in **Fig. 51** by introducing an ether at the C9 carbonyl group. We started with protection of the hydroxyl groups 10, 28 and 40 by TBS. For this reaction TBS-Cl was not reactive enough, so TBDMS-OTf had to be used. Under these conditions hydroxy group 28 and 40 were protected smoothly to give **71** with 80% yield. It was also possible to isolate the hemiacetal hydroxyl group 10 protected product **72** with 3% yield. With the double protected derivative **71** we next targeted the selective reduction of the C $\alpha$  carbonyl assuming that the  $\alpha$ -keto-amide would be the most electrophile position. The reduction proved to be very difficult. Using numerous different reaction conditions (Superhydride, LiAl(OtBu)<sub>3</sub>H, DIBAL, LiAlH<sub>4</sub>, NaBH<sub>4</sub>, NaB(OAc)<sub>3</sub>H) only trace amounts of product could be obtained. Finally we discovered reaction conditions (NaCNBH<sub>3</sub>, 0°C-50°C) that reduced the C9 carbonyl with moderate 20% yield.

We decided to further modify the obtained compound with a methyl group at the C9 hydroxy group. We explored different bases (Lutidine, K<sub>2</sub>CO<sub>3</sub>, LiHMDS, NaH) and MeI or MeOTf but until now no product could be isolated.

To overcome the problems of the aforementioned synthetic route we engaged in the synthesis of a C $\alpha$ -hydroxy, C $\alpha$ -allyl derivatized rapamycin analog. This was inspired by the results with the synthetic ligand **64a**. Mechanistic studies on rapamycin and ascomycin showed that the C9 carbonyl group is the most reactive in the molecule<sup>133, 134</sup>, so we planned a simplified synthetic route without protecting groups. We decided to start with allylmagnesium bromide but this reaction produced mono- to polyallylated compounds due to the high reactivity of the reagent also at -78°C. **Fig. 52** indicates the most reactive functional groups of rapamycin for an attack of allylmagnesium bromide. The most electrophilic positions of rapamycin are the C1 ester, the C9 carbonyl group, the C10 hemiacetal, and the two other carbonyl groups at C26 and C32. To improve the chemo selectivity we decided to use less reactive reagents and activate the C9 carbonyl by a lewis acid. We chose allyltrimethylsilane and tetraallyltin as allyl donors, while the carbonyl group was activated by In(OTf)<sub>3</sub>. Allyltrimethylsilane failed to produce any product but with tetraallyltin defined peaks of mono-, di-, tri and tetrasubstituted products were observed. By RP-HPLC it was possible to separate mono-allylated 24% **75-978**, di-allylated 7% **75-1021**, and tri-allylated 3% **75-1063** derivatives.

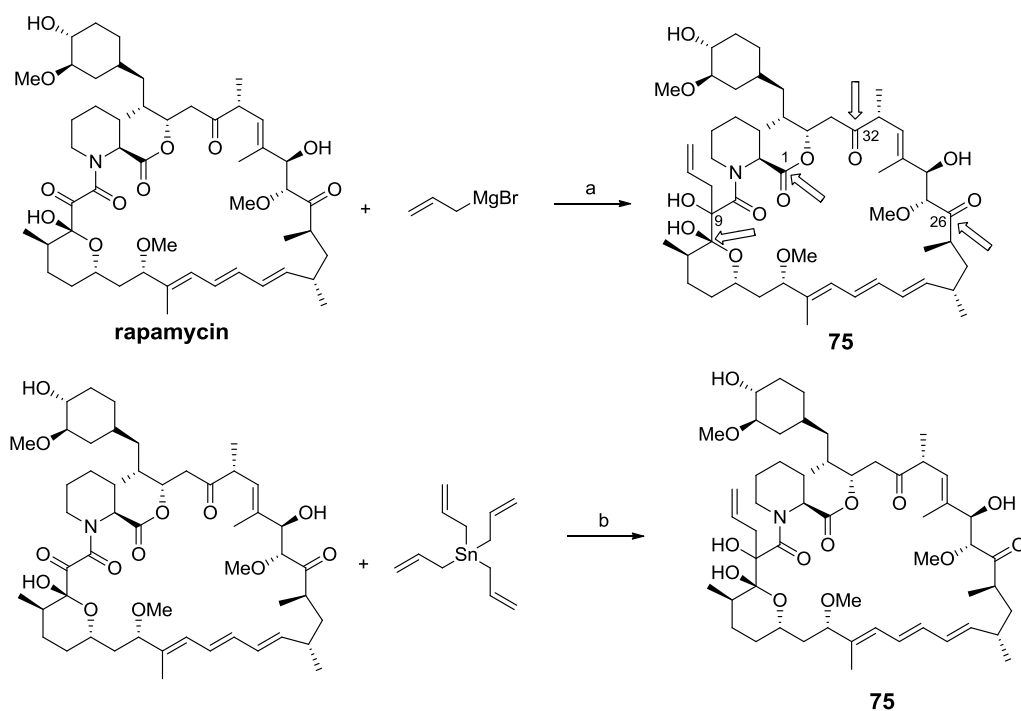


Fig. 52: (a) THF,  $-78^\circ\text{C}$ . (b)  $\text{InOTf}_3$ , THF, RT, 24,2%.

All of the alkylated rapamycin derivatives of **75** showed a dramatically decreased affinity for the wildtype and the F67V mutated FKBP proteins, and showed a selectivity for FKBP12 of greater than 100-fold. Unfortunately with the applied alkylation conditions no good binder could be isolated from the reaction mixture. Mono-allylated **75-978** binds to FKBP12 with an  $\text{IC}_{50}$  of around  $5\ \mu\text{M}$  whereas rapamycin binds in this assay to FKBP12 with an  $\text{IC}_{50}$  of around  $30\ \text{nM}$  which accounts to a 100-fold loss in binding affinity. Di- and tri allylated **75-1021** and **75-1063** lost affinity to FKBP12 in the same order of magnitude and showed only micromolar affinity. Binding affinity to FKBP51FK1/FKBP52FK1 wildtype and F67V mutant decreased to undetectable levels greater than  $100\ \mu\text{M}$ . From the  $\text{C}_\alpha$  hydroxy ligand series (**Chapter 2.2.3**) it is clear that the stereochemistry at  $\text{C}_\alpha$  is essential for binding. The stereochemistry of the reduction could not be determined of the isolated derivatives because not enough material for NMR interpretation was obtained.

## 2.3 Structural basis for the selectivity

### 2.3.1 Structure-activity relationship of the iFit ligands

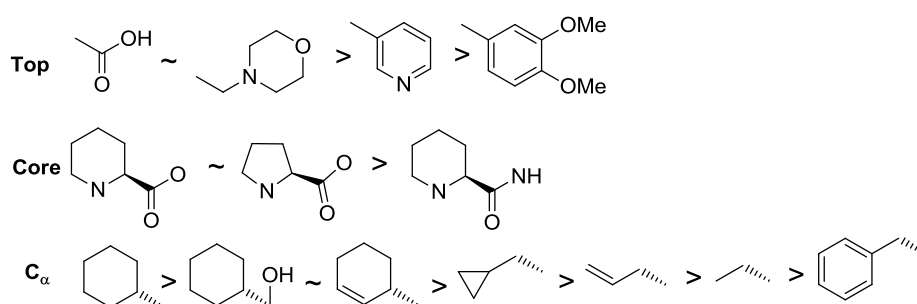
We synthesized a series of  $\text{C}_\alpha$ -substituted ligands to identify new compounds that induce the conformational change and thereby increase the selectivity. The exchange of the free acid substructure to the morpholine substructure increased the binding affinity in the allyl and

cyclopropylmethyl series substantially whereas in the cyclohexenyl/cyclohexyl series this exchange showed no additional increase in binding affinity. The Biricodar pyridine top-group lowered the affinity 2 fold compared to the free acid or morpholine analogs but decreases molecular weight and has one less stereocenter. We employed the even smaller monovalent top-group of **53** which resulted in a substantial loss in activity to micromolar levels.

The exchange from pipicolate to proline core is context-dependent and accounts only for minor changes in binding affinity whereas the piperidine-2-carboxamide core showed a 10-fold decrease in binding affinity.

We increased the C<sub>α</sub> substituent to cyclopropylmethyl which slightly increased the affinity. Upon increasing the size to cyclohexenyl/cyclohexyl the affinity could be increased to low nanomolar levels. These compounds are the first reported FKBP51 ligands that bind with sub-micromolar to low nanomolar affinity, and additionally show up to 10000-fold selectivity over FKBP52 and up to 10-fold selectivity over FKBP12. To determine if the alkene of the cyclohexenyl ring has an important effect on binding, we reduced the double bond. This further increased the binding affinity by almost 10-fold.

We synthesized the hydroxy compounds **64** and isolated the correct diastereomer which binds with similar affinity as the related compound **52**. Although we only synthesized one example yet it indicates that the C<sub>α</sub>-cyclohexyl/C<sub>α</sub>-hydroxy substitution is almost equivalent to C<sub>α</sub>-cyclohexenyl. We wanted to explore the limits of the induced binding pocket, so we enlarged the allyl/cyclopropylmethyl series to benzyl. This substituent is too large to be accommodated by the FKBP proteins. No binding affinity in the range of the assay could be measured.



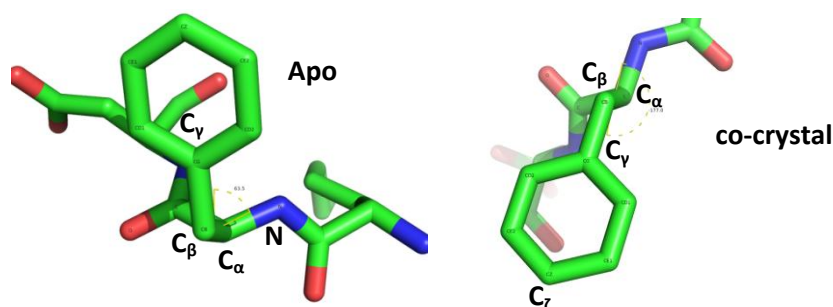
**Tab. 8:** SAR of iFit ligands (~ equal but context dependent)

The final SAR for binding of the iFit ligands to wildtype FKBP51 is shown in **Tab. 8**. The free acid showed in combination with cyclohexyl slightly better binding affinity than the morpholine top group, followed by the bipyridine substituent. The smallest monovalent top group showed the worst binding affinity. In combination with cyclohexenyl or cyclohexyl the pipicolinic core gave the best binding affinity, and for the C<sub>α</sub> substituents cyclohexyl was a little bit better than cyclohexenyl but

both of them were around 10 to 100-fold better than cyclopropylmethyl and allyl. The worst  $C_\alpha$  substituents were ethyl and benzyl.

### 2.3.2 Quantification of the induced conformational change

We quantified the conformational change in FKBP51 by measuring the distances from F67 to I87, W90 and F130, and the dihedral angle that defines the orientation of the phenyl ring of F67 (**Fig. 53**). We compared these values to the co-crystal structure of unselective ligands **FK506** and **SLF**, and to the apo structure. The distance from F67  $C_\zeta \leftrightarrow I87 C_\delta$  increased from 7.1-7.3 Å to 14.9-15.2 Å. In the same way, the distance between F67  $C_\zeta \leftrightarrow W90 C_\theta$  increased from 7.0-7.3 Å to 12.5-12.8 Å. The distance between F67  $C_\zeta \leftrightarrow F130 C_\zeta$  extended from 3.7-3.8 Å to 10.8-10.9 Å. The dihedral angle of F67 changed from 58.9°-63.8° to -152.2°-(-177.0°). All  $C_\alpha$  substituents synthesized by us varying from allyl to cyclohexyl are able to induce this conformational change in FKBP51. This induced conformation seems to be substantially less favorable for FKBP52, resulting in selectivities between 100 to 1000-fold. In addition cyclohexenyl and cyclohexyl strongly contribute to binding affinity.



	Name	F67 $C_\zeta \leftrightarrow I87 C_\delta$	F67 $C_\zeta \leftrightarrow W90 C_\theta$	F67 $C_\zeta \leftrightarrow F130 C_\zeta$	F67 $C_\zeta \leftrightarrow F67 C_\zeta$ apo	F67 N- $C_\alpha$ - $C_\beta$ - $C_\gamma$
selective	51FK1/24	15.2 Å	12.8 Å	10.9 Å	9.0 Å	-152,2°
	51FK1/27	14.9 Å	12.5 Å	10.8 Å	9.0 Å	-174,9°
	51FK1/42	15.0 Å	12.8 Å	10.8 Å	9.2 Å	-165,3°
	51FK1/51	15.2 Å	12.5 Å	10.9 Å	9.2 Å	-177,0°
unselective	51FK1/FK506	7.3 Å	7.3 Å	3.8 Å	0.3 Å	63,8°
	51FK1/SLF	7.1 Å	7.3 Å	3.7 Å	0.2 Å	58,9°
apo	51FK1 Apo	7.0 Å	7.0 Å	3.7 Å	--	63,5°

**Fig. 53:** Conformational reorganization of F67: **(A)** apo crystal structure of FKBP51FK1; **(B)** co-crystal structure FKBP51FK1 and **51**. The dihedral angle N- $C_\alpha$ - $C_\beta$ - $C_\gamma$  defining the conformational flip is indicated. **(C)** Distance of F67  $C_\zeta$  to I87  $C_\delta$ , F67  $C_\zeta$  W90  $C_\theta$  and F130  $C_\zeta$  in Å. Distance of F67  $C_\zeta$  of co-crystal structures to F67  $C_\zeta$  of the apo structure without ligand in Å. Dihedral angle of F67 N- $C_\alpha$ - $C_\beta$ - $C_\gamma$ .

## 2.3.3 Evaluation of the co-crystal structures

### 2.3.3.1 The C<sub>α</sub>-Substituent

To examine the structural basis for the unexpected selectivity of the iFit ligands for FKBP51 we solved four co-crystal structures with the FK1 domain of FKBP51 and compounds **24**, **27**, **42** and **51**. **Fig. 54** shows the induced subpocket in the protein and a spacefilling model of the ligands. **Fig. 54A** and **54B** show the allyl compounds **24** and **27**. As described in **Chapter 2.2.1** we enlarged the C<sub>α</sub> substituent to cyclopropylmethyl, because we hypothesized that a bigger substituent would fill the cavity better than allyl. By comparing the space filling models of the co-crystal structures of allyl ligands **24** and **27** (**Fig. 54A** and **B**) and the cyclopropyl of **42** our assumption proved to be true. It is easy to recognize that cyclopropyl fits much better into the hole than the allyl substituent of **27** (**Fig. 54C**), and thereby not only increases the binding affinity but also the selectivity for FKBP51. We observed that a substitution at C<sub>β</sub> would be tolerated, leading to the cyclized substituent cyclohexenyl (**Fig. 54D**). This substitution dramatically increased the affinity and selectivity further. **Fig. 16D** shows how nicely the cyclohexenyl fits into the cavity that it induces. The alkene moiety points into the pocket and the aliphatic part outwards. The alkene moiety per se however, does not seem to be essential since the reduced cyclohexenyl ligands interact even better with FKBP51. So we conclude that if the stereochemistry of the alkene could be better defined it would be suitable for further modifications.

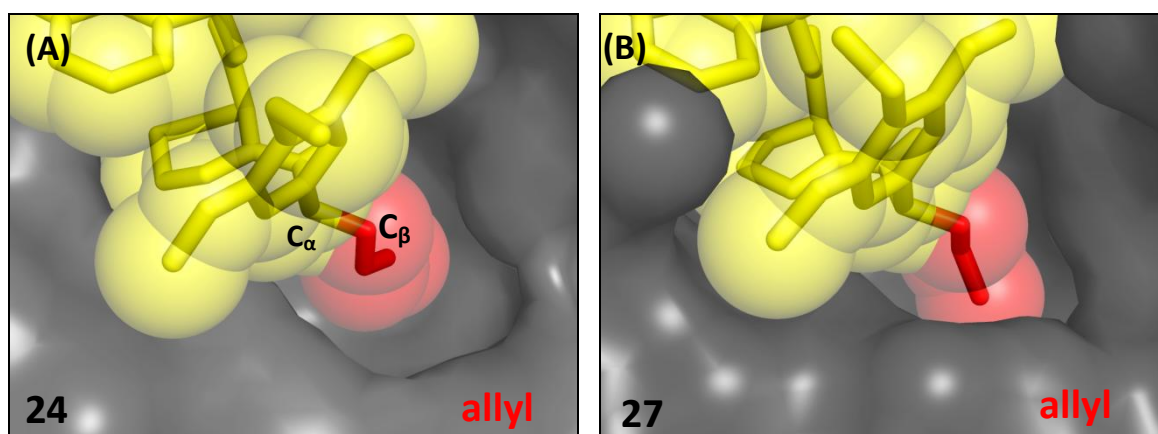


**Fig 54:** (A) Co-crystal structure of **24** and FKBP51FK1. (B) Co-crystal structure of **27** and FKBP51. For better visibility of the induced sub-pocket K121 was removed from the crystal structures.

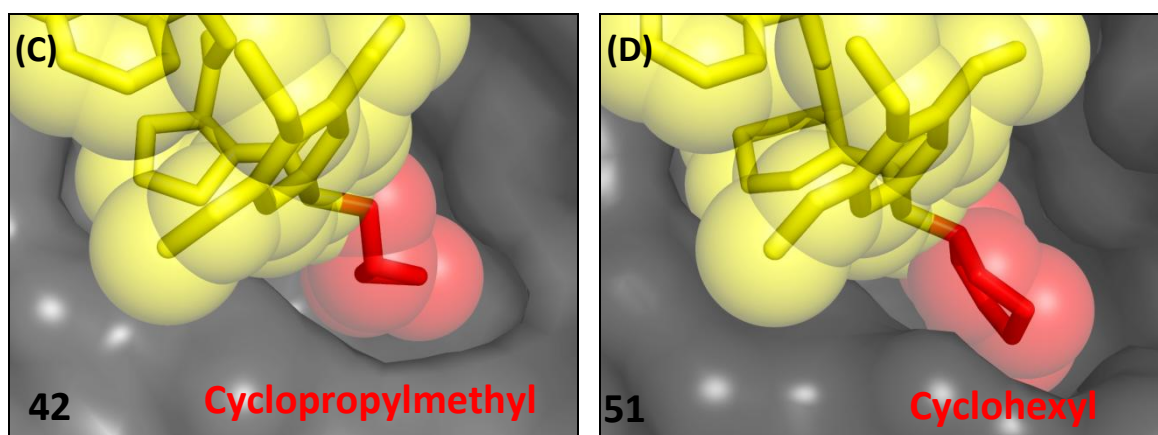


**Fig 54:** (C) Co-crystal structure of **42** and FKBP51. (D) Co-crystal structure of **51** and FKBP51. For better visibility of the induced sub-pocket K121 was removed from the crystal structures.

### 2.3.3.2 The Trimethoxyphenyl Moiety

**Fig. 55** shows the orientation of the trimethoxyphenyl moiety in the four co-crystal structures. The (S)-configuration at  $C_{\alpha}$  directs the trimethoxyphenyl ring out of the binding pocket. The movement is further limited by the top-group which does not allow it to turn. In all structures the ring adopts the same orientation. Only the para methoxy group seems to be free to change orientation, indicating that this methoxy might be less important. In our SAR we showed that by removing the methoxy groups the affinity drops dramatically. The crystal structures show van der Waals interaction between the methoxy groups and the side chains. Aromatic hydrogen bonds can be observed from the ortho positions of the trimethoxyphenyl ring to D68 on one side and to Y113 on the other side which are both in 3.4 Å distance. The side chains of the amino acids Y57, D68, Y113, S188 and I122 are in van der Waals distance to the trimethoxyphenyl ring. More different substructures have to be synthesized to perform a SAR study to better understand the structural implications of this part of the ligand.

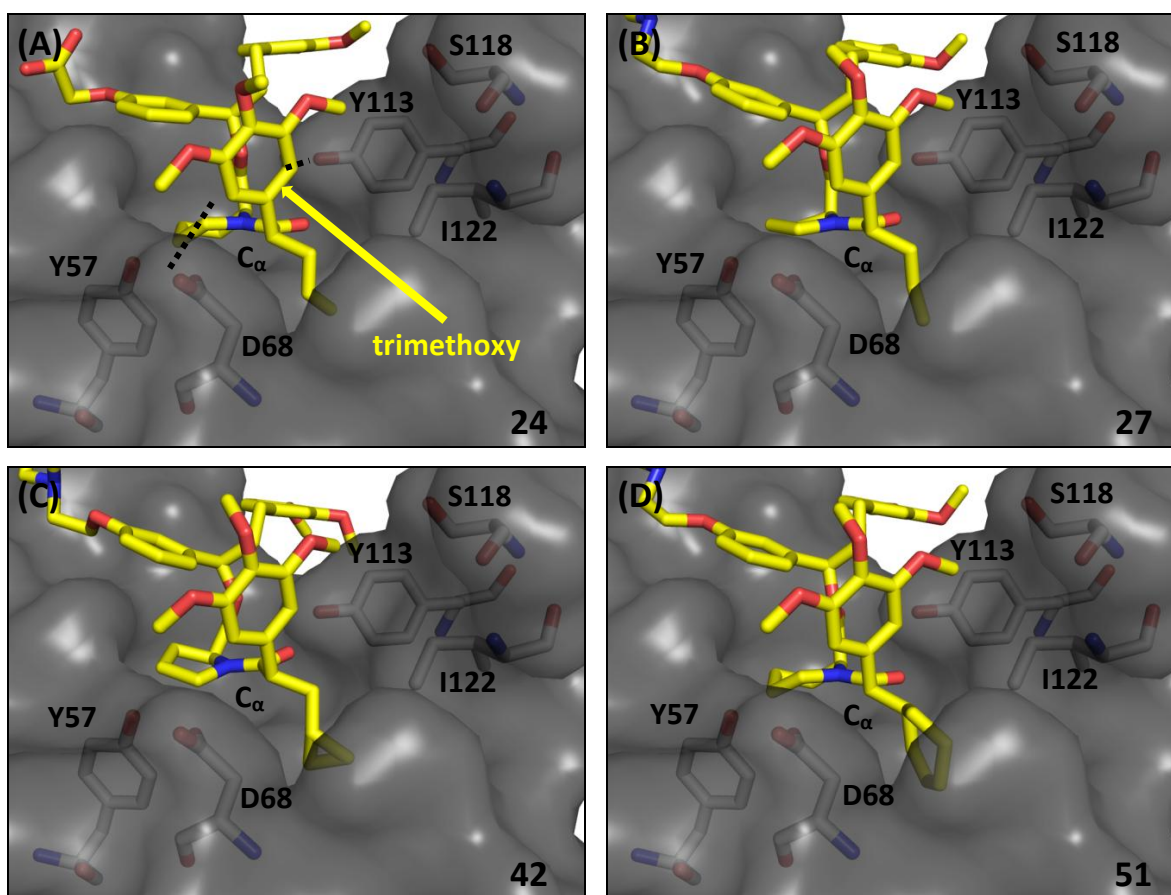


**Fig 55: Comparison of the trimethoxyphenyl moiety (A)** Co-crystalstructure of **24** and FKBP51FK1. Aromatic hydrogen bonds formed between D68/Y113 and the ortho positions of the trimethoxy phenyl ring **(B)** Co-crystalstructure of **27** and FKBP51FK1. **(C)** Co-crystalstructure of **42** and FKBP51FK1. **(D)** Co-crystalstructure of **51** and FKBP51FK1. For better visibility of the sub-pocket K121 was removed from the crystal structures

### 2.3.3.3 The Top Group

We tested four different top groups in our SAR study. Of these, two of them were crystallized, the morpholine substructure and the free acid substructure. In general, the morpholine and the free acid top groups show the best binding affinities in a similar range. Interestingly for smaller  $C_{\alpha}$  substituents like allyl and cyclopropylmethyl, the morpholine substructure performed around one order of magnitude better than the free acid top group. In contrast, the bigger cyclohexenyl/cyclohexyl substituents show only marginal differences between the two top groups. The free acid performed here around two times better than the morpholine. In the co-crystal structures the A and B phenyl rings all show almost the same conformation. Only in one of the **SLF** structures the A ring is rotated  $180^{\circ}$  compared to **24**, indicating the free acid is flexible and does not contribute substantially to the binding (**Fig. 56B-C**). Both rings sit nicely in shallow grooves on the surface of the protein, mainly

contributing to binding by non-directed hydrophobic interactions. In addition, in all co-crystal structures aromatic hydrogen bonds of both rings to the amino acid backbone are present.

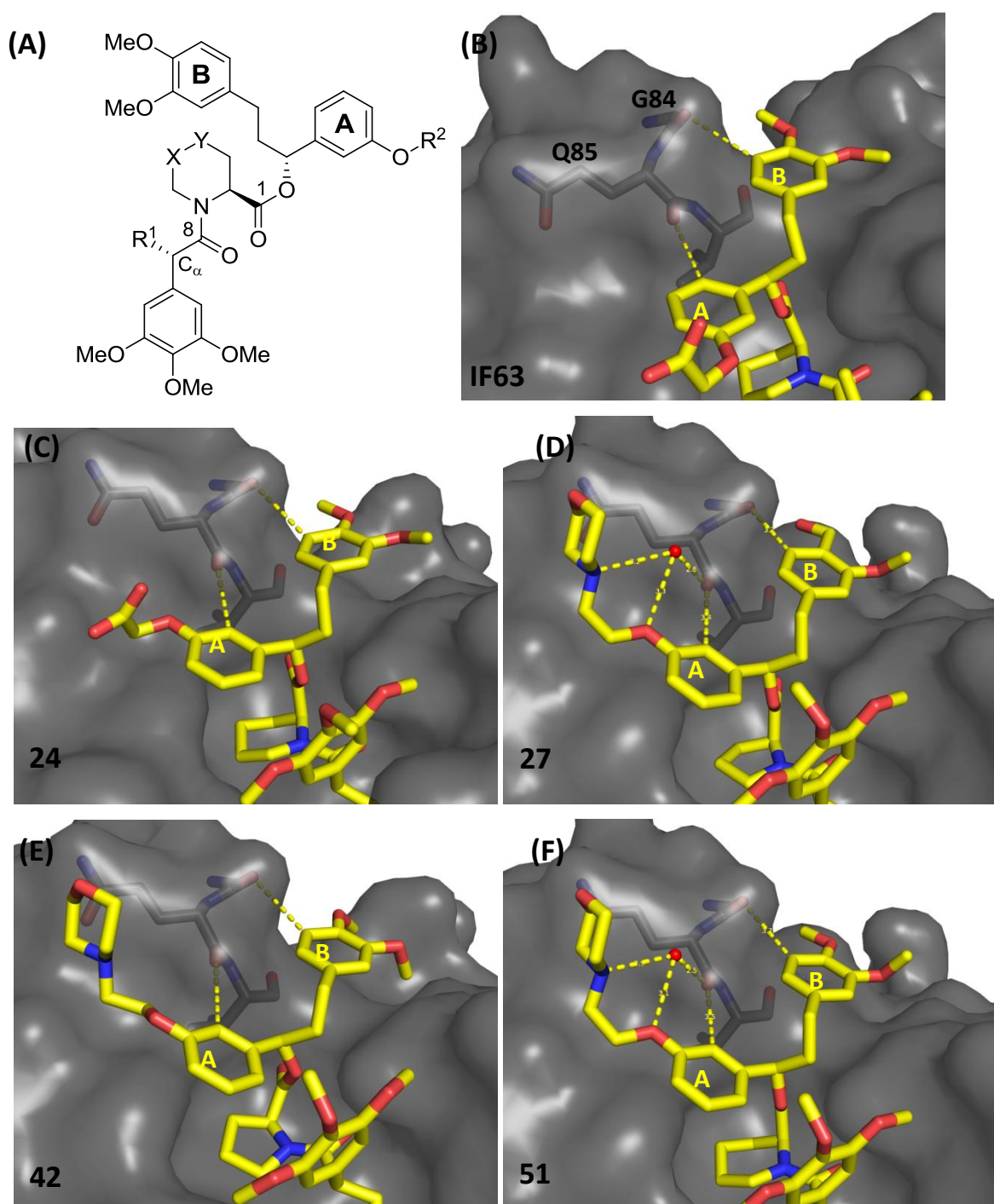


**Fig. 56:** (A) General structure of the ligands. (B) Co-crystal structure of FKBP51FK1 and IF63. (C) Co-crystal structure of FKBP51FK1 and 21. (D) Co-crystal structure of FKBP51FK1 and 27. (E) Co-crystal structure of FKBP51 and 42. (F) Co-crystal structure of FKBP51FK1 and 51.

Ring A forms a hydrogen bond from its ortho position to the amide carbonyl of Q85 and ring B from the meta position to the amide carbonyl of G84. In addition the morpholine co-crystal structures of

**27** and **51** show in addition a bridging water molecule which connects the morpholine amine with the amide carbonyl of Q85. These findings probably explain the strong gain in affinity for the ligands with small C $\alpha$  substituents but cannot explain why in the large cyclohexeny/cyclohexyl series this increase is not present or even reversed. More research on the top group has to be performed to evaluate the SAR.

### 3. Summary and Outlook on Selective FKBP Ligands

Taken together, by using functionally active FKBP51 and FKBP52 mutants that were sensitive to engineered inhibitors (FMSE inhibitors) we unambiguously demonstrate that FKBP ligands can have both neurite outgrowth-stimulating and neurite outgrowth-suppressing effects. Furthermore, the shown results provide a rationale for the design of selective ligands for FKBP51 by exploiting a conformational change which induces an extended binding pocket. We synthesized and evaluated the first selective FKBP51 ligands that bind with low nanomolar affinity and a selectivity of >1000-fold over FKBP52. We further applied these ligands in a cellular assay using mouse neuroblastoma cells (N2a) where selective inhibition of FKBP51 increased the neurite growth. These results replicated our results from the FSSE ligands under basal conditions. We showed that selective inhibition of endogenous FKBP51 has outgrowth-stimulating effects. The net effect of unselective FKBP inhibitors will thus depend on the relative importance of FKBP51 or FKBP52 in each cell type of interest. Neurite outgrowth-promoting substances have repeatedly been shown to enhance neuronal regeneration after neuronal insult, injury or degeneration. In the context of depression or related affective disorders the reduction of neuronal plasticity by the stress-induced FKBP51 is thought to contribute to the behavioral and cognitive deficits observed in these patients. Our results suggest that selective FKBP51 inhibitors could be superior to non-selective FKBP inhibitors at ameliorating these deficiencies.

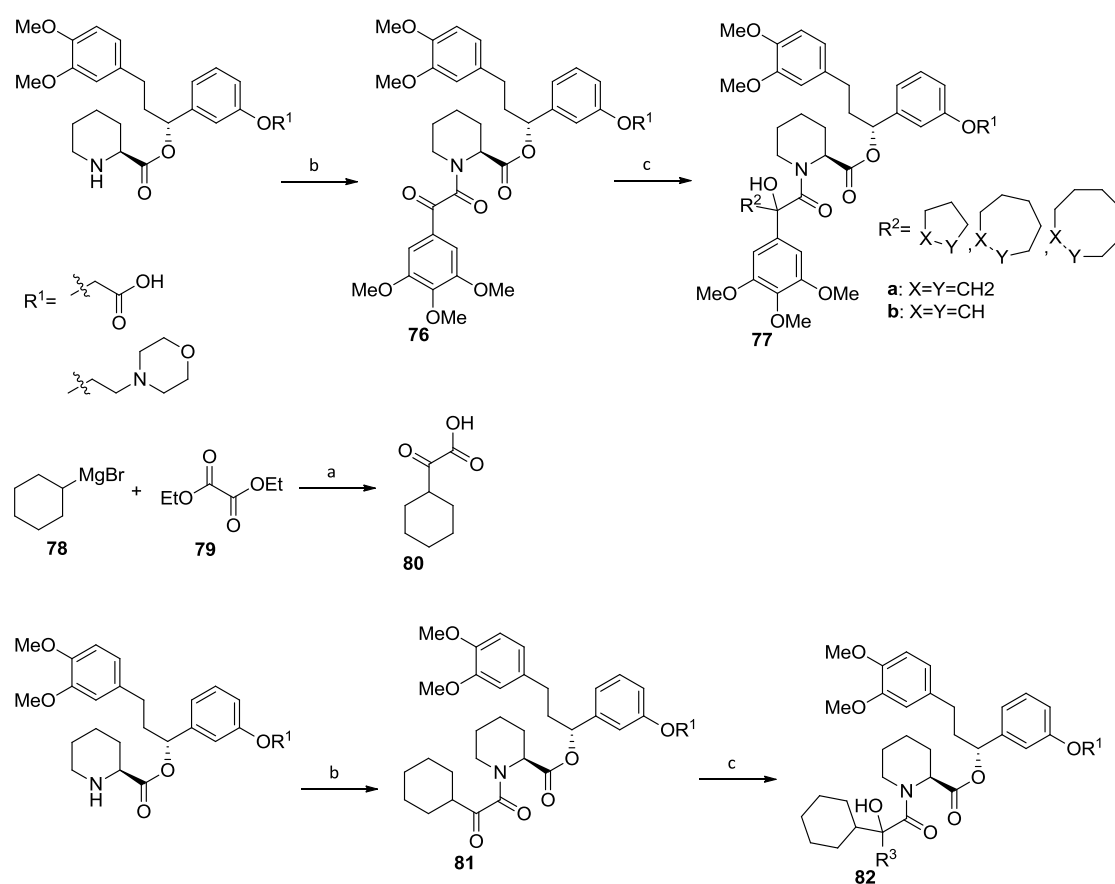
We postulate that our findings on iFit ligands represent a general phenomenon and that all compounds that induce the conformational change described by us will display a bias for FKBP51. Moreover, we believe that the induced additional pocket in FKBP51 discovered by us can be used to rationally design additional FKBP51-selective inhibitors.

Addition of cyclohexylmagnesium bromide to Biricodar in THF at -78°C readily produced **61** as a 1:1 mixture of diastereomers which could be successfully separated by preparative HPLC (**Fig. 57**). This allows for a broad spectrum of reaction types to be employed. The first step is analogous modification with different alkylmagnesium bromides and change to the morpholine top group, that has proven to give an increase in affinity (**Scheme 57**). Up to now cyclohexyl is the biggest C $\alpha$

substituent that is tolerated. Using the Grignard method it is easily possible to increase the ring to cycloheptane or cyclooctane or decrease it to cyclopentane. Further by using cycloalkenylmagnesium bromides it is possible to further modify the rings by Simmons-Smith cyclopropanation, oxidation, halogenation and so forth.

The method could be further optimized by using less reactive organometallic reagents like alkylboron or alkylzinc reagents which can be applied to stereoselective synthesis<sup>135-137</sup>.

With the same methodology but starting from cyclohexyl- $\alpha$ -keto-acetic acid, it is possible to investigate on the trimethoxy moiety. The starting point is 2-cyclohexylacetic acid<sup>138</sup> **80** which is coupled to form **81**. Then a screen with different commercially available aromatic or aliphatic Grignard reagents can be performed (**Scheme 57**) to probe different R<sup>3</sup> parts of the ligand.



**Scheme 57:** (a) HATU, DIPEA, CH<sub>3</sub>CN, RT. (b) RMgBr, THF, -78°C. (c) RMgBr, THF, -78°C.

## 4. Fluorescent Immunophilin Tracers

### 4.1 Synthesis of fluorescent rapamycin derivatives

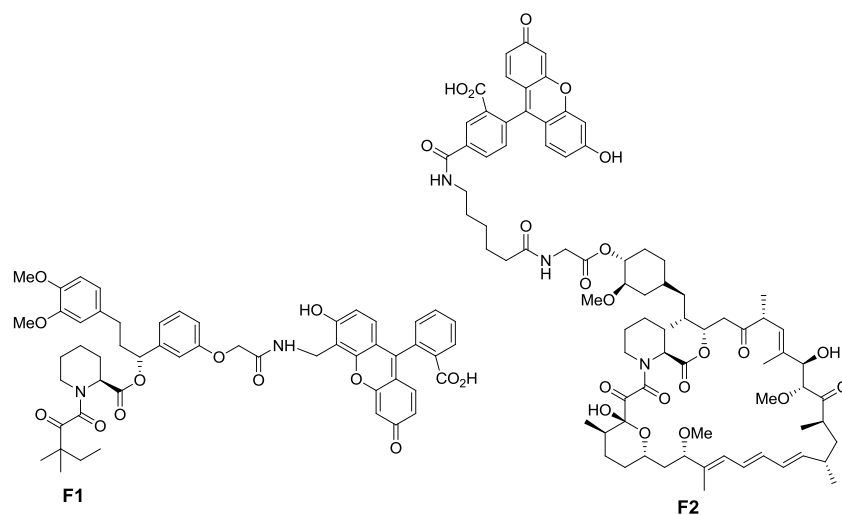


**Fig. 58:** Fluorescent FKBP ligand **F1** and Fluorescent rapamycin derivative **F2**

The best of our small molecule ligands reached the limits of the fluorescence polarization assay using the fluorescent tracer **F1**, due to its binding affinity to FKBP51FK1 of around 400 nM and to FKBP52FK1 of around 900 nM. Therefore using this tracer no compounds can be measured that bind better than around 200 nM for FKBP51. In our group the fluorescent rapamycin derivative **F2** was prepared (**Fig. 58**)<sup>108</sup>. This tracer showed affinity for FKBP51 below 1 nM, and for FKBP52 around 1 nM. With the fluorescence polarization mode of our Tecan plate reader it is possible to measure concentrations of fluorescein-labeled ligands as low as 1 nM. To measure  $K_i$  inhibition constants of ligands in a competition experiment it is necessary to use protein concentration equal to the  $K_i$  of the tracer, and tracer concentrations ideally below half the  $K_i$  value of the tracer. In this case **F2** would have to be used in picomolar concentrations, which is not measurable in polarization mode with our reader. We considered two possible solutions for that problem. First, using a tracer that can be diluted to even lower concentrations, meaning a brighter fluorophore has to be used. Alternatively, a tracer with binding affinity between **F1** and **F2** has to be synthesized. It is difficult to predict how a complex fluorophores like fluorescein would influence the affinity of the ligand, so we started to synthesize a series of fluorescent rapamycin derivatives. We synthesized the C40-glycine modified rapamycin analog **71** according to Kozany et al (**Fig. 59**)<sup>108</sup>. Then we couple different fluorophores bearing an active ester to it.

## B. Results and Discussion

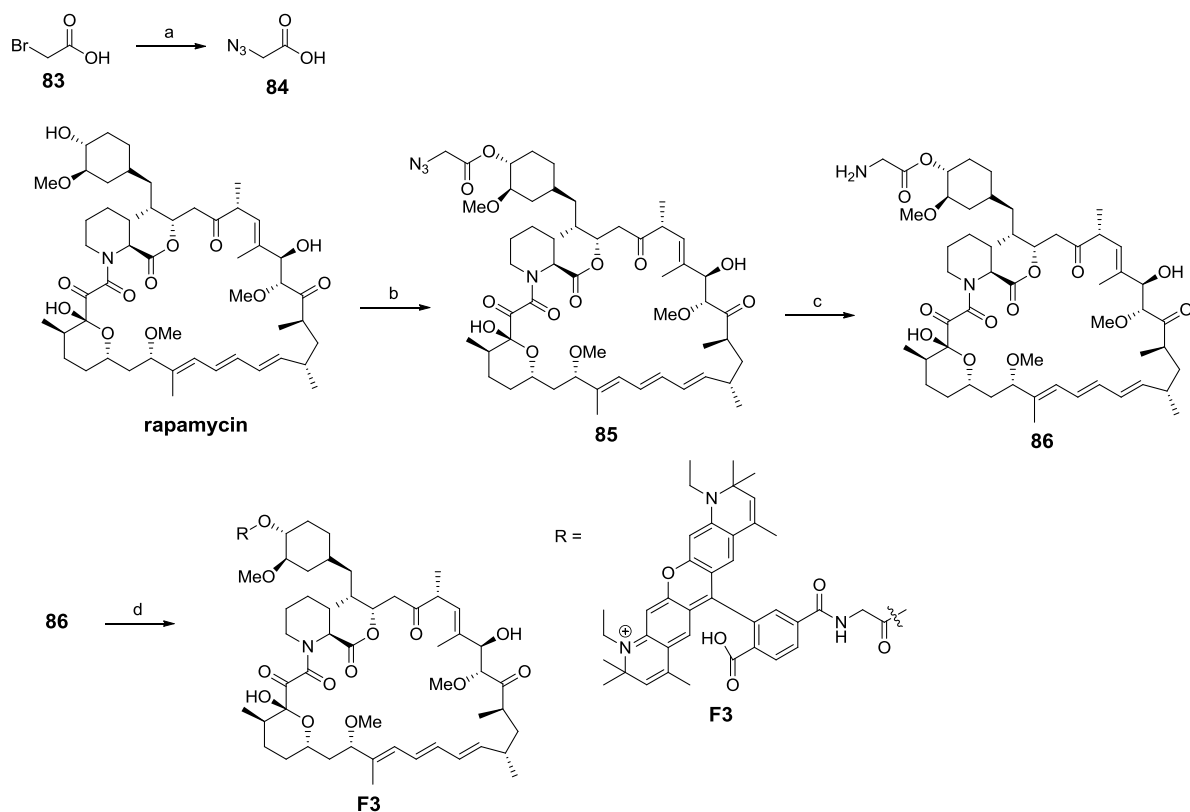


**Fig. 59:** (a)  $\text{NaN}_3$ ,  $\text{H}_2\text{O}$ ,  $0^\circ\text{C-RT}$ , 99%. (b) 2,4,6-trichlorobenzoyl chloride, TEA, DMAP, rapamycin, THF,  $0^\circ\text{C}$ , 33%. (c)  $\text{PPh}_3$ , 3:1 THF/ $\text{H}_2\text{O}$ , RT, 60%. (d) MFP590 (F3-oSu), DIPEA, DMF, RT, 20%.

The MFP590 fluorophore was the first to be employed. Compared to fluorescein it shows a red shifted emission spectrum with an absorption maximum of 597 nm and an emission maximum of 624 nm (**Fig 60**). Red shifted fluorophors offer better signal to noise ratios then green shifted fluorophors like fluorescein.

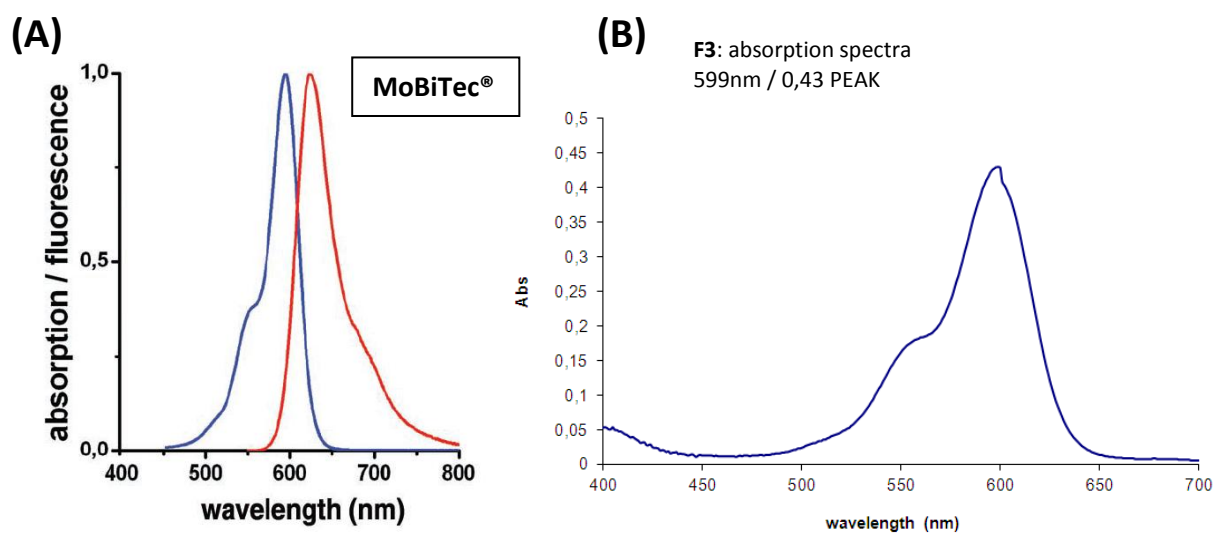


**Fig. 60 (A)** Absorption (blue)/Emission (red) spectra of MFP590  $\epsilon_{\text{Max}} = 1.2 \times 10^5 \text{ L mol}^{-1} \text{ cm}^{-1}$ . **(B)** Absorption spectra of F3, maximum 599 nm.

We recorded an absorption spectra of ligand **F3**, which resembled the reported absorption maxima of the MFP590 (**Fig. 60B**).

We titrated increasing concentrations of protein against **F3** with three concentrations (20 nM, 5 nM, 2 nM) unfortunately this fluorescent rapamycin derivative lost binding affinity for FKBP51FK1 completely. This result is consistent with the findings of Kozany et al who showed that binding affinity for FKBP51 is strongly dependent on the linker length between the ligand and the fluorophor.<sup>108</sup> More fluorophores with different linker length have to be coupled and tested.

## 4.2 Synthesis of a fluorescent iFit ligand

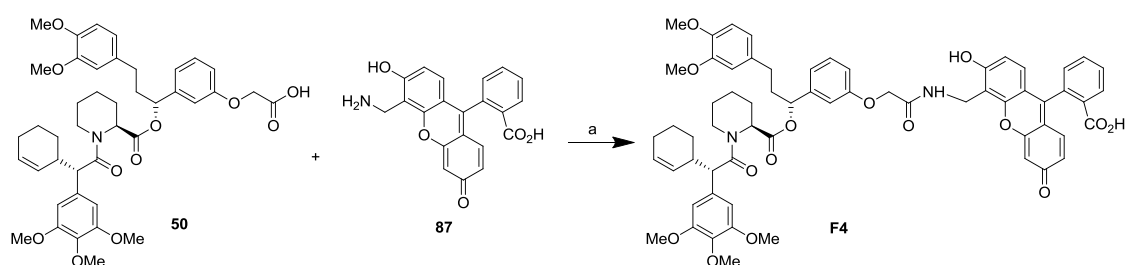


**Fig. 61:** (a) HATU, DIEPA, DMF, 23%

Due to the problems we encountered with the fluorescent rapamycin derivatives we decided to synthesize a fluorescent iFit ligand according to the synthesis of fluorescent derivative **F2** of **SLF** (**Fig. 61**).<sup>108</sup> The free acid of **50** was activated and reacted with aminomethyl-fluorescein to give **F4**.

We recorded an absorption spectra of **F4** which is in line with the spectra of fluorescein showing an absorption maximum at 498nm with an  $\epsilon_{\text{Max}}$  of 46900 L / (mol/cm) (**Fig. 62A**). We performed a FP binding assay and the ligand was able to bind to the FK1 domain of FKBP51 with an  $\text{EC}_{50}$  of  $5.8 \pm 0.3$  nM in addition we calculated the dissociation constant  $K_d = 4.4 \pm 1.2$  nM (**Fig. 62B**). To demonstrate the applicability of the tracer **F4** for the characterization of unlabeled ligands, we tested its performance in FP-competition assays (**Fig. 62C**). The unlabeled iFit ligand **50** was able to efficiently compete the tracer from FKBP51FK1. We determined an  $\text{IC}_{50}$  value of  $69.4 \pm 6.3$  nM and calculated the inhibition constant  $K_i = 23.5 \pm 4.0$  nM. We measured the binding of the fluorescent iFit ligand to FKBP52FK1 and as anticipated the affinity was 500 fold less than for FKBP51FK1. We assessed an  $\text{EC}_{50}$  of  $2611 \pm 340$  nM and calculated a  $K_D$  of  $2945 \pm 1920$  nM (**Fig. 62D**).

In summary, fluorescent iFit ligand **F4** binds 10 fold more potent to FKBP51FK1 than the unlabeled precursor compound **50**, likely due to additional contacts of the conjugated fluorescein. The tracer can be competed by non-labeled ligands which enables its use in FP competition assays. Most important its binding affinity for FKBP51 lies between that of **F1** and **F2** which enables for measuring

binding affinities below 200 nM which was necessary to evaluate our most advanced iFit ligands. Finally, **F4** further demonstrates nicely in a direct binding experiment to FKBP52FK1 the selectivity of the iFit ligands for FKBP51.

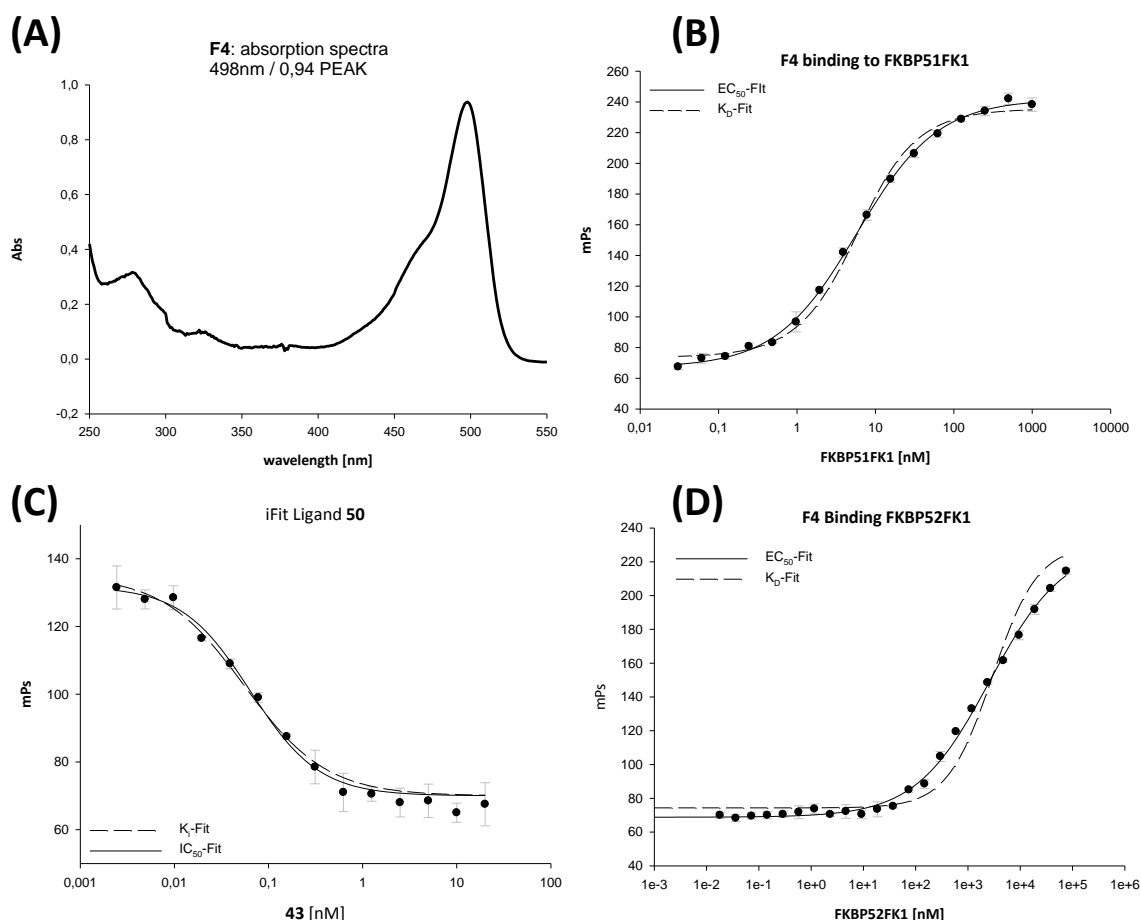


**Fig. 62:** (A) Absorption spectra of **F4** (5.4  $\mu\text{M}$ ), maximum 498 nm.  $\epsilon_{\text{Max}} = 46900 \text{ L} / \text{mol}^{-1} \text{ cm}^{-1}$ . (B) Binding of 3 nM **F4** to FKBP51FK1 measured by fluorescence polarization. (C) Competition of **F4** (3 nM) with **50** for the binding to FKBP51FK1 (4.5 nM). (D) Binding of 3 nM **F4** to FKBP52FK1 measured by fluorescence polarization.

### 4.3 Facile synthesis of a fluorescent CsA analogue to study Cyclophilin 40 and Cyclophilin 18 ligands

Cyp40 is a modulator of steroid hormone receptors and a further potential Hsp90 and SHR-associated drug target. To be able to screen for novel inhibitors for this immunophilin a fluorescein-labeled CsA analogue was synthesized.

This tracer was produced by a facile four step synthesis (**Scheme 23**). We show the binding of this tracer to Cyp40 and Cyp18 by measuring the fluorescent polarization change and demonstrate its

competition with Cyclosporin A. The binding data was confirmed using an enzymatic PPIase assay. The described tracer allows for a robust assay in a high throughput format to support the development of novel Cyp40 ligands. The results were published in Journal of medicinal chemistry letters (Gali et al).<sup>139</sup>

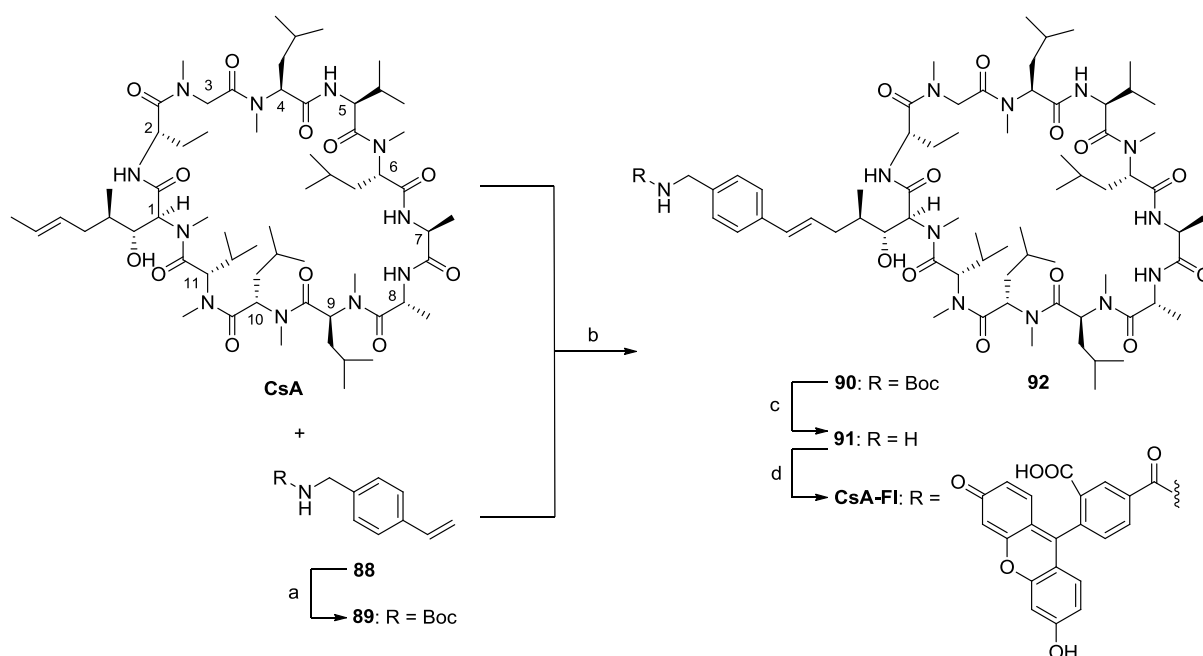


**Fig. 63:** (a) Boc<sub>2</sub>O, TEA, MeOH, RT, quant. (b) Grubbs Cat. II, Gen, DCM, reflux, 52% (c) 10% TFA, DCM, 0°C, 81%. (d) NHS-fluorescein, TEA, DCM/THF 2:1, RT, 23%.

#### 4.3.1 Synthesis of the tracer

The unselective cyclic undecapeptide cyclosporin A (CsA, **Scheme 23**) binds unspecifically to the class of cyclophilins in the nanomolar range. It is clinically used as an immunosuppressive drug<sup>140</sup>. We used **CsA** as a starting point for our tracer synthesis. By analyzing the co-crystal structure of Cyp18/**CsA** we noticed, that the terminal trans-alkene moiety of the unnatural aminoacid butenyl-methyl-L-threonine (position 1 of **CsA** in **Scheme 23**) points out of the binding pocket, and is solvent accessible.<sup>141</sup> This alkene is very suitable for a Grubbs metathesis reaction and thus can be used to introduce the fluorescent label.

We decided to attach an amine containing linker to **CsA** that could be easily coupled to carboxy-containing fluorophores. We first tried to couple Boc-allylamine or allylammoniumchloride to **CsA** which resulted in poor yields probably because metathesis catalysts are known to be sensitive to primary amines that are in close distance to the double bond. We thought to overcome this problem by using a longer linker. Therefore we first protected commercially available paravinylamino-

benzene **88** with  $\text{Boc}_2\text{O}$  to obtain **89** with quantitative yields. This was then coupled to CsA using second generation Grubbs catalyst to give **90** in good yields. The primary amine was liberated using 10% TFA to produce **91** which was reacted with 5/6-carboxyfluorescein N-hydroxysuccinimide (NHS-Fluorescein) to give the final compound **CsA-FI**.

#### 4.3.2 Development of a fluorescence polarization assay for cyclophilin 40 and Cyp18

The proteins Cyp40 and Cyp18 were cloned and expressed according to Gaali et al.<sup>139</sup> The functionality of the purified proteins was verified by a coupled enzymatic assay measuring their PPIase activity. We determined  $K_d$  values of  $106 \pm 13$  nM for Cyp40 and  $12 \pm 2$  nM for Cyp18 (Fig. 64A, Tab. 8). The absolute change in anisotropy was substantially larger for Cyp40 compared to Cyp18, likely reflecting the bigger size of the former. To verify the binding affinity of tracer **CsA-FI** to Cyp40 and Cyp18, a coupled enzymatic PPIase assay was performed (Fig. 65).<sup>142</sup> The measured values of  $101 \pm 24$  nM for Cyp40 and  $12 \pm 4$  nM for Cyp18 match very well with the FP-assay results shown above.

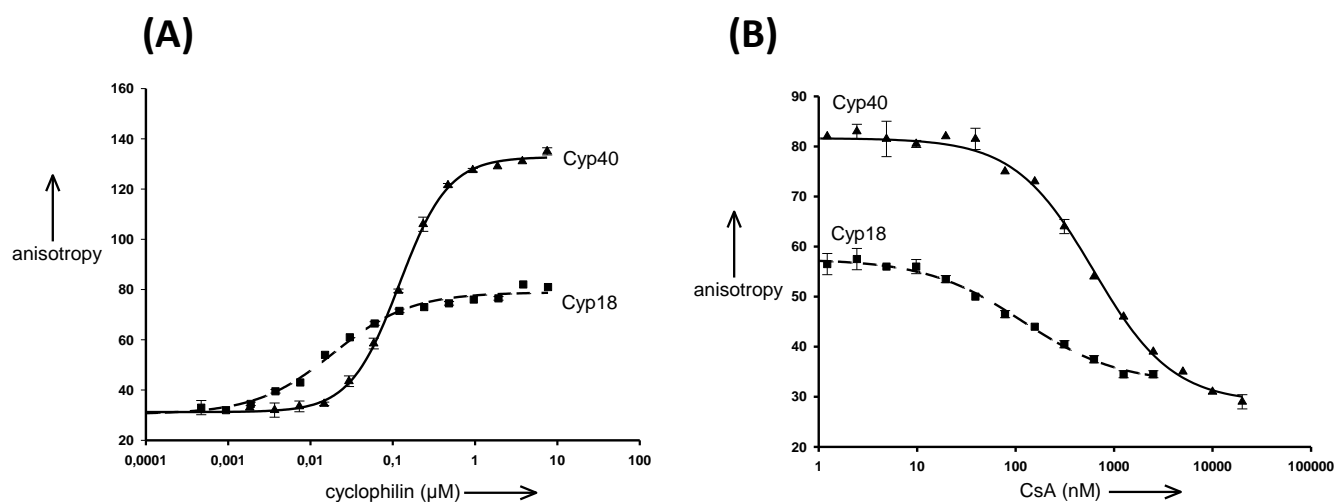


**Fig. 64:** (a) Binding of CsA-FI (10 nM) to Cyp18 and Cyp40 measured by fluorescence polarisation. (b) Competition of CsA with CsA-FI (10 nM) for the binding to Cyp18 (10 nM) and Cyp40 (100 nM) measured by fluorescence polarisation.

To demonstrate the use of the tracer **CsA-FI** for the characterization of unlabeled ligands, we tested its performance in FP-competition assays (Fig. 64B). The prototypic ligand **CsA** could efficiently compete with **CsA-FI** for the binding to Cyp40 and Cyp18. The measured  $K_d$  values were again

corroborated with a PPlase assay (**Fig. 65, Tab. 8**). For Cyp40 there was an excellent match between FP and PPlase results while for Cyp18 a slightly lower  $K_i$  was observed in the PPlase assay.

In general, **CsA-FI** binds slightly more potent to both Cyp18 and Cyp40 than CsA likely due to additional contacts of the conjugated fluorescein. The affinities measured in this work are consistent with the literature values for Cyp40 as well as with the majority of reports for Cyp 18. For Cyp18 substantial discrepancies in CsA affinities have been reported. The consensus values, however, match very well with the results reported in this work.<sup>29</sup>

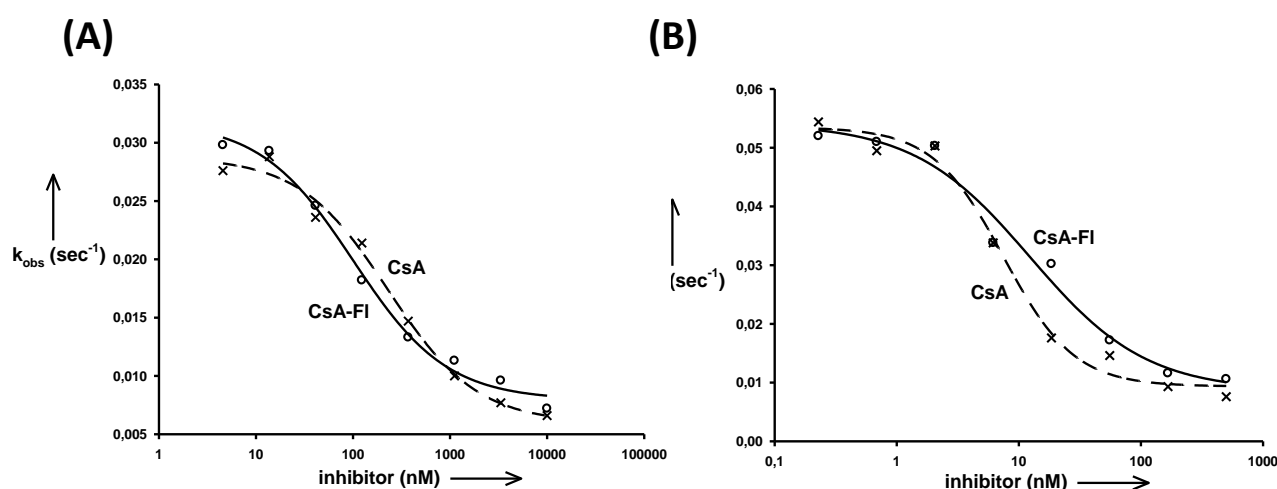


**Figure 65** : (A) Inhibition of the PPlase activity of Cyp40 (100 nM) by CsA (dashed, X) and CsA-FI (continuous, O). (A) Inhibition of the PPlase activity of Cyp18 (10 nM) by CsA (dashed, X) and CsA-FI (continuous, O).

	Cyclophilin	FP-assay ( $K_i$ or $K_D$ )	PPlase assay ( $K_i$ )
<b>CsA</b>	Cyp40	$227 \pm 22$	$231 \pm 55$
	Cyp18	$34 \pm 6$	$7 \pm 1$
<b>CsA-FI</b>	Cyp40	$106 \pm 13$	$101 \pm 24$
	Cyp18	$12 \pm 1$	$12 \pm 4$

**Table 8:** Binding and inhibition constants (nM) measured by fluorescence polarization or by an enzymatic PPlase assay

In summary, we developed a facile synthesis of a fluorescein-labelled tracer **CsA-FI**, which shows high affinity binding to Cyp40 and Cyp18. The tracer can be competed by CsA. Therefore **CsA-FI** enables a fluorescence polarisation assay in high throughput format, which can be used for screening and subsequent profiling of inhibitors of Cyp40 to identify structures for the development of potential new drugs against breast and prostate cancer.

## C. Experimental Section

### 1. Analytical Methods

#### 1.1 Nuclear magnetic resonance

$1D$   $^1H$ ,  $^{13}C$ -NMR and  $2D$  HSQC, HMBC and COSY were recorded at the department of chemistry and pharmacy of the LMU on a Bruker AC 300, a Bruker XL 400, or a Bruker AMX 600 at room temperature. Chemical shifts for  $^1H$  or  $^{13}C$  are given in ppm ( $\delta$ ) relative to tetramethylsilane (TMS) as internal standard.  $CDCl_3$  and  $d_6$ -DMSO were used as solvents.  $^1H$  and  $^{13}C$  spectra were calibrated on the specific solvent. The coupling constants (J) are given in Hertz (Hz). The multiplicities are abbreviated as singlet (s), doublet (d), triplet (t), quartet (q) and multiplet (m).

#### 1.2 Mass spectroscopy

Mass spectra ( $m/z$ ) were recorded on a Thermo Finnigan LCQ DECA XP Plus mass spectrometer at the Max Planck Institute of Psychiatry, while the high resolution mass spectrometry was carried out at MPI for Biochemistry (Microchemistry Core facility) on Varian Mat711 mass spectrometer.

#### 1.3 HPLC

The purity of the compounds was verified by reversed phase HPLC. All gradients were started after 1 min of equilibration with starting percentage of solvent mixture.

##### Analytical:

<b>Pump:</b>	Beckman System Gold 125S Solvent Module
<b>Detector:</b>	Beckman System Gold Diode Array Detector Module 168
<b>Column:</b>	Phenomenex Jupiter 4 $\mu$ Proteo 90Å, 250 x 4.6 mm 4 micron

## C. Experimental Section

---

**Solvent A:** 95% H<sub>2</sub>O  
5% CH<sub>3</sub>CN  
0.1% TFA

**Solvent B:** 95% CH<sub>3</sub>CN  
5% H<sub>2</sub>O  
0.1% TFA

**Standard Gradient:** 0-100% B in 20min, 1 ml/min

### Detection

**wavelength:** 220nm/280nm

### Chiral:

**Pump:** Waters 515 HPLC Pump

**Detector:** LDC Analytical Spectromonitor 5000 Photodiode Array Detector

**Column:** DAICEL Chemical Industries LTD. Chiralcel OD-H

**Solvent A:** Hexane

**Solvent B:** i-propanol

**Standard Gradient:** 1:1 60 min, 0.5 ml/min

**Detection**

**wavelength:** 220nm

### Preparative:

**Pump:** Beckman System Gold Programmable Solvent Module 126 NMP

**Detector:** Beckman Programmable Detector Module 166

**Column:** Phenomenex Jupiter 10 $\mu$  Proteo 90 Å, 250 x 21.2 mm 10 micron

**Methods:** Described at the specific compound

### Semi-

### preparative:

**Pump:** Beckman System Gold 125S Solvent Module

**Detector:** Beckman System Gold Diode Array Detector Module 168

**Column:** Phenomenex Jupiter 10 $\mu$  Proteo 90 Å, 250 x 10 mm 10 micron

**Methods:** Described at the specific compound

**LC-MS:**

<b>Pump:</b>	Beckman System Gold 125S Solvent Module
<b>Detector:</b>	System Gold Diode Array Detector Module 168
<b>Column:</b>	YMC Pack Pro C8, 100 x 4.6 mm, 3 $\mu$ m
<b>Solvent A:</b>	95% H <sub>2</sub> O 5% CH <sub>3</sub> CN 0.1% Formic acid
<b>Solvent B:</b>	95% CH <sub>3</sub> CN 5% H <sub>2</sub> O 0.1% Formic acid
<b>Standard Gradient:</b>	0-100% B in 11 min, 1 ml/min
<b>Detection wavelength:</b>	220nm, 280nm

## 1.4 Silica chromatography

For manual column chromatography, Silicagel 60 (Roth) with a particle size of 0.04-0.063 mm was used. Automated flash chromatography was performed, using an Interchim Puriflash 430 with an UV detector at 254 nm. Preparative thin layer chromatography (TLC) was performed on glass plates coated with 2 mm SiO<sub>2</sub> (Merck SIL-G-200, F-254,).

For TLC aluminum plates coated with SiO<sub>2</sub> (Merck 60, F-254) were used. The spots were visualized by UV light and/or by staining of the TLC plate with one of the solutions below followed, if necessary, by heating with a heat gun.

Hanessians: 5 g Ce(SO<sub>4</sub>)<sub>2</sub>, 25 g NH<sub>4</sub>Mo<sub>7</sub>O<sub>24</sub> 4 H<sub>2</sub>O, 450 mL H<sub>2</sub>O, 50 mL H<sub>2</sub>SO<sub>4</sub>

Ninhydrin: 0.5 g Ninhydrin, 100 mL EtOH, 5mL AcOH

Kaliumpermanganat: 1.5 g KMnO<sub>4</sub>, 10 g K<sub>2</sub>CO<sub>3</sub>, 1.25 mL 10% NaOH in 200 mL H<sub>2</sub>O

## 1.5 Data analysis of neurite outgrowth

The handling and treatment of N2a cells was performed by Alexander Kirschner. Pictures of cells were provided as image files. Data analysis was performed using the open source program ImageJ (<http://rsbweb.nih.gov/ij/>) and the plugin NeuronJ to measure the neurite length. Per lane of the diagrams neurites of 20-30 cells were measured and the average with standard error was plotted using Sigmaplot11.

## 2. Reagents and solvents

### 2.1 Reagents

Reagents were obtained from *ABCR, Aldrich, Alfa Aeser, Fluka, Merck, Novabiochem, Roth, Sigma Aldrich* and *Synchem* in common qualities puriss., p.a. or purum and used without further purification.

Compound name	CAS No.	Company	Product code	Purity
Allylmagnesium bromide 1M in THF	1730-25-2	Aldrich	225754	-
4'-(Aminomethyl)fluorescein hydrochloride	91539-64-9	Invitrogen	1032248	≥95
3-Bromocyclohexene	1521-51-3	ABCR	AB114158	95%
Benzoylformic acid	611-73-4	Merck	8.41629	95%
Cyclohexanone	108-94-1	Aldrich	398241	99%
Cyclohexene	110-83-8	Fluka	29230	≥99.5%
Cyclohexylmagnesium bromide (1 M, in THF)	931-50-0	ABCR	AB140471	-

### C. Experimental Section

---

Dicyclohexylacetic acid	52034-92-1	Aldrich	333840	99%
DCC	538-75-0	Aldrich	D,800-2	99%
Diphenylacetic acid	117-34-0	Aldrich	D204307	99%
3,4-Dimethoxybenzaldehyde	120-14-9	Aldrich	143758	99%
DIPEA	7087-68-5	Fluka	03440	99%
DMAP	1122-58-3	Aldrich	522805	99%
EDC	25952-53-8	Fluka	03449	≥99.0%
Formic acid	64-18-6	Roth	4724.3	≥98%
Grubbs Catalyst 2 <sup>nd</sup> Gen.	246047-72-3	Aldrich	569747	≥99
Fmoc-Pro-OH	71989-31-6	Novabiochem	852017	≥98%
HATU	148893-10-1	Novabiochem	8.51013	≥99%
HOAt	39968-33-7	ABCR	AB281963	-
HCl	7647-01-0	Roth	9277.1	37%
3'-Hydroxyacetophenone	121-71-1	Aldrich	328103	≥99%
1-Hydroxy-7-azabenzotriazole	39968-33-7	ABCR	AB281963	≥99
In(OTf) <sub>3</sub>	128008-30-0	Aldrich	442151	≥99%
Iodomethylcyclopropane	33574-02-6	Synchem	CIC048	95%
KMnO <sub>4</sub>	7722-64-7	Merck	1.05082	≥99%
K <sub>2</sub> CO <sub>3</sub>	584-08-7	Roth	X894.2	≥99.9%
KI	7681-11-0	Roth	8491.1	≥99 %
KOH	1310-58-3	Roth	6751.1	≥95%
LiCl	7447-41-8	Aldrich	L9650	≥99 %
LiHMDS 1M in THF	4039-32-1	Aldrich	22,577-0	-

### C. Experimental Section

---

L-Pipecolinic acid	3105-95-1	Alfa Aesar	L15373	99%
LiOH	1310-65-2	Sigma	545856	≥99 %
4-Methyl piperidine	626-58-4	Aldrich	M73206	96%
MgSO <sub>4</sub>	7487-88-9	Roth	0261.3	99%
NaCl	7647-14-5	VWR	27810.295	99.8 %
n-BuLi 2M in cyclohexane	109-72-8	Aldrich	302120	-
NaH 60% dispersion	7646-69-7	Aldrich	45,291-2	60%
NaHCO <sub>3</sub>	144-55-8	Roth	8551.1	≥ 99 %
NaHMDS 1M in THF	1070-89-9	Aldrich	24558-5	-
NaNO <sub>2</sub>	7632-00-0	Roth	8604.1	≥98.7%
NH <sub>4</sub> Cl	12125-02-9	Merck	1.01145	99.8 %
2-Nitrobenzenesulfonyl chloride	1694-92-4	Aldrich	N1,150-7	97%
Noyori catalyst	212143-24-3	ABCR	AB131601	90%
4-Phenoxystyrene	4973-29-9	ABCR	AB173746	90%
Pd/C	7440-05-3	Aldrich	75992	5%
Pentafluorophenol	771-61-9	Aldrich	103799	99%
(S)-4-iso-Propyloxazolidin-2-one	17016-83-0	Aldrich	298883	99%
(S)-Pyrrolidine-2-carboxylic acid	147-85-3	Fluka	81710	≥99%
(1S,2S)-(+)-Pseudoephedrine	90-82-4	Aldrich	287636	98%
Rapamycin	53123-88-9	Cfm Oskar Tropitzsch	53123-88-9	≥95%
tert-Butyl bromoacetate	5292-43-3	Fluka	17035	≥97%
Tetraallyltin	7393-43-3	VWR	C04W023	96%

### C. Experimental Section

---

Triethylamine	121-44-8	Merck	8.08352	99%
3,4,5-Trimethoxyphenyl acetic acid	951-82-6	ABCR	AB125360	99%
TFA	76-05-1	Roth	P088.2	≥99.9%

## 2.2 Non-commercial reagents

**5b**, **5c**, **5e**, **25** and **26** were provided by the Lead Discovery Center in Dortmund. **5d** was kindly provided by Yansong Wang (RG Hausch, MPI Psychiatry). The fluorescent tracers **F1** and **F2** were prepared as described in Kozany et al.<sup>108</sup> by Christoph Kress (RG Hausch, MPI Psychiatry).

## 2.3 Solvents

Solvents were purchased from Roth or Sigma Aldrich with qualities, ROTOSOLV, ROTIPURAN; ROTIDRY or HPLC quality with ≥99% purity. Anhydrous solvents were used from Sigma Aldrich with sure seals.

Compound name	CAS No.	Company	Product code	Purity
n-Hexane	110-54-3	Roth	7339.1	≥98%
Cyclohexane	110-82-7	Roth	6570.4	≥99.5%
Ethylacetate	141-78-6	Roth	CP42.6	≥ 99.5%
Chloroform	67-66-3	Roth	Y015.3	≥ 99%
CDCl <sub>3</sub>	865-49-6	Roth	Ae54.1	≥ 99.38 %
Dichloromethane	75-09-2	Roth	6053.5	≥ 99.5%
Dichloromethane sure seal,	75-09-2	Aldrich	270997	≥ 99.8%

≥99.8 anhydrous)

Tetrahydrofuran (sure seal, ≥99.9 anhydrous)	109-99-9	Aldrich	Ae07.1	≥ 99.9%
2-propanol	67-63-0	Roth	7343.1	≥ 99.9%
Acetone	67-64-1	Roth	5025.4	≥ 99.5 %
Methanol	67-56-1	Roth	8388.4	≥ 99 %
Methanol HPLC	67-56-1	Roth	7342.1	≥ 99.9 %
Acetonitrile HPLC	75-05-8	Roth	8825.2	≥ 99.9%
Toluene	108-88-3	Roth	Ae06.1	≥ 99.5 %
Diethylether	60-29-7	Roth	T900.1	≥ 99.8 %
DMF	68-12-2	Roth	A5291.1	99%
DMF (sure seal, ≥99.8 anhydrous)	68-12-2	Aldrich	227056	≥99.8

### 3. General procedures

All reactions were carried out with magnetic stirring and, when air or moisture sensitive, in flame-dried glassware under argon (Westfalen, 99.999 Vol% Klasse 5.0). Syringes were used to transfer reagents. Reagents used in very moisture-sensitive reactions were dried overnight under high vacuum ( $< 1 \times 10^{-2}$  mbar).

### 4. Synthesis of used compounds

#### 4.1 General synthesis procedure A for the coupling of morpholine containing top-groups

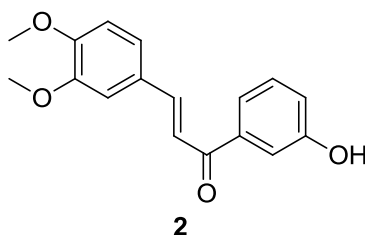
The alkylated acid (20 mg, 75  $\mu\text{mol}$ ) was dissolved in 300  $\mu\text{L}$  DCM or DMF, then DIPEA (41  $\mu\text{L}$ , 0.24 mmol) and HATU (46 mg, 0.12 mmol) were added and stirred for 15 min. Subsequently, the different top groups with a free secondary amine (32 mg, 60  $\mu\text{mol}$ ) in 300  $\mu\text{L}$  DCM were added and stirred for 14 h. The reaction mixture was concentrated and flash chromatographed or purified by preparative HPLC.

## 4.2 General synthesis procedure B for the coupling of free acid top-groups

The alkylated acid (57 mg, 0.21 mmol) and DIPEA (0.13 mL, 0.78 mmol) were dissolved in dry DCM (2 mL) at RT and stirred for 15min. Then, HATU (110 mg, 0.29 mmol) was added and stirred for another 15min. Subsequently, the different top groups with a free secondary amine (32 mg, 0.06 mmol) in 300 $\mu\text{L}$  DCM was added and stirred for 14 h. The raw product was purified with flash chromatography and then the acid was liberated using 10% TFA in DCM at RT for 5h. The reaction mixture was concentrated and flash chromatographed or purified by preparative HPLC.

## 4.3 Synthetic procedures

### (E)-3-(3,4-Dimethoxyphenyl)-1-(3-hydroxyphenyl)prop-2-en-1-one (2)



3,4-Dimethoxybenzaldehyd (30.6 g, 184 mmol) and 3-hydroxyacetophenone (25 g, 184 mmol) were dissolved in 250 mL EtOH and cooled to 0°C in an ice bath. KOH (41.2 g, 734 mmol) was dissolved in 200 mL H<sub>2</sub>O, cooled to ~10°C and added to the aforementioned ketone/aldehyde solution. The reaction mixture was allowed to warm to RT and stirred for 16 h. The solution was poured into an erlenmayer flask filled with ice. The ice-cooled solution was acidified with conc. HCl to pH<2. An

orange solid precipitated, which was filtered and afterwards dissolved in EtOAc. The product **2** was used without further purification (51.57g, 181 mmol, 99%).

**TLC** [EtOAc/n-hexane 1:1.5]:  $R_f = 0.31$ .

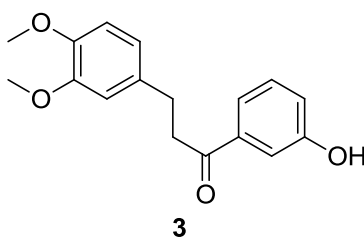
**HPLC** [0-100% Solvent B, 30 min]:  $R_t = 20.8$  min, purity (220 nm) = 95%

**$^1\text{H-NMR}$**  (300 MHz,  $\text{CDCl}_3$ ):  $\delta = 7.71$  (d,  $J = 6.6$  Hz, 2H), 7.61 (d,  $J = 7.7$  Hz, 1H), 7.53 (d,  $J = 1.7$  Hz, 1H), 7.47 (d,  $J = 1.7$  Hz, 1H), 7.39-7.34 (m, 2H), 7.07-7.00 (m, 2H), 3.87 (s, 3H), 3.82 (s, 3H).

**$^{13}\text{C-NMR}$**  (150 MHz,  $\text{CDCl}_3$ ):  $\delta = 189.3, 158.4, 151.6, 149.2, 144.5, 139.5, 129.9, 127.5, 123.9, 120.1, 119.8, 119.5, 114.7, 112.0, 111.1, 56.1, 55.8$ .

**Mass** ( $\text{ESI}^+$ ): calculated  $[\text{C}_{17}\text{H}_{16}\text{O}_4 + \text{H}]^+$  285.11, found 285.00  $[\text{M} + \text{H}]^+$ .

### 3-(3,4-Dimethoxyphenyl)-1-(3-hydroxyphenyl)propan-1-one (**3**)



100 mg Lindlar catalyst was placed into an autoclave (Modell II, Roth) and the autoclave was flushed with argon. (E)-3-(3,4-Dimethoxyphenyl)-1-(3-hydroxy-phenyl)prop-2-en-1-one **1** (25,6 g, 90 mmol) **1** was dissolved in 150 mL MeOH and poured into the autoclave, which was then closed and again flushed with argon. Then, 30 bar hydrogen gas (Westfalen, 99,999 Vol% Klasse 5.0) was introduced into the autoclave and the solution was stirred for 72 h at RT. The raw product was filtered through cellite and MeOH was evaporated *in vacuo*. Purification was performed by manual column chromatography with EtOAc/n-hexane 1:2 to afford **3** (22.65g, 79 mmol, 88%) as a white solid.

**TLC** [EtOAc/n-Hex 1:2]:  $R_f = 0.27$ .

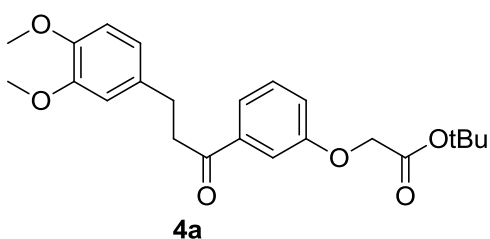
**HPLC** [0-100% Solvent B, 30 min]:  $R_t = 20.9$  min, purity (220 nm) = 96%

<sup>1</sup>H-NMR (300 MHz, CDCl<sub>3</sub>): δ = 7.55 - 7.45 (m, 2H), 7.31 - 7.24 (m, 1H), 7.05 (d, *J* = 1.8 Hz, 1H), 6.8 - 6.75 (m, 3H), 3.87 (s, 3H), 3.82 (s, 3H), 3.25 (t, *J* = 7.4 Hz, 2H), 2.98 (t, *J* = 7.5 Hz, 2H).

<sup>13</sup>C-NMR (150 MHz, CDCl<sub>3</sub>): δ = 200.1, 156.2, 149.5, 147.0, 139.1, 132.1, 130.0, 122.0, 120.3, 114.9, 112.3, 112.8, 56.1, 43.9, 30.9.

HRMS (EI<sup>+</sup>): calculated [C<sub>17</sub>H<sub>18</sub>O<sub>4</sub> + H]<sup>+</sup> 287.1205, found 287.1278 [M + H]<sup>+</sup>.

### tert-Butyl-2-[3-{3-(3,4-dimethoxyphenyl)propanoyl}phenoxy] acetate (4a)



To a solution of 3-(3,4-Dimethoxyphenyl)-1-(3-hydroxyphenyl)propan-1-one **3** (2 g, 7.0 mmol) and K<sub>2</sub>CO<sub>3</sub> (1.9 g, 14.0 mmol) in 20 mL acetone was added tert-butyl-bromoacetate (1.1 mL, 7.7 mmol) and stirred for 20 h at RT. K<sub>2</sub>CO<sub>3</sub> was filtered out and washed with acetone. The solvent was removed *in vacuo*. The raw product was dissolved in EtOAc and washed 3 times with brine. The aqueous phase was extracted with EtOAc. The combined organic layers were dried over MgSO<sub>4</sub>. The crude product was concentrated and purified by column chromatography (EtOAc/n-Hexane, 1:2) **4a** (2.06g, 5.14 mmol, 74%).

TLC [EtOAc/n-Hexane 1:2]: R<sub>f</sub> = 0.32

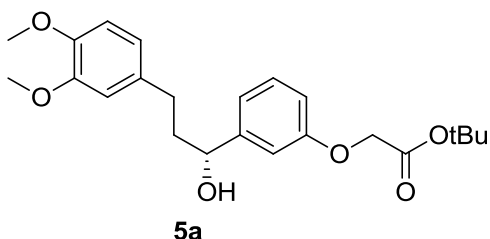
HPLC [0-100% Solvent B, 30 min]: R<sub>t</sub> = 26.2 min, purity (220 nm) = 98%

<sup>1</sup>H-NMR (300 MHz, CDCl<sub>3</sub>): δ = 7.59 (d<sub>q</sub>, *J* = 5.4 Hz, *J* = 0.9 Hz, 1H), 7.48 (d<sub>d</sub>, *J* = 1.2 Hz, *J* = 1.5 Hz, 1H), 7.38 (t, *J* = 8.1 Hz, 1H), 7.16 - 7.12 (m, 1H), 6.84 - 6.78 (m, 3H), 4.58 (s, 2H), 3.89 (s, 3H), 3.87 (s, 3H), 3.27 (t, *J* = 8.1 Hz, 2H), 3.02 (t, *J* = 6.9 Hz, 2H), 1.51 (s, 9H).

<sup>13</sup>C-NMR (150 MHz, CDCl<sub>3</sub>): δ = 198.9, 167.6, 158.2, 149.0, 147.5, 138.3, 133.8, 129.7, 121.5, 120.2, 120.1, 113.13, 111.9, 111.4, 82.62, 65.7, 56.0, 40.8, 29.8.

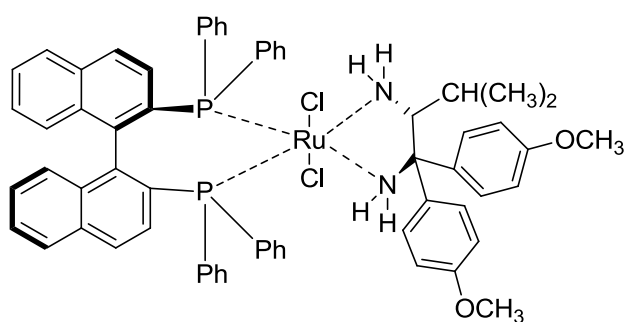
Mass (ESI<sup>+</sup>): calculated without t-butyl [C<sub>23</sub>H<sub>28</sub>O<sub>6</sub>+ H]<sup>+</sup> 345.13, found 345.20 [M + H]<sup>+</sup>.

**(R)-tert-Butyl-2-[3-{3-(3,4-dimethoxyphenyl)-1-hydroxypropyl}phenoxy]acetate (5a)**



tert-Butyl-2-[3-{3-(3,4-dimethoxyphenyl)propanoyl}phenoxy]acetate **4a** (2.06 g, 5.14 mmol) was dissolved in isopropanol and filled into an autoclave (Roth, Modell II). Then K<sub>2</sub>CO<sub>3</sub> (0.71 g, 5.14 mmol) was added and flushed with argon. Noyori catalyst (46 mg, 41 μmol, **Scheme. 24**) was added and after closing the autoclave, it was flushed again with argon. Now 35-40 bar hydrogen gas (Westfalen, 99,999 Vol% Klasse 5.0) was filled into the autoclave and the solution was stirred for 72h. The raw product was filtered through cellite and the solvent was removed under reduced pressure.

The product was purified by column chromatography (EtOAc/n-Hex, 1:2). **5a** (1.73g, 4.28 mmol, 83%) was obtained as a white solid. The enantiomeric excess (ee = 98%) was determined using chiral analytical HPLC.



**Noyori catalyst** (ABCR, AB131601)

**TLC** [EtOAc/n-Hex 1:2]: R<sub>f</sub> = 0.25.

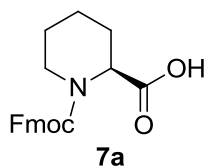
**HPLC** (Chiral): [i-Propanol/n-hexane, isochratic, 1:1 60 min]: R<sub>t</sub> = 37 min, purity (220 nm) = 97%

**<sup>1</sup>H-NMR** (300 MHz, CDCl<sub>3</sub>): δ = 7.29 – 7.21 (m, 1H), 6.98 – 6.90 (m, 2H), 6.80 – 6.70 (m, 4H), 4.69 – 4.66 (m, 1H), 4.52 (s, 2H), 3.86 (s, 3H), 3.85 (s, 3H), 2.70 – 2.60 (m, 2H), 2.11 – 1.95 (m, 2H), 1.49 (s, 9H).

**<sup>13</sup>C-NMR** (150 MHz, CDCl<sub>3</sub>): δ = 168.4, 160.7, 149.9, 147.1, 145.5, 134.4, 129.8, 122.5, 120.4, 112.2, 111.6, 108.8, 82.1, 74.2, 65.9, 56.1, 39.1, 29.4, 28.7.

**HRMS** (EI<sup>+</sup>): calculated für [C<sub>23</sub>H<sub>30</sub>O<sub>6</sub> + Na]<sup>+</sup> 425,1935, found 425,1946 [M + Na]<sup>+</sup>.

### (S)-1-(((9H-Fluoren-9-yl)methoxy)carbonyl)piperidine-2-carboxylic acid (**6a**)



L-pipecolinic acid **1** (3.6 g, 10 mmol) was dissolved in 40 mL 10 % aqueous Na<sub>2</sub>CO<sub>3</sub> solution and combined with a solution of Fmoc succinimide (3.4 g, 10 mmol) in 45 mL dioxane. The formed suspension was stirred for 22 h at RT. Then the reaction was quenched by addition of another 50 mL of H<sub>2</sub>O, followed by extraction with EtOAc. The aqueous phase was acidified to pH = 2, and again extracted with EtOAc. The organic phase was washed with 1 M HCl and brine, and dried over MgSO<sub>4</sub>) **7a** was concentrated (4.3 g, 8.3 mmol, 83%) and obtained as a white solid without further purification.

**TLC** [EtOAc/cyclohexane 1:1, 0.1% TFA] R<sub>f</sub> = 0.46.

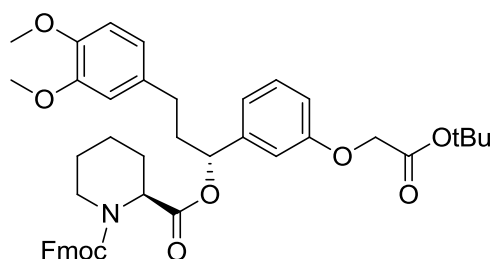
**HPLC** [0-100% Solvent B, 30 min]: R<sub>t</sub> = 24.5 min, purity (220 nm) = 97%

**<sup>1</sup>H-NMR** (300 MHz, CDCl<sub>3</sub>): δ (ppm) = 7.55-7.62 (m, 2H), 7.28-7.41 (m, 4H), .76-5.05(m, 1H), 4.37-4.49 (m, 2H), 4.05-4.33 (m, 2H), 3.15 (t, J= 13.2Hz, 1H), 2.19-2.37 (m, 1H), 1.77 (s, 2H), 1.69-1.82 (m, 3H), 1.28-1.53 (m, 2H).

**<sup>13</sup>C-NMR** (150 MHz, CDCl<sub>3</sub>): δ (ppm) = 177.69, 156.96, 156.18, 144.19, 141.63, 128.02, 127.39, 125.41, 120.30, 68.18, 67.91, 54.58, 54.48, 47.53, 42.27, 42.00, 27.07, 26.87, 25.02, 24.79, 21.07, 20.94.

**Mass:** (ESI<sup>+</sup>): calculated [C<sub>21</sub>H<sub>21</sub>NO<sub>4</sub> + H]<sup>+</sup> 514.41, found 514.43 [M + H]<sup>+</sup>.

**(S)-1-[9H-Fluoren-9-yl]methyl-ester-2-[(R)-1-{3-(2-tert-butoxy-2-oxoethoxy)phenyl}-3-(3,4-dimethoxyphenyl)propyl]piperidin-2-carboxylate**



Fmoc protected **8a**

**5a** (100 mg, 0.248 mmol), **7a** (96 mg, 0.27 mmol) were dissolved in 2 mL DCM at RT. Then EDC-HCl (52 mg, 0.27 mmol) was added and the mixture was stirred for 14 h at RT. After concentration *in vacuo* the raw product was subjected to column chromatography (EtOAc/n-Hexane, 1:2) to yield Fmoc protected **8a** as a slight yellow oil (139 mg, 0.19 mmol, 76%).

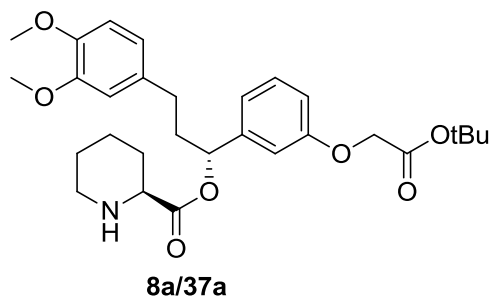
**TLC** [EtOAc/n-Hexane 1:2]: R<sub>f</sub> = 0.36.

**HPLC** [0-100% Solvent B, 20 min]: R<sub>t</sub> = 17.9 min, purity (220 nm) = 96%

**<sup>1</sup>H-NMR** (300 MHz, CDCl<sub>3</sub>): δ = 7.73 (m, 2H), 7.59 (t, J = 6.6 Hz, 1H), 7.16-7.49 (m, 6H), 6.94 (d, J = 7.6 Hz, 1H), 6.89 (s, 1H), 6.72-6.82 (m, 2H), 6.62 (m, 2H), 5.76 (br s, 1H), 5.02 (d, J = 3.7 Hz, 1H), 4.25-4.49 (m, 5H), 4.07-4.14 (m, 1H), 3.83 (s, 6H), 3.14 (t, J = 11.1 Hz, 1H), 2.46-2.54 (m, 2H), 2.16-2.33 (m, 2H), 2.00-2.07 (m, 1H), 1.68-1.78 (m, 4H), 1.46 (s, 9H), 1.39-1.56 (m, 1H).

**<sup>13</sup>C-NMR** (150 MHz, CDCl<sub>3</sub>): δ = 174.50, 171.33, 168.28, 158.48, 147.73, 144.30, 142.12, 133.90, 130.07, 128.07, 127.45, 125.48, 120.50, 120.35, 114.34, 113.66, 112.12, 111.74, 82.74, 76.82, 76.59, 68.20, 66.16, 56.32, 56.20, 47.63, 38.44, 31.98, 31.54, 28.42, 27.23, 25.18, 21.20.

**Mass** (ESI<sup>+</sup>): calculated [C<sub>44</sub>H<sub>49</sub>NO<sub>8</sub> + H]<sup>+</sup> 736.35 found 736.36 [M + H]<sup>+</sup>.

**(S)-[*(R)*-1-{3-(2-*tert*-Butoxy-2-oxoethoxy)phenyl}-3-(3,4-dimethoxyphenyl)propyl] piperidin-2-carboxylate (**8a/37a**)**

Fmoc-protected **8a/37a** (100 mg, 0.136 mmol) was dissolved in 1.8 mL dry DCM, then 0.2 mL 4-Methyl-Piperidine was added and stirred for 14h. The solvent was removed *in vacuo* and the raw product was purified with column chromatography (Gradient 50%-100% EtOAc in n-hexane) to afford **8a** as a colorless oil (345 mg, 0.66 mmol, 76%)

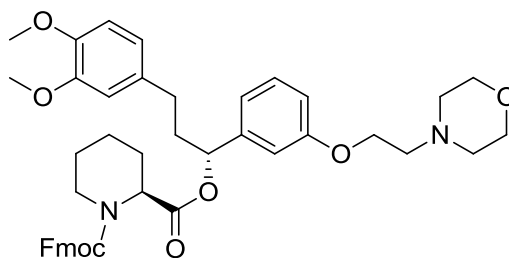
**TLC** [EtOAc/n-hexane 1:2]:  $R_f = 0.36$ .

**HPLC** [0-100% Solvent B, 20 min]:  $R_t = 15.5$  min, purity (220 nm) = 95%

**$^1\text{H-NMR}$**  (300 MHz,  $\text{CDCl}_3$ ):  $\delta = 7.28$  (t,  $J = 7.9$  Hz, 1H), 6.98 (d,  $J = 7.7$  Hz, 1H), 6.93 (s, 1H), 6.84 (m, 2H), 6.71 (d,  $J = 8.3$  Hz, 1H), 6.69 (s, 1H), 5.77 (dd,  $J = 6.3, 6.8$  Hz, 1H), 4.55 (s, 2H), 3.91 (s, 6H), 3.42 (m, 1H), 3.33 (s, 1H), 3.01 (m, 1H), 2.39-2.63 (m, 3H), 2.11-2.27 (m, 1H), 2.05-2.09 (m, 1H), 1.92 (m, 1H), 1.54 (s, 9H), 1.54-1.74 (m, 4H).

**$^{13}\text{C-NMR}$**  (150 MHz,  $\text{CDCl}_3$ ):  $\delta = 173.42, 168.29, 158.34, 149.20, 147.64, 142.54, 134.06, 129.92, 120.49, 120.19, 114.11, 113.54, 111.99, 111.60, 82.74, 75.21, 66.05, 61.45, 56.30, 56.21, 48.57, 38.55, 31.63, 29.41, 28.44, 25.70, 22.56$ .

**Mass** (ESI<sup>+</sup>): calculated  $[\text{C}_{29}\text{H}_{39}\text{NO}_7 + \text{H}]^+$  514.43, found 514.45  $[\text{M} + \text{H}]^+$ .

**Oxycarbonyl-2-((R)-3-(3,4-dimethoxyphenyl)-1-(3-(2-morpholinoethoxy)phenyl)propyl) (S)-1-(9H-Fluoren-9-yl)methylpiperidine-2-carboxylate**Fmoc protected **9a/37b**

A solution of alcohol **5b** (171 mg, 0.43 mmol), carboxylic acid **6a** (150 mg, 0.43 mmol), and DMAP (6 mg, 47  $\mu$ mol) in 10 mL DCM at room temperature was treated with DCC (113 mg, 0.51 mmol). The mixture was stirred for 14 h after which the organic solvent was removed *in vacuo*. The solid was dissolved in diethyl ether (50mL) and filtered through a plug of celite. The filtrate was concentrated and then flash chromatographed (DCM/MeOH 9.7:0.3) to afford Fmoc protected **8b** as brownish oil (280 mg, 0.38 mmol, 89%).

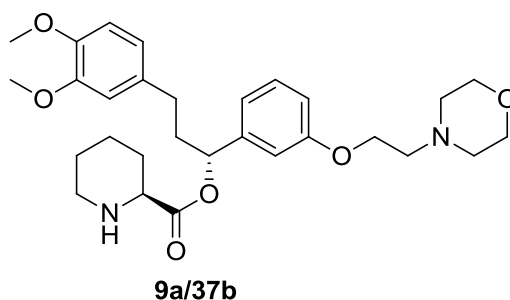
**TLC** [100% EtOAc]:  $R_f$  = 0.56.

**HPLC** [0-100% Solvent B, 15 min]:  $R_t$  = 8.8 min, purity (220 nm) = 98%

**$^1\text{H NMR}$**  (300 MHz,  $\text{CDCl}_3$ )  $\delta$  7.76 (dd,  $J$  = 14.6, 7.5 Hz, 2H), 7.60 (t,  $J$  = 6.6 Hz, 1H), 7.54 – 7.14 (m, 6H), 6.93 (d,  $J$  = 7.7 Hz, 3H), 6.89 – 6.80 (m, 1H), 6.76 (d,  $J$  = 8.3 Hz, 1H), 6.71 – 6.56 (m, 2H), 5.78 (s, 1H), 5.04 (s, 1H), 4.91 (s, 1H), 4.53 – 4.23 (m, 3H), 4.22 – 3.96 (m, 4H), 3.88 – 3.80 (m, 6H), 3.77 – 3.69 (m, 3H), 3.17 (t,  $J$  = 11.8 Hz, 1H), 2.99 (d,  $J$  = 12.0 Hz, 1H), 2.85 – 2.67 (m, 2H), 2.65 – 2.49 (m, 4H), 2.40 – 2.13 (m, 1H), 2.13 – 1.90 (m, 1H), 1.83 – 1.66 (m, 3H), 1.56 – 1.48 (m, 2H).

**$^{13}\text{C NMR}$**  (75 MHz,  $\text{CDCl}_3$ )  $\delta$  170.83, 158.70, 156.42, 155.77, 149.03, 147.28, 143.90, 143.88, 141.68, 141.23, 133.50, 129.63, 127.67, 127.06, 125.03, 120.06, 119.95, 119.05, 118.88, 113.94, 113.06, 111.66, 111.33, 67.76, 66.85, 65.59, 57.59, 54.89, 54.56, 54.06, 47.23, 38.10, 33.97, 31.17, 29.70, 27.01, 26.82, 25.61, 24.92, 24.57, 20.57.

**Mass:** (ESI<sup>+</sup>) calculated 735.40 [ $\text{C}_{44}\text{H}_{50}\text{N}_2\text{O}_8 + \text{H}$ ]<sup>+</sup>, found 735.57 [M + H]<sup>+</sup>.

**(S)-((R)-3-(3,4-Dimethoxyphenyl)-1-(3-(2-morpholinoethoxy)phenyl)propyl) piperidine-2-carboxylate (9a/37b)**

Fmoc protected **8b** (250 mg, 0.34 mmol) was treated with 20% 4-methylpiperidine in DCM at room temperature. The mixture was stirred for 14 h. 4-Methylpiperidine and DCM were evaporated under reduced pressure. The raw product was purified by column chromatography (EtOAc/cyclohexane 2:8, 0.2% TEA) to afford **9a/37b** as a slight yellow oil (160 mg, 0.31mmol, 84%).

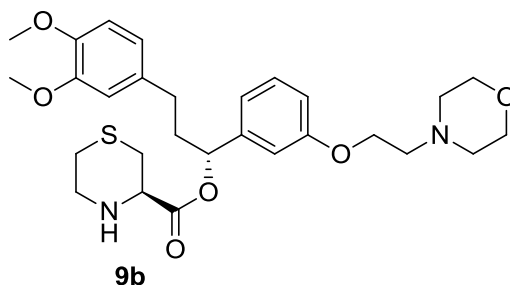
**TLC** [EtOAc/cyclohexane 2:8, 0.2% TEA]:  $R_f = 0.3$ .

**HPLC** [0-100% Solvent B, 20 min]:  $R_t = 11.6$  min, purity (220 nm) = 92%

**$^1\text{H NMR}$**  (300 MHz,  $\text{CDCl}_3$ )  $\delta = 7.19$  (t,  $J = 8.1$  Hz, 1H), 6.95 (s, 1H), 6.86 (d,  $J = 7.8$ Hz, 1H), 6.72-6.80 (m, 3H), 6.66-6.62 (m, 2H), 5.70 (t,  $J = 7.2$  Hz, 1H), 4.35-4.18 (m, 2H), 3.85-3.77 (m, 6H), 3.42-3.27 (m, 1H), 3.08 (s, 3H), 3.06 (s, 3H), 2.85 (s, 2H), 2.62-2.44 (m, 3H), 2.31-2.17 (m, 3H), 2.10-1.89- (m, 3H), 1.89-1.67 (m, 3H), 1.60-1.48 (m, 2H).

**$^{13}\text{C NMR}$**  (75 MHz,  $\text{CDCl}_3$ )  $\delta = 21.59, 22.00, 26.01, 31.15, 37.82, 44.12, 45.89, 55.91, 55.95, 56.67, 57.17, 64.55, 65.60, 77.65, 111.35, 111.83, 112.36, 111.72, 119.27, 120.18, 129.57, 133.31, 140.98, 147.29, 148.84, 158.45, 167.88$ .

**Mass:** (ESI<sup>+</sup>), calculated 513.32 [ $\text{C}_{29}\text{H}_{40}\text{N}_2\text{O}_6 + \text{H}$ ]<sup>+</sup>, found 513.29 [M + H]<sup>+</sup>.

**(R)-(R)-3-(3,4-Dimethoxyphenyl)-1-(3-(2-morpholinoethoxy)phenyl)propyl-thiomorpholine-3-carboxylate (9b)**

A solution of alcohol **5b** (0.10 g, 0.25 mmol), Fmoc-thiopipecolate (92 mg, 0.37 mmol), and catalytic amount of DMAP (3 mg, 25  $\mu$ mol) in 10 mL DCM was treated with EDC (53 mg, 0.28 mmol). The mixture was stirred for 14 h at RT. The crude product was concentrated, flash chromatographed (DCM/MeOH 97:3) and consequently dissolved in 1.8 mL DCM. Then 0.2 mL 4-methylpiperidine was added and the mixture was stirred for 14 h at RT. 4-Methylpiperidine and DCM were evaporated under reduced pressure. The raw product was purified by flash chromatography (DCM/MeOH 92:8). **9b** was obtained as a slight yellow oil (32 mg, 0.13 mmol, 48%).

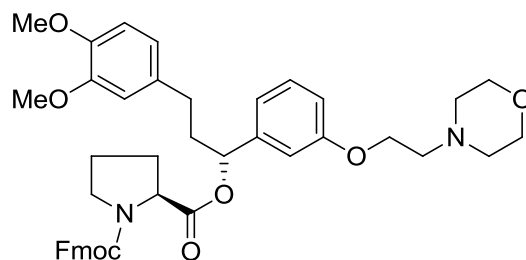
**TLC** [MeOH/DCM 8:92]:  $R_f$  = 0.18.

**HPLC** [0-100% Solvent B, 20 min]:  $R_t$  = 11.7 min, purity (220 nm) = 92%

**$^1\text{H NMR}$**  (300 MHz,  $d_6$ -DMSO)  $\delta$  7.24 – 7.16 (m, 1H), 6.91 – 6.73 (m, 5H), 6.66 (td,  $J$  = 8.2, 7.8, 2.0 Hz, 1H), 5.63 (dd,  $J$  = 8.4, 4.7 Hz, 1H), 4.09 – 4.00 (m, 2H), 3.97 (t,  $J$  = 3.6 Hz, 1H), 3.72 – 3.67 (m, 6H), 3.58 – 3.51 (m, 4H), 3.06 – 2.85 (m, 3H), 2.69 – 2.60 (m, 2H), 2.60 – 2.50 (m, 2H), 2.47 – 2.39 (m, 5H), 2.17 – 2.04 (m, 2H), 1.98 (d,  $J$  = 14.7 Hz, 2H).

**$^{13}\text{C NMR}$**  (75 MHz,  $d_6$ -DMSO)  $\delta$  170.62, 158.91, 148.86, 147.47, 142.32, 133.89, 129.68, 120.20, 118.75, 114.35, 112.88, 111.96, 74.91, 66.47, 65.39, 59.53, 57.34, 55.87, 54.09, 46.21, 38.16, 31.03, 28.82, 27.36.

**Mass:** (ESI $^+$ ), calculated 531.25 [ $\text{C}_{28}\text{H}_{38}\text{N}_2\text{O}_6\text{S}+\text{H}$ ] $^+$ , found 531.21 [ $\text{M}+\text{H}$ ] $^+$ .

**(S)-1-((9H-Fluoren-9-yl)methyl)ester-2-((R)-3-(3,4-dimethoxyphenyl)-1-(3-(2-morpholinoethoxy) phenyl)propyl) pyrrolidine-2-carboxylate**Fmoc protected **9c/36b**

**5b** (200 mg, 0.50 mmol), Fmoc-proline (185 mg, 0.55 mmol) and DMAP (12 mg, 0.10 mmol) were dissolved in DCM at 0°C then EDC (143 mg, 0.75 mmol) was added and the reaction was allowed to warm to RT, followed by stirring for 14 hours. The raw product was subjected to column chromatography (gradient 0%-5% MeOH in DCM). Fmoc protected **36b** (276 mg, 0.383 mmol, 77%) was obtained as a slight yellow oil.

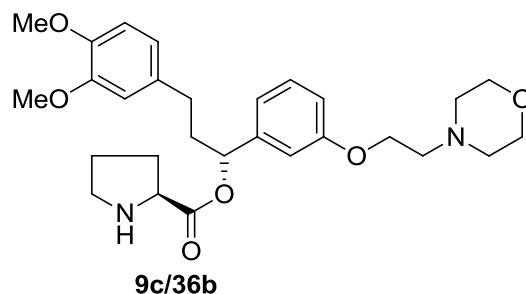
**TLC** [MeOH/DCM 5:95]:  $R_f = 0.2$ .

**HPLC** [0-100% Solvent B, 20 min]:  $R_t = 16.7$  min, purity (220 nm) = 98%

**$^1\text{H NMR}$**  (400 MHz,  $\text{CDCl}_3$ ):  $\delta$  7.78 – 7.67 (m, 2H), 7.65 – 7.53 (m, 1H), 7.53 – 7.45 (m, 1H), 7.42 – 7.26 (m, 3H), 7.25 – 7.18 (m, 1H), 6.94 – 6.53 (m, 7H), 5.73 (dt,  $J = 8.0, 5.8$  Hz, 1H), 4.49 (dt,  $J = 8.9, 3.7$  Hz, 1H), 4.41 (dd,  $J = 10.1, 6.8$  Hz, 2H), 4.34 – 4.13 (m, 1H), 4.14 – 4.07 (m, 2H), 3.85 – 3.82 (m, 6H), 3.77 – 3.66 (m, 4H), 3.31 (td,  $J = 9.1, 3.2$  Hz, 1H), 3.26 – 3.14 (m, 1H), 3.07 (dt,  $J = 10.4, 6.8$  Hz, 1H), 2.80 (dt,  $J = 6.9, 5.7$  Hz, 4H), 2.64 – 2.52 (m, 4H), 2.35 – 2.18 (m, 1H), 2.15 – 1.96 (m, 2H), 1.95 – 1.76 (m, 2H).

**$^{13}\text{C NMR}$**  (125 MHz,  $\text{CDCl}_3$ )  $\delta$  171.90, 159.63, 157.44, 150.39, 148.33, 144.14, 143.58, 139.48, 135.20, 129.28, 127.63, 126.29, 125.14, 121.85, 120.96, 119.20, 115.53, 114.12, 113.68, 113.06, 77.03, 67.50, 67.38, 66.80, 63.34, 56.83, 54.73, 52.94, 48.12, 47.31, 36.38, 34.08, 28.00, 24.98.

**Mass** (ESI<sup>+</sup>): calculated  $[\text{C}_{43}\text{H}_{48}\text{N}_2\text{O}_8 + \text{H}]^+$  721.35, found 721.25  $[\text{M} + \text{H}]^+$ .

**(S)-(R)-3-(3,4-Dimethoxyphenyl)-1-(3-(2-morpholinoethoxy)phenyl)propyl-pyrrolidine-2-carboxylate (9c/36b)**

Fmoc protected **9c/36b** (234 mg, 0.32 mmol) was dissolved in 1.8 mL dry DCM, then 200  $\mu$ L 4-methyl-piperidine was added and stirred for 14 h. The product was purified using flash chromatography (gradient 0%-10% MeOH in DCM) to obtain **36b** (140 mg, 0.28 mmol, 86%) as a yellow oil.

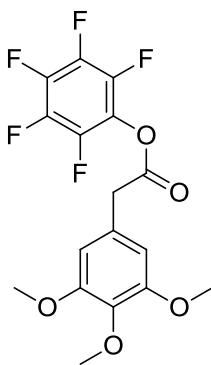
**TLC** [MeOH/DCM 6:94]:  $R_f = 0.10$ .

**HPLC** [0-100% Solvent B, 20 min]:  $R_t = 11.6$  min, purity (220 nm) = 92%.

**$^1\text{H NMR}$**  (300 MHz,  $\text{CDCl}_3$ )  $\delta$  7.25 – 7.18 (m, 1H), 6.94 – 6.83 (m, 2H), 6.83 – 6.72 (m, 2H), 6.70 – 6.61 (m, 2H), 5.72 (dd,  $J = 7.9, 5.9$  Hz, 1H), 4.64 (dd,  $J = 7.8, 5.3$  Hz, 1H), 4.14 – 4.07 (m, 2H), 3.85 – 3.82 (m, 6H), 3.77 – 3.66 (m, 4H), 3.31 (td,  $J = 9.1, 3.2$  Hz, 1H), 3.26 – 3.14 (m, 1H), 3.07 (dt,  $J = 10.4, 6.8$  Hz, 1H), 2.80 (dt,  $J = 6.9, 5.7$  Hz, 4H), 2.64 – 2.52 (m, 4H), 2.35 – 2.18 (m, 1H), 2.15 – 1.96 (m, 2H), 1.95 – 1.76 (m, 2H).

**$^{13}\text{C NMR}$**  (75 MHz,  $\text{CDCl}_3$ )  $\delta$  172.34, 158.73, 148.77, 147.17, 146.44, 141.28, 134.43, 133.35, 129.43, 119.09, 118.46, 113.45, 113.13, 111.75, 111.19, 73.61, 66.82, 65.70, 59.64, 57.63, 55.92, 54.05, 40.65, 31.64, 29.89, 24.75.

**Mass** ( $\text{ESI}^+$ ): calculated  $[\text{C}_{28}\text{H}_{38}\text{N}_2\text{O}_6 + \text{H}]^+$  499.28, found 499.22  $[\text{M} + \text{H}]^+$ .

**Pentafluorophenyl 2-(3,4,5-trimethoxyphenyl)acetate (20)****20**

2-(3,4,5-Trimethoxyphenyl)acetic acid (8.2 g, 36.2 mmol) was dissolved in 140 ml dry DCM, then EDC (10.4 g, 54.3 mmol) was added and stirred for 15 min at RT. 2,3,4,5,6-pentafluorophenol (10.0 g, 54.3 mmol) was dissolved in 60 ml dry DCM and added to the solution. The mixture was stirred for 6 h at RT and then concentrated and subjected to flash chromatography (EtOAc/cyclohexane, 2:8). **20** (13.4 g, 34.1 mmol, 94%) was obtained as a white solid.

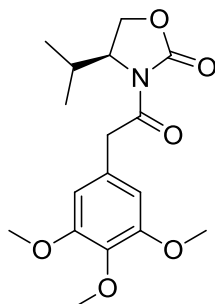
**TLC** [EtOAc/cyclohexane, 2:8]:  $R_f = 0.31$ .

**HPLC** [0-100% Solvent B, 30 min]:  $R_t = 25.8$  min, purity (220 nm) = 95%.

**$^1\text{H-NMR}$**  (300 MHz,  $\text{CDCl}_3$ ):  $\delta = 6.56$  (s, 2H), 3.90 (s, 2H), 3.87 (s, 6H), 3.85 (s, 3H).

**$^{13}\text{C-NMR}$**  (150 MHz,  $\text{CDCl}_3$ ):  $\delta = 167.39, 153.48, 137.59, 127.47, 106.19, 60.855, 56.12, 40.37$ .

**HRMS** ( $\text{ESI}^+$ ): calculated [ $\text{C}_{17}\text{H}_{13}\text{F}_5\text{O}_5 + \text{H}^+$ ] 393.0756, found 393.0711 [ $\text{M}$ ] +  $\text{H}^+$ .

**(S)-4-isopropyl-3-[2-(3,4,5-trimethoxyphenyl)acetyl]oxazolidin-2-one (21)****21**

n-Butyllithium (2.5 M in Cyclohexane, 1.4 mL, 3.6 mmol) was added to (S)-4-Isopropyl-oxazolidin-2-one (0.46 g, 3.6 mmol) dissolved in 17 mL dry THF at  $-78^{\circ}\text{C}$ , then was stirred for 1 h  $-78^{\circ}\text{C}$ . After that **20** (1.4 g, 3.6 mmol) dissolved in 17 mL dry THF was added to the above solution and stirred for 2h at  $-78^{\circ}\text{C}$  and 14 h at  $0^{\circ}\text{C}$ . The reaction mixture was quenched by adding sat.  $\text{NH}_4\text{Cl}$  solution. The aqueous solution was extracted with DCM. The org. phases were dried over  $\text{MgSO}_4$ . The crude product was concentrated and purified by column chromatography (EtOAc/cyclohexane, 1:2). **21** was afforded as a yellow oil (0.67 mg, 1.98 mmol, 53%).

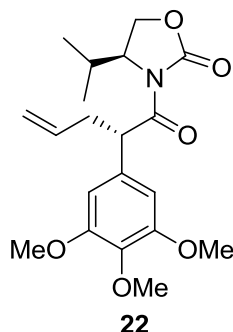
**TLC** [EtOAc/cyclohexane, 2:8]:  $R_f = 0.31$ .

**HPLC** [0-100% Solvent B, 30 min]:  $R_t = 22.4$  min, purity (220 nm) = 98%.

**$^1\text{H-NMR}$**  (300 MHz,  $\text{CDCl}_3$ ):  $\delta = 6.56$  (s, 2H), 4.43-4.41 (m, 2H), 4.38-4.17 (m, 3H), 3.85 (d, 9H), 2.38-2.27 (m, 1H), 0.96 (d,  $J = 6$  Hz, 3H), 0.85 (d,  $J = 6$  Hz, 3H).

**$^{13}\text{C-NMR}$**  (150 MHz,  $\text{CDCl}_3$ ):  $\delta = 167.39, 153.48, 137.59, 127.47, 106.19, 60.855, 56.12, 40.37$ .

**Mass** (ESI $^+$ ): calculated [ $\text{C}_{17}\text{H}_{23}\text{NO}_6 + \text{H}^+$ ] 338.16, found 338.20 [M] +  $\text{H}^+$ .

**(S)-4-Isopropyl-3-((S)-2-(3,4,5-trimethoxyphenyl)pent-4-enoyl)oxazolidin-2-one (22)**

**21** (2.0 g, 5.9 mmol) was dissolved in 5 mL anhydrous THF, cooled to  $-78^{\circ}\text{C}$  and then NaHMDS (7.1 mL, 7.1 mmol, 1M in THF) was added to the solution. After stirring for 30min at  $-78^{\circ}\text{C}$ , the reaction was stirred for another 30min at  $0^{\circ}\text{C}$ , then allylbromide (0.63 mL, 7.1 mmol) was added and stirred for 2h at  $-78^{\circ}\text{C}$ , and another 10 h at  $0^{\circ}\text{C}$ . The reaction was quenched by the addition of saturated  $\text{NH}_4\text{Cl}$  solution. The biphasic aqueous solution was extracted with DCM. The organic phases were combined and dried over  $\text{MgSO}_4$ . The crude mixture was concentrated and purified by column chromatography (EtOAc/cyclohexane, 2:8). **22** was obtained as yellow oil (1.0 g, 2.7 mmol, 45%, d.r. >95:5).

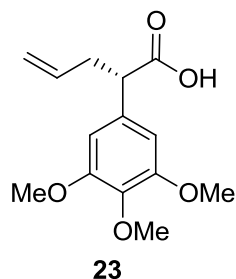
**TLC** [EtOAc/cyclohexane 2:8]:  $R_f = 0.31$ .

**HPLC** [0-100% Solvent B, 30 min]:  $R_t = 25.0$  min, purity (220 nm) = 98%.

**$^1\text{H NMR}$**  (600 MHz,  $\text{CDCl}_3$ )  $\delta$  6.60 (s, 2H), 5.80 – 5.70 (m, 1H), 5.20 – 5.15 (dd,  $J = 9.5, 5.8$  Hz, 1H), 5.14 – 5.07 (dq,  $J = 17.1, 1.6$  Hz, 1H), 5.04 – 4.98 (dq,  $J = 10.2, 1.1$  Hz, 1H), 4.40 – 4.34 (m, 1H), 4.18 – 4.13 (m, 2H), 3.85 – 3.82 (s, 6H), 3.83 – 3.79 (s, 3H), 2.93 – 2.84 (m, 1H), 2.52 – 2.44 (m, 1H), 2.43 – 2.35 (m, 1H), 0.92 – 0.84 (m, 6H).

**$^{13}\text{C NMR}$**  (150 MHz,  $\text{CDCl}_3$ )  $\delta$  173.36, 153.67, 153.04, 137.10, 135.07, 133.80, 117.14, 105.43, 62.99, 60.82, 58.93, 56.12, 47.79, 38.67, 28.37, 17.88, 14.58.

**HRMS** ( $\text{EI}^+$ ): calculated  $[\text{C}_{20}\text{H}_{27}\text{NO}_6 + \text{H}]^+$  378.19, found 378.13  $[\text{M} + \text{H}]^+$ .

**(S)-2-(3,4,5-Trimethoxyphenyl)pent-4-enoic acid (23)**

**22** (0.70 g, 1.86 mmol) was dissolved in 10 mL THF/H<sub>2</sub>O (1:1) and cooled to 0°C for 5 min. Then LiOH (89 mg, 3.71 mmol) was added followed by addition of H<sub>2</sub>O<sub>2</sub> (0.60 mL, 7.42 mmol). The reaction mixture was stirred at 0°C for 4 h. The reaction was quenched by the addition of 1.5 M Na<sub>2</sub>SO<sub>3</sub>. The aqueous solution was diluted with brine and extracted with DCM. Then, the aqueous phase was acidified to pH < 2 and further extracted with DCM. The organic layers were combined and dried over MgSO<sub>4</sub>. The raw product was concentrated and purified using flash chromatography (gradient 0%-30% EtOAc in n-hexane, 0.1% AcOH). **23** (324 mg, 1.22 mmol, 66%) was obtained as a yellow oil.

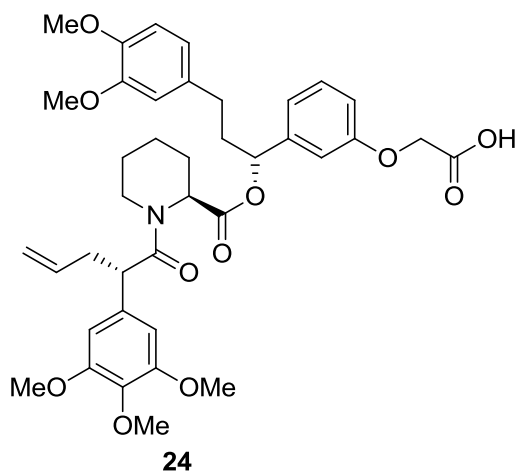
**TLC** [EtOAc/n-hexane 1:2]: R<sub>f</sub> = 0.22.

**HPLC** [0-100% Solvent B, 30 min]: R<sub>t</sub> = 17.9 min, purity (220 nm) = 98%.

**<sup>1</sup>H NMR** (300 MHz, CDCl<sub>3</sub>) δ 6.56 (d, *J* = 1.1 Hz, 2H), 5.84 – 5.67 (m, 1H), 5.19 – 5.00 (m, 2H), 3.87 – 3.84 (m, *J* = 0.7 Hz, 9H), 3.58 (dd, *J* = 8.6, 6.9 Hz, 1H), 2.88 – 2.75 (m, 1H), 2.53 (dtt, *J* = 14.5, 6.8, 1.4 Hz, 1H).

**<sup>13</sup>C NMR** (75 MHz, CDCl<sub>3</sub>) δ 178.95, 153.31, 137.47, 134.79, 133.38, 117.31, 105.08, 60.81, 56.14, 51.50, 37.18, 20.72.

**Mass:** (ESI+), calculated 287.12 [C<sub>14</sub>H<sub>18</sub>O<sub>5</sub> + H]<sup>+</sup>, found 287.13 [M + H]<sup>+</sup>.

**2-(3-((*R*)-3-(3,4-Dimethoxyphenyl)-1-(((*S*)-1-((*S*)-2-(3,4,5-trimethoxyphenyl)pent-4-enoyl)piperidine-2-carbonyloxy)propyl)phenoxy)acetic acid (**24**)**

General synthesis procedure **B** for free acid ligands with **37a** (0.10 g, 0.20 mmol) and **23** (57 mg, 0.21 mmol) was used. The crude product was purified using flash chromatography (gradient 0%-10% MeOH in DCM) to obtain **24** (38 mg, 54  $\mu$ mol, 55%) as a colorless oil. The diastereomeric rate was determined by HPLC.

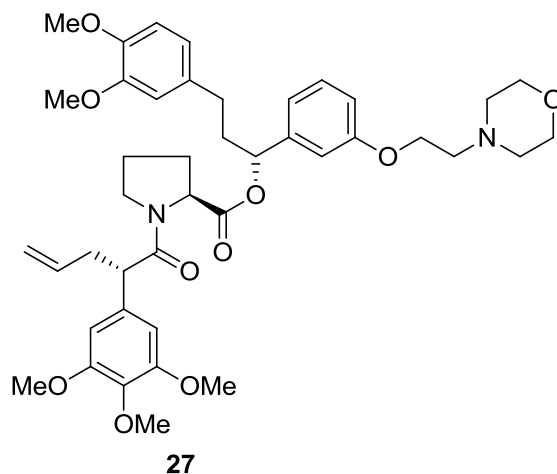
**TLC** [EtOAc/cyclohexane, 1:1, 1% AcOH]:  $R_f$  = 0.28.

**HPLC** [60-80% Solvent B, 20 min]:  $R_t$  = 8.1 min, purity (220 nm) = 95%, dr 95:5.

**$^1\text{H NMR}$**  (599 MHz,  $d_6$ -DMSO)  $\delta$  7.20 (dd,  $J$  = 7.8, 0.8 Hz, 1H), 6.85 – 6.71 (m, 4H), 6.67 (d,  $J$  = 2.0 Hz, 1H), 6.59 (s, 2H), 6.56 (dd,  $J$  = 8.2, 2.0 Hz, 1H), 5.76 – 5.64 (m, 1H), 5.48 (dd,  $J$  = 8.7, 4.6 Hz, 1H), 5.22 (dd,  $J$  = 5.9, 2.5 Hz, 1H), 5.03 – 4.92 (m, 2H), 4.65 (s, 2H), 3.71 (t,  $J$  = 2.3 Hz, 3H), 3.69 (s, 3H), 3.68 (s, 4H), 3.64 (s, 3H), 3.61 (s, 1H), 3.51 (s, 3H), 2.75 – 2.64 (m, 2H), 2.44 – 2.37 (m, 2H), 2.34 – 2.25 (m, 2H), 2.15 – 2.06 (m, 2H), 1.84 (ddd,  $J$  = 34.5, 8.0, 5.4 Hz, 2H), 1.63 – 1.52 (m, 2H), 1.05 – 0.95 (m, 2H).

**$^{13}\text{C NMR}$**  (151 MHz,  $\text{CDCl}_3$ )  $\delta$  176.94, 175.44, 175.30, 162.96, 157.84, 153.83, 152.17, 147.35, 141.80, 141.17, 140.09, 138.19, 134.63, 125.13, 123.41, 121.43, 117.28, 110.32, 80.06, 69.53, 64.83, 61.09, 60.78, 60.65, 60.51, 56.95, 52.14, 42.66, 35.80, 31.40, 29.98, 25.70.

**Mass:** (ESI<sup>+</sup>), calculated 728.30 [ $\text{C}_{39}\text{H}_{47}\text{NO}_{11}+\text{Na}$ ]<sup>+</sup>, found 728.40 [ $\text{M}+\text{H}$ ]<sup>+</sup>.

**(S)-(R)-3-(3,4-Dimethoxyphenyl)-1-(3-(2-morpholinoethoxy)phenyl)propyl-1-((S)-2-(3,4,5-trimethoxyphenyl)pent-4-enoyl)pyrrolidine-2-carboxylate (27)**

General synthesis procedure **A** for morpholine ligands with **9c** (31 mg, 62  $\mu\text{mol}$ ) and **23** (17 mg, 62  $\mu\text{mol}$ ) was used. Then the crude product was purified using flash chromatography (gradient 0%-10% MeOH in DCM) to obtain **27** (31 mg, 44  $\mu\text{mol}$ , 67%) as a light yellow oil. The diastereomeric rate was determined by HPLC.

**TLC** [MeOH/DCM, 3:97, 1% TEA]:  $R_f = 0.24$ .

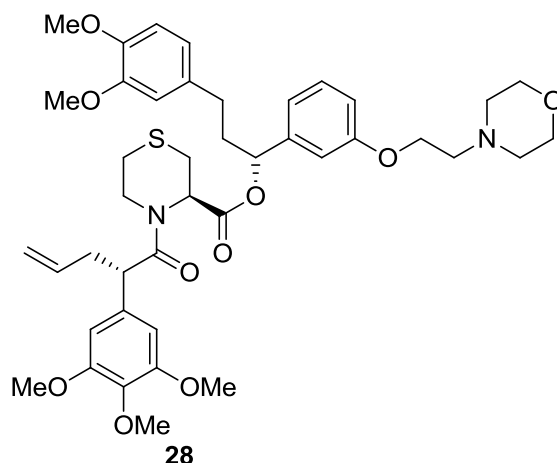
**HPLC** [0-100% Solvent B, 20 min]:  $R_t = 15.8$  min, purity (220 nm) = 95%, dr 95:5.

**$^1\text{H}$  NMR** (400 MHz,  $d_6$ -DMSO)  $\delta$  7.17 (t,  $J = 7.9$  Hz, 1H), 6.86 (t,  $J = 1.9$  Hz, 1H), 6.82 – 6.77 (m, 2H), 6.73 – 6.68 (m, 2H), 6.64 – 6.57 (m, 1H), 6.49 (s, 2H), 5.77 – 5.62 (m, 1H), 5.48 (dd,  $J = 8.3, 5.0$  Hz, 1H), 5.05 – 4.87 (m, 3H), 4.45 (dd,  $J = 8.7, 3.4$  Hz, 1H), 4.17 – 4.02 (m, 3H), 3.77 (dd,  $J = 8.5, 6.0$  Hz, 1H), 3.74 – 3.62 (m, 6H), 3.59 – 3.46 (m, 9H), 3.28 – 3.18 (m, 4H), 2.68 – 2.57 (m, 4H), 2.52 – 2.37 (m, 5H), 2.31 – 2.11 (m, 5H), 1.83 – 1.73 (m, 2H).

**$^{13}\text{C}$  NMR** (100 MHz,  $d_6$ -DMSO)  $\delta$  171.88, 170.71, 158.80, 153.15, 149.10, 147.33, 142.50, 137.04, 136.45, 135.00, 133.82, 129.55, 120.44, 118.37, 116.77, 114.28, 112.73, 112.34, 112.06, 105.68, 75.33, 66.60, 65.65, 60.08, 59.00, 57.39, 55.95, 54.07, 49.32, 46.83, 38.96, 38.10, 30.91, 29.17, 24.83.

Mass: (ESI+), calculated 747.39 [ $\text{C}_{42}\text{H}_{54}\text{N}_2\text{O}_{10} + \text{H}$ ] $^+$ , found 747.51 [ $\text{M} + \text{H}$ ] $^+$ .

**(R)-(R)-3-(3,4-Dimethoxyphenyl)-1-(3-(2-morpholinoethoxy)phenyl)propyl-4-((S)-2-(3,4,5-trimethoxyphenyl)pent-4-enoyl)thiomorpholine-3-carboxylate (28)**



General synthesis procedure **A** for morpholine ligands with **9b** (32 mg, 60  $\mu$ mol) and **23** (20 mg, 75  $\mu$ mol) was used. The crude product was purified using flash chromatography (gradient 0%-80% EtOAc in cyclohexane) to obtain **28** (31 mg, 4  $\mu$ mol, 67%) as a light yellow oil. The diastereomeric rate was determined by HPLC.

**TLC** [EtOAc/cyclohexane, 3:7, 4% AcOH]:  $R_f$  = 0.42.

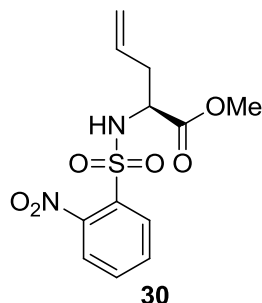
**HPLC** [0-100% Solvent B, 20 min]:  $R_t$  = 15.88 min, purity (220 nm) = 92%, dr  $\geq$  99:1.

**$^1\text{H NMR}$**  (400 MHz,  $d_6$ -DMSO)  $\delta$  7.29 – 7.23 (m, 1H), 7.16 (t,  $J$  = 7.8 Hz, 1H), 6.95 – 6.57 (m, 5H), 6.52 (s, 2H), 5.71 – 5.65 (m, 1H), 5.62 – 5.54 (m, 1H), 5.03 – 4.87 (m, 2H), 4.10 – 4.04 (m, 3H), 3.73 (d,  $J$  = 2.2 Hz, 3H), 3.69 (s, 3H), 3.69 – 3.67 (m, 6H), 3.62 (d,  $J$  = 2.3 Hz, 3H), 3.60 (s, 3H), 3.57 (s, 2H), 3.55 (s, 2H), 3.48 (d,  $J$  = 1.9 Hz, 1H), 3.32 (s, 1H), 3.14 – 3.08 (m, 1H), 2.91 (dd,  $J$  = 13.9, 4.0 Hz, 1H), 2.75 – 2.62 (m, 5H), 2.53 – 2.44 (m, 6H), 2.38 – 2.29 (m, 1H).

**$^{13}\text{C NMR}$**  (101 MHz,  $d_6$ -DMSO)  $\delta$  172.40, 168.83, 158.77, 153.39, 153.14, 149.03, 149.01, 147.44, 142.29, 142.22, 136.93, 136.73, 135.78, 135.03, 133.78, 129.93, 120.46, 116.81, 114.19, 112.68, 112.28, 105.51, 75.80, 66.52, 65.46, 60.19, 56.36, 56.00, 55.90, 55.79, 55.75, 55.35, 54.01, 52.52, 52.20, 51.58, 47.42, 44.49, 33.69, 31.73, 31.00, 26.99, 24.85, 22.54.

**Mass:** (ESI<sup>+</sup>), calculated 779.36 [C<sub>42</sub>H<sub>54</sub>N<sub>2</sub>O<sub>10</sub>S+H]<sup>+</sup>, found 779.37 [M+H]<sup>+</sup>.

### (S)-Methyl 2-(2-nitrophenylsulfonamido)pent-4-enoate (**30**)



**30** was synthesized according to Varray et al.<sup>129</sup>. L-Allyl-glycine (1.0 g, 8.69 mmol) was dissolved in 10 mL MeOH, cooled to 0°C, and then 3 mL TMS-Cl was added. The mixture was allowed to warm to RT and stirred for 24 h. The solvent was removed *in vacuo* and the resulting white oil was dissolved in hot EtOAc and precipitated with hexane. L-Allyl-glycine methylester (1.1 g, 8.51 mmol, 98%) was obtained as white crystals without further purification and reacted with *o*-nitrobenzenesulfonyl chloride (2.08 g, 9.37 mmol). For this it was dissolved in 15 mL anhydrous DCM, then TEA (1.40 mL, 17.03 mmol) was added and stirred for 5h. The reaction mixture was diluted with DCM and washed with brine. The aqueous phases were reextracted with DCM. The organic phases were combined, dried over MgSO<sub>4</sub>, and the solvent was removed *in vacuo*. The product was purified using flash chromatography (gradient 0%-30% EtOAc in cyclo-hexene). **30** (1.22 g, 3.88 mmol, 46%) was obtained as a slightly yellow solid.

**TLC** [EtOAc/cyclohexane, 1:1.5]: R<sub>f</sub> = 0.40.

**HPLC** [0-100% Solvent B, 20 min]: R<sub>t</sub> = 17.3 min, purity (220 nm) = 98%.

**HRMS** (EI<sup>+</sup>): calculated [C<sub>12</sub>H<sub>14</sub>N<sub>2</sub>O<sub>6</sub>S+ H]<sup>+</sup> 315.0651, found 315.0637 [M+ H]<sup>+</sup>.



chromatography (gradient 0%-40% EtOAc in cyclohexane) to give protected **32** (0.74 g, 2.27 mmol, 89%) as a dark brown oil.

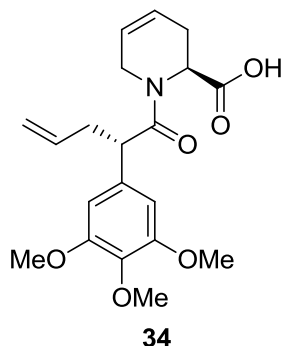
Protected **32** (0.64 g, 1.96 mmol) was dissolved in 1 mL dry CH<sub>3</sub>CN, then Cs<sub>2</sub>CO<sub>3</sub> (1.0 g, 3.10 mmol) and Thiophenol (0.23 mL, 2.25 mmol) was added and stirred for 1.5 h. The suspension turned from light yellow into a strong yellow slurry. The reaction mixture was subsequently diluted with DCM and extracted with H<sub>2</sub>O. The aqueous Phase was reextracted with DCM. The organic phases were combined and dried over MgSO<sub>4</sub>. The crude product was concentrated and purified using flash chromatography (gradient 0%-10% MeOH in DCM) to give **32** (0.22 g, 1.59 mmol, 81%) as a dark brown oil.

TLC [MeOH/DCM, 5:95]: R<sub>f</sub> = 0.25, stained with KMnO<sub>4</sub> stain

HPLC: not UV active.

HRMS (EI<sup>+</sup>): calculated [C<sub>7</sub>H<sub>11</sub>NO<sub>2</sub>+ H]<sup>+</sup> 142.0868, found 142.0864 [M+ H]<sup>+</sup>.

### (S)-Methyl-1-((S)-2-(3,4,5-trimethoxyphenyl)pent-4-enoyl)-1,2,3,6-tetrahydropyridine-2-carboxylate (**34**)



**23** (0.14 g, 0.53 mmol), HATU (0.22 g, 0.58 mmol) and DIPEA (0.36 mL, 2.13 mmol) were dissolved in 2 mL dry DCM and stirred for 15 min. Then **32** (75 mg, 0.53 mmol) in 1 mL dry DCM was added and stirred for 14 h at RT. The crude product was diluted with DCM and washed with brine. The organic layer was dried over MgSO<sub>4</sub>, concentrated and the methyl ester was cleaved by dissolving in 1 mL 1:1 THF/H<sub>2</sub>O and addition of LiOH (10 mg, 0.42 mmol). The mixture was stirred for 14 h then was diluted with brine and extracted with DCM. The aqueous layer was acidified to pH=2 and again extracted with DCM. The organic phases were combined and dried over MgSO<sub>4</sub>. **34** (84 mg, 0.22 mmol, 79%)

was obtained without further purification as a pale yellow oil. The diastereomeric rate was determined by HPLC.

**TLC** [EtOAc/cyclohexane, 2:1]:  $R_f = 0.60$ .

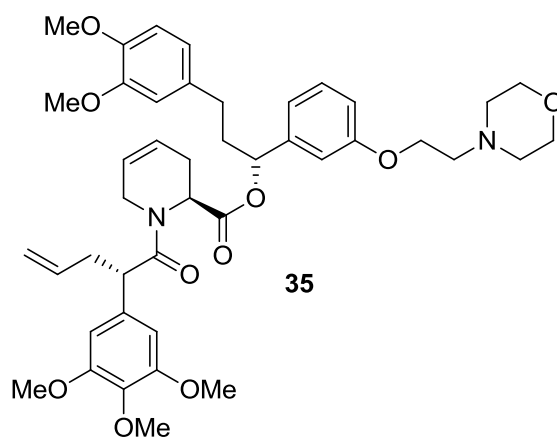
**HPLC** [0-100% Solvent B, 20 min]:  $R_t = 15.6$  min, purity (220 nm) = 95%, dr 95:5.

**$^1\text{H}$  NMR** (300 MHz,  $\text{CDCl}_3$ )  $\delta$  6.45 (s, 2H), 5.81 (ddd,  $J = 13.8, 6.9, 3.9$  Hz, 1H), 5.76 – 5.66 (m, 1H), 5.62 (dd,  $J = 6.7, 1.6$  Hz, 1H), 5.56 (dd,  $J = 10.2, 2.9$  Hz, 1H), 5.09 – 4.97 (m, 2H), 4.12 – 4.03 (m, 1H), 3.83 (s, 6H), 3.81 (s, 3H), 3.79 – 3.72 (m, 2H), 3.63 – 3.51 (m, 1H), 2.85 (d,  $J = 6.4$  Hz, 1H), 2.70 (dd,  $J = 17.4, 5.9$  Hz, 1H), 2.43 (m, 2H).

**$^{13}\text{C}$  NMR** (75 MHz,  $\text{CDCl}_3$ )  $\delta$  176.22, 172.77, 153.28, 136.85, 136.32, 133.90, 123.33, 122.98, 116.51, 105.05, 60.86, 56.11, 50.17, 49.37, 43.19, 39.33, 26.36.

**Mass:** ( $\text{ESI}^+$ ), calculated 376.18 [ $\text{C}_{20}\text{H}_{25}\text{NO}_6 + \text{H}$ ] $^+$ , found 376.28 [ $\text{M} + \text{H}$ ] $^+$ .

**2-(3-((*R*)-3-(3,4-Dimethoxyphenyl)-1-(((*S*)-1-((*S*)-2-(3,4,5-trimethoxyphenyl)pent-4-enoyl)-1,2,3,6-tetrahydropyridine-2-carbonyl)oxy)propyl)phenoxy)acetic acid (**35**)**



**34** (20 mg, 53  $\mu\text{mol}$ ), DMAP (1.0 mg, 5.3  $\mu\text{mol}$ ) and DCC (7.0 mg, 59  $\mu\text{mol}$ ) were dissolved in 1 mL DCM at 0°C and stirred for 15 min. Then **37b** (23 mg, 59  $\mu\text{mol}$ ) in 500  $\mu\text{L}$  DCM was added, and the mixture was allowed to warm to RT and stirred for 14 h. The crude product was concentrated and

purified using flash chromatography (gradient 0%-8% MeOH in DCM). **35** (17 mg, 22.4  $\mu$ mol, 42 %) was obtained as a colorless oil. The diastereomeric rate was determined by HPLC.

**TLC** [MeOH/DCM, 6:94]:  $R_f$  = 0.42.

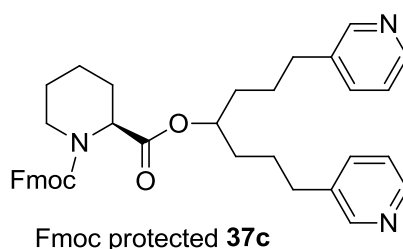
**HPLC** [0-100% Solvent B, 20 min]:  $R_t$  = 16.6 min, purity (220 nm) = 98%, dr 95:5.

**$^1\text{H}$  NMR** (400 MHz,  $d_6$ -DMSO)  $\delta$  7.23 (ddd,  $J$  = 10.0, 7.7, 3.1 Hz, 1H), 7.14 – 7.08 (m, 1H), 6.88 – 6.77 (m, 2H), 6.72 – 6.56 (m, 3H), 6.55 (s, 1H), 6.44 (d,  $J$  = 7.7 Hz, 1H), 5.71 – 5.63 (m, 1H), 5.57 (d,  $J$  = 2.8 Hz, 1H), 5.49 – 5.45 (m, 1H), 5.38 (dd,  $J$  = 8.5, 5.1 Hz, 1H), 5.29 (dt,  $J$  = 5.7, 2.6 Hz, 1H), 4.98 (dd,  $J$  = 17.2, 2.1 Hz, 1H), 4.91 (dd,  $J$  = 10.2, 2.2 Hz, 1H), 4.08 – 4.03 (m, 3H), 3.72 – 3.69 (m, 3H), 3.67 -3.63 (m, 6H), 3.60 (s, 3H), 3.57 (s, 3H), 3.55 (s, 2H), 3.54 (s, 2H), 3.50 – 3.47 (m, 2H), 2.69 (dd,  $J$  = 12.8, 6.1 Hz, 2H), 2.67 – 2.61 (m, 3H), 2.43 (t,  $J$  = 5.0 Hz, 3H), 2.30 (dd,  $J$  = 8.8, 7.0 Hz, 2H), 2.24 (t,  $J$  = 7.4 Hz, 2H), 1.95 (d,  $J$  = 6.5 Hz, 2H).

**$^{13}\text{C}$  NMR** (101 MHz,  $d_6$ -DMSO)  $\delta$  173.73, 172.42, 158.74, 153.18, 149.05, 147.40, 142.24, 136.62, 134.74, 133.73, 133.41, 130.14, 124.03, 122.95, 120.36, 118.25, 116.77, 114.02, 112.69, 112.22, 105.67, 75.54, 66.62, 65.79, 60.30, 57.54, 56.39, 56.30, 56.02, 55.92, 55.75, 54.07, 51.56, 49.97, 49.38, 48.03, 42.98, 33.65, 31.71, 27.03, 26.55, 24.84.

**Mass:** (ESI $^+$ ), calculated 759.39 [ $\text{C}_{43}\text{H}_{54}\text{N}_2\text{O}_{10}+\text{H}$ ] $^+$ , found 759.42 [ $\text{M}+\text{H}$ ] $^+$ .

### (S)-1-((9H-Fluoren-9-yl)methyl)ester-2-(1,7-di(pyridin-3-yl)heptan-4-yl) piperidine-2-dicar-boxylate



A solution of alcohol **5c** (0.30 g, 1.1 mmol) and carboxylic acid **6a** (0.39 g, 1.1 mmol) in 10 mL DCM was treated with EDC (0.23 g, 1.2 mmol). The reaction mixture was stirred for 14 h at RT. The solvent

## C. Experimental Section

---

was removed *in vacuo* and the crude mixture was purified by flash chromatography (gradient 0%-100% EtOAc in cyclohexane) to afford Fmoc protected **37c** as a yellow oil (0.49 g, 0.8 mmol, 73%).

**TLC** [EtOAc 99% + 1% TEA]:  $R_f = 0.2$ .

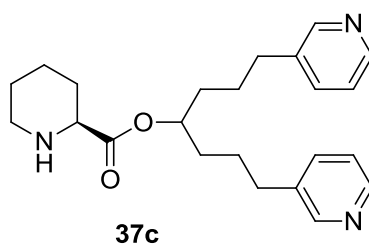
**LCMS**: [0-100% Solvent B, 10 min]:  $R_t = 7.1$  min, purity (220 nm) = 96%.

**$^1\text{H NMR}$**  (300 MHz,  $\text{CDCl}_3$ )  $\delta$  8.47 – 8.34 (m, 4H), 7.77 (d,  $J = 7.1$  Hz, 2H), 7.63 – 7.56 (m, 2H), 7.53 – 7.45 (m, 2H), 7.45 – 7.27 (m, 4H), 7.24 – 7.06 (m, 2H), 4.93 (dd,  $J = 29.0, 23.9$  Hz, 2H), 4.50 – 4.23 (m, 3H), 4.23 – 4.01 (m, 1H), 2.67 – 2.47 (m, 4H), 2.23 (d,  $J = 13.3$  Hz, 1H), 1.82 – 1.38 (m, 10H), 1.35 – 1.16 (m, 4H).

**$^{13}\text{C NMR}$**  (75 MHz,  $\text{CDCl}_3$ )  $\delta$  171.54, 156.48, 149.32, 147.14, 143.57, 141.28, 137.13, 135.83, 127.71, 127.04, 125.09, 123.28, 120.07, 74.16, 67.71, 60.38, 54.22, 47.09, 41.86, 33.45, 32.37, 29.69, 26.28, 24.46, 21.27, 20.55, 14.25.

**Mass**: (ESI<sup>+</sup>), calculated 604.32 [ $\text{C}_{38}\text{H}_{41}\text{N}_3\text{O}_4 + \text{H}$ ]<sup>+</sup>, found 604.30 [M + H]<sup>+</sup>.

### (S)-1,7-Di(pyridin-3-yl)heptan-4-yl piperidine-2-carboxylate (**37c**)



Fmoc-protected **37c** (0.44 g, 0.73 mmol) was dissolved in 1.8 mL dry DCM, then 0.2 mL 4-Methylpiperidin was added and stirred for 14 h at RT. The crude mixture was concentrated and purified by flash chromatography (gradient 0%-15% MeOH in DCM). **37c** (0.22 g, 0.58 mmol, 80%) was obtained as a slight yellow oil.

**TLC** [MeOH/DCM 10:90]:  $R_f = 0.42$ .

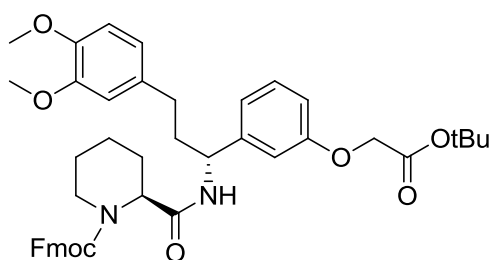
**HPLC** [0-50% Solvent B, 20 min]:  $R_t = 9.0$  min, purity (220 nm) = 90%.

$^1\text{H NMR}$  (300 MHz,  $\text{CDCl}_3$ )  $\delta$  8.46 – 8.38 (m, 4H), 7.42-7.38 (m, 2H), 7.18-7.14 (m,  $J = 7.5$  Hz, 2H), 4.83 (tt,  $J = 6.3, 4.9$  Hz, 1H), 3.16 – 3.03 (m, 2H), 2.73 (dt,  $J = 12.2, 5.2$  Hz, 1H), 2.62 – 2.56 (m, 4H), 2.12 (ddt,  $J = 12.0, 7.5, 5.9$  Hz, 1H), 2.00 (s, 1H), 1.78 – 1.69 (m, 1H), 1.69 – 1.63 (m, 4H), 1.62 – 1.56 (m, 3H), 1.55 – 1.51 (m, 1H), 1.51 – 1.46 (m, 4H).

$^{13}\text{C NMR}$  (75 MHz,  $\text{CDCl}_3$ )  $\delta$  169.23, 149.61, 147.27, 137.42, 137.13, 136.99, 136.08, 135.90, 123.48, 75.55, 56.98, 45.31, 43.48, 36.56, 32.26, 27.26, 26.20, 22.20.

**Mass:** (ESI<sup>+</sup>), calculated 382.25 [ $\text{C}_{23}\text{H}_{31}\text{N}_3\text{O}_2 + \text{H}$ ]<sup>+</sup>, found 382.20 [ $\text{M} + \text{H}$ ]<sup>+</sup>.

**(S)-1-((9H-Fluoren-9-yl)methyl)ester-2-((R)-1-(3-(2-(tert-butoxy)-2-oxoethoxy)phenyl)-3-(3,4-dimethoxyphenyl)propyl) piperidine-2-carboxylate**



Fmoc protected **37e**

**6a** (0.25 g, 0.71 mmol), DIPEA (0.37 g, 2.85 mmol) and HATU (410 mg, 1.07 mmol) were dissolved in 1.5 mL DMF and stirred for 30 min. Then (*R*)-tert-butyl-2-(3-(1-amino-3-(3,4-dimethoxyphenyl)propyl)phenoxy)acetate **5e** (0.29 g, 0.71 mmol) dissolved in 2 mL DCM was added to the reaction mixture and stirred at RT for 14 h. The solvent was removed *in vacuo* and the crude product was purified by flash chromatography (EtOAc/cyclohexane 3:7) to afford Fmoc protected **37e** (0.48 g, 0.65 mmol, 92%) as a slightly yellow solid.

**TLC** [EtOAc/cyclohexane 3:7]:  $R_f = 0.25$ .

**HPLC** [0-100% Solvent B, 20 min]:  $R_t = 20.5$  min, purity (220 nm) = 98%

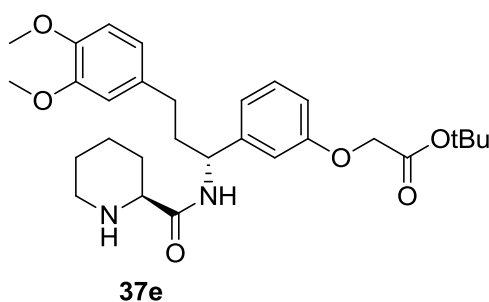
$^1\text{H NMR}$  (400 MHz, DMSO)  $\delta$  7.83-7.80 (m, 2H), 7.63-7.58 (m, 2H), 7.46 – 7.39 (m, 4H), 7.32 – 7.20 (m, 2H), 7.04-7.02 (m, 2H), 6.88-6.84 (m, 3H), 6.80 – 6.74 (m, 2H), 5.20-5.17 (m, 1H), 5.00 – 4.93 (m, 4H),

4.83 (t,  $J = 6.2$  Hz, 1H), 4.17-4.11 (m, 1H), 3.83 (s, 3H), 3.75 (s, 3H), 3.53-3.47 (m, 1H), 2.82 (t,  $J = 4.3$  Hz, 1H), 2.69 (t,  $J = 7.9$  Hz, 2H), 2.34-2.20 (m, 2H), 2.08-1.91 (m, 2H), 1.79-1.66 (m, 3H), 1.34 (s, 9H).

$^{13}\text{C}$  NMR (101 MHz, DMSO)  $\delta$  170.45, 168.32, 162.49, 158.23, 155.70, 148.71, 147.54, 145.61, 144.45, 141.16, 134.01, 129.35, 128.18, 127.22, 125.45, 120.40, 119.48, 113.43, 112.65, 112.08, 81.47, 64.94, 59.93, 55.91, 54.51, 51.97, 46.97, 41.90, 38.41, 36.27, 32.22, 31.25, 28.31, 26.80, 24.78, 21.20.

**Mass:** (ESI<sup>+</sup>), calculated 531.25 [C<sub>44</sub>H<sub>50</sub>N<sub>2</sub>O<sub>8</sub>+H]<sup>+</sup>, found 531.21 [M+H]<sup>+</sup>.

**tert-Butyl-2-(3-((*R*)-3-(3,4-dimethoxyphenyl)-1-((*S*)-piperidine-2-carboxamido)propyl) phenoxy) acetate (37e)**



Fmoc protected **37e** (0.43 mg, 0.59 mmol) was dissolved in 4.5 mL dry DCM, then was added 0.5 mL 4-methylpiperidine and stirred for 14 h. The raw product was concentrated and subjected to flash chromatography (gradient 0-100% EtOAc in cyclohexane, then EtOAc/MeOH 99:1, 1% TEA). **37e** (160 mg, 0.312, 53%) was obtained as a white solid.

**TLC** [EtOAc/MeOH 99:1, 1% TEA]:  $R_f = 0.20$ .

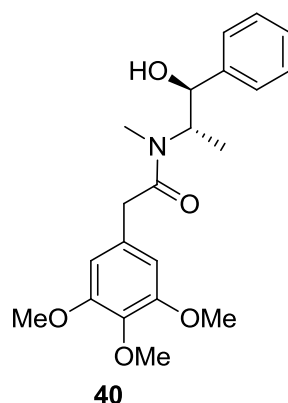
**HPLC** [0-100% Solvent B, 20 min]:  $R_t = 14.8$  min, purity (220 nm) = 95%

$^1\text{H}$  NMR (300 MHz, CDCl<sub>3</sub>)  $\delta$  7.26 – 7.20 (m, 1H), 7.18 (d,  $J = 9.4$  Hz, 1H), 6.94 – 6.88 (m, 1H), 6.86 (dd,  $J = 2.6, 1.5$  Hz, 1H), 6.78 – 6.72 (m, 2H), 6.69 – 6.64 (m, 2H), 4.96 (q,  $J = 7.7$  Hz, 1H), 4.49 (s, 2H), 3.85 (s, 3H), 3.83 (s, 3H), 3.23 – 3.15 (m, 1H), 3.02 – 2.91 (m, 1H), 2.68 – 2.58 (m, 1H), 2.59 – 2.50 (m, 2H), 2.21 – 2.00 (m, 4H), 1.98 – 1.87 (m, 1H), 1.80 – 1.70 (m, 1H), 1.59 – 1.49 (m, 1H), 1.47 (s, 9H).

$^{13}\text{C}$  NMR (75 MHz,  $\text{CDCl}_3$ )  $\delta$  172.71, 167.65, 158.24, 148.73, 146.82, 144.02, 133.90, 129.60, 120.08, 119.82, 113.37, 112.87, 111.74, 111.20, 82.20, 65.69, 60.12, 55.90, 52.51, 45.68, 37.93, 32.24, 29.75, 28.02, 25.69, 23.88.

**Mass:** (ESI+), calculated 530.30 [ $\text{C}_{29}\text{H}_{40}\text{N}_2\text{O}_6+\text{H}$ ] $^+$ , found 530.28 [ $\text{M}+\text{H}$ ] $^+$ .

**N-((1*S*,2*S*)-1-Hydroxy-1-phenylpropan-2-yl)-N-methyl-2-(3,4,5-trimethoxyphenyl)acetamide (40)**



Trimethoxyphenyl acetic acid **11** (5.0 g, 22.1 mmol), triethylamine (3.5 mL, 46.0 mmol), EDC-HCl (3.9 g, 20.26 mmol) and HOAt (2.76 g, 20.26 mmol) were dissolved in DCM at 0°C. Then (*S,S*)-pseudoephedrine (3.0 g, 18.4 mmol) was added and the reaction was stirred at RT for 14 h. The crude product was concentrated and purified using flash chromatography (gradient 0%-100% EtOAc in cyclohexane). **40** (6.37 g, 17.06 mmol, 92%) was obtained as a white solid.

**TLC** [EtOAc, 1% TEA]:  $R_f$  = 0.33.

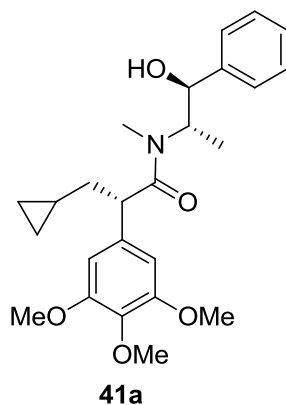
**HPLC** [0-100% Solvent B, 20 min]:  $R_t$  = 14.4 min, purity (220 nm)  $\geq$  99%.

$^1\text{H}$  NMR (300 MHz,  $\text{CDCl}_3$ )  $\delta$  7.38 – 7.20 (m, 5H), 6.47 (s, 2H), 4.66 – 4.40 (m, 1H), 4.25 – 3.94 (m, 1H), 3.84 (s, 6H), 3.82 (s, 3H), 3.65 (s, 2H), 2.85 (s, 3H), 1.11 – 1.02 (m, 3H).

$^{13}\text{C}$  NMR (75 MHz,  $\text{CDCl}_3$ )  $\delta$  173.11, 153.10, 142.00, 136.81, 130.26, 128.65, 128.40, 127.78, 126.77, 126.49, 105.74, 75.43, 60.81, 58.73, 56.13, 42.02, 32.76, 14.40.

**Mass:** (ESI<sup>+</sup>), calculated 374.20 [C<sub>21</sub>H<sub>27</sub>NO<sub>5</sub>+H]<sup>+</sup>, found 374.20 [M+H]<sup>+</sup>.

**(S)-3-Cyclopropyl-N-((1S,2S)-1-hydroxy-1-phenylpropan-2-yl)-N-methyl-2-(3,4,5-trimethoxyphenyl)propanamide (41a)**



**40** (1.0 g, 2.7 mmol) and Lithiumchloride (0.68 mg, 16.07 mmol) were put each into a Schlenck flask and kept under high vacuum for 14 h. Additionally LiCl was heated to 150°C using an oil bath. Then **40** was dissolved in 18 mL anhydrous THF and added to the dry LiCl. The mixture was cooled to -78°C. LDA (2.95 mL, 5.89 mmol, 2.0 M in THF/heptane/ethylbenzene) was added dropwise and then stirred for 1h. The reaction mixture was warmed to 0°C, and stirred for 15 min, finally warmed briefly to RT, then cooled again to 0°C and treated with cyclopropylmethylbromide (1.3 mL, 13.4 mmol). The reaction mixture was stirred for 2h at 0°C then slowly warmed to RT and stirred for another 14 h. The raw product was diluted with brine, acidified with 1 M HCl to pH~2 and extracted with DCM. The organic phases were combined and dried over MgSO<sub>4</sub>. The crude product was concentrated and purified by flash chromatography (gradient 0%-50% EtOAc in cyclohexane). **41a** (0.65 g, 1.51 mmol, 56%) was obtained as yellow crystals.

**TLC** [MeOH/DCM, 5:95]: R<sub>f</sub> = 0.40.

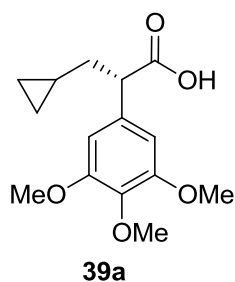
**HPLC** [0-100% Solvent B, 20 min]: R<sub>t</sub> = 14.4 min, purity (220 nm) = 98%, dr 95:5.

•  
**<sup>1</sup>H NMR** (300 MHz, CDCl<sub>3</sub>) δ 7.41 (s, 1H), 7.38 – 7.31 (m, 2H), 7.28 (d, *J* = 1.0 Hz, 2H), 6.52 (s, 2H), 4.58 (d, *J* = 6.3 Hz, 1H), 4.14 (d, *J* = 7.1 Hz, 1H), 3.87 – 3.80 (m, 9H), 3.65 (t, *J* = 7.2 Hz, 1H), 2.79 (s, 3H), 2.12 – 1.93 (m, 1H), 1.58 – 1.46 (m, 1H), 1.14 (d, *J* = 6.8 Hz, 3H), 0.67 (s, 1H), 0.43 (dd, *J* = 8.5, 4.6 Hz, 2H), 0.23 – -0.00 (m, 2H).

$^{13}\text{C}$  NMR (75 MHz,  $\text{CDCl}_3$ )  $\delta$  175.54, 153.41, 142.33, 136.85, 135.47, 128.31, 127.60, 126.37, 104.71, 75.45, 60.83, 56.18, 50.68, 40.34, 27.33, 14.17, 9.42, 4.66, 4.63.

**Mass:** ( $\text{ESI}^+$ ), calculated 428.24 [ $\text{C}_{25}\text{H}_{33}\text{NO}_5+\text{H}$ ] $^+$ , found 428.52 [ $\text{M}+\text{H}$ ] $^+$ .

### (S)-3-cyclopropyl-2-(3,4,5-trimethoxyphenyl)propanoic acid (39a)



**41a** (0.28 mg, 0.66 mmol) was dissolved in 4 mL dioxane at RT. 4 mL of a 4 M solution of  $\text{H}_2\text{SO}_4$  in water were added dropwise. The mixture was refluxed for 4h (150°C). The reaction was quenched by addition of 50% (w/v) NaOH followed by extraction with DCM. The aqueous phase was acidified with 1 M HCl to pH<2 and extracted again. The organic layers of the acidic extraction were combined and dried over  $\text{MgSO}_4$ . The raw product was concentrated and purified using preparative TLC (MeOH/DCM, 9:91, 1% AcOH). **39a** (68 mg, 0.24 mmol, 37%) was obtained as a yellow oil.

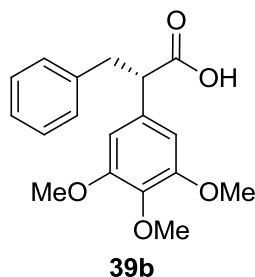
**TLC** [EtOAc/cyclohexane, 1:1, 1% AcOH]:  $R_f$  = 0.35.

**HPLC** [0-100% Solvent B, 20 min]:  $R_t$  = 15.1 min, purity (220 nm) = 95%.

$^1\text{H}$  NMR (300 MHz,  $\text{CDCl}_3$ )  $\delta$  6.57 (s, 2H), 3.87 (s, 6H), 3.84 (s, 3H), 3.62 (dd,  $J$  = 8.2, 7.0 Hz, 1H), 1.91 (dt,  $J$  = 13.9, 7.8 Hz, 1H), 1.75 (dt,  $J$  = 13.7, 6.8 Hz, 1H), 0.75 – 0.61 (m, 1H), 0.49 – 0.41 (m, 2H), 0.16 – 0.04 (m, 2H).

$^{13}\text{C}$  NMR (75 MHz,  $\text{CDCl}_3$ )  $\delta$  179.79, 153.24, 137.35, 134.17, 105.09, 60.44, 56.14, 52.16, 38.39, 9.20, 4.46.

**Mass:** ( $\text{ESI}^+$ ), calculated 281.14 [ $\text{C}_{15}\text{H}_{20}\text{O}_5+\text{H}$ ] $^+$ , found 281.37 [ $\text{M}+\text{H}$ ] $^+$ .

**(S)-3-phenyl-2-(3,4,5-trimethoxyphenyl)propanoic acid (39b)**

**40** (0.5 g, 1.34 mmol) and dry Lithiumchloride (0.34 g, 8.03 mmol, dried as described for **41a**) were dissolved in 5 mL anhydrous THF and cooled to  $-78^{\circ}\text{C}$ . LDA (1.4 mL, 2.95 mmol) was added and stirred for 1 h. The reaction mixture was warmed to  $0^{\circ}\text{C}$ , and stirred for 15 min, finally warmed briefly to RT, then cooled again to  $0^{\circ}\text{C}$  and treated with Benzylbromide (0.8 mL, 6.69 mmol). The reaction mixture was stirred at  $0^{\circ}\text{C}$  for 14 h. The crude product was concentrated and purified by flash chromatography (gradient, 0%-40% EtOAc in cyclohexane). **41b** (0.33 mg, 0.77 mmol, 58%) was obtained as a yellow oil which was directly further reacted.

**TLC** [EtOAc/cyclohexane, 2:1]:  $R_f = 0.33$ .

**HPLC** [0-100% Solvent B, 20 min]:  $R_t = 23.5$  min, purity (220 nm) = 95%, dr = 95:5.

**Mass** (ESI<sup>+</sup>), calculated 464.24 [C<sub>28</sub>H<sub>33</sub>NO<sub>5</sub>+H]<sup>+</sup>, found 464.27 [M+H]<sup>+</sup>.

**41b** (0.28 mg, 0.60 mmol) was dissolved in 4 mL dioxane and then 3.5 mL of a 4 M aq solution of H<sub>2</sub>SO<sub>4</sub> was added. The mixture was refluxed for 4h. ( $150^{\circ}\text{C}$ ). The reaction was quenched by addition of 50% (w/v) NaOH then was extracted with DCM. Now was acidified with 1 M HCl to pH<2 and again extracted. These organic layers were combined and dried over MgSO<sub>4</sub>. The raw product was purified using preparative TLC (EtOAc/cyclohexane, 3:7, 4% AcOH). **39b** (113 mg, 0.36 mmol, 60%) was obtained as a yellow oil.

**TLC** [EtOAc/cyclohexane, 3:7, 4% AcOH]:  $R_f = 0.42$ .

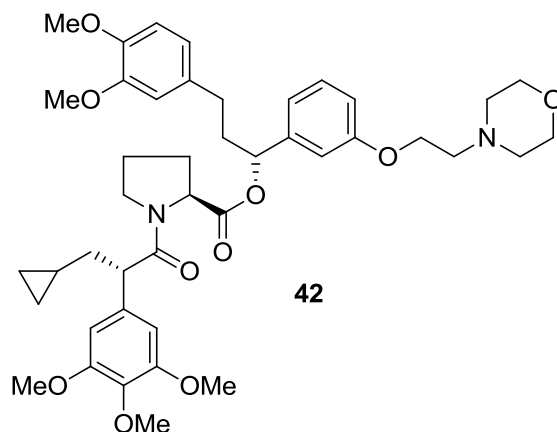
**HPLC** [0-100% Solvent B, 20 min]:  $R_t = 19.9$  min, purity (220 nm)  $\geq 99\%$ .

$^1\text{H NMR}$  (300 MHz,  $\text{CDCl}_3$ )  $\delta$  7.29 – 7.20 (m, 3H), 7.14 (dd,  $J = 7.9, 1.7$  Hz, 2H), 6.53 (s, 2H), 3.85 (s, 6H), 3.84 (s, 3H), 3.40 (dd,  $J = 13.8, 8.5$  Hz, 2H), 3.04 (dd,  $J = 13.7, 6.8$  Hz, 1H).

$^{13}\text{C NMR}$  (75 MHz,  $\text{cdCl}_3$ )  $\delta$  178.92, 153.27, 138.58, 137.50, 133.49, 130.37, 128.90, 128.41, 126.54, 105.19, 60.84, 56.16, 53.59, 39.38, 20.76, 1.03.

**Mass:** ( $\text{ESI}^+$ ), calculated 317.14 [ $\text{C}_{18}\text{H}_{20}\text{O}_5+\text{H}$ ] $^+$ , found 317.13 [ $\text{M}+\text{H}$ ] $^+$ .

**(S)-(R)-3-(3,4-dimethoxyphenyl)-1-(3-(2-morpholinoethoxy)phenyl)propyl-1-((S)-3-cyclopropyl-2-(3,4,5-trimethoxyphenyl)propanoyl)pyrrolidine-2-carboxylate (42)**



General synthesis procedure **A** for morpholine ligands with **36b** (40 mg, 80  $\mu\text{mol}$ ) and **39a** (22 mg, 80  $\mu\text{mol}$ ) was used. Then was purified using preparative HPLC (gradient 55%-70% Solvent B in Solvent A, 20min) to obtain **42** (17 mg, 7.7  $\mu\text{mol}$ , 28%) as a colorless oil. The diastereomeric rate was determined by HPLC.

**TLC** [ $\text{MeOH}/\text{DCM}$ , 8:92]:  $R_f = 0.44$ .

**HPLC** [0-100% Solvent B, 20 min]:  $R_t = 16.3$  min, purity (220 nm) = 95%, dr 95:5

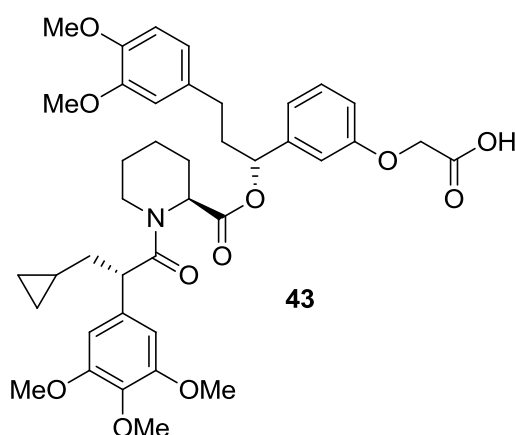
$^1\text{H NMR}$  (400 MHz,  $\text{d}_6\text{-DMSO}$ )  $\delta$  7.52 (d,  $J = 7.7$  Hz, 1H), 7.33 – 7.20 (m, 1H), 6.97 – 6.85 (m, 2H), 6.84 – 6.78 (m, 2H), 6.64 – 6.56 (m, 2H), 6.50 (s, 1H), 5.54 (ddd,  $J = 37.2, 8.3, 4.8$  Hz, 2H), 4.46 (dd,  $J = 8.6, 3.4$  Hz, 1H), 4.41 – 4.29 (m, 3H), 3.84 – 3.74 (m, 3H), 3.73 – 3.69 (m, 5H), 3.69 – 3.67 (m, 5H), 3.61 – 3.58 (m, 3H), 3.56 – 3.49 (m, 6H), 2.59 (s, 4H), 2.47 (p,  $J = 1.8$  Hz, 1 H), 2.38 – 2.28 (m, 1H), 2.23 – 2.05

(m, 2H), 1.93 – 1.76 (m, 2H), 1.75 – 1.65 (m, 1H), 1.37 – 1.26 (m, 1H), 1.22 (dt,  $J = 12.1, 6.8$  Hz, 2H), 0.60 (s, 1H), 0.36 – 0.22 (m, 2H), 0.02 (qd,  $J = 10.2, 4.6$  Hz, 2H).

$^{13}\text{C}$  NMR (101 MHz, d6-DMSO)  $\delta$  171.83, 171.50, 158.19, 153.15, 152.99, 149.04, 147.39, 142.69, 136.39, 135.86, 133.76, 133.68, 123.98, 120.49, 114.37, 112.75, 112.42, 105.67, 75.17, 63.75, 62.51, 60.23, 56.30, 55.99, 55.78, 52.16, 49.87, 46.13, 30.78, 29.12, 24.88, 21.14, 14.40, 9.61, 8.81, 4.85.

Mass: (ESI<sup>+</sup>), calculated 761.40 [C<sub>43</sub>H<sub>56</sub>N<sub>2</sub>O<sub>10</sub>+H]<sup>+</sup>, found 761.41 [M+H]<sup>+</sup>.

**2-(3-((*R*)-1-(((*S*)-1-((*S*)-3-cyclopropyl-2-(3,4,5-trimethoxyphenyl)propanoyl) piperidine-2-carbonyl)oxy)-3-(3,4-dimethoxyphenyl)propyl)phenoxy)acetic acid (**43**)**



General synthesis procedure **B** for free acid ligands with **37a** (100 mg, 0.20 mmol) and **39a** (55 mg, 0.20 mmol) (57.0 mg, 0.21 mmol) was used. The crude product was concentrated and purified using flash chromatography (gradient 0%-10% MeOH in DCM) to obtain **43** (38 mg, 54  $\mu\text{mol}$ , 55%) as a colorless oil. The diastereomeric rate was determined by HPLC.

TLC [MeOH/DCM, 6:94]:  $R_f = 0.27$ .

HPLC [0-100% Solvent B, 20 min]:  $R_t = 19.3$  min, purity (220 nm) = 95%, dr = 95:5.

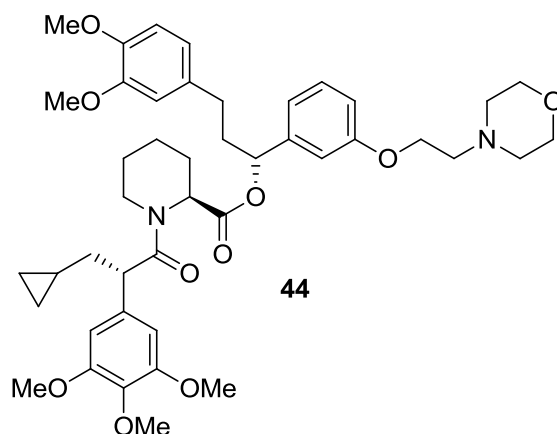
$^1\text{H}$  NMR (400 MHz, d6-DMSO)  $\delta$  7.22 (s, 1H), 7.12 (dd,  $J = 15.6, 7.9$  Hz, 1H), 6.85 – 6.69 (m, 3H), 6.63 – 6.55 (m, 2H), 6.51 (s, 1H), 5.50 (dd,  $J = 8.2, 5.2$  Hz, 1H), 5.25 (s, 1H), 4.64 (s, 2H), 3.71 (d,  $J = 2.0$  Hz,

2H), 3.68 (s, 3H), 3.67 (s, 3H), 3.60 (d,  $J = 2.5$  Hz, 1H), 3.56 (s, 6H), 3.53 (s, 3H), 2.68 – 2.60 (m, 1H), 2.52 (t,  $J = 5.3$  Hz, 2H), 2.45 – 2.40 (s, 2H), 2.38 – 2.33 (m, 2H), 2.14 (d,  $J = 12.0$  Hz, 1H), 1.94 – 1.84 (m, 2H), 1.64 – 1.57 (m, 4H), 0.63 – 0.56 (m, 1H), 0.36 – 0.28 (m, 2H), 0.07 – -0.03 (m, 2H).

$^{13}\text{C}$  NMR (101 MHz,  $d_6$ -DMSO)  $\delta$  172.66, 170.73, 170.52, 158.01, 153.09, 149.14, 147.59, 142.39, 136.43, 135.93, 133.44, 129.79, 120.34, 113.88, 112.82, 112.64, 112.34, 109.94, 105.52, 75.34, 64.87, 60.20, 57.45, 56.30, 55.95, 55.88, 52.05, 47.92, 43.37, 30.92, 26.67, 21.10, 14.38, 9.71, 4.73.

Mass: (ESI<sup>+</sup>), calculated 720.34 [ $\text{C}_{40}\text{H}_{49}\text{NO}_{11}+\text{H}$ ]<sup>+</sup>, found 720.32 [M+H]<sup>+</sup>.

**(S)-(R)-3-(3,4-dimethoxyphenyl)-1-(3-(2-morpholinoethoxy)phenyl)propyl-1-((S)-3-cyclopropyl-2-(3,4,5-trimethoxyphenyl)propanoyl)piperidine-2-carboxylate (44)**



General synthesis procedure **A** for morpholine ligands with **39a** (8 mg, 29  $\mu\text{mol}$ ) and **37b** (14 mg, 27  $\mu\text{mol}$ ) was used. Then was purified using flash chromatography (gradient 0%-10% MeOH in DCM) to obtain **44** (6 mg, 7.74  $\mu\text{mol}$ , 29%) as a colorless oil. The diastereomeric rate was determined by HPLC.

TLC [MeOH/DCM, 8:92]:  $R_f = 0.52$ .

HPLC [0-100% Solvent B, 20 min]:  $R_t = 15.1$  min, purity (220 nm) = 95%, dr 95:5

$^1\text{H}$  NMR (600 MHz,  $\text{CDCl}_3$ )  $\delta$  7.26-7.24 (m, 1H), 7.02 – 6.97 (m, 1H), 6.90 – 6.71 (m, 5H), 6.60 (s, 2H), 5.45-5.43 (m, 1H), 4.88-4.86 (m, 1H), 4.08-4.05 (m, 2H), 3.84 – 3.74 (m, 6H), 3.72 – 3.70 (m, 8H), 3.70

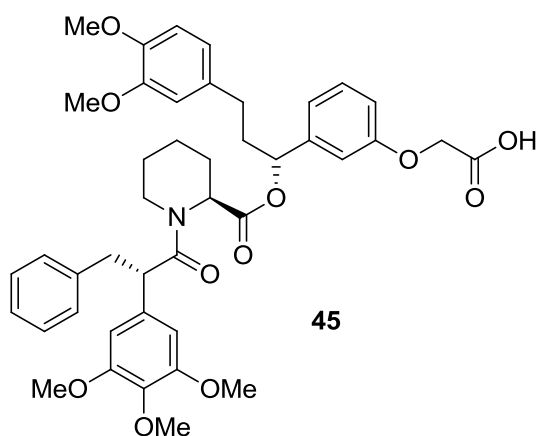
### C. Experimental Section

– 3.59 (m, 2H), 3.55–3.53 (m,  $J = 4.7$  Hz, 4H), 3.49 – 3.45 (m, 1H), 2.76 – 2.64 (m, 4H), 2.53 – 2.41 (m, 5H), 2.16 – 2.06 (m, 3H), 1.99–1.97 (m,  $J = 7.2$  Hz, 1H), 1.92 – 1.82 (m, 3H), 1.74 – 1.60 (m, 3H), 0.88 – 0.75 (m, 1H), 0.31 – 0.20 (m, 2H), 0.05 – -0.06 (m, 2H).

$^{13}\text{C}$  NMR (125 MHz,  $\text{CDCl}_3$ )  $\delta$  175.62, 170.15, 159.63, 156.01, 150.39, 148.33, 143.58, 137.88, 135.20, 132.08, 129.28, 121.85, 119.20, 115.53, 114.12, 113.68, 113.06, 107.04, 77.03, 67.38, 66.80, 60.70, 58.74, 56.83, 54.73, 52.94, 48.18, 43.29, 36.38, 34.08, 33.96, 25.91, 25.47, 22.24, 9.61, 7.11.

**Mass:** (ESI<sup>+</sup>), calculated 775.42 [ $\text{C}_{44}\text{H}_{58}\text{N}_2\text{O}_{10} + \text{H}$ ]<sup>+</sup>, found 775.48 [M+H]<sup>+</sup>.

### 2-(3-((*R*)-3-(3,4-dimethoxyphenyl)-1-(((*S*)-1-((*S*)-3-phenyl-2-(3,4,5-trimethoxyphenyl) propanoyl)piperidine-2-carbonyl)oxy)propyl)phenoxy)acetic acid (**45**)



General synthesis procedure **B** for free acid ligands with **41b** (68 mg, 0.21 mmol) and **37a** (100 mg, 0.20 mmol) was used. Then was purified using reversed phase flash (Gradient 40%–70% MeOH in  $\text{H}_2\text{O}$  + 1%AcOH) to obtain **45** (49 mg, 0.13 mmol, 49%) as a slight yellow oil. The diastereomeric rate was determined by HPLC.

**TLC** [MeOH/DCM, 8:92]:  $R_f = 0.20$ .

**HPLC** [isochratic 60% B, 20 min]:  $R_t = 10.4$  min, purity (220 nm) = 98%, dr 95:5.

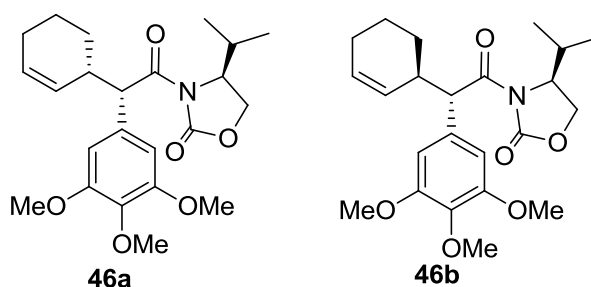
$^1\text{H}$  NMR (599 MHz,  $d_6$ -DMSO)  $\delta$  7.27 – 7.03 (m, 6H), 6.86 – 6.65 (m, 5H), 6.59 (s, 2H), 5.50 (dd,  $J = 8.2$ , 5.1 Hz, 1H), 5.19 (dd,  $J = 6.0$ , 2.5 Hz, 1H), 4.61 (s, 2H), 4.35 (dd,  $J = 8.9$ , 6.0 Hz, 1H), 3.99 (d,  $J = 13.2$  Hz, 1H), 3.70 (s, 3H), 3.69 (s, 3H), 3.66 (s, 1H), 3.62 (s, 6H), 3.53 (d,  $J = 0.7$  Hz, 3H), 3.31 – 3.26 (m, 2H),

2.85 (dd,  $J = 13.5, 5.9$  Hz, 1H), 2.70 (td,  $J = 13.4, 2.9$  Hz, 1H), 2.43 (ddd,  $J = 14.0, 9.0, 5.7$  Hz, 1H), 2.33 (dt,  $J = 14.0, 8.1$  Hz, 1H), 2.08 (d,  $J = 13.4$  Hz, 1H), 1.88 (qd,  $J = 8.5, 8.0, 5.4$  Hz, 2H), 1.54 – 1.44 (m, 2H), 1.44 – 1.35 (m, 1H), 1.12 – 1.03 (m, 1H), 1.01 – 0.93 (m, 1H).

$^{13}\text{C}$  NMR (151 MHz,  $d_6$ -DMSO)  $\delta$  172.30, 170.60, 158.34, 153.05, 149.12, 147.61, 142.67, 140.25, 136.47, 135.16, 133.44, 130.00, 129.79, 129.59, 129.38, 129.37, 128.49, 128.26, 126.26, 120.50, 118.49, 113.89, 112.61, 112.53, 112.42, 105.76, 75.42, 65.12, 60.25, 56.09, 55.98, 55.86, 55.72, 52.13, 49.02, 43.34, 41.21, 38.10, 31.04, 26.52, 20.78.

Mass: (ESI), calculated 756.34 [ $\text{C}_{43}\text{H}_{49}\text{NO}_{11}+\text{H}$ ] $^-$ , found 756.33 [ $\text{M}+\text{H}$ ] $^+$ .

**(S)-3-((S)-2-((S)-cyclohex-2-en-1-yl)-2-(3,4,5-trimethoxyphenyl)acetyl)-4-isopropyl-oxazolidin-2-one (46a)**



dr = 85 : 15

**21** (3.0 g, 8.89 mmol) was dissolved in 1 mL anhydrous THF and cooled to  $-78$  °C. Then NaHMDS (14.23 mL, 14.23 mmol, 1 M in THF) was added dropwise and stirred for 1h. The reaction mixture was briefly warmed to  $0$  °C and cooled again to  $-78$  °C. Cyclohexene bromide (1.0 mL, 8.9 mmol) was added dropwise and stirred for 1h at  $-78$  °C finally it was slowly warmed to  $0$  °C and stirred for another 14 h. The reaction mixture was quenched with sat.  $\text{NH}_4\text{Cl}$  solution and extracted with DCM. The organic phase was dried over  $\text{MgSO}_4$  and the solvent was removed *in vacuo*. The raw product was purified using column chromatography (EtOAc/cyclohexane 1:3) to obtain a mixture of **46a/b** (2.03 g, 4.9 mmol, 55%) as yellow orange solid. A dr at  $\text{C}_\beta$  of 85:15 was determined via  $^{13}\text{C}$  NMR (**Annex Fig. D**). The distribution shown above is based on the co-crystal structure with **51**.

TLC [EtOAc/n-hexane 1:2]:  $R_f = 0.5$ .

**HPLC 46a/b** [55-65% Solvent B, 20 min]: Rt = 20.3 min, purity (220 nm)  $\geq$  99%.

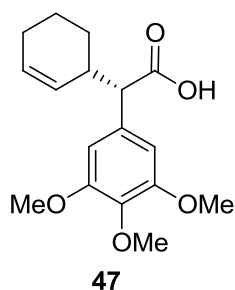
**HPLC 46a/b** [55-65% Solvent B, 20 min]: Rt = 16.6 min, purity (220 nm)  $\geq$  99%.

**<sup>1</sup>H NMR** (300 MHz, d<sub>6</sub>-DMSO) major diastereomer  $\delta$  6.54 – 6.53 (s, 2H), 5.74 – 5.66 (m, 1H), 5.61 – 5.54 (dd, J = 10.3, 2.3 Hz, 1H), 4.73 – 4.67 (d, J = 11.2 Hz, 1H), 4.49 – 4.42 (m, 1H), 4.34 – 4.27 (m, 1H), 4.20 – 4.15 (dd, J = 9.0, 3.1 Hz, 1H), 3.70 – 3.69 (s, 6H), 3.62 – 3.60 (s, J = 1.9 Hz, 3H), 1.68 – 1.55 (m, 3H), 1.47 – 1.35 (m, 2H), 1.34 – 1.20 (dd, J = 14.4, 7.5 Hz, 2H), 1.11 – 0.98 (m, 1H), 0.73 – 0.69 (d, J = 7.0 Hz, 3H), 0.35 – 0.32 (d, J = 6.8, 3H).

**<sup>13</sup>C NMR** (75 MHz, d<sub>6</sub>-DMSO) major diastereomer  $\delta$  172.85, 172.83, 153.81, 153.09, 137.22, 133.09, 129.97, 128.88, 106.30, 63.53, 60.45, 57.97, 56.30, 54.06, 37.30, 28.12, 26.52, 25.25, 20.99, 17.56, 14.44.

**Mass:** (ESI<sup>+</sup>), calculated 418.22 [C<sub>23</sub>H<sub>31</sub>NO<sub>6</sub>+H]<sup>+</sup>, found 418.25 [M+H]<sup>+</sup>.

### **(S)-2-((R)-Cyclohex-2-en-1-yl)-2-(3,4,5-trimethoxyphenyl)acetic acid (47)**



**46** (0.65 mg, 1.56 mmol) was dissolved in 13 mL THF/H<sub>2</sub>O 8:5 at RT. Then lithium hydroxide (75 mg, 3.12 mmol) and hydrogen peroxide (0.68 mL, 28.1 mmol) were added and stirred until complete dissolved. The reaction mixture was cooled to 0°C and stirred for 4h and another 2h at RT. Finally the reaction was quenched with 5 mL 1.5 M Na<sub>2</sub>SO<sub>3</sub> solution and was subsequently diluted with brine and extracted with DCM. The aqueous phase was acidified to pH<2 and extracted again with DCM. All organic phases were checked with TLC and LCMS, product containing phases were combined, dried over MgSO<sub>4</sub> and concentrated. **47** (470 mg, 1.53 mmol, 96%) was obtained without further purification as a yellow oil with a dr 85:15 (determined via <sup>13</sup>C NMR).

**TLC** [EtOAc/n-hexane 1:1.5, 1% AcOH]: R<sub>f</sub> = 0.40.

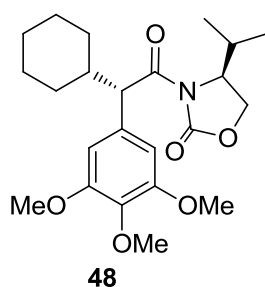
**HPLC** [55-65% Solvent B, 20 min]: Rt = 19.0 min, purity (220 nm) = 98%.

**<sup>1</sup>H NMR** (300 MHz, d<sub>6</sub>-DMSO) major diastereomer δ 6.61 (s, 2H), 5.72 (dd, *J* = 10.0, 2.3 Hz, 1H), 5.61 (d, *J* = 10.3 Hz, 1H), 3.72 (s, 6H), 3.62 (s, 3H), 3.50 (dtd, *J* = 8.6, 6.1, 1.1 Hz, 1H), 3.13 (dd, *J* = 11.1, 4.6 Hz, 1H), 1.91 (s, 2H), 1.41 – 1.20 (m, 3H), 1.10 – 0.91 (m, 1H).

**<sup>13</sup>C NMR** (75 MHz, d<sub>6</sub>-DMSO) major diastereomer δ 174.80, 159.27, 153.00, 136.89, 134.47, 129.95, 128.78, 105.95, 60.30, 57.67, 56.28, 38.26, 26.37, 25.16, 20.75,

**Mass:** (ESI<sup>+</sup>), calculated 307.15 [C<sub>17</sub>H<sub>22</sub>O<sub>5</sub> +H]<sup>+</sup>, found 307.18 [M+H]<sup>+</sup>.

**(S)-3-((S)-2-Cyclohexyl-2-(3,4,5-trimethoxyphenyl)acetyl)-4-isopropyl oxazolidin-2-one (48)**



**46** (0.20 mg, 0.48 mmol) was dissolved in 10 mL of MeOH and placed in an autoclave (Roth, Lab autoclave model II). Palladium on activated charcoal (10% Pd basis, 20 mg, 18.8 μmol) was added and the autoclave was flushed with argon and hydrogen gas. Finally it was filled with 30 bar hydrogen gas and the reaction mixture stirred for 2 d. The reaction progress was monitored by LCMS. If educt was still present another amount of Palladium on activated charcoal (10% Pd basis, 10 mg, 9.40 μmol) was added and above described procedure repeated. The palladium containing crude product was filtered through celite and concentrated. **48** (188 mg, 0.45 mmol, 94%, dr 99:1) was obtained as slight yellow oil and used without further purification. No residual **46** could be observed in the NMR spectra. The diastereomeric rate was determined by HPLC.

**TLC** [EtOAc/n-hexane 1:2]: R<sub>f</sub> = 0.5.

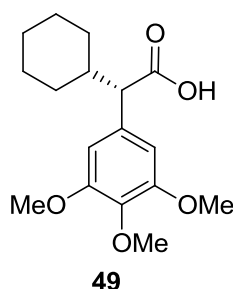
**HPLC** [60-70% Solvent B, 20 min]:  $R_t = 17.9$  min, purity (220 nm) = 98%, dr  $\geq$  99:1.

**$^1\text{H}$  NMR** (300 MHz,  $d_6$ -DMSO)  $\delta$  6.56 (s, 2H), 4.79 (d,  $J = 10.6$  Hz, 1H), 4.38 (dt,  $J = 7.3, 3.5$  Hz, 1H), 4.27 – 4.21 (m, 2H), 3.71 (s, 6H), 3.61 (s, 3H), 2.25 (td,  $J = 7.0, 3.4$  Hz, 1H), 2.04 (d,  $J = 10.9$  Hz, 1H), 1.65 (d,  $J = 11.0$  Hz, 2H), 1.56 (d,  $J = 8.0$  Hz, 2H), 1.25 – 0.99 (m, 6H), 0.84 (d,  $J = 1.6$  Hz, 3H), 0.80 (d,  $J = 6.9$  Hz, 3H).

**$^{13}\text{C}$  NMR** (75 MHz,  $d_6$ -DMSO)  $\delta$  173.58, 154.13, 153.06, 137.13, 133.36, 108.74, 106.47, 63.15, 60.37, 58.76, 56.19, 53.74, 31.49, 30.26, 28.33, 26.28, 25.80, 25.66, 17.88, 14.63.

**Mass:** (ESI<sup>+</sup>), calculated 420.24 [ $\text{C}_{23}\text{H}_{33}\text{NO}_6 + \text{H}$ ]<sup>+</sup>, found 420.25 [M+H]<sup>+</sup>.

### (S)-2-Cyclohexyl-2-(3,4,5-trimethoxyphenyl)acetic acid (**49**)



**48** (0.50 g, 1.19 mmol) was dissolved in 6 mL THF/ $\text{H}_2\text{O}$  8:5 and cooled to 0°C, then lithium hydroxide (57.1 mg, 2.38 mmol) and hydrogen peroxide (0.52 mL, 21.45 mmol) were added and stirred for 24 h. Subsequently the reaction mixture was quenched by adding 5 mL of a 1.5 M  $\text{Na}_2\text{SO}_3$  solution. Finally the reaction was quenched with 5 mL 1.5 M  $\text{Na}_2\text{SO}_3$  solution and was subsequently diluted with brine and extracted with DCM. The aqueous phase was acidified to pH<2 and extracted again with DCM. All organic phases were checked with TLC and LCMS, product containing phases were combined, dried over  $\text{MgSO}_4$  and concentrated. **49** (220 mg, 0.71 mmol, 60%) was obtained as a pale yellow oil without further purification.

**TLC** [EtOAc/n-hexane 1:1.5, 1% AcOH]:  $R_f = 0.33$ .

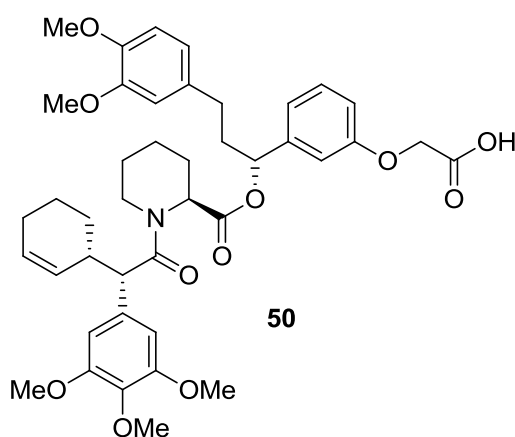
**HPLC** [60-70% Solvent B, 20 min]:  $R_t = 14.4$  min, purity (220 nm) = 95%

$^1\text{H NMR}$  (300 MHz,  $\text{CDCl}_3$ )  $\delta$  6.54 (s, 2H), 3.84 (s, 6H), 3.82 (s, 3H), 3.12 (d,  $J = 10.7$  Hz, 1H), 2.01 – 1.83 (m, 3H), 1.81 – 1.59 (m, 3H), 1.42 – 1.21 (m, 2H), 1.20 – 0.99 (m, 3H).

$^{13}\text{C NMR}$  (75 MHz,  $\text{CDCl}_3$ )  $\delta$  179.31, 153.13, 137.33, 132.79, 105.60, 60.80, 58.89, 56.12, 40.86, 31.91, 30.25, 26.23, 25.91.

**Mass:** ( $\text{ESI}^+$ ), calculated 309.17 [ $\text{C}_{17}\text{H}_{24}\text{O}_5 + \text{H}$ ] $^+$ , found 309.20 [ $\text{M} + \text{H}$ ] $^+$ .

**2-(3-((*R*)-1-(((*S*)-1-((*S*)-2-((*S*)-Cyclohex-2-en-1-yl)-2-(3,4,5-trimethoxyphenyl)acetyl)piperidine-2-carbonyloxy)-3-(3,4-dimethoxyphenyl)propyl)phenoxy)acetic acid (**50**)**



General synthesis procedure **B** for free acid ligands with **37a** (50 mg, 0.20 mmol) and **47** (29.8 mg, 0.20 mmol) was used. Then was purified using flash chromatography (gradient 0%-4% MeOH in DCM) to obtain **50** (25 mg, 33.5  $\mu\text{mol}$ , 67%, dr 85:15) as a slight yellow oil. The dr was determined by NMR.

**TLC** [MeOH/DCM, 6:94]:  $R_f = 0.12$ .

**HPLC** [0-100% Solvent B, 20 min]:  $R_t = 20.0$  min, purity (220 nm) = 98%.

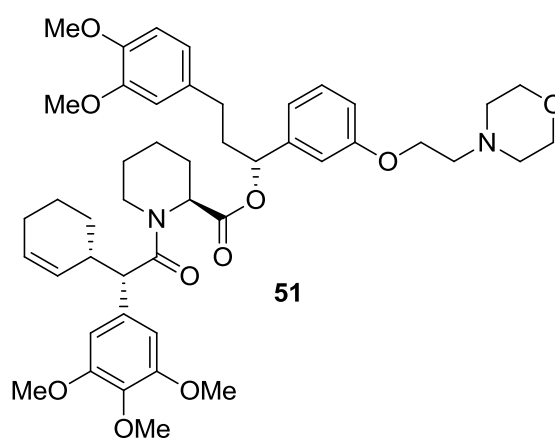
$^1\text{H NMR}$  (600 MHz,  $d_6$ -DMSO) major diastereomer  $\delta$  7.08 (td,  $J = 8.1, 1.7$  Hz, 1H), 6.80 (dd,  $J = 8.3, 1.1$  Hz, 1H), 6.75 (ddd,  $J = 8.3, 2.6, 0.9$  Hz, 1H), 6.69 – 6.66 (m, 2H), 6.64 (d,  $J = 11.4$  Hz, 2H), 6.60 – 6.58 (m, 1H), 6.38 – 6.34 (m, 1H), 5.69 – 5.65 (m, 1H), 5.59 (dq,  $J = 9.8, 3.6$  Hz, 1H), 5.52 (dd,  $J = 10.0, 2.4$  Hz, 1H), 5.47 – 5.40 (m, 1H), 5.30 – 5.25 (m, 1H), 4.62 (d,  $J = 1.3$  Hz, 1H), 4.13 (d,  $J = 13.4$  Hz, 1H), 3.71

(d,  $J = 0.8$  Hz, 1H), 3.69 (s, 3H), 3.68 (s, 3H), 3.62 – 3.61 (m, 3H), 3.59 (s, 3H), 3.57 (s, 3H), 3.53 (d,  $J = 0.7$  Hz, 3H), 2.82 – 2.71 (m, 2H), 2.67 – 2.53 (m, 1H), 2.42 – 2.32 (m, 1H), 2.25 (ddt,  $J = 24.0, 13.8, 8.2$  Hz, 2H), 2.11 (d,  $J = 12.9$  Hz, 1H), 1.90 (s, 2H), 1.84 – 1.73 (m, 2H), 1.62 – 1.51 (m, 2H), 1.24 – 1.12 (m, 1H), 1.06 (dtd,  $J = 22.1, 12.1, 3.1$  Hz, 1H)

$^{13}\text{C}$  NMR (151 MHz,  $d_6$ -DMSO) major diastereomer  $\delta$  171.70, 170.42, 158.01, 152.87, 149.01, 147.50, 142.19, 136.44, 133.42, 129.78, 128.05, 120.17, 118.44, 113.74, 112.91, 112.46, 112.01, 106.25, 105.80, 75.23, 64.94, 60.03, 56.06, 56.05, 55.92, 55.76, 52.41, 51.92, 43.29, 38.91, 38.02, 30.80, 26.69, 25.42, 21.21.

Mass: (ESI<sup>+</sup>), calculated 746.35 [ $\text{C}_{42}\text{H}_{51}\text{NO}_{11}+\text{H}$ ]<sup>+</sup>, found 746.38 [M+H]<sup>+</sup>.

**(S)-(R)-3-(3,4-Dimethoxyphenyl)-1-(3-(2-morpholinoethoxy)phenyl)propyl-1-((S)-2-((S)-cyclohex-2-en-1-yl)-2-(3,4,5-trimethoxyphenyl)acetyl)piperidine-2-carboxylate (51)**



General synthesis procedure **A** for morpholine ligands with **47** (10 mg, 33  $\mu\text{mol}$ ) and **37b** (17 mg, 33  $\mu\text{mol}$ ) was used. The product was purified using flash chromatography (gradient 0%-6% MeOH in DCM). **51** (16 mg, 20  $\mu\text{mol}$ , 75%, dr 85:15) was obtained as a colorless oil. The dr was determined by NMR.

TLC [MeOH/DCM, 6:94]:  $R_f = 0.22$ .

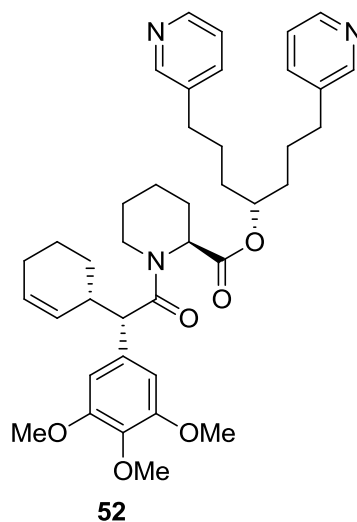
HPLC [50-60% Solvent B, 20 min]:  $R_t = 10.5$  min, purity (220 nm) = 98%.

<sup>1</sup>H NMR (400 MHz, d<sub>6</sub>-DMSO) major diastereomer δ 7.08 (t, *J* = 7.9 Hz, 1H), 6.93 – 6.87 (m, 1H), 6.83 – 6.76 (m, 2H), 6.72 (q, *J* = 2.5, 2.0 Hz, 1H), 6.68 (d, *J* = 2.0 Hz, 1H), 6.62 (d, *J* = 11.1 Hz, 2H), 6.36 (t, *J* = 7.1 Hz, 1H), 5.69 – 5.63 (m, 1H), 5.55 – 5.49 (m, 1H), 5.47 – 5.38 (m, 1H), 5.26 (s, 1H), 4.06 (dd, *J* = 14.6, 6.1 Hz, 2H), 3.72 – 3.70 (m, 2H), 3.69 (s, 3H), 3.67 (s, 3H), 3.61 (t, *J* = 1.5 Hz, 1H), 3.58 (s, 1H), 3.55 (s, 2H), 3.53 (s, 2H), 3.29 – 3.27 (m, 10H), 2.82 – 2.70 (m, 2H), 2.65 – 2.56 (m, 1H), 2.32 – 2.22 (m, 2H), 2.11 (d, *J* = 13.2 Hz, 2H), 1.90 (s, 2H), 1.80 (dt, *J* = 14.9, 6.8 Hz, 3H), 1.59 (d, *J* = 13.8 Hz, 3H), 1.49 – 1.36 (m, 1H), 1.21 (d, *J* = 3.6 Hz, 3H), 0.88 – 0.77 (m, 2H).

<sup>13</sup>C NMR (101 MHz, d<sub>6</sub>-DMSO) major diastereomer δ 172.07, 170.39, 158.51, 153.10, 148.83, 147.53, 142.35, 136.56, 133.51, 130.70, 129.85, 128.16, 120.38, 118.26, 114.15, 112.85, 112.65, 112.33, 106.17, 75.31, 66.60, 65.63, 60.20, 60.11, 57.40, 56.45, 56.04, 55.93, 55.77, 54.00, 52.60, 52.01, 51.96, 43.13, 37.92, 30.92, 28.64, 28.01, 26.71, 25.32, 22.42, 21.21, 20.82.

Mass: (ESI<sup>+</sup>), calculated 801.43 [C<sub>46</sub>H<sub>60</sub>N<sub>2</sub>O<sub>10</sub>+H]<sup>+</sup>, found 801.42 [M+H]<sup>+</sup>.

**(S)-1,7-Di(pyridin-3-yl)heptan-4-yl-1-((S)-2-((S)-cyclohex-2-en-1-yl)-2-(3,4,5-trimethoxy phenyl) acetyl)piperidine-2-carboxylate (52)**



**47** (42 mg, 0.14 mmol) was dissolved in 500 μL DMF, then HATU (91 mg, 0.25 mmol) and DIPEA (86 μL, 0.50 mmol) were added and stirred for 30 min. Then **37c** (48 mg, 0.14 mmol) in 500 μL DMF was added and stirred for 14 h. Subsequently, 3 mL H<sub>2</sub>O/MeOH 1:1 with 0.1% TFA was added and subjected to reversed phase flash chromatography (gradient 0%-45% MeOH in H<sub>2</sub>O + 0.1% TFA). **52** (53 mg, 79 μmol, 63%, 85:15) was obtained as a yellow oil. The dr was determined by NMR.

**TLC** [MeOH/DCM, 15:85]:  $R_f = 0.25$ .

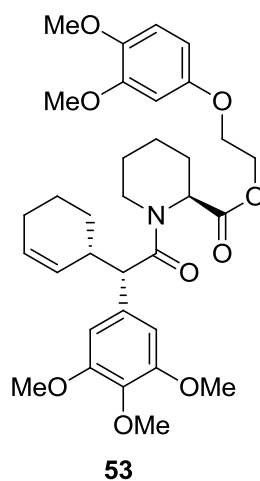
**HPLC** [0-100% Solvent B, 20 min]:  $R_t = 13.2$  min, purity (220 nm) = 95%.

**$^1\text{H NMR}$**  (300 MHz,  $\text{CDCl}_3$ ) major diastereomer  $\delta$  8.69 (d,  $J = 15.8$  Hz, 4H), 8.23 (dd,  $J = 24.2, 7.7$  Hz, 2H), 7.81 (s, 2H), 6.51 (d,  $J = 12.9$  Hz, 2H), 5.83 – 5.68 (m, 1H), 5.65 – 5.48 (m, 1H), 5.30 (s, 1H), 4.84 (s, 1H), 3.85 – 3.82 (m, 1H), 3.81 (s, 3H), 3.78 (s, 6H), 3.63 – 3.43 (m, 1H), 2.95 – 2.84 (m, 2H), 2.80 – 2.67 (m, 4H), 2.21 (d,  $J = 12.9$  Hz, 2H), 1.99 (s, 3H), 1.76 – 1.34 (m, 14H), 1.12 (d,  $J = 11.3$  Hz, 1H).

**$^{13}\text{C NMR}$**  (75 MHz,  $\text{CDCl}_3$ ) major diastereomer  $\delta$  172.71, 172.51, 171.03, 170.84, 152.77, 145.17, 144.97, 141.86, 141.49, 139.45, 136.89, 133.18, 130.02, 128.94, 126.52, 105.84, 72.97, 60.90, 56.13, 53.91, 52.42.

**Mass:** (ESI<sup>+</sup>), calculated 670.39 [ $\text{C}_{40}\text{H}_{51}\text{N}_3\text{O}_6+\text{H}$ ]<sup>+</sup>, found 670.39 [M+H]<sup>+</sup>.

**(S)-2-(3,4-Dimethoxyphenoxy)ethyl-1-((S)-2-((R)-cyclohex-2-en-1-yl)-2-(3,4,5-trimethoxy phenyl)acetyl)piperidine-2-carboxylate (53)**



**47** (45 mg, 0.15 mmol) was dissolved in 700  $\mu\text{L}$  dry DMF then N-ethyl-N-isopropylpropan-2-amine (102  $\mu\text{L}$ , 0.60 mmol) and HATU (83 mg, 0.22 mmol) was added and stirred for 15 min. Then **37d** (45 mg, 0.15 mmol) was dissolved in 600  $\mu\text{L}$  DCM/DMF 1:1 and added to the reaction mixture. Then was stirred for 14 h at RT. The product was purified using flash chromatography (Gradient 0%-50% EtOAc in cyclohexane). **53** (12 mg, 20  $\mu\text{mol}$ , 13%, dr 85:15) was obtained as a slight yellow oil. The dr was determined by NMR.

**TLC** [EtOAc/cyclohexane, 1:1]:  $R_f = 0.29$ .

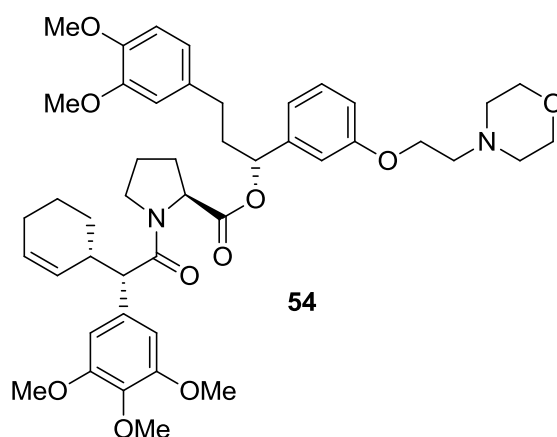
**HPLC** [60-80% Solvent B, 20 min]:  $R_t = 12.0$  min, purity (220 nm) = 95%.

**$^1\text{H NMR}$**  (400 MHz,  $d_6$ -DMSO) major diastereomer  $\delta$  6.81 – 6.77 (m, 1H), 6.67 (d,  $J = 6.9$  Hz, 1H), 6.59 (s, 2H), 6.46 (d,  $J = 2.7$  Hz, 1H), 5.68 – 5.63 (m, 1H), 5.55 – 5.52 (m, 1H), 5.15 – 5.12 (m, 1H), 4.44 – 4.39 (m, 1H), 4.16 – 4.10 (m, 2H), 4.02 – 3.95 (m, 2H), 3.82 – 3.76 (m, 1H), 3.69 (s, 3H), 3.67 (s, 6H), 3.66 (s, 3H), 3.62 – 3.60 (m, 3H), 3.59 – 3.52 (m, 1H), 2.73 – 2.66 (m, 2H), 2.09 – 2.01 (m, 1H), 1.98 – 1.86 (m, 3H), 1.84 – 1.73 (m, 2H), 1.70 – 1.52 (m, 3H), 1.32 (d,  $J = 7.5$  Hz, 2H).

**$^{13}\text{C NMR}$**  (101 MHz,  $d_6$ -DMSO) major diastereomer  $\delta$  172.25, 171.15, 153.21, 152.92, 150.00, 143.62, 136.44, 134.87, 133.53, 131.40, 128.24, 113.13, 106.42, 104.61, 101.36, 66.53, 63.39, 60.70, 56.48, 56.37, 56.19, 55.83, 52.76, 52.36, 43.22, 38.91, 26.91, 26.74, 26.58, 25.39, 21.13, 20.93.

**Mass:** (ESI+), calculated 598.30 [ $\text{C}_{33}\text{H}_{43}\text{NO}_9 + \text{H}$ ] $^+$ , found 598.28 [ $\text{M} + \text{H}$ ] $^+$ .

**(S)-(R)-3-(3,4-dimethoxyphenyl)-1-(3-(2-morpholinoethoxy)phenyl)propyl-1-((S)-2-((R)-cyclohex-2-en-1-yl)-2-(3,4,5-trimethoxyphenyl)acetyl)pyrrolidine-2-carboxylate (54)**



General synthesis procedure **A** for morpholine ligands with **47** (30 mg, 98  $\mu\text{mol}$ ) and **37b** (40 mg, 80  $\mu\text{mol}$ ). The product was purified using flash chromatography. **54** (44 mg, 20  $\mu\text{mol}$ , 70%, dr 85:15) was obtained as colorless oil. The dr was determined by NMR.

**TLC** [MeOH/DCM, 8:92]:  $R_f = 0.29$ .

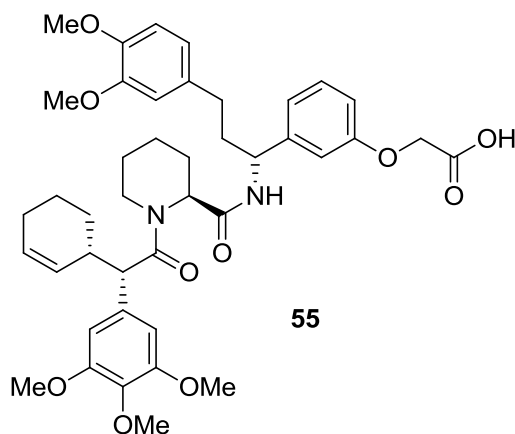
**HPLC** [0-100% Solvent B, 20 min]:  $R_t = 16.6$  min, purity (220 nm) = 98%.

**$^1\text{H NMR}$**  (400 MHz,  $d_6$ -DMSO) major diastereomer  $\delta$  7.24 – 7.14 (m, 1H), 6.94 (d,  $J = 29.5$  Hz, 1H), 6.88 – 6.78 (m, 2H), 6.70 (dd,  $J = 6.1, 2.0$  Hz, 1H), 6.68 – 6.63 (m, 1H), 6.63 – 6.59 (m, 1H), 6.57 (d,  $J = 5.9$  Hz, 2H), 5.72 – 5.64 (m, 1H), 5.58 (ddd,  $J = 14.8, 10.1, 2.2$  Hz, 1H), 5.41 (ddd,  $J = 12.6, 8.2, 5.0$  Hz, 1H), 5.09 (dd,  $J = 10.2, 2.5$  Hz, 1H), 4.47 (ddd,  $J = 14.3, 8.6, 3.1$  Hz, 1H), 4.22 – 4.13 (m, 1H), 3.73 – 3.71 (m, 1H), 3.70 (s, 2H), 3.68 (s, 3H), 3.64 – 3.61 (m, 3H), 3.55 (s, 3H), 3.54 (d,  $J = 1.5$  Hz, 4H), 3.32 (s, 9H), 3.23-3.19 (m, 1H), 2.89 – 2.74 (m, 2H), 2.75 – 2.61 (m, 2H), 2.46 – 2.24 (m, 2H), 2.25 – 2.13 (m, 2H), 1.97 – 1.86 (m, 2H), 1.80 – 1.67 (m, 3H), 1.67 – 1.54 (m, 1H), 1.53 – 1.29 (m, 3H), 1.27 – 1.14 (m, 1H).

**$^{13}\text{C NMR}$**  (101 MHz,  $d_6$ -DMSO) major diastereomer  $\delta$  171.90, 171.05, 159.55, 153.08, 149.26, 147.35, 142.64, 136.73, 133.54, 130.79, 129.87, 129.38, 128.68, 120.50, 114.23, 112.82, 112.32, 106.54, 106.04, 75.16, 67.84, 66.99, 60.86, 59.81, 58.96, 57.75, 56.19, 54.80, 53.88, 47.26, 32.66, 30.54, 29.34, 28.63, 25.48, 24.79, 21.81, 21.31.

**Mass:** (ESI<sup>-</sup>), calculated 787.42 [ $\text{C}_{45}\text{H}_{58}\text{N}_2\text{O}_{10} + \text{H}$ ]<sup>-</sup>, found 787.35 [ $\text{M} + \text{H}$ ]<sup>+</sup>.

**2-(3-((*R*)-1-((*S*)-1-((*S*)-2-((*R*)-Cyclohex-2-en-1-yl)-2-(3,4,5-trimethoxyphenyl)acetyl)piper-idine-2-carboxamido)-3-(3,4-dimethoxyphenyl)propyl)phenoxy)acetic acid (**55**)**



General synthesis procedure **B** for free acid ligands with **37e** (50 mg, 0.20 mmol) and **47** (30 mg, 0.20 mmol) was used. The product was purified using preparative TLC (MeOH/DCM 8:92) to obtain **55** (25 mg, 33.5  $\mu$ mol, 67%, dr 85:15) as a slight yellow oil. The diastereomeric rate was determined by NMR.

**TLC** [MeOH/DCM, 8:92]:  $R_f$  = 0.29.

**HPLC** [0-100% Solvent B, 20 min]:  $R_t$  = 11.7 min, purity (220 nm) = 98%.

**<sup>1</sup>H NMR** (400 MHz, dmsO) major diastereomer  $\delta$  7.10 – 7.05 (m, 1H), 6.92 – 6.86 (m, 1H), 6.81 (t,  $J$  = 8.4 Hz, 1H), 6.72 (dq,  $J$  = 11.8, 2.0 Hz, 2H), 6.69 – 6.64 (m, 1H), 6.63 – 6.57 (m, 1H), 6.56 – 6.51 (m, 2H), 5.70 – 5.61 (m, 1H), 5.53 (d,  $J$  = 10.2 Hz, 1H), 5.12 – 5.04 (m, 1H), 4.79 – 4.66 (m, 2H), 4.66 – 4.53 (m, 3H), 3.73 – 3.69 (m, 2H), 3.69 – 3.66 (m, 6H), 3.62 – 3.60 (m, 1H), 3.55 – 3.51 (m, 9H), 2.93 – 2.81 (m, 2H), 2.79 – 2.67 (m, 2H), 2.40 – 2.27 (m, 2H), 2.16 – 2.02 (m, 2H), 1.96 – 1.84 (m, 2H), 1.84 – 1.73 (m, 3H), 1.56 (d,  $J$  = 8.2 Hz, 2H), 1.31 (d,  $J$  = 9.6 Hz, 1H).

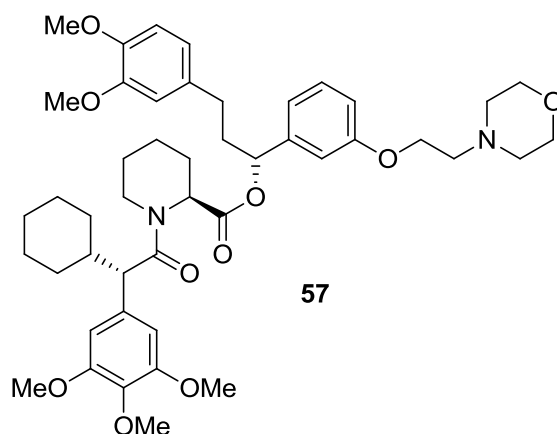
**<sup>13</sup>C NMR** (101 MHz, dmsO)  $\delta$  172.44, 170.72, 170.56, 158.10, 152.97, 149.05, 147.45, 145.74, 136.42, 134.04, 133.70, 131.15, 129.51, 128.15, 120.46, 113.07, 112.76, 112.70, 112.19, 106.01, 64.77, 63.52, 60.15, 56.41, 55.97, 55.92, 55.78, 52.86, 52.23, 51.90, 43.24, 38.97, 38.62, 32.03, 27.78, 27.48, 26.54, 25.31, 21.12, 20.41.



$^{13}\text{C}$  NMR (151 MHz,  $d_6$ -DMSO)  $\delta$  172.48, 172.08, 170.61, 158.61, 152.66, 149.15, 147.47, 142.13, 136.20, 134.32, 133.43, 120.48, 118.07, 113.80, 113.07, 112.53, 112.13, 106.25, 75.16, 66.46, 60.33, 56.62, 55.90, 55.74, 53.12, 52.03, 43.53, 41.10, 37.94, 32.41, 31.32, 30.58, 29.98, 26.87, 26.32, 25.93, 25.38, 20.93.

Mass: (ESI<sup>-</sup>), calculated 748.37 [ $\text{C}_{42}\text{H}_{53}\text{NO}_{11} + \text{H}$ ]<sup>+</sup>, found 768.41[M+H]<sup>+</sup>.

**(S)-(R)-3-(3,4-dimethoxyphenyl)-1-(3-(2-morpholinoethoxy)phenyl)propyl-1-((S)-2-cyclohexyl-2-(3,4,5-trimethoxyphenyl)acetyl)piperidine-2-carboxylate (57)**



General synthesis procedure **A** for morpholine ligands with **49** (30 mg, 97  $\mu\text{mol}$ ) and **37b** (50 mg, 97  $\mu\text{mol}$ ). The product was purified using flash chromatography (gradient 0%-15% MeOH in DCM). **57** (11 mg, 13.6  $\mu\text{mol}$ , 14%) was obtained as a colorless oil.

TLC [MeOH/DCM 6:94]:  $R_f$  = 0.44.

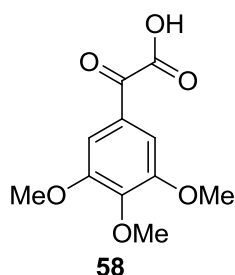
HPLC [0-100% Solvent B, 20 min]:  $R_t$  = 17.7 min, purity (220 nm) = 98%.

$^1\text{H}$  NMR (400 MHz,  $d_6$ -DMSO)  $\delta$  7.08 (t,  $J$  = 7.9 Hz, 1H), 6.93 – 6.87 (m, 1H), 6.83 – 6.76 (m, 2H), 6.72 (q,  $J$  = 2.5, 2.0 Hz, 1H), 6.68 (d,  $J$  = 2.0 Hz, 1H), 6.62 (d,  $J$  = 11.1 Hz, 2H), 6.36 (t,  $J$  = 7.1 Hz, 1H), 5.47 – 5.38 (m, 1H), 5.26 (s, 1H), 4.06 (dd,  $J$  = 14.6, 6.1 Hz, 2H), 3.72 – 3.70 (m, 2H), 3.69 (s, 3H), 3.67 (s, 3H), 3.61 (t,  $J$  = 1.5 Hz, 1H), 3.58 (s, 1H), 3.55 (s, 3H), 3.53 (s, 3H), 3.29 – 3.27 (m, 10H), 2.82 – 2.70 (m, 2H), 2.65 – 2.56 (m, 1H), 2.32 – 2.22 (m, 2H), 2.11 (d,  $J$  = 13.2 Hz, 2H), 1.90 (s, 2H), 1.80 (dt,  $J$  = 14.9, 6.8 Hz, 4H), 1.59 (d,  $J$  = 13.8 Hz, 4H), 1.49 – 1.36 (m, 1H), 1.21 (d,  $J$  = 3.6 Hz, 3H), 0.88 – 0.77 (m, 2H).

$^{13}\text{C}$  NMR (151 MHz,  $d_6$ -DMSO)  $\delta$  172.55, 170.94, 162.94, 153.03, 149.33, 147.72, 137.03, 133.56, 129.26, 120.19, 112.20, 75.37, 60.37, 56.68, 55.84, 55.30, 53.99, 51.62, 46.53, 43.54, 36.39, 32.08, 30.77, 27.00, 25.93, 25.39, 21.16, 17.17, 9.63.

**Mass:** (ESI<sup>-</sup>), calculated 803.34 [ $\text{C}_{46}\text{H}_{62}\text{N}_2\text{O}_{10}+\text{H}$ ]<sup>+</sup>, found 803.38[M+H]<sup>+</sup>.

## 2-Oxo-2-(3, 4, 5-trimethoxyphenyl) acetic acid **58**



1-(3,4,5-Trimethoxyphenyl)ethanone (2.93g, 13.9mmol) and selenium dioxide (2.32 g, 20.9 mmol) in 60 mL pyridine were heated to 100°C for 14 h. The mixture was filtered through celite, concentrated *in vacuo* and purified with flash chromatography (EtOAc/cyclohexane 15:1, 1% AcOH). **58** (2.2 g, 9.1 mmol, 65%) was obtained as a yellow solid.

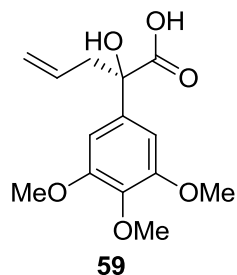
**TLC** [EtOAc/cyclohexane, 15:1, + 1% AcOH]:  $R_f$  = 0.14.

**HPLC** [0-100% B, 20 min]:  $R_t$  = 10.8 min, purity (220 nm) 90%.

$^1\text{H}$ NMR (600 MHz,  $\text{CDCl}_3$ )  $\delta$  = 3.91(s, 6H), 3.95(s, 3H), 7.50 (s, 2H).

$^{13}\text{C}$  NMR (150 MHz,  $\text{CDCl}_3$ )  $\delta$  = 56.31, 61.03, 108.04, 127.55, 144.19, 153.06, 165.74, 186.94.

**HRMS**(EI<sup>+</sup>), calculated 240.0634[ $\text{C}_{11}\text{H}_{12}\text{O}_6+\text{H}$ ]<sup>+</sup>.found 240.0624[M+H]<sup>+</sup>

**(R)-2-hydroxy-2-(3,4,5-trimethoxyphenyl)pent-4-enoic acid (59)**

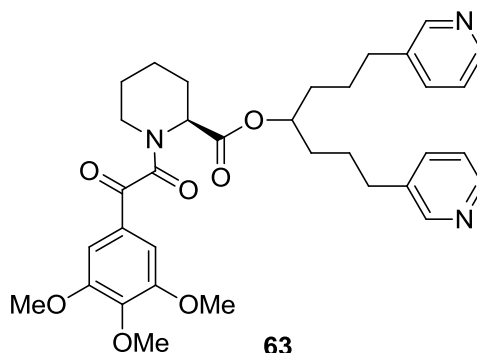
**58** (100 mg, 0.42 mmol) was dissolved in 3.5 ml dry THF and cooled to  $-78^{\circ}\text{C}$  then Allylmagnesiumbromid (1 M in THF, 0.42 mL, 0.42 mmol) was added dropwise, stirred for 4 h then was allowed to warm to RT and the reaction mixture was quenched, using  $\text{NH}_4\text{Cl}$  (sat). The aqueous phase was extracted with DCM and the product was purified by silica chromatography (EtOAc/cyclohexane, 1:1 +1% AcOH). **59** (88mg, 0.36 mmol, 87%) was obtained as white crystals.

**TLC** [EtOAc/cyclohexane, 1:1 + 5% AcOH]:  $R_f = 0.38$ .

**HPLC** [0-100% Solvent B, 20 min]:  $R_t = 17.7$  min, purity (220 nm) = 98%.

**$^1\text{H NMR}$**  (300 MHz,  $\text{CDCl}_3$ )  $\delta$  6.89 (s, 2H), 5.79 (dt,  $J = 17.2, 8.3$  Hz, 1H), 5.32 – 5.21 (m, 2H), 3.89 (s, 6H), 3.86 (s, 3H), 3.03 (dd,  $J = 13.9, 7.3$  Hz, 1H), 2.80 (dd,  $J = 14.0, 7.0$  Hz, 1H).

**Mass:** (ESI<sup>-</sup>), calculated 281.10 [ $\text{C}_{14}\text{H}_{18}\text{O}_6 + \text{H}$ ]<sup>-</sup>, found 281.13 [ $\text{M} + \text{H}$ ]<sup>+</sup>.

**(S)-1,7-Di(pyridin-3-yl)heptan-4-yl-1-(2-oxo-2-(3,4,5-trimethoxyphenyl)acetyl)piperidine-2-carboxylate (63)**

**58** (94 mg, 0.40 mmol) was dissolved in 500  $\mu$ L DMF, then HATU (191 mg, 0.52 mmol) and DIPEA (0.18 mL, 1.05 mmol) were added and stirred for 30min. Subsequently, **37c** (0.10 g, 0.26 mmol) in 500  $\mu$ L DMF was added and stirred for 14 h at RT. The solvent was reduced *in vacuo*. The crude product was dissolved in 4 mL MeOH/H<sub>2</sub>O 1:1 solution and purified with reversed phase flash chromatography (Column: Interchim puriFlash IR-50C18-20G, gradient 0%-20% MeOH in H<sub>2</sub>O + 1% TEA). **63** was obtained as a slight brown oil (104 mg, 0.17 mmol, 66%)

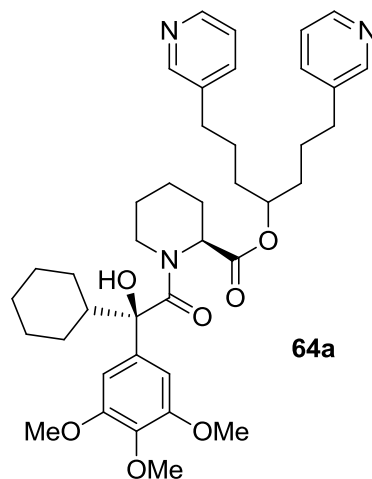
**TLC** [MeOH/DCM 20:80]:  $R_f$  = 0.15.

**HPLC** [0-100% Solvent B, 20 min]:  $R_t$  = 11.6 min, purity (220 nm) = 95%.

**<sup>1</sup>H NMR** (300 MHz, d<sub>6</sub>-DMSO)  $\delta$  8.67 (dd,  $J$  = 11.4, 5.7 Hz, 4H), 8.26 – 8.18 (m, 2H), 7.77 (td,  $J$  = 8.3, 5.4 Hz, 2H), 7.22 (s, 2H), 5.17 (d,  $J$  = 5.7 Hz, 1H), 4.97 (s, 1H), 3.82 (s, 6H), 3.77 (s, 3H), 3.31 (d,  $J$  = 13.1 Hz, 1H), 3.13 – 3.05 (m, 1H), 2.78 – 2.70 (m, 4H), 2.16 (d,  $J$  = 13.8 Hz, 1H), 1.83 – 1.69 (m, 1H), 1.70 – 1.56 (m, 6H), 1.53 – 1.45 (m, 1H), 1.45 – 1.31 (m, 2H), 1.28 – 1.19 (m, 2H), 1.19 – 1.11 (m, 1H).

**<sup>13</sup>C NMR** (75 MHz, d<sub>6</sub>-DMSO)  $\delta$  190.83, 190.80, 170.86, 170.67, 170.12, 167.75, 167.53, 158.66, 158.59, 153.87, 153.48, 144.31, 144.16, 142.19, 141.00, 127.91, 126.57, 118.59, 107.23, 75.25, 60.99, 56.71, 51.82, 44.25, 33.28, 31.93, 26.27, 26.10, 24.53, 20.99.

**Mass:** (ESI<sup>-</sup>), calculated 604.30 [C<sub>34</sub>H<sub>41</sub>N<sub>3</sub>O<sub>7</sub>+H]<sup>+</sup>, found 604.31[M+H]<sup>+</sup>.

**(S)-1,7-Di(pyridin-3-yl)heptan-4-yl-1-((R)-2-cyclohexyl-2-hydroxy-2-(3,4,5-trimethoxy phenyl)acetyl)piperidine-2-carboxylate (64a)**

**63/Biricodar** (69 mg, 0.11 mmol) was dissolved in 700  $\mu\text{L}$  anhydrous THF and cooled to  $-78^\circ\text{C}$ . Then cyclohexylmagnesium bromide (1 M in THF, 343  $\mu\text{L}$ , 0.34 mmol) was added and stirred for 2h. The reaction mixture was quenched with  $\text{NH}_4\text{Cl}$  (sat) solution and extracted with DCM. The organic phases were combined and dried over  $\text{MgSO}_4$ . The diastereomers were separated using preparative HPLC (Gradient 45%-60% solvent B in Solvent A) yielding **64a** (14 mg, 20  $\mu\text{mol}$ , 20%). The diastereomeric rate was determined by HPLC.

**TLC** [MeOH/DCM 5:95]:  $R_f = 0.45$ .

**HPLC 64a** [25-40% Solvent B, 20 min]:  $R_t = 15.7$  min, purity (220 nm) = 95%, dr  $\geq 99:1$

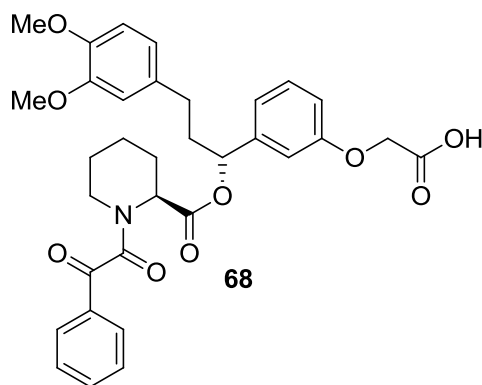
**HPLC 64b** [25-40% Solvent B, 20 min]:  $R_t = 16.7$  min, purity (220 nm) = 95%, dr  $\geq 99:1$

**$^1\text{H}$  NMR** (599 MHz,  $\text{d}_6\text{-DMSO}$ )  $\delta$  8.31 (t,  $J = 7.9$  Hz, 2H), 8.22 – 8.09 (m, 2H), 7.74 (s, 2H), 7.71 – 7.64 (m, 2H), 6.49 (d,  $J = 18.9$  Hz, 2H), 4.92 – 4.85 (m, 1H), 4.04 (dd,  $J = 11.4, 3.6$  Hz, 1H), 3.66 (s, 6H), 3.64 (s, 3H) 2.77 – 2.63 (m, 6H), 2.19 – 2.15 (m, 2H), 1.99 (dd,  $J = 14.2, 3.3$  Hz, 2H), 1.79 – 1.43 (m, 14H), 1.37 – 1.11 (m, 4H), 1.11 – 0.95 (m, 4H).

**$^{13}\text{C}$  NMR** (101 MHz,  $\text{d}_6\text{-DMSO}$ )  $\delta$  177.12, 170.90, 156.48, 151.65, 146.83, 141.45, 135.84, 135.72, 123.83, 104.86, 84.10, 79.16, 60.70, 58.79, 56.83, 43.78, 40.62, 35.64, 31.32, 29.27, 27.81, 26.75, 26.02, 25.91, 25.47, 22.24.

**Mass:** (ESI<sup>+</sup>), calculated 688.40 [C<sub>40</sub>H<sub>53</sub>N<sub>3</sub>O<sub>7</sub>+H]<sup>+</sup>, found 688.39 [M-H]<sup>+</sup>.

**2-(3-((*R*)-3-(3,4-Dimethoxyphenyl)-1-(((*S*)-1-(2-oxo-2-phenylacetyl)piperidine-2-carbonyl) oxy)propyl)phenoxy)acetic acid (68)**



General synthesis procedure **B** for free acid ligands with **37a** (50 mg, 97  $\mu$ mol) and Phenylglyoxylic acid (16 mg, 0.11 mmol) was used. The crude mixture was concentrated and purified using flash chromatography (Gradient 0%-60% EtOAc in cyclohexane +0.1 % AcOH) to obtain **68** (33 mg, 72  $\mu$ mol, 89%) as a brownish oil.

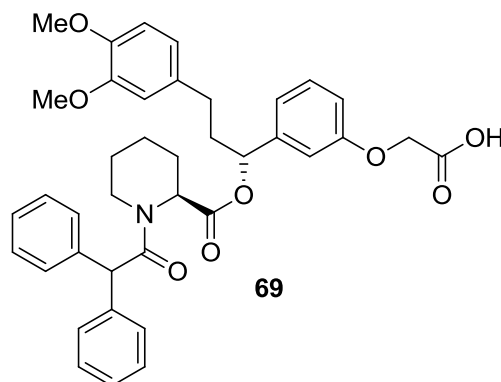
**TLC** [EtOAc/cyclohexane 45:50 + 5% AcOH]: R<sub>f</sub> = 0.18.

**HPLC** [0-100% Solvent B, 20 min]: R<sub>t</sub> = 16.1 min, purity (220 nm) = 98%

<sup>1</sup>H NMR (600 MHz, CDCl<sub>3</sub>)  $\delta$  7.81 (dd, *J* = 7.5, 1.5 Hz, 2H), 7.61 – 7.53 (m, 1H), 7.53 – 7.45 (m, 2H), 7.25 (d, *J* = 14.9 Hz, 1H), 7.04 – 6.97 (m, 2H), 6.90 – 6.83 (m, 2H), 6.82 – 6.74 (m, 2H), 5.68 (t, *J* = 7.0 Hz, 1H), 4.64 (s, 2H), 4.48 (t, *J* = 8.3 Hz, 1H), 3.83 (s, 3H), 3.75 (s, 3H), 3.66 (dt, *J* = 12.2, 6.0 Hz, 1H), 3.54 (dt, *J* = 12.3, 6.0 Hz, 1H), 2.65 (t, *J* = 7.9 Hz, 2H), 2.28 (td, *J* = 7.9, 6.9 Hz, 1H), 2.08 – 1.96 (m, 2H), 1.81 (ddt, *J* = 12.3, 8.4, 5.6 Hz, 1H), 1.74 – 1.54 (m, 4H).

<sup>13</sup>C NMR (125 MHz, CDCl<sub>3</sub>)  $\delta$  190.18, 171.80, 170.15, 163.11, 159.07, 150.39, 148.33, 144.02, 135.46, 135.20, 133.32, 130.12, 129.38, 129.32, 121.85, 119.24, 115.58, 114.12, 113.68, 113.54, 77.03, 66.03, 59.12, 56.83, 42.84, 36.38, 34.08, 25.91, 25.47, 22.24.

**Mass:** (ESI<sup>+</sup>), calculated 612.22 [C<sub>33</sub>H<sub>35</sub>NO<sub>9</sub>+Na]<sup>+</sup>, found 612.24 [M-Na]<sup>+</sup>.

**2-(3-((*R*)-3-(3,4-dimethoxyphenyl)-1-(((*S*)-1-(2,2-diphenylacetyl)piperidine-2-carbonyl)oxy)propyl)phenoxy)acetic acid (**69**)**

General synthesis procedure **B** for free acid ligands with **37a** (50 mg, 0,097 mmol) and Diphenyl acetic acid (22 mg, 0.11 mmol) was used. Then was purified using flash chromatography (Gradient 0%-50% EtOAc in cyclohexane +0.1 % AcOH) to obtain **69** (42 mg, 72  $\mu$ mol, 89%) as a brownish oil.

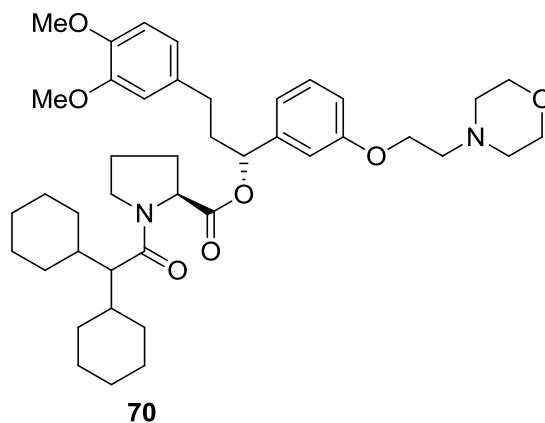
**TLC** [EtOAc/cyclohexane 45:50 + 5% AcOH]:  $R_f$  = 0.34.

**HPLC** [0-100% Solvent B, 20 min]:  $R_t$  = 19.8 min, purity (220 nm) = 95%

**$^1\text{H NMR}$**  (600 MHz,  $\text{CDCl}_3$ )  $\delta$  7.39 – 7.35 (m, 6H), 7.27 – 7.23 (m, 1H), 7.23 – 7.19 (m, 4H), 7.02 – 6.98 (m, 1H), 6.95 – 6.92 (m, 1H), 6.89 – 6.84 (m, 2H), 6.81 – 6.74 (m, 2H), 5.92 (t,  $J$  = 7.0 Hz, 1H), 4.82 (s, 1H), 4.69 – 4.60 (m, 3H), 3.83 (s, 3H), 3.75 (s, 3H), 3.74 – 3.66 (m, 1H), 3.45 (dt,  $J$  = 12.2, 6.1 Hz, 1H), 2.64 – 2.54 (m, 2H), 2.47 – 2.38 (m, 1H), 2.27 – 2.19 (m, 1H), 2.06 – 1.97 (m, 1H), 1.76 – 1.56 (m, 5H).

**$^{13}\text{C NMR}$**  (125 MHz,  $\text{CDCl}_3$ )  $\delta$  172.91, 171.80, 170.15, 159.07, 150.39, 148.33, 144.02, 137.82, 135.20, 130.60, 129.38, 128.97, 127.61, 121.85, 119.24, 115.58, 114.12, 113.68, 113.54, 77.03, 66.03, 58.74, 56.83, 56.11, 43.29, 36.38, 34.08, 25.91, 25.47, 22.24.

**Mass:** ( $\text{ESI}^+$ ), calculated 674.27 [ $\text{C}_{39}\text{H}_{41}\text{NO}_8+\text{Na}$ ] $^+$ , found 674.30 [ $\text{M}-\text{Na}$ ] $^+$ .

**(S)-(R)-3-(3,4-Dimethoxyphenyl)-1-(3-(2-morpholinoethoxy)phenyl)propyl-1-(2,2-dicyclohexylacetyl)pyrrolidine-2-carboxylate (70)**

General synthesis procedure **A** for morpholine ligands with **65** (18 mg, 80  $\mu$ mol) and **37b** (39 mg, 80  $\mu$ mol) was used. The crude product was concentrated and purified using flash chromatography (gradient 0%-15% MeOH in DCM). **70** (14 mg, 30  $\mu$ mol, 38%) was obtained as a slight yellow oil.

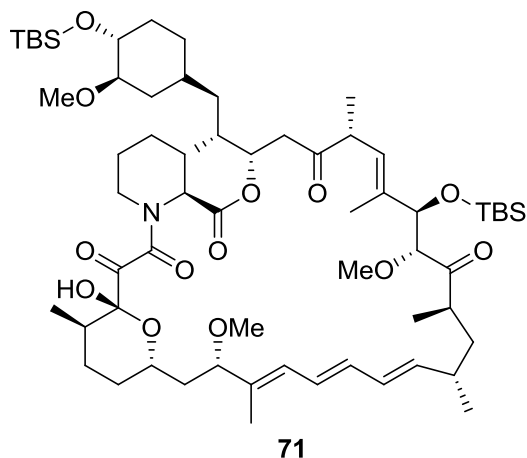
**TLC** [MeOH/DCM 5:95]:  $R_f$  = 0.39.

**HPLC** [0-100% Solvent B, 20 min]:  $R_t$  = 14.7 min, purity (220 nm)  $\geq$  99%.

**$^1\text{H NMR}$**  (600 MHz,  $\text{CDCl}_3$ )  $\delta$  7.30-7.25 (m, 1H), 7.03 – 6.94 (m, 3H), 6.90 – 6.74 (m, 3H), 5.61 (t,  $J$  = 6.8 Hz, 1H), 4.63 (t,  $J$  = 4.0 Hz, 1H), 4.06 (t,  $J$  = 3.8 Hz, 2H), 3.83 (s, 3H), 3.75 (s, 3H), 3.57 (t,  $J$  = 4.8 Hz, 4H), 3.52 – 3.37 (m, 4H), 2.73 – 2.63 (m, 2H), 2.50 (t,  $J$  = 4.7 Hz, 4H), 2.44 (dt,  $J$  = 6.7, 5.6 Hz, 1H), 2.34 (dt,  $J$  = 6.8, 5.7 Hz, 1H), 2.21 – 2.17 (m, 1H), 2.10-1.98 (m, 3H), 1.95 – 1.86 (m, 6H), 1.71-1.59 (m, 4H), 1.64-1.62 (m, 3H), 1.32-1.25 (m, 4H), 1.12-1.11 (m, 2H), 0.97-0.81 (m, 4H).

**$^{13}\text{C NMR}$**  (125 MHz,  $\text{CDCl}_3$ )  $\delta$  176.24, 171.90, 159.63, 150.39, 148.33, 143.58, 135.20, 129.28, 121.85, 119.20, 115.53, 114.12, 113.68, 113.06, 77.03, 67.38, 66.80, 61.22, 56.83, 54.73, 52.94, 52.72, 46.25, 41.21, 38.97, 36.38, 34.08, 32.08, 30.69, 28.00, 26.27, 26.02, 25.90, 25.55, 24.98.

**Mass:** (ESI $^+$ ), calculated 705.45 [ $\text{C}_{42}\text{H}_{60}\text{N}_2\text{O}_7+\text{H}$ ] $^+$ , found 705.35 [M-H] $^+$ .

**TBS-Rap (71)**

Rapamycin (50 mg, 55  $\mu\text{mol}$ ) was dissolved in 1 mL DCM and cooled to 0°C. Then TBDMS-OTf (65 mg, 0.25 mmol) and 2,6-Lutidine (38  $\mu\text{L}$ , 0.33 mmol) was added. Then it was stirred further at 0°C for 2h. The reaction was quenched, using  $\text{NH}_4\text{Cl}$  (sat) solution. The aqueous phase was extracted with DCM. The organic phase was dried over  $\text{MgSO}_4$ . The product was purified using column chromatography (EtOAc/cyclohexane 2:8). **71** (95 mg, 83  $\mu\text{mol}$ , 38%).

**TLC** [EtOAc/cyclohexane 2:8]:  $R_f = 0.29$ .

**HPLC reversed phase** [isocratic 100% Solvent B without TFA, 20 min]:  $R_t = 27.8$  min, purity (220 nm) = 98%.

**HPLC normal phase\*** [isocratic EtOAc/n-hexane 1:1, 30 min]:  $R_t = 3.9$  min, purity (280 nm) = 98%.

\*(Phenomenex Luna Silica (2) column, Waters 515 HPLC pump, LCD Analytical spectromonitor 5000 detector, 277 nm)

**$^1\text{H NMR}$**  (599 MHz,  $\text{CDCl}_3$ )  $\delta$  6.41 (dd,  $J = 14.8, 11.1$  Hz, 1H), 6.34 – 6.26 (m, 1H), 6.15 (dd,  $J = 15.1, 10.3$  Hz, 1H), 6.04 (d,  $J = 10.9$  Hz, 1H), 5.33 – 5.22 (m, 2H), 5.05 (d,  $J = 4.2$  Hz, 1H), 4.17 (dd,  $J = 13.0, 6.4$  Hz, 1H), 3.83 (d,  $J = 5.7$  Hz, 1H), 3.80 (s, 1H), 3.71 (dd,  $J = 9.2, 6.0$  Hz, 1H), 3.64 (s, 1H), 3.41 (s, 3H), 3.38 – 3.35 (m, 2H), 3.35 – 3.32 (m, 1H), 3.27 (s, 3H), 3.13 (d,  $J = 6.6$  Hz, 3H), 2.92 – 2.84 (m, 1H), 2.70 – 2.64 (m, 1H), 2.60 (dd,  $J = 16.0, 8.1$  Hz, 1H), 2.39 (dd,  $J = 15.9, 3.5$  Hz, 1H), 2.33 – 2.24 (m, 2H), 2.03 – 1.94 (m, 2H), 1.86 – 1.80 (m, 2H), 1.80 – 1.75 (m, 2H), 1.64 (s, 3H), 1.62 – 1.55 (m, 3H), 1.54 – 1.45 (m, 3H), 1.44 – 1.35 (m, 3H), 1.35 – 1.30 (m, 3H), 1.27 – 1.23 (m, 2H), 1.22 – 1.14 (m, 2H), 1.12 – 1.09 (m, 2H), 1.06 (dd,  $J = 6.7, 2.3$  Hz, 2H), 1.02 (d,  $J = 6.6$  Hz, 3H), 1.00 – 0.96 (m, 3H), 0.93 – 0.89 (m, 4H),

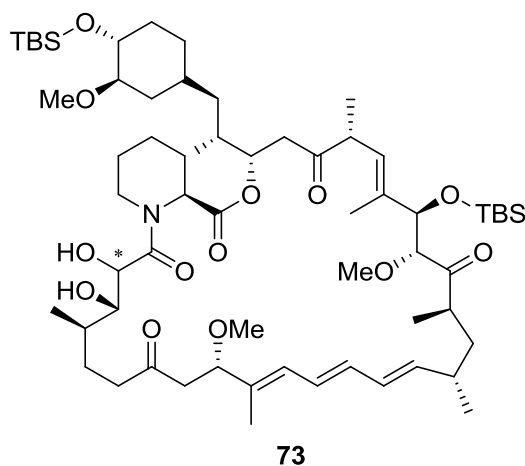
### C. Experimental Section

0.90-0.87 (m, 18H), 0.82 (d,  $J = 11.0$  Hz, 8H), 0.70 (q,  $J = 12.1$  Hz, 2H), 0.07 (s, 3H), 0.05 (s, 3H), -0.01 (s, 3H), -0.07 (s, 3H).

$^{13}\text{C}$  NMR (151 MHz,  $\text{CDCl}_3$ )  $\delta$  210.83, 208.14, 193.46, 169.38, 166.11, 139.10, 137.78, 135.90, 132.82, 130.58, 129.24, 127.05, 126.68, 98.58, 84.70, 84.29, 84.12, 78.81, 75.43, 66.89, 58.25, 57.93, 55.85, 51.20, 46.84, 44.05, 42.20, 41.66, 40.09, 38.77, 38.52, 35.99, 35.00, 34.09, 33.86, 32.88, 31.71, 31.07, 27.20, 26.85, 25.85, 25.75, 25.64, 25.16, 21.40, 20.50, 18.12, 16.08, 15.53, 15.11, 14.18, 13.81, 12.68, 10.13, -4.52, -4.77, -5.00.

**Mass:** (ESI<sup>+</sup>), calculated 1164.72 [ $\text{C}_{63}\text{H}_{107}\text{NO}_{13}\text{Si}_2+\text{Na}$ ]<sup>+</sup>, found 1164.73 [M-Na]<sup>+</sup>.

### TBS-Rap-OH (72)



To a stirred solution of **71** (132 mg, 0.12 mmol) in 3.5 mL Methanol at  $-5^\circ\text{C}$  (ice/Aceton bath) was added in several portions  $\text{NaCNBH}_3$  (145 mg, 2.31 mmol). After addition was complete reaction was allowed to warm to RT and then heated to  $50^\circ\text{C}$  and stirred for 1h. The reaction was quenched, using  $\text{NaHCO}_3$  (sat) solution and extracted with DCM. The organic phases were dried over  $\text{MgSO}_4$ . The product was purified using flash chromatography (gradient 0%-50% i-Propanol in cyclohexane). **73** (27 mg, 24  $\mu\text{mol}$ , 20%) was obtained as a slight yellow oil.

**TLC** [EtOAc/cyclohexane 1:1]:  $R_f = 0.42$ .

**HPLC** [10-30% Solvent B, 20 min]:  $R_t = 14.7$  min, purity (280 nm) 96%.

**HPLC normal phase\*** [10-30% EtOAc in n-hexane, 30 min]:  $R_t = 18.3$  min, purity (220 nm) = 98%.

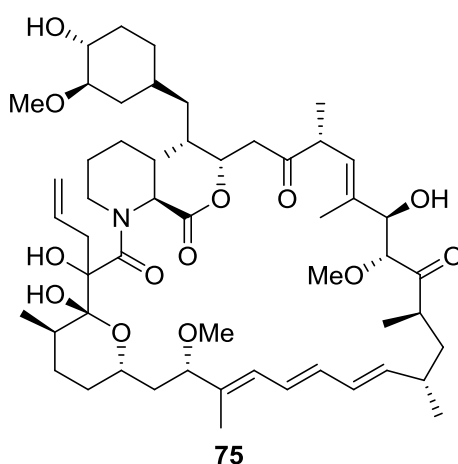
\*(Phenomenex Luna Silica (2) column, Beckmann 126s solvent module, detector 168, 220/280 nm)

$^1\text{H NMR}$  (600 MHz,  $\text{CDCl}_3$ )  $\delta$  6.36 (dd,  $J = 14.6, 11.0$  Hz, 1H), 6.21 (dd,  $J = 14.7, 10.6$  Hz, 1H), 6.16 – 6.08 (m, 2H), 5.53 (dd,  $J = 14.9, 8.7$  Hz, 1H), 5.27 – 5.20 (m, 2H), 5.18 (dt,  $J = 8.2, 4.3$  Hz, 1H), 4.23 (tdd,  $J = 10.8, 5.4, 3.3$  Hz, 2H), 4.16 (dd,  $J = 7.2, 2.4$  Hz, 1H), 4.13 – 4.06 (m, 1H), 3.85 (dd,  $J = 7.2, 3.5$  Hz, 1H), 3.81 (t,  $J = 7.1$  Hz, 1H), 3.38 (s, 3H), 3.36 (dd,  $J = 10.6, 5.9$  Hz, 1H), 3.34 – 3.29 (m, 1H), 3.25 (s, 3H), 3.14 (s, 3H), 2.89 – 2.81 (m, 1H), 2.75 (dtd,  $J = 13.6, 6.5, 3.5$  Hz, 1H), 2.65 – 2.56 (m, 2H), 2.47 – 2.37 (m, 1H), 2.31 (s, 1H), 2.23 (d,  $J = 15.0$  Hz, 1H), 2.03 – 1.94 (m, 2H), 1.86 – 1.80 (m, 2H), 1.80 – 1.75 (m, 2H), 1.64 (s, 3H), 1.62 – 1.55 (m, 3H), 1.54 – 1.45 (m, 3H), 1.44 – 1.35 (m, 3H), 1.35 – 1.30 (m, 3H), 1.27 – 1.23 (m, 2H), 1.22 – 1.14 (m, 2H), 1.12 – 1.09 (m, 2H), 1.06 (dd,  $J = 6.7, 2.3$  Hz, 2H), 1.02 (d,  $J = 6.6$  Hz, 3H), 1.00 – 0.96 (m, 3H), 0.93 – 0.89 (m, 4H), 0.88 (d,  $J = 2.5$  Hz, 12H), 0.82 (d,  $J = 11.0$  Hz, 8H), 0.70 (q,  $J = 12.1$  Hz, 2H), 0.07 (s, 3H), 0.05 (s, 3H), -0.01 (s, 3H), -0.07 (s, 3H).

$^{13}\text{C NMR}$  (150 MHz,  $\text{CDCl}_3$ )  $\delta$  213.07, 207.99, 174.14, 171.78, 169.84, 139.27, 137.70, 135.61, 133.14, 130.26, 129.22, 127.79, 126.64, 84.16, 82.81, 78.85, 75.63, 74.88, 60.02, 58.05, 55.83, 52.74, 46.67, 43.10, 41.28, 40.64, 40.01, 39.03, 38.57, 36.02, 34.85, 33.83, 33.21, 33.08, 31.83, 31.52, 30.94, 29.73, 29.14, 28.43, 26.33, 24.79, 22.60, 21.62, 20.55, 18.11, 17.97, 17.36, 15.34, 15.27, 14.16, 11.81, 10.96, -4.43, -4.53, -4.74, -5.12.

**Mass:** (ESI<sup>+</sup>), calculated 1166.73 [ $\text{C}_{63}\text{H}_{108}\text{NO}_{13}\text{Si}_2+\text{Na}$ ]<sup>+</sup>, found 1166.73 [M-Na]<sup>+</sup>.

## Allyl-Rap (75)



Rapamycin (20 mg, 22  $\mu\text{mol}$ ) was placed in a flask and dried over night at high vacuum. Then it was dissolved in 200  $\mu\text{L}$  anhydrous THF and cooled to  $-78^\circ\text{C}$ . Indium(III) trifluoromethanesulfonate (18 mg, 33  $\mu\text{mol}$ ) and a tetraallylstannane (98  $\mu\text{L}$ , 98  $\mu\text{mol}$ , 1 M in THF) were added dropwise. The reaction mixture was stirred for 1 h at  $-78^\circ\text{C}$  and 14 h at  $-20^\circ\text{C}$ . The raw product was diluted with 4 mL

### C. Experimental Section

---

MeOH, filtered and the variously substituted products were purified with preparative HPLC (gradient 50%-70% CH<sub>3</sub>CN in H<sub>2</sub>O without TFA). Fractions containing compounds with masses + allyl

**HPLC (75-978)** [65%-75% solvent B in 20min]: R<sub>t</sub> = 13.1 min, purity (220 nm) = 97%

**UV spectra** ( $\lambda_{\text{max}}$ ): 210nm, 265 nm, 278 nm, 288 nm (characteristic for triene moiety of rapamycin based on Sehgal et al<sup>143</sup>,  $\lambda_{\text{max}}$ : 267 nm, 277 nm, 288 nm)

**Mass:** (ESI<sup>+</sup>), calculated 978.59 [C<sub>54</sub>H<sub>85</sub>NO<sub>13</sub>+Na]<sup>+</sup>, found 978.57 [M-Na]<sup>+</sup>.

**HPLC (75-1021)** [65%-75% solvent B in 20min]: R<sub>t</sub> = 18.0 min, purity (220 nm) = 90%

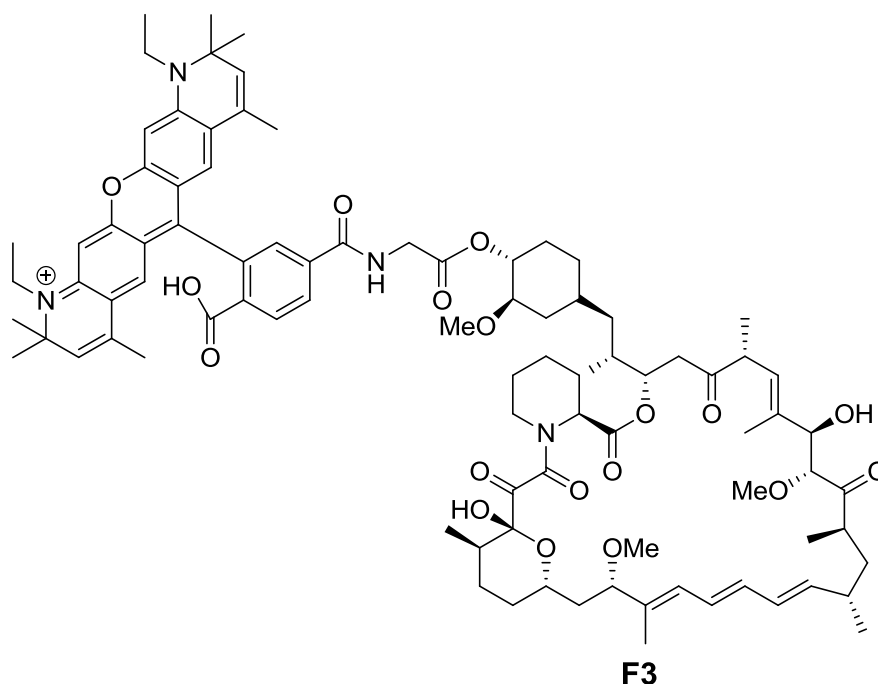
**UV spectra** ( $\lambda_{\text{max}}$ ): 220 nm, 268 nm, 278 nm, 289 nm

**Mass:** (ESI<sup>+</sup>), calculated 1020.64 [C<sub>57</sub>H<sub>91</sub>NO<sub>13</sub>+Na]<sup>+</sup>, found 1020.60 [M-Na]<sup>+</sup>.

**HPLC (75-1062)** [70%-100% solvent B in 20min]: R<sub>t</sub> = 13.3 min, purity (220 nm) = 85%

**UV spectra** ( $\lambda_{\text{max}}$ ): 220 nm, 265 nm, 278 nm, 289 nm

**Mass:** (ESI<sup>+</sup>), calculated 1062.69 [C<sub>60</sub>H<sub>97</sub>NO<sub>13</sub>+Na]<sup>+</sup>, found 1062.72 [M-Na]<sup>+</sup>.

**MFP590-Rap (F3)**

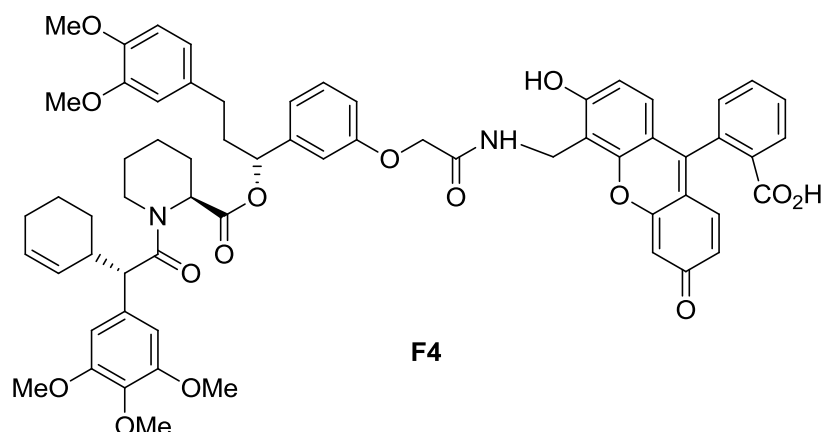
C40-Glycyl-rapamycin **87** was synthesized as described.<sup>144</sup> **87** (1 mg, 1.0  $\mu\text{mol}$ ) was dissolved in 10  $\mu\text{L}$  DMF, then DIEPA (2  $\mu\text{L}$ , 2.1  $\mu\text{mol}$ ) was added. MFP590 (0.5 mg, 0.6  $\mu\text{mol}$ ) was dissolved in 20  $\mu\text{L}$  DMF and was added to the above solution and stirred for 48h. The crude product was diluted with 2 mL  $\text{CH}_3\text{CN}/\text{H}_2\text{O}$  80:20 filtered and purified with semi preparative HPLC (gradient 60%-100%  $\text{CH}_3\text{CN}$  in  $\text{H}_2\text{O}$ ). **F3** was obtained as 183  $\mu\text{M}$  solution in DMSO. The concentration was determined by absorption spectroscopy using  $\epsilon_{597} = 1.2 \times 10^5 \text{ M}^{-1}\text{cm}^{-1}$  of MFP590.

**HPLC** [60%-80% solvent B in 20 min]:  $R_t = 18.2$  min.

**UV spectra** ( $\lambda_{\text{max}}$ ): 267 nm, 278 nm, 289 nm, 597 nm (characteristic for triene moiety of rapamycin based on Sehgal et al<sup>143</sup>,  $\lambda_{\text{max}}$ : 267 nm, 277 nm, 288 nm)

**UV/Vis spectra** (80 % MeOH, 20 % Tris-HCl, 5 mM, pH 8.8) 10  $\mu\text{M}$ :  $\epsilon_{597} = 1.2 \times 10^5 \text{ M}^{-1}\text{cm}^{-1}$

**Mass:** (ESI<sup>+</sup>), calculated 1543.85 [ $\text{C}_{90}\text{H}_{119}\text{F}_3\text{N}_4\text{O}_{18}$ ]<sup>+</sup>, found 1543.80 [M]<sup>+</sup>.

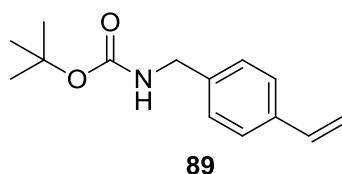
**Fluorescent iFit ligand (F4)**

**50** (5 mg, 6.7  $\mu\text{mol}$ ) was dissolved in 50  $\mu\text{L}$  DCM then HATU (5 mg, 13  $\mu\text{mol}$ ) and DIPEA (5  $\mu\text{L}$ , 29  $\mu\text{mol}$ ) was added and stirred for 15min. Subsequently 4'-(Aminomethyl)-fluorescein (2 mg, 6.7  $\mu\text{mol}$ ) was added and stirred at RT for 2.5 h. The crude product was diluted with 1 mL MeOH and purified with preparative HPLC (gradient 50%-90% MeOH in  $\text{H}_2\text{O}$  without TFA, 30 min,  $R_t = 20 - 22$  min, 220 nm). **F4** was obtained as a yellow fluorescent solid (1.7 mg, 1.6  $\mu\text{mol}$ , 23%).

**HPLC** [60%-90% solvent B, 20 min]:  $R_t = 13.0$  min, purity (220 nm) = 98%

**UV/Vis spectra** (80 % MeOH, 20 % Tris-HCl, 5 mM, pH 8.8) 5.4  $\mu\text{M}$ :  $\epsilon_{278} = 15850 \text{ M}^{-1}\text{cm}^{-1}$ ,  $\epsilon_{280} = 15650 \text{ M}^{-1} \text{ cm}^{-1}$ ,  $\epsilon_{498} = 46900 \text{ M}^{-1}\text{cm}^{-1}$ .

**Mass:** (ESI<sup>+</sup>), calculated 1089.44 [ $\text{C}_{63}\text{H}_{64}\text{N}_2\text{O}_{15} + \text{H}$ ]<sup>+</sup>, found 1089.40 [M+H]<sup>+</sup>.

**tert-Butyl 4-vinylbenzylcarbamate (89)**

To 4-vinylaminobenzene (1 g, 7.5 mmol, TCI Europe) and TEA (0.73 mL, 9.0 mmol) dissolved in 20 mL dry MeOH was added Boc-anhydride (2.5 g, 11.3 mmol). After stirring for 14 h, the resulting reaction

mixture was concentrated in vacuo and flash chromatographed (silica gel, EtOAc/i-Hex) to obtain **74** as a white solid (1.75g, quant. yield).

**TLC** [EtOAc/i-Hex 1:9]:  $R_f = 0.38$ .

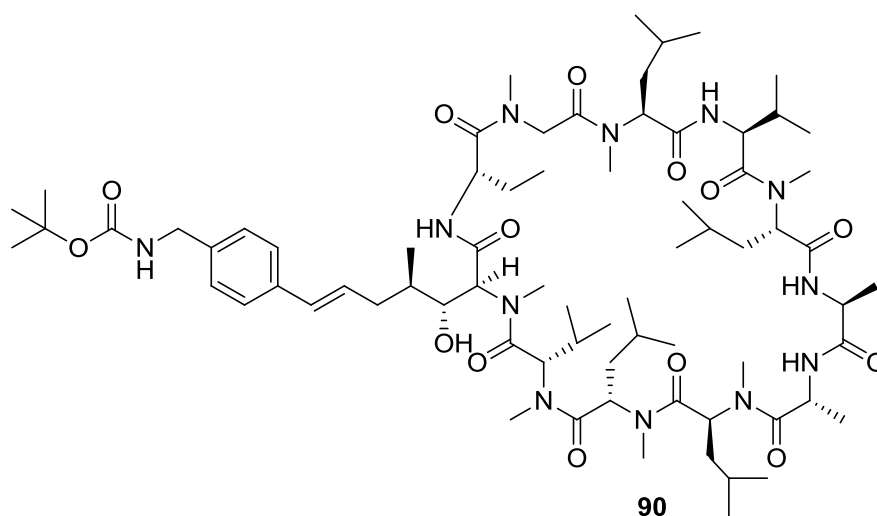
**HPLC** [0%-100% solvent B, 20 min]:  $R_t = 25.0$  min, purity (220 nm) = 98%

**$^1\text{H}$  NMR** (300 MHz,  $\text{CDCl}_3$ ):  $\delta = 7.38$  (d,  $J = 9$  Hz, 2 H), 7.26 (d,  $J = 9$  Hz, 2 H), 6.72 (dd,  $J = 10.86$  Hz, 17.61 Hz 1H), 5.75 (dd,  $J = 0.93$  Hz, 17.60 Hz, 1 H), 5.25 (dd,  $J = 0.92$  Hz, 10.88 Hz, 1 H), 4.31 (d,  $J = 5.00$  Hz, 2 H), 1.48 (s, 9 H).

**$^{13}\text{C}$  NMR** (75 MHz,  $\text{CDCl}_3$ ):  $\delta = 155.87, 138.55, 136.72, 136.43, 127.65, 126.42, 113.77, 44.45, 28.41$ .

**HRMS**: calculated 234.1494 [ $\text{C}_{14}\text{H}_{19}\text{NO}_2 + \text{H}$ ] $^+$ , found: 234.1481 [ $\text{M} + \text{H}$ ] $^+$ .

### Cyclosporin with linker (**90**)



**CsA** (100 mg, 84  $\mu\text{mol}$ ) and Grubbs catalyst 2nd Generation (3.5 mg, 4.2  $\mu\text{mol}$ , Aldrich) were dissolved in 1 mL dry DCM. Then **89** (196 mg, 0.84 mmol) was added and refluxed for 20 h. The resulting mixture was filtered through celite, concentrated in vacuo and flash chromatographed (silica gel, EtOAc/i-hexane) to obtain **90** as a brown oil (60 mg, 43  $\mu\text{mol}$ , 52 % yield).

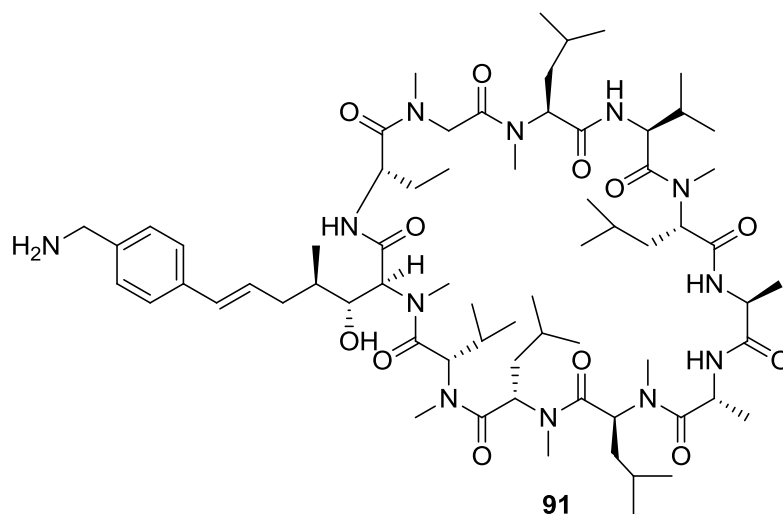
**TLC** [EtOAc, 100% ]:  $R_f = 0.36$ .

**HPLC** [65%-85% solvent B, 20 min]:  $R_t = 18.1$  min, purity (220 nm) = 95%

**$^1\text{H}$  NMR** (600 MHz,  $\text{CDCl}_3$ ):  $\delta = 8.00$  (d,  $J = 9.76$  Hz, 1H), 7.64 (d,  $J = 7.68$  Hz, 1H), 7.50 (d,  $J = 8.24$  Hz, 1H), 7.29 (d, 8.18 Hz, 2H), 7.20 (d,  $J = 8.04$  Hz, 2H), 7.10 (d,  $J = 8.00$  Hz, 1H), 6.30 (d,  $J = 15.82$  Hz, 1H), 6.15 (m, 1H), 5.68 (dd,  $J = 4.38$  Hz, 10.98 Hz, 1H), 5.56, (d,  $J = 5.65$  Hz, 1H), 5.32, (dd, 3.94 Hz, 11.55 Hz, 1H), 5.12 (d,  $J = 10.82$  Hz, 1H), 5.04 (dd,  $J = 7.09$  Hz 14.11 Hz, 2H), 4.93 (d,  $J = 6.02$  Hz, 1H), 4.91 (d,  $J = 6.14$  Hz, 1H), 4.82 (m, 1H), 4.74 (d,  $J = 13.93$  Hz, 1H), 4.66 (m, 1H), 4.54 (t,  $J = 7.41$  Hz, 7.41 Hz, 1H), 4.27 (s,  $J = 7.68$  Hz, 2H), 3.78 (m, 1H), 3.53 (s, 3H), 3.40 (s, 3H), 3.26 (s, 3H), 3.11 (s, 3H), 3.09 (s, 3H), 2.70 (s, 3H), 2.68 (s, 3H), 2.44 (m, 2H), 2.12 (m, 2H), 1.98 (m, 2H), 1.78 (m, 2H), 1.72 (m, 2H), 1.61 (m, 2H), 1.45 (s, 9H), 1.34 (d,  $J = 7.27$  Hz, 6H), 1.24 (d,  $J = 6.89$  Hz, 6H), 1.21 (d,  $J = 6.11$  Hz, 6H), 1.08 (d,  $J = 6.55$  Hz, 6H), 1.03 (d,  $J = 6.78$  Hz, 6H), 0.96-0.83 (m, 21H), 0.80 (d,  $J = 6.60$  Hz, 3H), 0.71 (d,  $J = 6.36$  Hz, 3H).

**$^{13}\text{C}$  NMR** (150 MHz,  $\text{CDCl}_3$ ):  $\delta = 173.96, 173.78, 173.70, 173.43, 171.58, 171.34, 171.10, 170.54, 170.31, 170.16, 170.08, 155.82, 137.09, 130.86, 129.69, 128.87, 127.65, 126.24, 75.22, 64.41, 58.94, 57.84, 57.58, 55.52, 55.48, 55.45, 50.35, 48.75, 48.49, 48.18, 45.11, 40.39, 39.56, 38.92, 37.53, 36.85, 36.60, 36.60, 34.21, 31.51, 31.34, 31.17, 29.79, 29.78, 29.51, 29.22, 28.40, 25.34, 24.87, 24.60, 24.30, 23.82, 23.69, 23.64, 23.46, 23.39, 21.82, 21.09, 20.40, 19.93, 18.69, 18.38, 18.20, 16.83, 16.03, 9.91.$

**HRMS**: calculated 1393.8377 [ $\text{C}_{73}\text{H}_{124}\text{N}_{12}\text{O}_{14}+\text{H}$ ] $^+$ , found 1393.8974 [ $\text{M}+\text{H}$ ] $^+$ .

**Cyclosporin with deprotected linker (91)**

**90** (40 mg, 29  $\mu$ mol) was dissolved in 1.8 mL dry DCM and cooled to 0°C in an ice bath. Then 200  $\mu$ L TFA was added drop wise. The reaction was stirred for 2h. DCM/TFA was evaporated via air blow. The mixture was flash chromatographed (MeOH/DCM, 5:95, 1%TEA) to obtain **91** as white solid (30 mg, 23  $\mu$ mol, 81% yield).

**TLC** [MeOH/DCM,5:95 + 1% TEA]:  $R_f$  = 0.28.

**HPLC** [30%-70% solvent B, 20 min]:  $R_t$  = 18.6 min, purity (220 nm) = 90 %

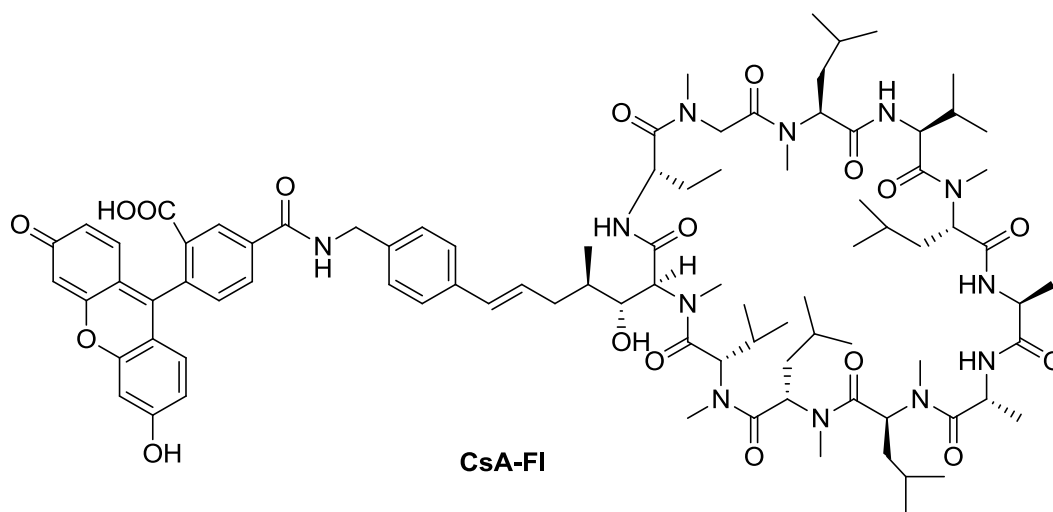
**$^1\text{H NMR}$**  (600 Mhz,  $\text{CDCl}_3$ ):  $\delta$  = 7.98 (d,  $J$  = 9.75 Hz, 1H), 7.64 (d,  $J$  = 7.60 Hz, 1H), 7.52 (m, 1H), 7.49 (d,  $J$  = 8.32 Hz, 1H), 7.29 (d, 8.29 Hz, 2H), 7.20 (d,  $J$  = 8.04 Hz, 2H), 7.09 (d,  $J$  = 7.95 Hz, 1H), 6.29 (d,  $J$  = 18.00 Hz, 1H), 6.14 (m, 1H), 5.67 (dd,  $J$  = 4.30 Hz, 11.06 Hz, 1H), 5.53, (d,  $J$  = 5.75 Hz, 1H), 5.30 (dd, 3.96 Hz, 11.41 Hz, 1H), 5.11 (d,  $J$  = 15.00 Hz, 1H), 5.03 (m, 2H), 4.92 (dd,  $J$  = 3.96 Hz, 11.41 Hz, 1H), 4.81 (m, 1H), 4.71 (d,  $J$  = 13.99 Hz, 1H), 4.64 (dd,  $J$  = 8.44 Hz, 9.66 Hz, 1H), 4.52 (m, 1H), 3.89 (s, 1H) 3.78 (m, 1H), 3.51 (s, 3H), 3.38 (s, 3H), 3.23 (s, 3H), 3.08 (s, 3H), 3.07 (s, 3H), 2.69 (s, 3H), 2.66 (s, 3H), 2.42 (ddd,  $J$  = 6.66 Hz, 13.45 Hz, 16.19 Hz, 2H), 2.11 (m, 2H), 1.98 (m, 2H), 1.76 (m, 2H), 1.70 (m, 2H), 1.59 (m, 2H), 1.33 (d,  $J$  = 7.07 Hz, 6H), 1.22 (d,  $J$  = 6.91 Hz, 6H), 1.22 (d,  $J$  = 6.09 Hz, 6H), 1.09 (s, 3H), 1.08 (s, 3H) 1.06 (d,  $J$  = 6.69 Hz, 6H), 1.01 (d,  $J$  = 6.64 Hz, 6H), 0.97-0.83 (m, 18H), 0.79 (d,  $J$  = 6.00 Hz, 3H), 0.71 (d,  $J$  = 6.00 Hz, 3H).

**$^{13}\text{C NMR}$**  (150 MHz,  $\text{CDCl}_3$ ):  $\delta$  = 173.88, 173.73, 173.68, 173.43, 171.53, 173.31, 171.08, 170.48, 170.32, 170.17, 170.09, 137.43, 130.80, 129.79, 128.21, 127.75, 127.35, 75.73, 67.94, 58.88, 57.85,

57.62, 57.55, 55.47, 55.42, 55.40, 50.33, 48.75, 48.48, 48.17, 45.10, 40.38, 39.50, 38.92, 37.50, 36.72, 36.47, 35.95, 34.14, 31.56, 31.31, 31.20, 29.79, 29.77, 29.51, 29.19, 28.60, 25.58, 25.33, 24.86, 24.60, 24.29, 23.80, 23.68, 23.63, 23.45, 23.37, 23.32, 21.07, 20.38, 19.88, 18.67, 19.37, 18.17, 16.83, 16.02, 9.83.

**HRMS:** calculated 1293.8914 [C<sub>68</sub>H<sub>116</sub>N<sub>12</sub>O<sub>12</sub>+H]<sup>+</sup>, found 1293.8667 [M+H]<sup>+</sup>

### CsA-FI



**92** (5 mg, 4  $\mu$ mol) and TEA (1  $\mu$ L, 12  $\mu$ mol, Roth) was dissolved in 600  $\mu$ L DCM/THF then 5(6)-carboxyfluorescein N-hydroxy-succinimide (2 mg, 4  $\mu$ mol) was added and stirred at RT for 2h. 1 mL 80:20 MeOH/H<sub>2</sub>O was added and filtrated. The crude mixture was purified by preparative HPLC (gradient: 65%-85% MeOH in H<sub>2</sub>O, + 0.1% TFA). **CsA-FI** (0.54 mg, 0.9  $\mu$ mol, 23%) was obtained as a yellow solid.

**HPLC:** [gradient 65%-85% solvent B in solvent A]: R<sub>t</sub> = 9 min, purity (220 nm) = 96 %

**UV/Vis spectra** (80 % MeOH, 20 % Tris-HCl, 5 mM, pH 8.8) 10  $\mu$ M:  $\epsilon_{254} = 22100 \text{ M}^{-1}\text{cm}^{-1}$ ,  $\epsilon_{280} = 12100 \text{ M}^{-1}\text{cm}^{-1}$ ,  $\epsilon_{468} = 7500 \text{ M}^{-1}\text{cm}^{-1}$ .

**HRMS:** calculated 1651.9391 [C<sub>89</sub>H<sub>126</sub>N<sub>12</sub>O<sub>18</sub>+H]<sup>+</sup>, found 1651.8666 [M+H]<sup>+</sup>

## 4.4 Biochemical Methods

All biochemical assays were performed under the guidance of Dr. Christian Kozany and Bastian Hoogeland.

### Inhibition of the cis–trans peptidyl–prolyl isomerase activity

The PPIase activity was determined as described<sup>108</sup> using Suc-AAPF-pNA (Sigma–Aldrich) as peptide substrate. The peptide substrate (4 mM) was dissolved in a solution of LiCl (470 mM) in dry trifluoroethanol and stored under argon. All solutions and buffers used were precooled to 4°C.

A 40x concentrated protein solution (25 µL, 400 nM Cyp18 or 4 µM Cyp40), 5 µL DMSO or 5 µL of a 200x stock of CsA or CsA-FI in DMSO were added to 845 µL assay buffer (50 mM HEPES pH 8, 100 mM NaCl). The samples were incubated in protein low binding cups (Eppendorf) for 30 minutes at room temperature and were then transferred to cuvettes. After addition of chymotrypsin (100 µL, 60 mg/mL; Carl Roth GmbH) the reaction was started by addition of the peptide substrate (25 µL, 4 mM). The increase in absorption was recorded at 390 nm and 4°C. The amount of released p-nitroanilide (pNA) is directly proportional to the trans isomer of the peptide substrate, starting from a cis–trans mixture. The measured absorption units were correlated to release pNA by the molar extinction coefficient of 13,300 M<sup>-1</sup> cm<sup>-1</sup> at 390 nm. The curves were analyzed by using Sigma Plot11 and fitted with a three parameter fit (single) for an exponential rise to a maximum. Since subsaturating final substrate concentration (100 µM) were ( $[S] \ll K_M$ ) the measured IC<sub>50</sub> could be directly converted to K<sub>i</sub>.

### Fluorescence polarization assay for the binding of CsA-FI to cyclophilins

For fluorescence polarization assays a 10 µM stock solution of proteins was serially diluted 1:1 in assay buffer (20 mM HEPES pH 8, 0.01% Triton-X100). 30 µL of each protein dilution was mixed with 30 µL of CsA-FI (20 nM in assay buffer) and transferred to a black 384-well assay plate (No.: 3575; Corning Life Sciences B.V.). After incubation at room temperature for 30 min the fluorescence anisotropy was measured with a plate reader (GENios Pro, Tecan) by using an excitation filter of 485/20 nm and emission filters of 535/25 nm. The binding assays were performed in duplicates. The binding curves were analysed by using SigmaPlot 11. Data were fitted to the equation according to Kozany et al. to derive K<sub>D</sub> values.<sup>108</sup>

## Fluorescence polarization competition assay for binding of unlabelled cyclophilin ligands

A 2 mM stock solution of CsA dissolved in DMSO was serially diluted 1:1 in DMSO. Every sample of this serial dilution was diluted by a factor of 50 in assay buffer (20 mM HEPES pH 8, 0.01% Triton-X100) supplemented with 20 nM ligand CsA-FI. To 30  $\mu$ L of each of these competitive ligand mixtures, 30  $\mu$ L of protein (20 nM Cyp18, 200 nM Cyp40) dissolved in assay buffer were added. The samples were transferred to black 384-well assay plates (No.: 3575; Corning Life Sciences) and treated as described above. The competition curves were analyzed by using Sigma Plot 11. For the analysis of  $K_i$  values, data were fitted according to Kozany et al.<sup>108</sup>.

## Fluorescence polarization assay for the binding of fluorescent iFit ligand F4 to FKBP51

For fluorescence polarization assays a 97  $\mu$ M stock solution of protein was serially diluted 1:1 in assay buffer (20 mM HEPES pH 8, 0.01% Triton-X100). 20  $\mu$ L of each protein dilution was mixed with 20  $\mu$ L of **F4** (20 nM in assay buffer) and transferred to a black 384-well assay plate (No.: 3575; Corning Life Sciences B.V.). After incubation at room temperature for 30 min the fluorescence anisotropy was measured with a plate reader (GENios Pro, Tecan) by using an excitation filter of 485/20 nm and emission filters of 535/25 nm. The binding assays were performed in duplicates. The binding curves were analysed by using SigmaPlot 11. Data were fitted to the equation according to Kozany et al. to derive  $K_D$  values.<sup>108</sup>

## Fluorescence polarization competition assay for binding of unlabelled FKBP ligands

A stock solution of test compound was dissolved in DMSO and serially diluted 1:1 in DMSO. Every sample of this serial dilution was diluted by a factor of 33,33 in assay buffer (20 mM HEPES pH 8, 0.01% Triton-X100) supplemented with 3 nM ligand **F4**. To 20  $\mu$ L of each of these competitive ligand mixtures, 20  $\mu$ L of protein (4.5 nM FKBP51FK1) dissolved in assay buffer were added. The samples were transferred to black 384-well assay plates (No.: 3575; Corning Life Sciences) and measured as described above. The competition curves were analyzed by using Sigma Plot 11. For the analysis of  $K_i$  values, data were fitted according to Kozany et al.<sup>108</sup>

## D. Abbreviations

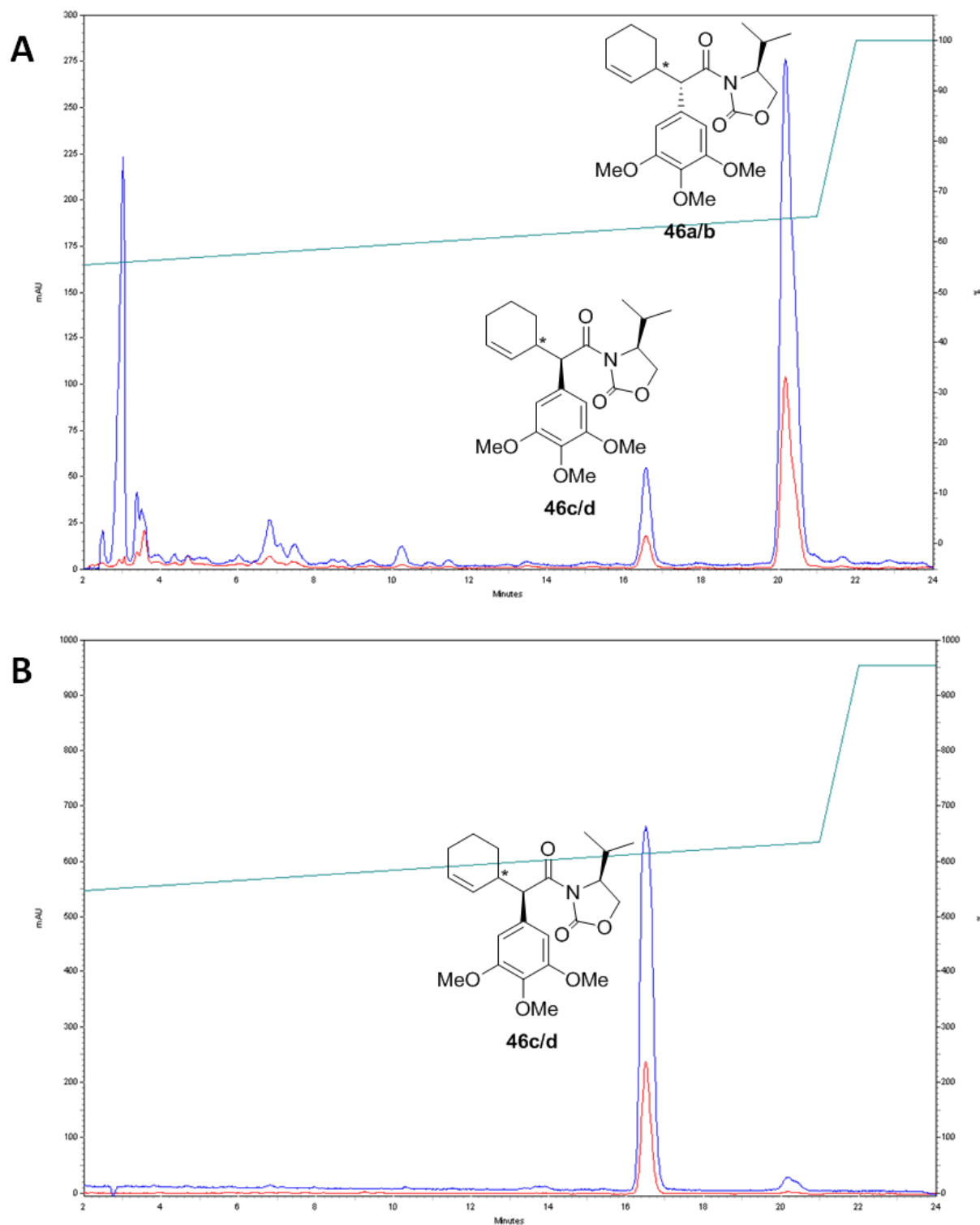
ACTH	Adrenocorticotrophic Hormone
AR	Androgen Receptor
Brine	Saturated NaCl solution
BuLi	n-butyllithium
CID	Chemical Inducer of Dimerization
CK2	Casein Kinase 2
CN	Calcineurin
CRH	Corticotropin Releasing Hormone
CsA	Cyclosporine A
Cyp	Cyclophilin
DCM	Dichloromethane
DCC	N,N'-Dicyclohexylcarbodiimide
DIPEA	N,N-Diisopropylethylamine
EDC	1-Ethyl-3-(3-dimethylaminopropyl)carbodiimid
EE	Ethyl acetate
ER	Estrogen Receptor
F	Phenylalanine
FKBP	FK506 binding protein
FP	Fluorescence Polarisation
GR	Glucocorticoid receptor
HOAt	1-Hydroxy-7-azabenzotriazole
HATU	O-(7-Azabenzotriazol-1-yl)-N,N,N',N'-tetramethyluronium hexafluorophosphate
HPA	Hypothalamus pituitary adrenal
HPLC	High Pressure Liquid Chromatography
Hsp90	Heat shock protein 90
LDC	Lead Discovery Center
LiHMDS	Lithium hexamethyldisilazid
LiOH	Lithium hydroxide
LMU	Ludwig Maximilian University
MeOH	Methanol

#### D. Abbreviations

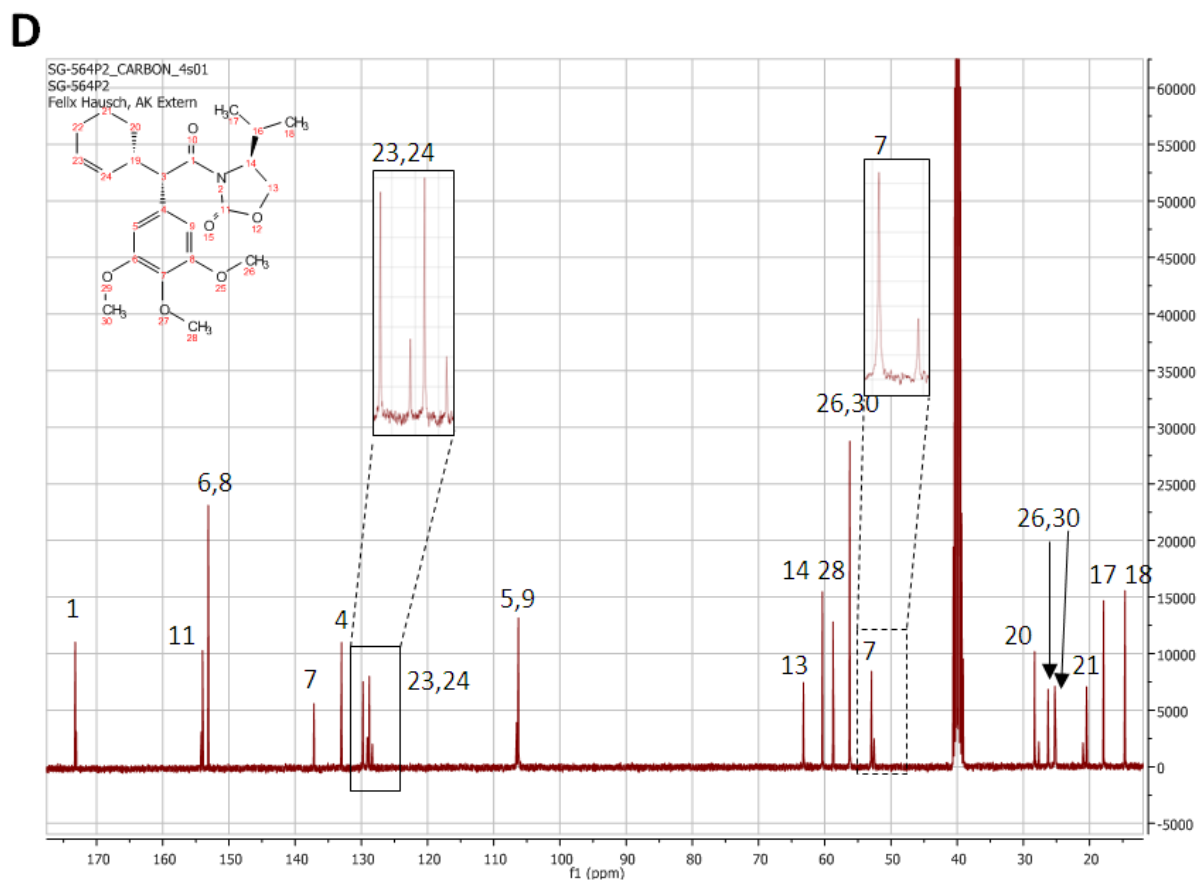
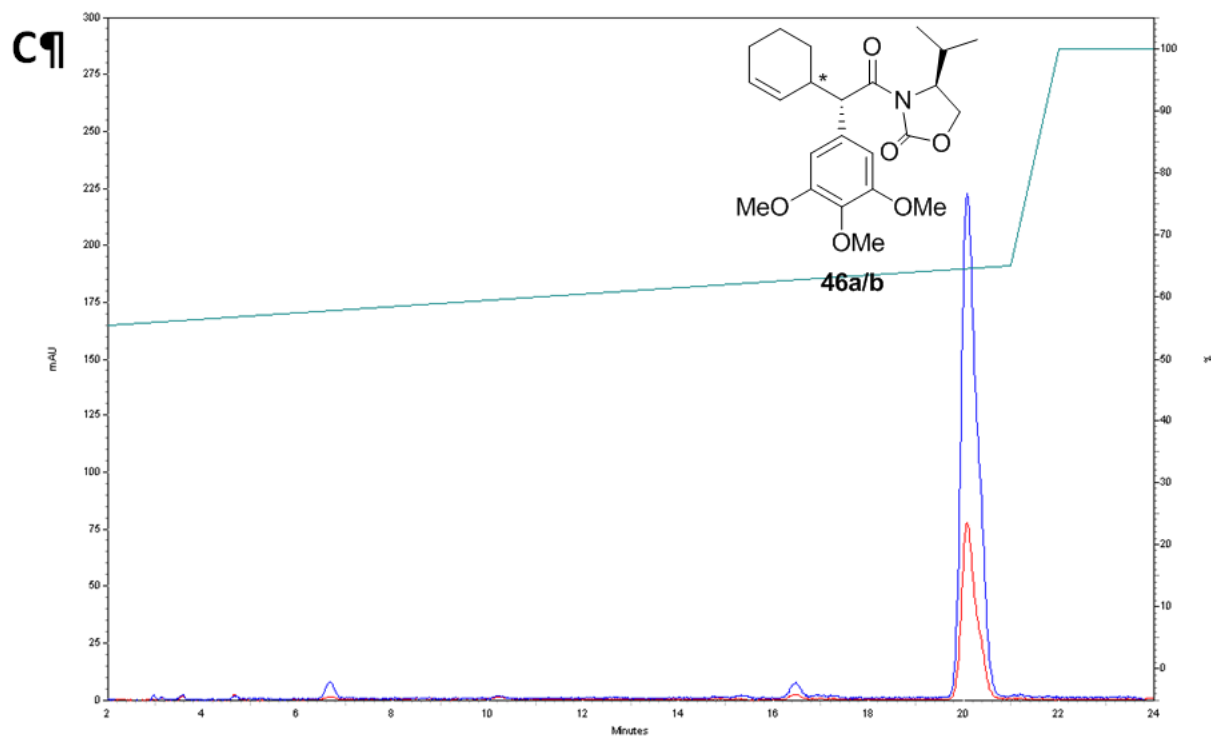
---

MD	Major depression
MPI	Max Planck Institute
MR	Mineralcorticoid Receptor
mTOR	mammalian target of rapamycin
NaHMDS	Natrium hexamethyl disilazid
NF-AT	Nuclear factor of activated T-cells
n-Hex	n-Hexane
NMR	Nuclear magnetic resonance
PPIase	Peptidyl-prolyl-cis/trans-Isomerase
PR	Progesterone Receptor
PTSD	Post-traumatic stress disorder
Rap	Rapamycin
RT	Room Temperature
SAR	Structure Activity Relationship
SHR	Steroid Hormone Receptor
TFA	Trifluoroacetic acid
TEA	Triethylamine
TLC	Thin layer chromatography
THF	Tetrahydrofuran
V	Valine
WT	Wildtype

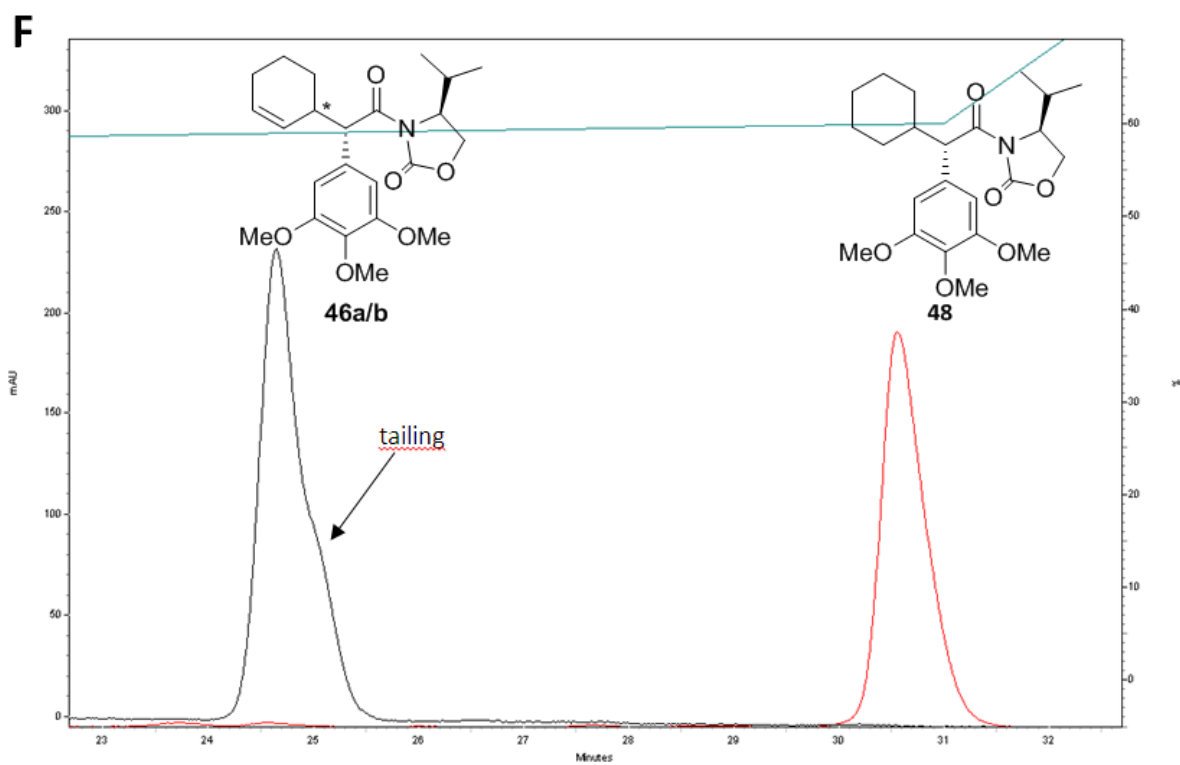
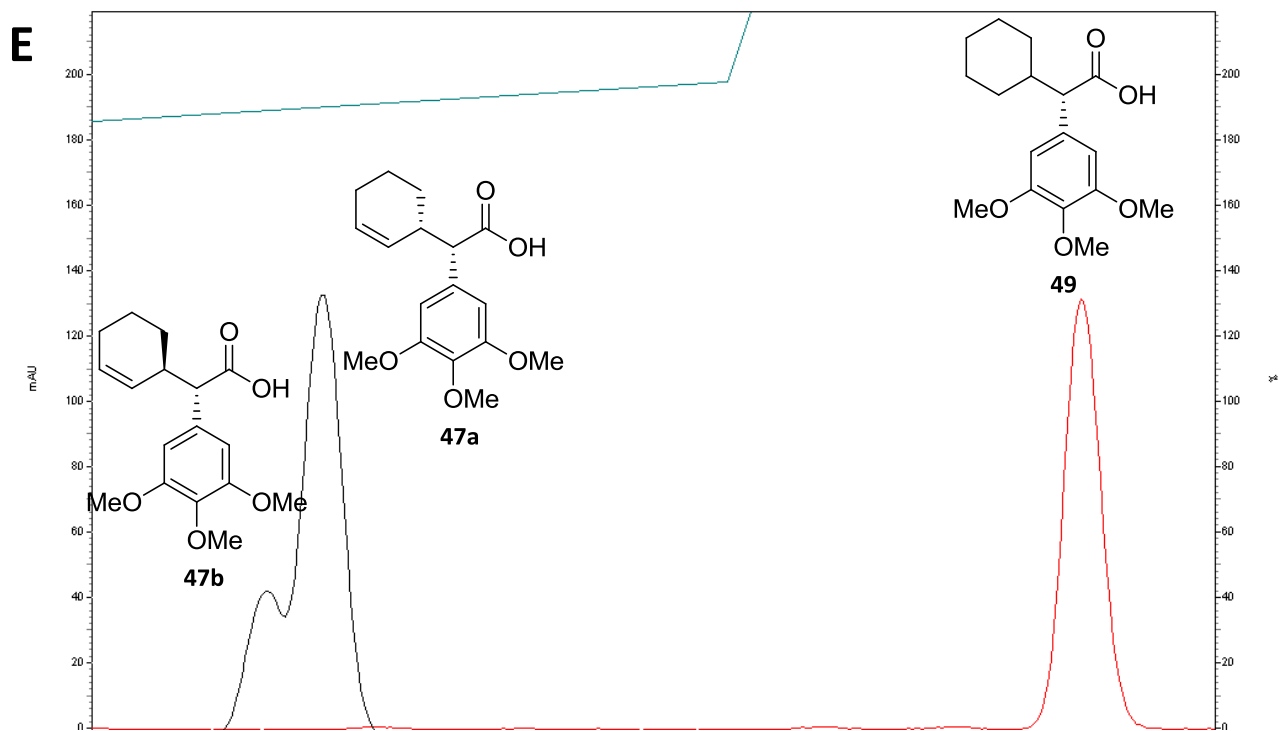
## E. Annex



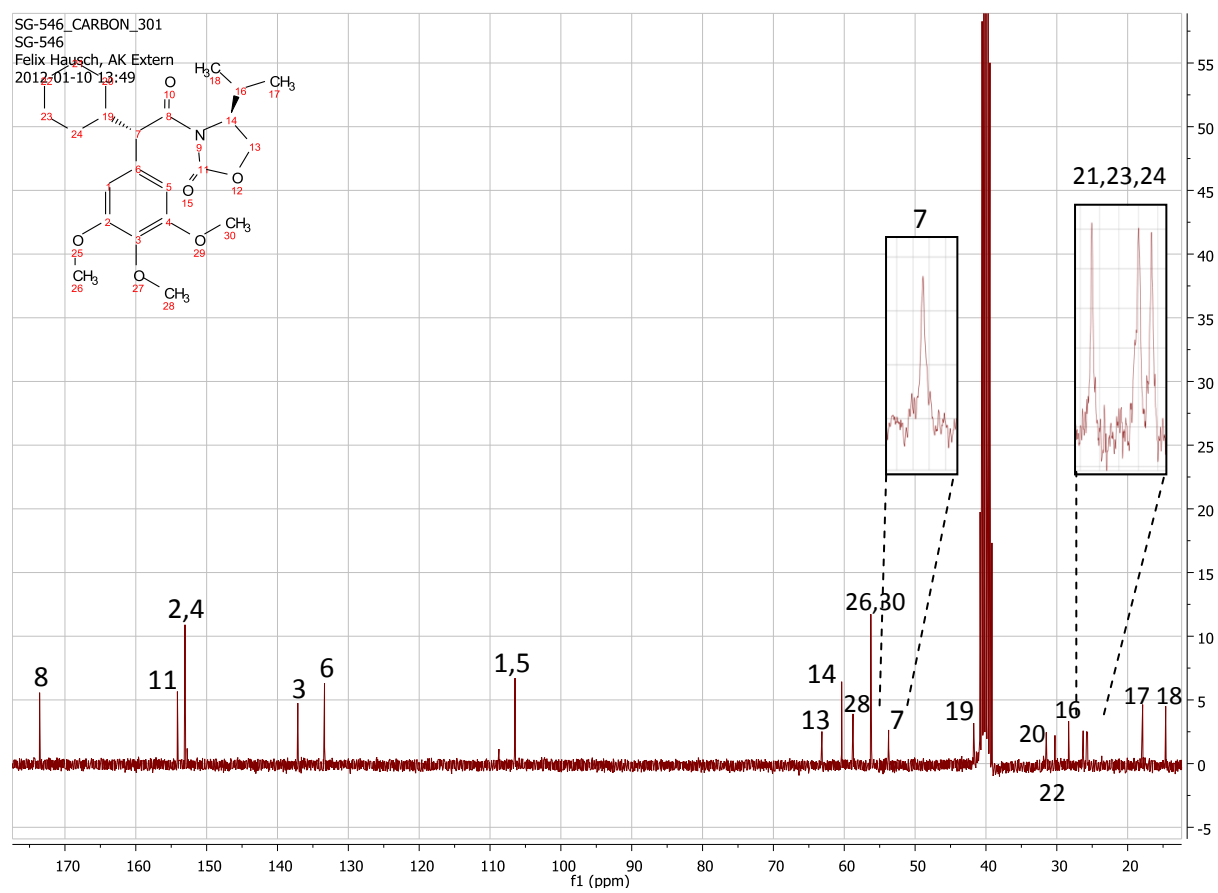
Annex: (A) Crude product of 46. (B) Purified minor product 46c/d.



Annex: (C) Purified major product 46a/b. (B)  $^{13}\text{C}$  spectra of 46a/b as a mixture of diastereomers



Annex: (E) Partial resolution of **47a/b**, no tailing for the reduced **49**. (F) Tailing of **46a/b**, no tailing for the reduced **48**.



Annex: (G)  $^{13}\text{C}$  NMR of 49. No diastereomers can be observed.

## F. References

1. Wedemeyer, W. J.; Welker, E.; Scheraga, H. A., Current Topics/Perspectives Proline Cis-Trans Isomerization and Protein Folding. *Biochemistry* **2002**, 41, (50), 14637-14644.
2. Weiwad, M.; Edlich, F.; Kilka, S.; Erdmann, F.; Jarczowski, F.; Dorn, M.; Moutty, M. C.; Fischer, G., Comparative analysis of calcineurin inhibition by complexes of immunosuppressive drugs with human FK506 binding proteins. *Biochemistry* **2006**, 45, (51), 15776-84.
3. Crabtree, G. R.; Schreiber, S. L., SnapShot: Ca<sup>2+</sup>-calcineurin-NFAT signaling. *Cell* **2009**, 138, (1), 210, 210 e1.
4. Zoncu, R.; Efeyan, A.; Sabatini, D. M., mTOR: from growth signal integration to cancer, diabetes and ageing. *Nat Rev Mol Cell Biol* **12**, (1), 21-35.
5. Galat, A., Functional drift of sequence attributes in the FK506-binding proteins (FKBPs). *J Chem Inf Model* **2008**, 48, (5), 1118-30.
6. Harding, M. W.; Galat, A.; Uehling, D. E.; Schreiber, S. L., A receptor for the immunosuppressant FK506 is a cis-trans peptidyl-prolyl isomerase. *Nature* **1989**, 341, (6244), 758-60.
7. Aghdasi, B.; Ye, K.; Resnick, A.; Huang, A.; Ha, H. C.; Guo, X.; Dawson, T. M.; Dawson, V. L.; Snyder, S. H., FKBP12, the 12-kDa FK506-binding protein, is a physiologic regulator of the cell cycle. *Proceedings of the National Academy of Sciences* **2001**, 98, (5), 2425-2430.
8. Zissimopoulos, S.; Lai, F. A., Interaction of FKBP12.6 with the Cardiac Ryanodine Receptor C-terminal Domain. *Journal of Biological Chemistry* **2005**, 280, (7), 5475-5485.
9. Lam, E.; Martin, M. M.; Timerman, A. P.; Sabers, C.; Fleischer, S.; Lukas, T.; Abraham, R. T.; O'Keefe, S. J.; O'Neill, E. A.; Wiederrecht, G. J., A novel FK506 binding protein can mediate the immunosuppressive effects of FK506 and is associated with the cardiac ryanodine receptor. *J Biol Chem* **1995**, 270, (44), 26511-22.
10. Cheung, K. L. Y.; Bates, M.; Ananthanarayanan, V. S., Effect of FKBP65, a putative elastin chaperone, on the coacervation of tropoelastin in vitro. *Biochemistry and Cell Biology* **2010**, 88, (6), 917-925.
11. Jarczowski, F.; Fischer, G.; Edlich, F., FKBP36 Forms Complexes with Clathrin and Hsp72 in Spermatocytes. *Biochemistry* **2008**, 47, (26), 6946-6952.
12. Jarczowski, F.; Jahreis, G. n.; Erdmann, F.; Schierhorn, A.; Fischer, G.; Edlich, F., FKBP36 Is an Inherent Multifunctional Glyceraldehyde-3-phosphate Dehydrogenase Inhibitor. *Journal of Biological Chemistry* **2009**, 284, (2), 766-773.
13. Kuzhandaivelu, N.; Cong, Y. S.; Inouye, C.; Yang, W. M.; Seto, E., XAP2, a novel hepatitis B virus X-associated protein that inhibits X transactivation. *Nucleic Acids Res* **1996**, 24, (23), 4741-50.
14. Sohocki, M. M.; Bowne, S. J.; Sullivan, L. S.; Blackshaw, S.; Cepko, C. L.; Payne, A. M.; Bhattacharya, S. S.; Khaliq, S.; Qasim Mehdi, S.; Birch, D. G.; Harrison, W. R.; Elder, F. F.; Heckenlively, J. R.; Daiger, S. P., Mutations in a new photoreceptor-pineal gene on 17p cause Leber congenital amaurosis. *Nat Genet* **2000**, 24, (1), 79-83.
15. Shirane, M.; Nakayama, K. I., Inherent calcineurin inhibitor FKBP38 targets Bcl-2 to mitochondria and inhibits apoptosis. *Nat Cell Biol* **2003**, 5, (1), 28-37.
16. Baughman, G.; Wiederrecht, G. J.; Campbell, N. F.; Martin, M. M.; Bourgeois, S., FKBP51, a novel T-cell-specific immunophilin capable of calcineurin inhibition. *Mol Cell Biol* **1995**, 15, (8), 4395-402.
17. Callebaut, I.; Renoir, J. M.; Lebeau, M. C.; Massol, N.; Burny, A.; Baulieu, E. E.; Mornon, J. P., An immunophilin that binds M(r) 90,000 heat shock protein: main structural features of a mammalian p59 protein. *Proc Natl Acad Sci U S A* **1992**, 89, (14), 6270-4.
18. Galat, A.; Lane, W. S.; Standaert, R. F.; Schreiber, S. L., A rapamycin-selective 25-kDa immunophilin. *Biochemistry* **1992**, 31, (8), 2427-2434.
19. Galat, A., Function-dependent clustering of orthologues and paralogues of cyclophilins. *Proteins* **2004**, 56, (4), 808-20.

20. Sanglier, J. J.; Quesniaux, V.; Fehr, T.; Hofmann, H.; Mahnke, M.; Memmert, K.; Schuler, W.; Zenke, G.; Gschwind, L.; Maurer, C.; Schilling, W., Sanglifehrins A, B, C and D, novel cyclophilin-binding compounds isolated from *Streptomyces* sp. A92-308110. I. Taxonomy, fermentation, isolation and biological activity. *J Antibiot (Tokyo)* **1999**, 52, (5), 466-73.
21. Sanchez, E. R., Hsp56: a novel heat shock protein associated with untransformed steroid receptor complexes. *J Biol Chem* **1990**, 265, (36), 22067-70.
22. Smith, D. F.; Faber, L. E.; Toft, D. O., Purification of unactivated progesterone receptor and identification of novel receptor-associated proteins. *J Biol Chem* **1990**, 265, (7), 3996-4003.
23. Pirkl, F.; Buchner, J., Functional analysis of the Hsp90-associated human peptidyl prolyl cis/trans isomerases FKBP51, FKBP52 and Cyp40. *J Mol Biol* **2001**, 308, (4), 795-806.
24. Wu, B.; Li, P.; Liu, Y.; Lou, Z.; Ding, Y.; Shu, C.; Ye, S.; Bartlam, M.; Shen, B.; Rao, Z., 3D structure of human FK506-binding protein 52: implications for the assembly of the glucocorticoid receptor/Hsp90/immunophilin heterocomplex. *Proc Natl Acad Sci U S A* **2004**, 101, (22), 8348-53.
25. Sinars, C. R.; Cheung-Flynn, J.; Rimerman, R. A.; Scammell, J. G.; Smith, D. F.; Clardy, J., Structure of the large FK506-binding protein FKBP51, an Hsp90-binding protein and a component of steroid receptor complexes. *Proc Natl Acad Sci U S A* **2003**, 100, (3), 868-73.
26. Cox, M. B.; Riggs, D. L.; Hessling, M.; Schumacher, F.; Buchner, J.; Smith, D. F., FK506-Binding Protein 52 Phosphorylation: A Potential Mechanism for Regulating Steroid Hormone Receptor Activity. *Mol Endocrinol* **2007**, 21, (12), 2956-2967.
27. Cox, M. B.; Smith, D. F., *Functions of the Hsp90-Binding FKBP Immunophilins*. Austin, 2007.
28. Cheung-Flynn, J.; Prapapanich, V.; Cox, M. B.; Riggs, D. L.; Suarez-Quian, C.; Smith, D. F., Physiological role for the cochaperone FKBP52 in androgen receptor signaling. *Mol Endocrinol* **2005**, 19, (6), 1654-66.
29. Riggs, D. L.; Roberts, P. J.; Chirillo, S. C.; Cheung-Flynn, J.; Prapapanich, V.; Ratajczak, T.; Gaber, R.; Picard, D.; Smith, D. F., The Hsp90-binding peptidylprolyl isomerase FKBP52 potentiates glucocorticoid signaling in vivo. *Embo J* **2003**, 22, (5), 1158-67.
30. Tranguch, S.; Cheung-Flynn, J.; Daikoku, T.; Prapapanich, V.; Cox, M. B.; Xie, H.; Wang, H.; Das, S. K.; Smith, D. F.; Dey, S. K., Cochaperone immunophilin FKBP52 is critical to uterine receptivity for embryo implantation. *Proc Natl Acad Sci U S A* **2005**, 102, (40), 14326-31.
31. Storer, C. L.; Dickey, C. A.; Galigniana, M. D.; Rein, T.; Cox, M. B., FKBP51 and FKBP52 in signaling and disease. *Trends Endocrinol Metab* **2011**.
32. Riggs, D. L.; Cox, M. B.; Tardif, H. L.; Hessling, M.; Buchner, J.; Smith, D. F., Noncatalytic role of the FKBP52 peptidyl-prolyl isomerase domain in the regulation of steroid hormone signaling. *Mol Cell Biol* **2007**, 27, (24), 8658-69.
33. Witchel, S. F.; DeFranco, D. B., Mechanisms of disease: regulation of glucocorticoid and receptor levels--impact on the metabolic syndrome. *Nat Clin Pract Endocrinol Metab* **2006**, 2, (11), 621-31.
34. Galigniana, M. D.; Echeverria, P. C.; Erlejman, A. G.; Piwien-Pilipuk, G., Role of molecular chaperones and TPR-domain proteins in the cytoplasmic transport of steroid receptors and their passage through the nuclear pore. *Nucleus* **2010**, 1, (4), 299-308.
35. Piwien Pilipuk, G.; Vinson, G. P.; Gomez Sanchez, C.; Galigniana, M. D., Evidence for NL1-Independent Nuclear Translocation of the Mineralocorticoid Receptor. *Biochemistry* **2007**, 46, (5), 1389-1397.
36. Galigniana, M. D.; Radanyi, C.; Renoir, J. M.; Housley, P. R.; Pratt, W. B., Evidence that the peptidylprolyl isomerase domain of the hsp90-binding immunophilin FKBP52 is involved in both dynein interaction and glucocorticoid receptor movement to the nucleus. *J Biol Chem* **2001**, 276, (18), 14884-9.
37. Yong, W.; Yang, Z.; Periyasamy, S.; Chen, H.; Yucel, S.; Li, W.; Lin, L. Y.; Wolf, I. M.; Cohn, M. J.; Baskin, L. S.; Sánchez, E. R.; Shou, W., Essential Role for Co-chaperone Fkbp52 but Not Fkbp51 in Androgen Receptor-mediated Signaling and Physiology. *Journal of Biological Chemistry* **2007**, 282, (7), 5026-5036.
38. Yang, Z.; Wolf, I. M.; Chen, H.; Periyasamy, S.; Chen, Z.; Yong, W.; Shi, S.; Zhao, W.; Xu, J.; Srivastava, A.; Sanchez, E. R.; Shou, W., FK506-binding protein 52 is essential to uterine reproductive

- physiology controlled by the progesterone receptor A isoform. *Mol Endocrinol* **2006**, *20*, (11), 2682-94.
39. Touma, C.; Gassen, N. C.; Herrmann, L.; Cheung-Flynn, J.; BÄ¼ll, D. R.; Ionescu, I. A.; Heinzmann, J.-M.; Knapman, A.; Siebertz, A.; Depping, A.-M.; Hartmann, J.; Hausch, F.; Schmidt, M. V.; Holsboer, F.; Ising, M.; Cox, M. B.; Schmidt, U.; Rein, T., FK506 Binding Protein 5 Shapes Stress Responsiveness: Modulation of Neuroendocrine Reactivity and Coping Behavior. *Biological Psychiatry* **2011**, *70*, (10), 928-936.
40. Hartmann, J.; Wagner, K. V.; Liebl, C.; Scharf, S. H.; Wang, X.-D.; Wolf, M.; Hausch, F.; Rein, T.; Schmidt, U.; Touma, C.; Cheung-Flynn, J.; Cox, M. B.; Smith, D. F.; Holsboer, F.; MÄ¼ller, M. B.; Schmidt, M. V., The involvement of FK506-binding protein 51 (FKBP5) in the behavioral and neuroendocrine effects of chronic social defeat stress. *Neuropharmacology* **2012**, *62*, (1), 332-339.
41. O'Leary, J. C., III; Dharia, S.; Blair, L. J.; Brady, S.; Johnson, A. G.; Peters, M.; Cheung-Flynn, J.; Cox, M. B.; de Erausquin, G.; Weeber, E. J.; Jinwal, U. K.; Dickey, C. A., A New Anti-Depressive Strategy for the Elderly: Ablation of FKBP5/FKBP51. *PLoS ONE* **2011**, *6*, (9), e24840.
42. de Kloet, E. R.; Joels, M.; Holsboer, F., Stress and the brain: from adaptation to disease. *Nat Rev Neurosci* **2005**, *6*, (6), 463-75.
43. Reynolds, P. D.; Ruan, Y.; Smith, D. F.; Scammell, J. G., Glucocorticoid resistance in the squirrel monkey is associated with overexpression of the immunophilin FKBP51. *J Clin Endocrinol Metab* **1999**, *84*, (2), 663-9.
44. Denny, W. B.; Prapapanich, V.; Smith, D. F.; Scammell, J. G., Structure-function analysis of squirrel monkey FK506-binding protein 51, a potent inhibitor of glucocorticoid receptor activity. *Endocrinology* **2005**, *146*, (7), 3194-201.
45. Binder, E. B.; Salyakina, D.; Lichtner, P.; Wochnik, G. M.; Ising, M.; Putz, B.; Papiol, S.; Seaman, S.; Lucae, S.; Kohli, M. A.; Nickel, T.; Kunzel, H. E.; Fuchs, B.; Majer, M.; Pfennig, A.; Kern, N.; Brunner, J.; Modell, S.; Baghai, T.; Deiml, T.; Zill, P.; Bondy, B.; Rupprecht, R.; Messer, T.; Kohnlein, O.; Dabitz, H.; Bruckl, T.; Muller, N.; Pfister, H.; Lieb, R.; Mueller, J. C.; Lohmussaar, E.; Strom, T. M.; Bettecken, T.; Meitinger, T.; Uhr, M.; Rein, T.; Holsboer, F.; Muller-Myhsok, B., Polymorphisms in FKBP5 are associated with increased recurrence of depressive episodes and rapid response to antidepressant treatment. *Nat Genet* **2004**, *36*, (12), 1319-25.
46. Kirchheiner, J.; Lorch, R.; Lebedeva, E.; Seeringer, A.; Roots, I.; Sasse, J.; BrockmÄ¼ller, J. r., Genetic variants in FKBP5 affecting response to antidepressant drug treatment. *Pharmacogenomics* **2008**, *9*, (7), 841-846.
47. Lekman, M.; Laje, G.; Charney, D.; Rush, A. J.; Wilson, A. F.; Sorant, A. J. M.; Lipsky, R.; Wisniewski, S. R.; Manji, H.; McMahon, F. J.; Paddock, S., The FKBP5-Gene in Depression and Treatment Response - an Association Study in the Sequenced Treatment Alternatives to Relieve Depression (STAR\*D) Cohort. *Biological Psychiatry* **2008**, *63*, (12), 1103-1110.
48. Willour, V. L.; Chen, H.; Toolan, J.; Belmonte, P.; Cutler, D. J.; Goes, F. S.; Zandi, P. P.; Lee, R. S.; MacKinnon, D. F.; Mondimore, F. M.; Schweizer, B.; DePaulo, J. R., Jr.; Gershon, E. S.; McMahon, F. J.; Potash, J. B., Family-based association of FKBP5 in bipolar disorder. *Mol Psychiatry* **2009**, *14*, (3), 261-8.
49. Brent, D.; Melhem, N.; Ferrell, R.; Emslie, G.; Wagner, K. D.; Ryan, N.; Vitiello, B.; Birmaher, B.; Mayes, T.; Zelazny, J.; Onorato, M.; Devlin, B.; Clarke, G.; DeBar, L.; Keller, M., Association of FKBP5 polymorphisms with suicidal events in the Treatment of Resistant Depression in Adolescents (TORDIA) study. *Am J Psychiatry* **2010**, *167*, (2), 190-7.
50. Supriyanto, I.; Sasada, T.; Fukutake, M.; Asano, M.; Ueno, Y.; Nagasaki, Y.; Shirakawa, O.; Hishimoto, A., Association of FKBP5 gene haplotypes with completed suicide in the Japanese population. *Prog Neuropsychopharmacol Biol Psychiatry* **2011**, *35*, (1), 252-6.
51. Roy, A.; Gorodetsky, E.; Yuan, Q.; Goldman, D.; Enoch, M. A., Interaction of FKBP5, a stress-related gene, with childhood trauma increases the risk for attempting suicide. *Neuropsychopharmacology* **2010**, *35*, (8), 1674-83.

52. Roy, A.; Hodgkinson, C. A.; Deluca, V.; Goldman, D.; Enoch, M. A., Two HPA axis genes, CRHBP and FKBP5, interact with childhood trauma to increase the risk for suicidal behavior. *J Psychiatr Res* **2012**, *46*, (1), 72-9.
53. Ising, M.; Depping, A. M.; Siebertz, A.; Lucae, S.; Unschuld, P. G.; Kloiber, S.; Horstmann, S.; Uhr, M.; Muller-Myhsok, B.; Holsboer, F., Polymorphisms in the FKBP5 gene region modulate recovery from psychosocial stress in healthy controls. *Eur J Neurosci* **2008**, *28*, (2), 389-98.
54. Koenen, K. C.; Saxe, G.; Purcell, S.; Smoller, J. W.; Bartholomew, D.; Miller, A.; Hall, E.; Kaplow, J.; Bosquet, M.; Moulton, S.; Baldwin, C., Polymorphisms in FKBP5 are associated with peritraumatic dissociation in medically injured children. *Mol Psychiatry* **2005**, *10*, (12), 1058-1059.
55. Ozer, E. J.; Best, S. R.; Lipsey, T. L.; Weiss, D. S., Predictors of posttraumatic stress disorder and symptoms in adults: a meta-analysis. *Psychol Bull* **2003**, *129*, (1), 52-73.
56. Yehuda, R.; Cai, G.; Golier, J. A.; Sarapas, C.; Galea, S.; Ising, M.; Rein, T.; Schmeidler, J.; Muller-Myhsok, B.; Holsboer, F.; Buxbaum, J. D., Gene expression patterns associated with posttraumatic stress disorder following exposure to the World Trade Center attacks. *Biol Psychiatry* **2009**, *66*, (7), 708-11.
57. Stechschulte, L. A.; Sanchez, E. R., FKBP51-a selective modulator of glucocorticoid and androgen sensitivity. *Curr Opin Pharmacol* **2011**, *11*, (4), 332-7.
58. O'Malley, K. J.; Dhir, R.; Nelson, J. B.; Bost, J.; Lin, Y.; Wang, Z., The expression of androgen-responsive genes is Up-Regulated in the epithelia of benign prostatic hyperplasia. *The Prostate* **2009**, *69*, (16), 1716-1723.
59. Ni, L.; Yang, C. S.; Gioeli, D.; Frierson, H.; Toft, D. O.; Paschal, B. M., FKBP51 promotes assembly of the Hsp90 chaperone complex and regulates androgen receptor signaling in prostate cancer cells. *Mol Cell Biol* **2010**, *30*, (5), 1243-53.
60. Periyasamy, S.; Warriar, M.; Tillekeratne, M. P.; Shou, W.; Sanchez, E. R., The immunophilin ligands cyclosporin A and FK506 suppress prostate cancer cell growth by androgen receptor-dependent and -independent mechanisms. *Endocrinology* **2007**, *148*, (10), 4716-26.
61. Schulke, J. P.; Wochnik, G. M.; Lang-Rollin, I.; Gassen, N. C.; Knapp, R. T.; Berning, B.; Yassouridis, A.; Rein, T., Differential impact of tetratricopeptide repeat proteins on the steroid hormone receptors. *PLoS One* **2010**, *5*, (7), e11717.
62. Mukaide, H.; Adachi, Y.; Taketani, S.; Iwasaki, M.; Koike-Kiriyama, N.; Shigematsu, A.; Shi, M.; Yanai, S.; Yoshioka, K.; Kamiyama, Y.; Ikehara, S., FKBP51 expressed by both normal epithelial cells and adenocarcinoma of colon suppresses proliferation of colorectal adenocarcinoma. *Cancer Invest* **2008**, *26*, (4), 385-90.
63. Rees-Unwin, K. S.; Craven, R. A.; Davenport, E.; Hanrahan, S.; Totty, N. F.; Dring, A. M.; Banks, R. E.; G, J. M.; Davies, F. E., Proteomic evaluation of pathways associated with dexamethasone-mediated apoptosis and resistance in multiple myeloma. *Br J Haematol* **2007**, *139*, (4), 559-67.
64. Avellino, R.; Romano, S.; Parasole, R.; Bisogni, R.; Lamberti, A.; Poggi, V.; Venuta, S.; Romano, M. F., Rapamycin stimulates apoptosis of childhood acute lymphoblastic leukemia cells. *Blood* **2005**, *106*, (4), 1400-6.
65. Romano, S.; Di Pace, A.; Sorrentino, A.; Bisogni, R.; Sivero, L.; Romano, M. F., FK506 binding proteins as targets in anticancer therapy. *Anticancer Agents Med Chem* **2010**, *10*, (9), 651-6.
66. Pei, H.; Li, L.; Fridley, B. L.; Jenkins, G. D.; Kalari, K. R.; Lingle, W.; Petersen, G.; Lou, Z.; Wang, L., FKBP51 affects cancer cell response to chemotherapy by negatively regulating Akt. *Cancer Cell* **2009**, *16*, (3), 259-66.
67. De Leon, J. T.; Iwai, A.; Feau, C.; Garcia, Y.; Balsiger, H. A.; Storer, C. L.; Suro, R. M.; Garza, K. M.; Lee, S.; Kim, Y. S.; Chen, Y.; Ning, Y. M.; Riggs, D. L.; Fletterick, R. J.; Guy, R. K.; Trepel, J. B.; Neckers, L. M.; Cox, M. B., Targeting the regulation of androgen receptor signaling by the heat shock protein 90 cochaperone FKBP52 in prostate cancer cells. *Proc Natl Acad Sci U S A* **2011**, *108*, (29), 11878-83.
68. Nakamura, N.; Shimaoka, Y.; Tougan, T.; Onda, H.; Okuzaki, D.; Zhao, H.; Fujimori, A.; Yabuta, N.; Nagamori, I.; Tanigawa, A.; Sato, J.; Oda, T.; Hayashida, K.; Suzuki, R.; Yukioka, M.; Nojima, H.; Ochi, T., Isolation and expression profiling of genes upregulated in bone marrow-derived mononuclear cells of rheumatoid arthritis patients. *DNA Res* **2006**, *13*, (4), 169-83.

69. Matsushita, R.; Hashimoto, A.; Tomita, T.; Yoshitawa, H.; Tanaka, S.; Endo, H.; Hirohata, S., Enhanced expression of mRNA for FK506-binding protein 5 in bone marrow CD34 positive cells in patients with rheumatoid arthritis. *Clin Exp Rheumatol* **2010**, *28*, (1), 87-90.
70. Park, J.; Kim, M.; Na, G.; Jeon, I.; Kwon, Y. K.; Kim, J. H.; Youn, H.; Koo, Y., Glucocorticoids modulate NF-kappaB-dependent gene expression by up-regulating FKBP51 expression in Newcastle disease virus-infected chickens. *Mol Cell Endocrinol* **2007**, *278*, (1-2), 7-17.
71. Jiang, W.; Cazacu, S.; Xiang, C.; Zenklusen, J. C.; Fine, H. A.; Berens, M.; Armstrong, B.; Brodie, C.; Mikkelsen, T., FK506 binding protein mediates glioma cell growth and sensitivity to rapamycin treatment by regulating NF-kappaB signaling pathway. *Neoplasia* **2008**, *10*, (3), 235-43.
72. Kelly, M. M.; King, E. M.; Rider, C. F.; Gwozd, C.; Holden, N. S.; Eddleston, J.; Zuraw, B.; Leigh, R.; O'Byrne, P. M.; Newton, R., Corticosteroid-induced gene expression in allergen-challenged asthmatic subjects taking inhaled budesonide. *British Journal of Pharmacology* **2012**, *165*, (6), 1737-1747.
73. Holownia, A.; Mroz, R. M.; Kolodziejczyk, A.; Chyczewska, E.; Braszko, J. J., Increased FKBP51 in induced sputum cells of chronic obstructive pulmonary disease patients after therapy. *Eur J Med Res* **2009**, *14* Suppl 4, 108-11.
74. Imai, A.; Sahara, H.; Tamura, Y.; Jimbow, K.; Saito, T.; Ezoe, K.; Yotsuyanagi, T.; Sato, N., Inhibition of endogenous MHC class II-restricted antigen presentation by tacrolimus (FK506) via FKBP51. *Eur J Immunol* **2007**, *37*, (7), 1730-8.
75. Costantini, L. C.; Cole, D.; Pravin, C.; Isacson, O., Immunophilin ligands can prevent progressive dopaminergic degeneration in animal models of Parkinson's disease. *European Journal of Neuroscience* **2001**, *13*, (6), 1085-1092.
76. Li, F.; Otori, N.; Hayashi, T.; Jin, G.; Sato, K.; Nagano, I.; Shoji, M.; Abe, K., Protection against ischemic brain damage in rats by immunophilin ligand GPI-1046. *J Neurosci Res* **2004**, *76*, (3), 383-9.
77. Gold, B. G.; Katoh, K.; Storm-Dickerson, T., The immunosuppressant FK506 increases the rate of axonal regeneration in rat sciatic nerve. *J Neurosci* **1995**, *15*, (11), 7509-16.
78. Jones, J. W.; Gruber, S. A.; Barker, J. H.; Breidenbach, W. C., Successful hand transplantation. One-year follow-up. Louisville Hand Transplant Team. *N Engl J Med* **2000**, *343*, (7), 468-73.
79. Labrande, C.; Velly, L.; Canolle, B.; Guillet, B.; Masmejean, F.; Nieoullon, A.; Pisano, P., Neuroprotective effects of tacrolimus (FK506) in a model of ischemic cortical cell cultures: role of glutamate uptake and FK506 binding protein 12 kDa. *Neuroscience* **2006**, *137*, (1), 231-9.
80. Steiner, J. P.; Hamilton, G. S.; Ross, D. T.; Valentine, H. L.; Guo, H.; Connolly, M. A.; Liang, S.; Ramsey, C.; Li, J. H.; Huang, W.; Howorth, P.; Soni, R.; Fuller, M.; Sauer, H.; Nowotnik, A. C.; Suzdak, P. D., Neurotrophic immunophilin ligands stimulate structural and functional recovery in neurodegenerative animal models. *Proc Natl Acad Sci U S A* **1997**, *94*, (5), 2019-24.
81. Steiner, J. P.; Connolly, M. A.; Valentine, H. L.; Hamilton, G. S.; Dawson, T. M.; Hester, L.; Snyder, S. H., Neurotrophic actions of nonimmunosuppressive analogues of immunosuppressive drugs FK506, rapamycin and cyclosporin A. *Nat Med* **1997**, *3*, (4), 421-8.
82. Gold, B. G.; Densmore, V.; Shou, W.; Matzuk, M. M.; Gordon, H. S., Immunophilin FK506-binding protein 52 (not FK506-binding protein 12) mediates the neurotrophic action of FK506. *J Pharmacol Exp Ther* **1999**, *289*, (3), 1202-10.
83. Edlich, F.; Weiwad, M.; Wildemann, D.; Jarczowski, F.; Kilka, S.; Moutty, M. C.; Jahreis, G.; Lucke, C.; Schmidt, W.; Striggow, F.; Fischer, G., The specific FKBP38 inhibitor N-(N',N'-dimethylcarboxamidomethyl)cycloheximide has potent neuroprotective and neurotrophic properties in brain ischemia. *J Biol Chem* **2006**, *281*, (21), 14961-70.
84. Gaali, S.; Gopalakrishnan, R.; Wang, Y.; Kozany, C.; Hausch, F., The Chemical Biology of Immunophilin Ligands. *Current Medicinal Chemistry* **2011**, *18*.
85. Gerard, M.; Deleersnijder, A.; Demeulemeester, J.; Debyser, Z.; Baekelandt, V., Unraveling the role of peptidyl-prolyl isomerases in neurodegeneration. *Mol Neurobiol* **2011**, *44*, (1), 13-27.
86. Quinta, H. R.; Maschi, D.; Gomez-Sanchez, C.; Piwien-Pilipuk, G.; Galigniana, M. D., Subcellular rearrangement of hsp90-binding immunophilins accompanies neuronal differentiation and neurite outgrowth. *J Neurochem* **2010**, *115*, (3), 716-34.

87. Jinwal, U. K.; Koren, J., 3rd; Borysov, S. I.; Schmid, A. B.; Abisambra, J. F.; Blair, L. J.; Johnson, A. G.; Jones, J. R.; Shults, C. L.; O'Leary, J. C., 3rd; Jin, Y.; Buchner, J.; Cox, M. B.; Dickey, C. A., The Hsp90 cochaperone, FKBP51, increases Tau stability and polymerizes microtubules. *J Neurosci* **2010**, *30*, (2), 591-9.
88. Chambraud, B.; Sardin, E.; Giustiniani, J.; Dounane, O.; Schumacher, M.; Goedert, M.; Baulieu, E. E., A role for FKBP52 in Tau protein function. *Proc Natl Acad Sci U S A* **2010**, *107*, (6), 2658-63.
89. Harrison, D. E.; Strong, R.; Sharp, Z. D.; Nelson, J. F.; Astle, C. M.; Flurkey, K.; Nadon, N. L.; Wilkinson, J. E.; Frenkel, K.; Carter, C. S.; Pahor, M.; Javors, M. A.; Fernandez, E.; Miller, R. A., Rapamycin fed late in life extends lifespan in genetically heterogeneous mice. *Nature* **2009**, *460*, (7253), 392-5.
90. Spilman, P.; Podlutskaya, N.; Hart, M. J.; Debnath, J.; Gorostiza, O.; Bredesen, D.; Richardson, A.; Strong, R.; Galvan, V., Inhibition of mTOR by rapamycin abolishes cognitive deficits and reduces amyloid-beta levels in a mouse model of Alzheimer's disease. *PLoS One* **2010**, *5*, (4), e9979.
91. Malagelada, C.; Jin, Z. H.; Jackson-Lewis, V.; Przedborski, S.; Greene, L. A., Rapamycin protects against neuron death in in vitro and in vivo models of Parkinson's disease. *J Neurosci* **2010**, *30*, (3), 1166-75.
92. Ravikumar, B.; Vacher, C.; Berger, Z.; Davies, J. E.; Luo, S.; Oroz, L. G.; Scaravilli, F.; Easton, D. F.; Duden, R.; O'Kane, C. J.; Rubinsztein, D. C., Inhibition of mTOR induces autophagy and reduces toxicity of polyglutamine expansions in fly and mouse models of Huntington disease. *Nat Genet* **2004**, *36*, (6), 585-95.
93. Cirstea, D.; Hideshima, T.; Rodig, S.; Santo, L.; Pozzi, S.; Vallet, S.; Ikeda, H.; Perrone, G.; Gorgun, G.; Patel, K.; Desai, N.; Sportelli, P.; Kapoor, S.; Vali, S.; Mukherjee, S.; Munshi, N. C.; Anderson, K. C.; Raje, N., Dual inhibition of akt/mammalian target of rapamycin pathway by nanoparticle albumin-bound-rapamycin and perifosine induces antitumor activity in multiple myeloma. *Mol Cancer Ther* **2010**, *9*, (4), 963-75.
94. Gold, B. G.; Storm-Dickerson, T.; Austin, D. R., The immunosuppressant FK506 increases functional recovery and nerve regeneration following peripheral nerve injury. *Restor Neurol Neurosci* **1994**, *6*, (4), 287-96.
95. Ruan, B.; Pong, K.; Jow, F.; Bowlby, M.; Crozier, R. A.; Liu, D.; Liang, S.; Chen, Y.; Mercado, M. L.; Feng, X.; Bennett, F.; von Schack, D.; McDonald, L.; Zaleska, M. M.; Wood, A.; Reinhart, P. H.; Magolda, R. L.; Skotnicki, J.; Pangalos, M. N.; Koehn, F. E.; Carter, G. T.; Abou-Gharbia, M.; Graziani, E. I., Binding of rapamycin analogs to calcium channels and FKBP52 contributes to their neuroprotective activities. *Proc Natl Acad Sci U S A* **2008**, *105*, (1), 33-8.
96. Kupina, N. C.; Detloff, M. R.; Dutta, S.; Hall, E. D., Neuroimmunophilin ligand V-10,367 is neuroprotective after 24-hour delayed administration in a mouse model of diffuse traumatic brain injury. *J Cereb Blood Flow Metab* **2002**, *22*, (10), 1212-21.
97. Yamazaki, S.; Yamaji, T.; Murai, N.; Yamamoto, H.; Price, R. D.; Matsuoka, N.; Mutoh, S., FK1706, a novel non-immunosuppressive immunophilin ligand, modifies the course of painful diabetic neuropathy. *Neuropharmacology* **2008**, *55*, (7), 1226-30.
98. Liu, D.; McIlvain, H. B.; Fennell, M.; Dunlop, J.; Wood, A.; Zaleska, M. M.; Graziani, E. I.; Pong, K., Screening of immunophilin ligands by quantitative analysis of neurofilament expression and neurite outgrowth in cultured neurons and cells. *J Neurosci Methods* **2007**, *163*, (2), 310-20.
99. Summers, M. Y.; Leighton, M.; Liu, D.; Pong, K.; Graziani, E. I., 3-normeridamycin: a potent non-immunosuppressive immunophilin ligand is neuroprotective in dopaminergic neurons. *J Antibiot (Tokyo)* **2006**, *59*, (3), 184-9.
100. Revill, W. P.; Voda, J.; Reeves, C. R.; Chung, L.; Schirmer, A.; Ashley, G.; Carney, J. R.; Fardis, M.; Carreras, C. W.; Zhou, Y.; Feng, L.; Tucker, E.; Robinson, D.; Gold, B. G., Genetically engineered analogs of ascomycin for nerve regeneration. *J Pharmacol Exp Ther* **2002**, *302*, (3), 1278-85.
101. Voda, J.; Yamaji, T.; Gold, B. G., Neuroimmunophilin ligands improve functional recovery and increase axonal growth after spinal cord hemisection in rats. *J Neurotrauma* **2005**, *22*, (10), 1150-61.

102. Gold, B. G.; Armistead, D. M.; Wang, M. S., Non-FK506-binding protein-12 neuroimmunophilin ligands increase neurite elongation and accelerate nerve regeneration. *J Neurosci Res* **2005**, *80*, (1), 56-65.
103. Armistead, D. M.; Badia, M. C.; Deininger, D. D.; Duffy, J. P.; Saunders, J. O.; Tung, R. D.; Thomson, J. A.; DeCenzo, M. T.; Futer, O.; Livingston, D. J.; Murcko, M. A.; Yamashita, M. M.; Navia, M. A., Design, synthesis and structure of non-macrocyclic inhibitors of FKBP12, the major binding protein for the immunosuppressant FK506. *Acta Crystallogr D Biol Crystallogr* **1995**, *51*, (Pt 4), 522-8.
104. Harper, S.; Bilsland, J.; Young, L.; Bristow, L.; Boyce, S.; Mason, G.; Rigby, M.; Hewson, L.; Smith, D.; O'Donnell, R.; O'Connor, D.; Hill, R. G.; Evans, D.; Swain, C.; Williams, B.; Hefti, F., Analysis of the neurotrophic effects of GPI-1046 on neuron survival and regeneration in culture and in vivo. *Neuroscience* **1999**, *88*, (1), 257-67.
105. Birge, R. B.; Wadsworth, S.; Akakura, R.; Abeyasinghe, H.; Kanojia, R.; Maclelag, M.; Desbarats, J.; Escalante, M.; Singh, K.; Sundarababu, S.; Parris, K.; Childs, G.; August, A.; Siekierka, J.; Weinstein, D. E., A role for schwann cells in the neuroregenerative effects of a non-immunosuppressive fk506 derivative, jnj460. *Neuroscience* **2004**, *124*, (2), 351-66.
106. Bocquet, A.; Lorent, G.; Fuks, B.; Grimee, R.; Talaga, P.; Daliers, J.; Klitgaard, H., Failure of GPI compounds to display neurotrophic activity in vitro and in vivo. *Eur J Pharmacol* **2001**, *415*, (2-3), 173-80.
107. Keenan, T.; Yaeger, D. R.; Courage, N. L.; Rollins, C. T.; Pavone, M. E.; Rivera, V. M.; Yang, W.; Guo, T.; Amara, J. F.; Clackson, T.; Gilman, M.; Holt, D. A., Synthesis and activity of bivalent FKBP12 ligands for the regulated dimerization of proteins. *Bioorg Med Chem* **1998**, *6*, (8), 1309-35.
108. Kozany, C.; Marz, A.; Kress, C.; Hausch, F., Fluorescent probes to characterise FK506-binding proteins. *Chembiochem* **2009**, *10*, (8), 1402-10.
109. Gopalakrishnan, R.; Kozany, C.; Gaali, S.; Kress, C.; Hoogeland, B.; Bracher, A.; Hausch, F., Evaluation of Synthetic FK506 Analogs as Ligands for the FK506-Binding Proteins 51 and 52. *Journal of Medicinal Chemistry* **2012**.
110. Bracher, A.; Kozany, C.; Thost, A. K.; Hausch, F., Structural characterization of the PPIase domain of FKBP51, a cochaperone of human Hsp90. *Acta Crystallogr D Biol Crystallogr* **2011**, *67*, (Pt 6), 549-59.
111. Gopalakrishnan, R.; Kozany, C.; Wang, Y.; Schneider, S.; Hoogeland, B.; Bracher, A.; Hausch, F., Exploration of Pipecolate Sulfonamides as Binders of the FK506-Binding Proteins 51 and 52. *Journal of Medicinal Chemistry* **2012**.
112. Wei, L.; Wu, Y.; Wilkinson, D. E.; Chen, Y.; Soni, R.; Scott, C.; Ross, D. T.; Guo, H.; Howorth, P.; Valentine, H.; Liang, S.; Spicer, D.; Fuller, M.; Steiner, J.; Hamilton, G. S., Solid-phase synthesis of FKBP12 inhibitors: N-sulfonyl and N-carbamoylpropyl/pipecolyl amides. *Bioorg Med Chem Lett* **2002**, *12*, (10), 1429-33.
113. Choi, C.; Li, J. H.; Vaal, M.; Thomas, C.; Limburg, D.; Wu, Y. Q.; Chen, Y.; Soni, R.; Scott, C.; Ross, D. T.; Guo, H.; Howorth, P.; Valentine, H.; Liang, S.; Spicer, D.; Fuller, M.; Steiner, J.; Hamilton, G. S., Use of parallel-synthesis combinatorial libraries for rapid identification of potent FKBP12 inhibitors. *Bioorg Med Chem Lett* **2002**, *12*, (10), 1421-8.
114. Spencer, D. M.; Wandless, T. J.; Schreiber, S. L.; Crabtree, G. R., Controlling signal transduction with synthetic ligands. *Science* **1993**, *262*, (5136), 1019-24.
115. Amara, J. F.; Clackson, T.; Rivera, V. M.; Guo, T.; Keenan, T.; Natesan, S.; Pollock, R.; Yang, W.; Courage, N. L.; Holt, D. A.; Gilman, M., A versatile synthetic dimerizer for the regulation of protein-protein interactions. *Proc Natl Acad Sci U S A* **1997**, *94*, (20), 10618-23.
116. Clackson, T.; Yang, W.; Rozamus, L. W.; Hatada, M.; Amara, J. F.; Rollins, C. T.; Stevenson, L. F.; Magari, S. R.; Wood, S. A.; Courage, N. L.; Lu, X.; Cerasoli, F.; Gilman, M.; Holt, D. A., Redesigning an FKBP-ligand interface to generate chemical dimerizers with novel specificity. *Proceedings of the National Academy of Sciences* **1998**, *95*, (18), 10437-10442.
117. Blau, C. A.; Peterson, K. R.; Drachman, J. G.; Spencer, D. M., A proliferation switch for genetically modified cells. *Proc Natl Acad Sci U S A* **1997**, *94*, (7), 3076-81.

118. Yang, X.; Chang, H. Y.; Baltimore, D., Autoproteolytic activation of pro-caspases by oligomerization. *Mol Cell* **1998**, 1, (2), 319-25.
119. Li, Z. Y.; Otto, K.; Richard, R. E.; Ni, S.; Kirillova, I.; Fausto, N.; Blau, C. A.; Lieber, A., Dimerizer-induced proliferation of genetically modified hepatocytes. *Mol Ther* **2002**, 5, (4), 420-6.
120. Belshaw, P. J.; Spencer, D. M.; Crabtree, G. R.; Schreiber, S. L., Controlling programmed cell death with a cyclophilin-cyclosporin-based chemical inducer of dimerization. *Chem Biol* **1996**, 3, (9), 731-8.
121. Trujillo, M. E.; Pajvani, U. B.; Scherer, P. E., Apoptosis through targeted activation of caspase 8 ("ATTAC-mice"): novel mouse models of inducible and reversible tissue ablation. *Cell Cycle* **2005**, 4, (9), 1141-5.
122. Pajvani, U. B.; Trujillo, M. E.; Combs, T. P.; Iyengar, P.; Jelicks, L.; Roth, K. A.; Kitsis, R. N.; Scherer, P. E., Fat apoptosis through targeted activation of caspase 8: a new mouse model of inducible and reversible lipodystrophy. *Nat Med* **2005**, 11, (7), 797-803.
123. Banaszynski, L. A.; Chen, L. C.; Maynard-Smith, L. A.; Ooi, A. G.; Wandless, T. J., A rapid, reversible, and tunable method to regulate protein function in living cells using synthetic small molecules. *Cell* **2006**, 126, (5), 995-1004.
124. Bishop, A. C.; Ubersax, J. A.; Petsch, D. T.; Matheos, D. P.; Gray, N. S.; Blethrow, J.; Shimizu, E.; Tsien, J. Z.; Schultz, P. G.; Rose, M. D.; Wood, J. L.; Morgan, D. O.; Shokat, K. M., A chemical switch for inhibitor-sensitive alleles of any protein kinase. *Nature* **2000**, 407, (6802), 395-401.
125. Shokat, K.; Velleca, M., Novel chemical genetic approaches to the discovery of signal transduction inhibitors. *Drug Discov Today* **2002**, 7, (16), 872-9.
126. Evans, D. A.; Ennis, M. D.; Le, T.; Mandel, N.; Mandel, G., Asymmetric acylation reactions of chiral imide enolates. The first direct approach to the construction of chiral .beta.-dicarbonyl synthons. *Journal of the American Chemical Society* **1984**, 106, (4), 1154-1156.
127. Paquette, L. A.; Guevel, R.; Sakamoto, S.; Kim, I. H.; Crawford, J., Convergent Enantioselective Synthesis of Vinigrol, an Architecturally Novel Diterpenoid with Potent Platelet Aggregation Inhibitory and Antihypertensive Properties. 1. Application of Anionic Sigmatropy to Construction of the Octalin Substructure. *The Journal of Organic Chemistry* **2003**, 68, (16), 6096-6107.
128. Kliman, L. T.; Mlynarski, S. N.; Morken, J. P., Pt-Catalyzed Enantioselective Diboration of Terminal Alkenes with B<sub>2</sub>(pin)<sub>2</sub>. *Journal of the American Chemical Society* **2009**, 131, (37), 13210-13211.
129. Varray, S. p.; Gauzy, C.; Lamaty, F. d. r.; Lazaro, R.; Martinez, J., Synthesis of Cyclic Amino Acid Derivatives via Ring Closing Metathesis on a Poly(ethylene glycol) Supported Substrate. *The Journal of Organic Chemistry* **2000**, 65, (20), 6787-6790.
130. Myers, A. G.; Yang, B. H.; Chen, H.; McKinstry, L.; Kopecky, D. J.; Gleason, J. L., Pseudoephedrine as a Practical Chiral Auxiliary for the Synthesis of Highly Enantiomerically Enriched Carboxylic Acids, Alcohols, Aldehydes, and Ketones. *Journal of the American Chemical Society* **1997**, 119, (28), 6496-6511.
131. Peifer, C.; Selig, R.; Kinkel, K.; Ott, D.; Totzke, F.; Schal`chtele, C.; Heidenreich, R.; Ro`cken, M.; Schollmeyer, D.; Laufer, S., Design, Synthesis, and Biological Evaluation of Novel 3-Aryl-4-(1H-indole-3yl)-1,5-dihydro-2H-pyrrole-2-ones as Vascular Endothelial Growth Factor Receptor (VEGF-R) Inhibitors. *Journal of Medicinal Chemistry* **2008**, 51, (13), 3814-3824.
132. Armistead, D. M.; Saunders, J. O.; Boger, J. S., 1-(2-oxoacetyl)piperidine-2-carboxylic acid derivatives as multi-drug-resistant cancer cell sensitizers. *WO 9407858* **1994**.
133. Baumann, K.; Hoegenauer, K.; Knapp, H.; Bacher, M.; Steck, A.; Wagner, T., On the reactivity of ascomycin at the binding domain. Part 3: Reactivity of the binding domain towards diazomethane. *Tetrahedron* **2005**, 61, (20), 4819-4829.
134. Luengo, J. I.; Rozamus, L. W.; Holt, D. A., Studies on selective reductions of rapamycin. *Tetrahedron Letters* **1994**, 35, (35), 6469-6472.
135. Wieland, L. C.; Deng, H.; Snapper, M. L.; Hoveyda, A. H., Al-Catalyzed Enantioselective Alkylation of  $\alpha$ -Ketoesters by Dialkylzinc Reagents. Enhancement of Enantioselectivity and Reactivity by an Achiral Lewis Base Additive. *Journal of the American Chemical Society* **2005**, 127, (44), 15453-15456.

136. Tokuda, O.; Kano, T.; Gao, W.-G.; Ikemoto, T.; Maruoka, K., A Practical Synthesis of (S)-2-Cyclohexyl-2-phenylglycolic Acid via Organocatalytic Asymmetric Construction of a Tetrasubstituted Carbon Center. *Organic Letters* **2005**, *7*, (22), 5103-5105.
137. Yanagisawa, A.; Terajima, Y.; Sugita, K.; Yoshida, K., Asymmetric Aldol Reaction of Ketones with Alkenyl Trichloroacetates Catalyzed by Dibutyltin Dimethoxide and BINAP·Silver(I) Complex: Construction of a Chiral Tertiary Carbon Center. *Advanced Synthesis & Catalysis* **2009**, *351*, (11-12), 1757-1762.
138. Senanayake, C. H.; Bakale, R. P.; Fang, Q. K.; Grover, P. T.; Heefner, D. L.; Rossi, R. F.; Wald, S. A., Preparation of cycloalkylphenylglycolate enantiomers by asymmetric synthesis. *WO9950205* **1999**.
139. Gaali, S.; Kozany, C.; Hoogeland, B.; Klein, M.; Hausch, F., Facile Synthesis of a Fluorescent Cyclosporin A Analogue To Study Cyclophilin 40 and Cyclophilin 18 Ligands. *ACS Medicinal Chemistry Letters* **2010**, *1*, (9), 536-539.
140. Ruegger, A.; Kuhn, M.; Lichti, H.; Loosli, H. R.; Huguenin, R.; Quiquerez, C.; von Wartburg, A., [Cyclosporin A, a Peptide Metabolite from *Trichoderma polysporum* (Link ex Pers.) Rifai, with a remarkable immunosuppressive activity]. *Helv Chim Acta* **1976**, *59*, (4), 1075-92.
141. Ke, H.; Mayrose, D.; Belshaw, P. J.; Alberg, D. G.; Schreiber, S. L.; Chang, Z. Y.; Etkorn, F. A.; Ho, S.; Walsh, C. T., Crystal structures of cyclophilin A complexed with cyclosporin A and N-methyl-4-[(E)-2-butenyl]-4,4-dimethylthreonine cyclosporin A. *Structure* **1994**, *2*, (1), 33-44.
142. Kofron, J. L.; Kuzmic, P.; Kishore, V.; Colon-Bonilla, E.; Rich, D. H., Determination of kinetic constants for peptidyl prolyl cis-trans isomerases by an improved spectrophotometric assay. *Biochemistry* **1991**, *30*, (25), 6127-34.
143. Sehgal, S. N.; Baker, H.; Vezina, C., Rapamycin (AY-22,989), a new antifungal antibiotic. II. Fermentation, isolation and characterization. *J Antibiot (Tokyo)* **1975**, *28*, (10), 727-32.
144. Banaszynski, L. A.; Liu, C. W.; Wandless, T. J., Characterization of the FKBP.rapamycin.FRB ternary complex. *J Am Chem Soc* **2005**, *127*, (13), 4715-21.

## G. Curriculum Vitae

**Steffen Paul-Günter Gaali**

Born 13<sup>th</sup> of January 1981 in Munich/Großhadern

### **Professional experience**

---

Since 04/08 Ph.D. student at Max-Planck-Institut of Psychiatry in the Hausch lab: *Design and Synthesis of selective ligands for the FK506-binding protein 51*

### **Academic Qualification**

---

#### **University**

11/05-03/08 Master of Science (M.Sc.), Chemistry, Ludwig-Maximilians-University

11/02-11/05 Bachelor of Science (B.Sc.), Chemistry and Biochemistry, Ludwig-Maximilians-University

11/01-11/05 Bachelor of Science, Bioinformatik, Ludwig-Maximilians-University

#### **Education**

#### **School**

06/01 Abitur at the Erasmus-Grasser-Gymnasium in Laim

### **Publications**

---

**Steffen Gaali**, Christian Kozany, Bastiaan Hoogeland, Marielle Klein, and Felix Hausch, Facile Synthesis of a Fluorescent Cyclosporin A Analogue To Study Cyclophilin 40 and Cyclophilin 18 Ligands, ACS Med. Chem. Lett., 2010, 1 (9), pp 536–539

**Gaali, S.**;Gopalakrishnan, R.;Wang, Y.;Kozany, C.;Hausch, F., The Chemical Biology of Immunophilin Ligands, Current Medicinal Chemistry, 2011, 18, 5355-5379

Ranganath Gopalakrishnan, Christian Kozany, **Steffen Gaali**, Christoph Kress, Bastiaan Hoogeland, Andreas Bracher, Felix Hausch. Evaluation of Synthetic FK506 Analogs as Ligands for FKBP51 and FKBP52. JMC, DOI: 10.1021/jm201747c

**Posters**

---

**Gaali S**, Kozany C, Hoogeland B, Klein M, Hausch F., Institute Symposium, 2010, Fluorescence Polarisation Assay for the Hsp90 Cochaperone Cyclophilin 40

**Gaali S**, Kozany C, Hoogeland B, Klein M, Hausch F., AGNP 2011, Development of Fluorescence Polarisation Assays for the Immunophilins FKBP51/52 and Cyp40.